Chemical and biological studies on bioactive secondary metabolites from fungal source

DISSERTATION

zur Erlangung des Doktorgrades der Naturwissenschaften

(Dr. rer. nat.)

der

Naturwissenschaftlichen Fakultät II

Chemie, Physik und Mathematik

der Martin-Luther-Universität

Halle-Wittenberg

vorgelegt von

Herrn Dipl.-Pharmazeut Alexander Otto

geb. am 30. Dezember 1986 in Halle (Saale)

This dissertation has been developed under the supversision of Prof. Dr. Ludger Wessjohann and mentorship of Dr. Norbert Arnold at the Leibniz Institute of Plant Biochemistry (IPB) in cooperation with the Martin Luther University of Halle-Wittenberg.

The results presented in this thesis have been published as eight peer-reviewed original research articles as well as one European patent specification.

1st Reviewer: Prof. Dr. Ludger Wessjohann

2nd Reviewer: PD Dr. Bernd Schneider

Date of public defense: 20th March 2017

Look deep into nature, and then you will understand everything better.

Albert Einstein

Table of contents

List of abbreviations

$[\alpha]^T_D$	Specific optical rotation	FT-ICR	Fourier transform ion cyclotron resonance
^{13}C	Carbon 13		
Ac$_2$O	Acetanhydride	GC	Gas chromatography
amu	Atomic mass units	h	Hour(s)
BCA	Biological control agent	HCD	Higher-collision energy dissociation
br	Broad signal		
calc.	Calculated	HMBC	Heteronuclear multiple bond correlation
CC	Column chromatography		
CD	Circular dichroism	HPLC	High-performance liquid chromatography
CE	Cotton effect		
CH$_2$Cl$_2$	Dichloromethane	HR	High-resolution
CH$_3$CN	Acetonitrile	HSQC	Heteronuclear single quantum correlation
CHCl$_3$	Chloroform		
CID	Collision induced dissociation	IC$_{50}$	Concentration of a compound needed to inhibit the growth by half
CoA	Coenzyme A		
coll.	Collection	IR	Infrared
COSY	Correlated spectroscopy	*J*	Coupling constant
d	Doublet	KSH	Kultursammlung Halle
Da	Dalton	LC-MS	Liquid chromatography/mass spectrometry
DEPT	Distortionless enhancement by polarization transfer		
		m	Multiplet
DMSO	Dimethylsulfoxide	m.p.	Melting point
dpi	Days post inoculation	*m/z*	Mass-to-charge ratio
DSMZ	Deutsche Sammlung für Mikro-organismen und Zellkulturen	MALDI	Matrix assisted laser desorption/ ionization
EI	Electron impact	MeOH	Methanol
eq.	Equivalent(s)	MIC	Minimum inhibitory concentration
ESI	Electrospray ionization	min	Minute(s)
EtOAc	Ethyl acetate	MPA	Malt peptone agar
EUCAST	European Committee on Anti-microbial Susceptibility Testing	MRSA	Methicillin-resistant *Staphylo-coccus aureus*
FA	Formic acid	MS	Mass spectrometry
Fig.	Figure	MS^n	Multistage mass spectrometry
		MTP	Microtiter plate

NMR	Nuclear magnetic resonance	**sp./spec.**	Species
NOE	Nuclear Overhauser effect	**SPE**	Solid-phase extraction
NOESY	Nuclear Overhauser enhancement spectroscopy	**spp.**	Species (more than one)
		SPPS	Solid-phase peptide synthesis
NRPS	Non-ribosomal peptide synthetase	**SRM**	Selected reaction monitoring
OD	Optical density	**t**	Triplet
ppm	Parts per million	**t-Bu**	*Tert*-butyl
PPP	Pentose phosphate pathway	**TFA**	Trifluoroacetic acid
PTFE	Polytetrafluoroethylene	**TFFH**	Tetramethylfluoroformamidinium hexafluorophosphate
q	Quartet		
r.t.	Room temperature	**TLC**	Thin-layer chromatography
rel. int.	Relative intensity	**TMS**	Tetramethylsilane
R_f	Retention factor	**TOCSY**	Total correlation spectroscopy
ROESY	Rotational frame Overhauser effect spectroscopy	**TOF**	Time of flight
		t_R	Retention time
s	Singlet	**UV/Vis**	Ultraviolet/visible
s.l.	Sensu lato	**VRE**	Vancomycin-resistant *Entero-coccus faecium*
SIM	Selected ion monitoring		

Summary

Fungi are an exceptional source of biologically active natural products, which had and possibly will have a significant influence on the development of pharmaceutical and agricultural products. Since only less than 10% of the world's estimated fungal species are described by now (Schüffler and Anke, 2014), it can be estimated that there is still an enormous potential to find new leads for crop protectants or drugs from chemically unexplored fungal sources. The goal of the present thesis was thus the isolation as well as the structural and biosynthetic characterization of bioactive secondary metabolites from fungal source by using different concepts and methods of natural product chemistry. Furthermore, the biological activity was evaluated with special focus on phytopathogenic organisms.

Five new hygrophorones (**6.1**–**6.5**) were isolated from fruiting bodies of *Hygrophorus abieticola*. The hygrophorones B^{12} (**6.1**), B^{10} (**6.2**), and E^{12} (**6.3**) belong to previously discovered hygrophorone types, while hygrophorone H^{12} (**6.4**) and its corresponding 2,3-dihydro derivative **6.5** are novel tetrahydroxylated hygrophorones. Hygrophorone B^{12} (**6.1**) was subsequently synthesized in an enantiomerically pure form (in cooperation), allowing for an unambiguous determination of the absolute configuration of B-type hygrophorones. The stereostructure of the E and H series hygrophorones was elucidated as well. Moreover, semisynthetic derivatives were generated by acetylation to obtain initial structure-activity relationships. In addition, structurally related pseudohygrophorones A^{12} (**5.1**) and B^{12} (**5.2**), featuring a six-membered ring system, were isolated from *H. abieticola* as well. Pseudohygrophorones **5.1** and **5.2** represent the first naturally occurring alkyl cyclohexenones from a fungal source. The absolute configuration of the three stereogenic centers in the diastereomeric compounds **5.1** and **5.2** was established with the aid of coupling constant and NOE analyses in conjunction with conformational studies and quantum chemical calculation of CD spectra.

Furthermore, the biosynthesis of hygrophorone B^{12} (**6.1**) in *H. abieticola* was investigated by feeding experiments in the field using ^{13}C labelled samples of D-glucose and sodium acetate in combination with spectroscopic analyses. It could be demonstrated that hygrophorone B^{12} (**6.1**) is derived from a fatty acid-polyketide route instead of a 1,4-α-D-glucan derived anhydrofructose pathway. The experiment with [2-^{13}C]-acetate revealed an unexpected incorporation pattern in the cyclopentenone system of **6.1**, indicating the formation of a symmetrical intermediate during the biosynthesis of hygrophorone B^{12} (**6.1**).

The biological activity of the isolated and semisynthetic (pseudo-)hygrophorones was evaluated against the phytopathogenic organisms *Botrytis cinerea*, *Septoria tritici*, and *Phytophthora infestans*. The highest activity was observed for hygrophorone B^{12} (**6.1**), followed by hygrophorone B^{10} (**6.2**) and the pseudohygrophorones A^{12} (**5.1**) and B^{12} (**5.2**). The semisynthetic hygrophorone B^{12} acetyl derivatives **6.1a**–**c** exhibited weaker effects in comparison to hygrophorone B^{12} (**6.1**). The hygrophorones E^{12} (**6.3**) and H^{12} (**6.4**) lacking the endocyclic

carbonyl function exhibited only modest activities, while 2,3-dihydrohygrophorone H^{12} (**6.5**) without the double bond was inactive against all organisms tested. These results indicate, that an α,β-unsaturated carbonyl structure seems to be a prerequisite for potent bioactivity, which might react as a Michael acceptor with biological nucleophiles. This was supported by the rapid Michael addition of L-cysteine to hygrophorone B^{12} (**6.1**).

In addition, five sesquiterpene carboxylic acids **7.1**–**7.5** and one nor-sesquiterpene carboxylic acid **7.6** of the rare ventricosane type, named penarines A–F, were isolated from fruiting bodies of *Hygrophorus penarius*. This is the first report of (nor-)sesquiterpenes isolated from basidiocarps of the family Hygrophoraceae. Additionally, the only known member of this rare type of sesquiterpenes, ventricos-7(13)-ene (**7.7**) isolated from the liverwort *Lophozia ventricosa*, could be identified *via* headspace GC–MS analysis in fruiting bodies of *H. penarius*. Penarines A–F (**7.1**–**7.6**) were devoid of significant antifungal activity against *Cladosporium cucumerinum*.

In continuation of our search for new bioactive compounds from fungi, ten new and two known peptaibols were isolated from semi-solid cultures of *Sepedonium* and *Gliocladium* species (Hypocreaceae). Two new linear 15-residue peptaibols, named chilenopeptins A (**8.1**) and B (**8.2**), together with the known peptaibols tylopeptins A (**8.3**) and B (**8.4**) were isolated from the Chilean *Sepedonium* aff. *chalcipori* KSH 883. The taxonomic status of the *Sepedonium* strain KSH 883, parasitizing on the endemic mushroom *Boletus loyo*, was investigated by using molecular phylogenetic and chemical data. Additionally, the synthesis of the peptides **8.1** and **8.2** was accomplished by a solid-phase approach confirming the absolute configuration of all chiral amino acids as L.

The albupeptins A–D (**9.1**–**9.4**) are new 11-mer peptaibols, which were obtained from *Gliocladium album*. The absolute configuration of **9.1**–**9.4** was unambiguously assigned by proton NMR chemical shift analyses in conjunction with solid-phase peptide synthesis. Albupeptins B (**9.2**) and D (**9.4**) belong to the rare class of peptaibols that exhibit both stereoisomers of isovaline (L- and D-) in the same sequence.

Four new 19-residue peptaibols, named tulasporins A–D (**10.1**–**10.4**) were isolated from *Sepedonium tulasneanum*. Constituents **10.1**–**10.4** represent the first peptaibols from *Sepedonium* strains that produce at the same time oval, hyaline aleurioconidia instead of round, yellow colored ones.

All isolated peptaibols show activity against phytopathogenic organisms. The strongest antiphytopathogenic effects were observed for the 19-residue tulasporins A–D (**10.1**–**10.4**), followed by the 15-mer chilenopeptins and tylopeptins. The biological activity of the tested peptaibols thus correlated with the length of the amino acid sequence.

Zusammenfassung

Pilze sind eine außergewöhnliche Quelle von biologisch aktiven Naturstoffen, die einen wesentlichen Einfluss auf die Entwicklung von pharmazeutischen und landwirtschaftlichen Produkten hatten und vermutlich auch in Zukunft haben werden. Da bislang erst weniger als 10% der weltweit geschätzten Pilzarten beschrieben sind (Schüffler and Anke, 2014), kann von einem enormen Potential ausgegangen werden, neue Leitstrukturen als Grundlage für die Entwicklung neuartiger Pflanzenschutzmittel oder Arzneimittel in bislang chemisch unerforschten Pilzquellen zu entdecken. Ziel der vorliegenden Arbeit war daher die Isolierung sowie die strukturelle und biosynthetische Charakterisierung von bioaktiven Sekundärmetaboliten aus pilzlicher Quelle unter Anwendung unterschiedlicher Konzepte und Methoden der Naturstoffchemie. Weiterhin wurde die biologische Aktivität, insbesondere gegen phytopathogene Organismen, evaluiert.

Fünf neue Hygrophorone (**6.1**–**6.5**) wurden aus Fruchtkörpern von *Hygrophorus abieticola* isoliert. Hygrophoron B^{12} (**6.1**), B^{10} (**6.2**) und E^{12} (**6.3**) gehören zu den zuvor beschriebenen Hygrophoron-Typen, währenddessen Hygrophoron H^{12} (**6.4**) und das entsprechende 2,3-dihydro-Derivat **6.5** neue tetrahydroxylierte Hygrophorone sind. Hygrophoron B^{12} (**6.1**) wurde außerdem in enantiomerenreiner Form synthetisiert (in Kooperation), so dass die absolute Konfiguration von Hygrophoronen der B Serie zweifelsfrei bestimmt werden konnte. Die Konfiguration der Hygrophoron E- und H-Typen konnte ebenfalls aufgeklärt werden. Außerdem wurden halb-synthetische Derivate von **6.1** durch Acetylierung dargestellt, um Aussagen über erste Struktur-Aktivitäts-Beziehungen treffen zu können. Die strukturell verwandten Pseudohygrophorone A^{12} (**5.1**) und B^{12} (**5.2**), welche ein sechsgliedriges Ringsystem aufweisen, wurden ebenfalls aus *H. abieticola* isoliert. Die Pseudohygrophorone **5.1** und **5.2** stellen die ersten natürlich vorkommenden Alkylcyclohexenone aus pilzlicher Quelle dar. Die absolute Konfiguration der drei Stereozentren in den diastereomeren Verbindungen **5.1** und **5.2** wurde durch die Analyse von Kopplungskonstanten und NOE Interaktionen in Verbindung mit Konformationsstudien und quantenchemischen Berechnungen der CD-Spektren bestimmt.

Weiterhin wurde die Biosynthese von Hygrophoron B^{12} (**6.1**) in *H. abieticola* durch Verfütterungsexperimente mit ^{13}C markierten Proben von D-Glucose und Natriumacetat in Kombination mit spektroskopischen Analysen untersucht. Es konnte gezeigt werden, dass Hygrophoron B^{12} (**6.1**) über den Fettsäure-Polyketidweg anstatt des 1,4-α-D-Glucan abgeleiteten Anhydrofructoseweges biosynthetisiert wird. Das Experiment mit [2-^{13}C]-Acetat zeigte ein unerwartetes Einbaumuster in das Cyclopentenon-System von **6.1**, welches auf die Bildung eines symmetrischen Intermediates während der Biosynthese von Hygrophoron B^{12} (**6.1**) hindeutet.

Die biologische Aktivität der isolierten und halbsynthetischen (Pseudo-)hygrophorone wurde gegen die phytopathogenen Organismen *Botrytis cinerea*, *Septoria tritici* und *Phytophthora infestans* evaluiert. Die höchste Aktivität wurde für Hygrophoron B^{12} (**6.1**) beobachtet, gefolgt von Hygrophoron B^{10} (**6.2**) und den Pseudohygrophoronen A^{12} (**5.1**) und B^{12} (**5.2**). Die

halbsynthetischen Acetylderivative von Hygrophoron B^{12} **6.1a–c** zeigten im Vergleich zu Hygrophoron B^{12} (**6.1**) geringere Aktivitäten. Die Hygrophorone E^{12} (**6.3**) und H^{12} (**6.4**) ohne die endocyclische Carbonylfunktion zeigten nur mäßige Aktivitäten, währenddessen 2,3-Dihydrohygrophoron H^{12} (**6.5**) ohne die Doppelbindung gegen alle getesteten Organismen inaktiv war. Diese Ergebnisse deuten darauf hin, dass eine α,β-ungesättigte Carbonylstruktur eine Voraussetzung für die biologische Aktivität ist, welche als Michael-Akzeptor mit biologischen Nukleophilen reagieren könnte. Diese Beobachtung wurde durch die rasche Michael-Addition von L-Cystein an Hygrophoron B^{12} (**6.1**) unterstützt.

Diese Arbeit beschreibt weiterhin fünf Sesquiterpen-carbonsäuren **7.1–7.5** und eine Norsesquiterpen-carbonsäure **7.6** des seltenen Ventricosan-Typs, genannt Penarine A–F, aus Fruchtkörpern von *Hygrophorus penarius*. (Nor-)sesquiterpene wurden damit zum ersten Mal aus Fruchtkörpern der Familie Hygrophoraceae isoliert. Zusätzlich konnte das einzige bekannte Ventricosan-Sesquiterpen, Ventricos-7(13)-en (**7.7**) aus dem Lebermoos *Lophozia ventricosa*, mittels Headspace-GC-MS-Analyse auch in Fruchtkörpern von *H. penarius* identifiziert werden. Die Penarine A–F (**7.1–7.6**) wiesen keine antimykotische Aktivität gegen *Cladosporium cucumerinum* auf.

Im Zuge weiterer naturstoffchemischen Untersuchungen konnten zehn neue und zwei zuvor beschriebene Peptaibole aus Kulturen von *Sepedonium* und *Gliocladium* Arten (Hypocreaceae) isoliert werden. Die neuen, linearen 15-mer Peptaibole namens Chilenopeptin A (**8.1**) und B (**8.2**) wurden zusammen mit den bekannten Peptaibolen Tylopeptin A (**8.3**) und B (**8.4**) aus dem chilenischen Stamm von *Sepedonium* aff. *chalcipori* KSH 883 isoliert. Der taxonomische Status von *Sepedonium* Stamm KSH 883, welcher in Chile auf dem endemischen Pilz *Boletus loyo* parasitierte, wurde mit Hilfe von molekularen und chemischen Daten untersucht. Des Weiteren wurden die Peptide **8.1** und **8.2** an Festphase synthetisiert und damit die absolute Konfiguration aller chiralen Aminosäuren als L bestimmt.

Die Albupeptine A–D (**9.1–9.4**) sind neue 11-mer Peptaibole, welche aus dem Kulturfiltrat von *Gliocladium album* erhalten wurden. Die absolute Konfiguration von **9.1–9.4** wurde durch Analyse von ^{1}H NMR chemischen Verschiebungen in Verbindung mit Festphasenpeptidsynthese bestimmt. Die Albupeptine B (**9.2**) und D (**9.4**) gehören zur seltenen Klasse der Peptaibole, welche beide Stereoisomere von Isovalin (L- und D-) in der gleichen Sequenz aufweisen.

Vier neue 19-mer Peptaibole, genannt Tulasporine A–D (**10.1–10.4**), wurden aus *Sepedonium tulasneanum* isoliert. Die Verbindungen **10.1–10.4** stellen die ersten Peptaibole aus *Sepedonium*-Kulturen dar, welche gleichzeitig ovale, hyaline Aleuriokonidien anstatt runder, gelb gefärbter produzieren.

Alle isolierten Peptaibole zeigen eine Aktivität gegen pflanzenpathogene Organismen. Die 19-mer Tulasporine A–D (**10.1–10.4**) zeigten die stärksten antiphytopathogenen Effekte, gefolgt von den 15-mer Chilenopeptinen und Tylopeptinen. Damit korrelierte die Stärke der biologischen Aktivität mit der Aminosäuresequenzlänge der getesteten Peptaibole.

1   Introduction and objectives

Fungi are from an evolutionary point of view very old organisms and occur ubiquitously in aquatic and terrestrial environments. The total number of fungal species is estimated at 1.5 million (Hawksworth, 2001), of which only about 100.000 species have been described to date (Schüffler and Anke, 2014). Fungal phenotypes are highly diverse, ranging from unicellular yeasts to complex multicellular organisms that can form fruiting bodies.

Unlike plants, fungi are heterotrophic organisms, as they are not capable of photosynthesis. Many fungi obtain nutrients such as sugars or amino acids by ectomycorrhizal symbiosis with plants; others are associated with algae (lichens), occur as epithelial or internal parasites, or are decomposers of dead organic material (Deacon, 2006). Due to these lifestyles and less pronounced mechanical protection from predators and competitors, fungi have evolved highly effective secondary metabolites with exceptional chemical diversity and striking biological activities. However, the ecological role of most fungal secondary metabolites is poorly understood (Spiteller, 2015).

Certain fungi are of great importance in our daily life. For instance, the metabolic physiology of yeast has been used since ancient times for preparing cheese, bread, and alcoholic beverages. The occurrence of biologically active compounds in fungi had been recognized by humans more than 5000 years ago, since fruiting bodies of *Piptoporus betulinus* were found among the belongings of the Iceman "Ötzi" (Alresly et al., 2016; Capasso, 1998). This fungus was most likely used for medicinal purposes due to its antimicrobial properties (Pöder, 1993).

For the past 50 years, fungal secondary metabolites have revolutionized natural product research, affording drugs and drug leads of enormous medicinal and agricultural potential (Aly et al., 2011). For instance, penicillins (e.g. penicillin G, **1.1**) and cephalosporins (e.g. cephalotin, **1.2**), β-lactam antibiotics firstly isolated from *Penicillium* and *Acremonium* species, are still among the world's blockbuster drugs, representing about 50% of the total antibiotic market in 2009 (Aly et al., 2011; Hamad, 2010). The antifungal agent griseofulvin (**1.3**, Fulvicin®), that was isolated from the mold *Penicillium griseofulvum* (Grove et al., 1952), is approved for the treatment of dermatophyte infections of the skin, nails and hair of humans (Aly et al., 2011). Another important group of fungal derived drugs are the antihyperlipidemic statins, for instance lovastatin (**1.4**, Mevacor®), isolated from *Aspergillus terreus* (Alberts et al., 1980), *Monascus ruber* (Negishi et al., 1986), and *Pleurotus ostreatus* (Alarcón et al., 2003), or the semisynthetic analogue simvastatin (**1.5**, Zocor®). Statins are competitive inhibitors of the 3-hydroxy-3-methyl-glutaryl coenzyme A (HMG-CoA) reductase, an enzyme involved in cholesterol metabolism (Alberts, 1988).

A new era in immunopharmacology began with the discovery of the cyclic undecapeptide cyclosporin A (**1.6**, Sandimmune®), isolated from the fermentation broth of *Tolypocladium inflatum* (originally misidentified as *Trichoderma polysporum*) (Gams, 1971a; Rüegger et al.,

1976). It is widely used as an immunosuppressant to prevent rejection of transplanted organs (Wenger, 1985).

penicillin G (**1.1**)

cephalotin (**1.2**)

griseofulvin (**1.3**)

	R
lovastatin (**1.4**)	H
simvastatin (**1.5**)	CH$_3$

cyclosporin A (**1.6**)
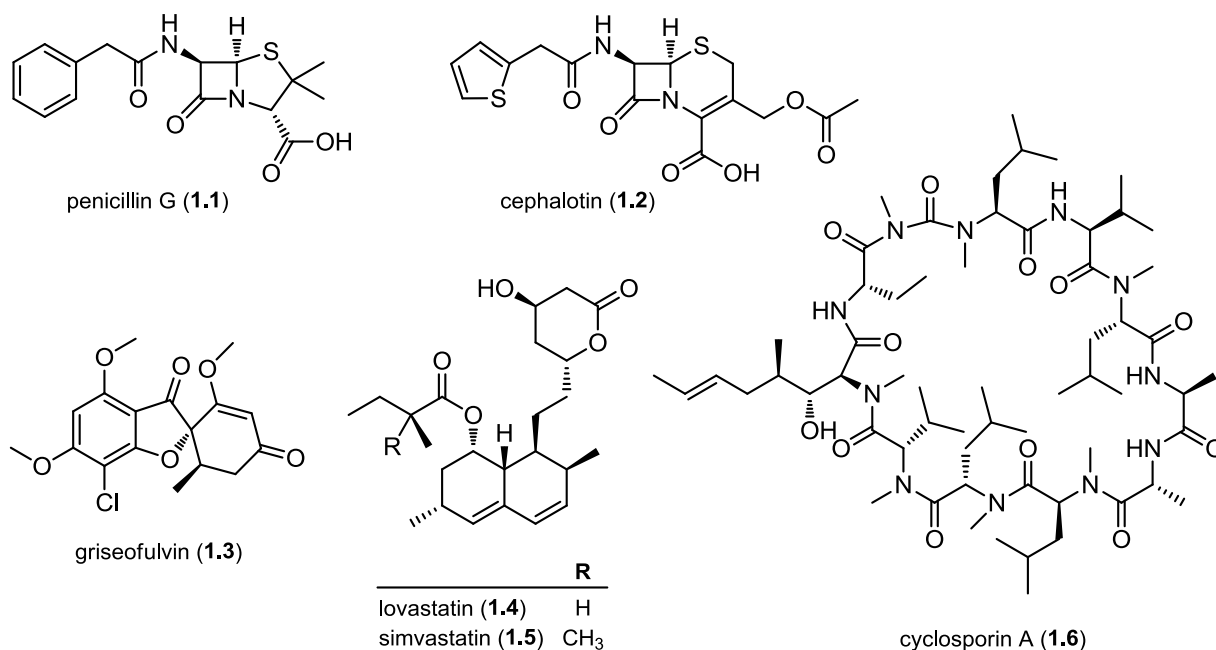
Fungal natural products also had a significant impact on agricultural crop protection, e.g., the discovery of the strobilurin fungicides. In 1977, the first naturally occurring strobilurins A (**1.7**) and B (**1.8**) were isolated from cultures of the pinecone cap *Strobilurus tenacellus* (Anke et al., 1977). Strobilurins are fungicidal β-methoxyacrylic acid derivatives that have been isolated additionally from basidiomycetes of many other genera (Anke and Erkel, 2002).

Despite the photolability of the natural strobilurins, they served as a chemical lead that allowed the synthesis of strobilurin analogues with enhanced light stability and efficacy, systemic properties without phytotoxicity, and a broader spectrum of action (Aly et al., 2011; Thind, 2007). For instance, the photolabile triene functionality could be stabilized by introducing an arene system, such as in the enoletherstilbene **1.9** and the diphenylether **1.10** (Sauter et al., 1999). These compounds were the basis for the development of today's commercial strobilurins such as azoxystrobin (**1.11**, Amistar®), kresoxim-methyl (**1.12**, Discus®), and pyraclostrobin (**1.13**, Signum®). As of 2009, strobilurins accounted for around 22% of the global fungicide market, reaching over 2.6 billion dollars of annual sales (Sauter et al., 2012). Thus, strobilurin fungicides represent the most important class of crop protection agents, followed by the formerly leading triazoles (Sauter et al., 2012).

The strobilurins are the so-called quinone outside inhibitors (QoI), as they inhibit the fungal cell respiration by blocking the electron transfer at the quinol oxidation (Qo) site of the cytochrome bc$_1$ complex, and thus prevent ATP formation (Balba, 2007; Bartlett et al., 2001). In spite of this mechanism of action, their toxicity for humans and other warm blooded animals is very low (Schüffler and Anke, 2014). Most strobilurins are broad spectrum fungicides, acting against a diverse range of diseases caused by fungi and fungus-like oomycetes (Bartlett et al.,

2001). Unfortunately, strobilurins are rather susceptible to resistance formation (Sauter et al., 2012). Thus, demand for novel fungicides will rise in the future.
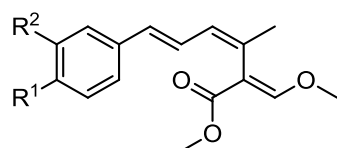
	R^1	R^2
strobilurin A (**1.7**)	H	H
strobilurin B (**1.8**)	Cl	OCH$_3$
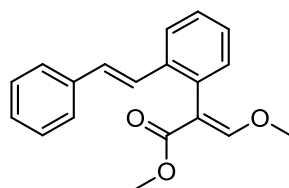
enoletherstilbene derivative **1.9**
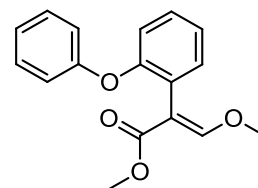
diphenylether derivative **1.10**
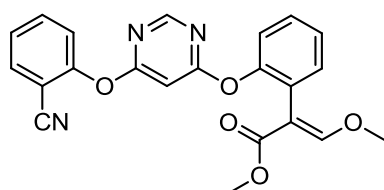
azoxystrobin (**1.11**)
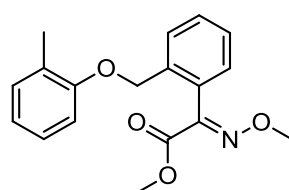
kresoxim-methyl (**1.12**)
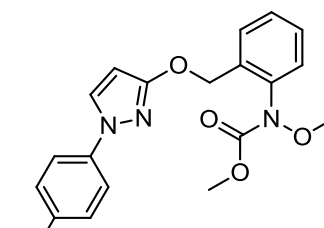
pyraclostrobin (**1.13**)

Diseases caused by fungal and fungus-like phytopathogens are economically extremely significant, accounting for more than 70% of the major crop diseases (Deacon, 2006) and destroying more than 125 million tons of the top five food crops (rice, wheat, maize, potato, and soybean) every year (Kupferschmidt, 2012).

Table 1.1 provides an overview of economically important phytopathogenic fungi and oomycetes. The majority of fungal phytopathogens belong to the Ascomycetes, Basidiomcyetes and Fungi imperfecti (mainly anamorphic ascomycetes). For instance, the blast fungus *Magnaporthe grisea* (anamorph *Pyricularia grisea*) causes a serious disease on grasses including rice, wheat, and barley (Talbot, 2003). The basidiomycetous fungi *Ustilago maydis* (boil smut) and *Puccinia graminis* (rust) are responsible for devastating diseases on cereal crops (Dean et al., 2012). The most relevant phytopathogenic anamorphic (asexual stage) fungi include *Botrytis cinerea*, the causal agent of grey mold on various crops, and *Septoria tritici*, responsible for the septoria leaf blotch which is the most prevalent disease on wheat worldwide (Suffert et al., 2011).

The fungus-like oomycetes, often referred to as water molds, also cause a number of economically significant diseases such as downy mildew (*Peronospora* spp., *Pseudoperonospora* spp., *Plasmopara* spp.), root rot (*Pythium* spp.), or late blight (*Phytophthora infestans*). The latter pathogen was responsible for the Irish potato famine in the 1840s that led to death and emigration of over two million Irish people (Martin et al., 2013).

Two major challenges have to be faced in fungicide crop protection. On the one hand, the loss of commercial fungicides due to new regulations is higher than the number of new active substances being introduced to the market (Krämer et al., 2012). On the other hand, the high input of fungicides in combating such phytopathogen diseases has led to a dramatic increase of strains showing resistance to chemical fungicides. For instance, isolates of *Septoria tritici* resistant to strobilurin fungicides were discovered in Europe for the first time at the end of the 2002 season,

and have spread since then to Northern America (Estep et al., 2013) and Northern Africa (Siah et al., 2014; Taher et al., 2014).

Table 1.1. Overview of economically relevant plant pathogenic fungi and oomycetes, modified from Doohan (2011) and FRAC (2013).

Pathogen	Hosts	Common name
Ascomycota (anamorph)		
Botrytis cinerea	ornamentals and fruit trees	grey mold
Alternaria solani	potato, tomato	alternaria blight (early blight)
Cladosporium cucumerinum	cucumber, cucurbit, melon	scab
Septoria tritici	cereals (primarily wheat)	septoria leaf blotch
Fusarium oxysporum	various (e.g. cotton, tobacco, banana, soybean, coffee, turfgrass, ginger)	fusarium wilt
Verticillium spp.	various (e.g. cotton, tomato, potato, pepper)	verticillium wilt
Ascomycota (teleomorph)		
Venturia inequalis	apple	apple scab
Magnaporthe grisea	rice	rice blast
Oomycota		
Phytophthora infestans	potato, tomato	late blight
Plasmopara viticola	grapevine	downy mildew
Pseudoperonospora spp.	cucurbit, cucumber	downy mildew
Pythium spp.	various (e.g. potato, corn, soybean)	root rot, damping-off
Basidiomycota		
Puccinia graminis	cereals	black stem rust
Ustilago maydis	corn	smut
Rhizoctonia solani	various (e.g. carrot, wheat, barley, cotton, bean)	damping-off, root and stem rot

Hence, there is an urgent need for novel resistance-breaking lead structures, yielding inexpensive fungicides that exert enhanced efficacy, lower toxicity, and less environmental impact than the products already established on the market (Aly et al., 2011). The fact that less than 10% of the world's biodiversity have been evaluated for their biological activity provides an enormous chance to explore more useful lead structures from natural sources (Harvey, 2000).

The general objective of the present thesis was thus the isolation and identification of new natural products from fungal sources that can potentially serve as lead structures for the development of novel plant protective fungicides and/or pharmaceutical drugs. In particular, the investigations were focused on the following aspects:

- Isolation, characterization and structural elucidation of biologically active secondary metabolites from fungal sources

- Evaluation of their biological activity with special focus on phytopathogenic organisms such as *B. cinerea*, *S. tritici*, and *P. infestans*

- Semisynthesis of derivatives for activity enhancement and initial structure-activity relationship (SAR) studies

- Assignment of the absolute configuration by (semi-)synthetic or chiroptical studies

- Investigations towards the biosynthesis of selected natural products

References

Alarcón, J., Águila, S., Arancibia-Avila, P., Fuentes, O., Zamorano-Ponce, E., Hernández, M., 2003. Production and purification of statins from *Pleurotus ostreatus* (Basidiomycetes) strains. *Z. Naturforsch.* 58c, 62–64.

Alberts, A.W., 1988. Discovery, biochemistry and biology of lovastatin. *Am. J. Cardiol.* 62, J10–J15.

Alberts, A.W., Chen, J., Kuron, G., Hunt, V., Huff, J., Hoffman, C., Rothrock, J., Lopez, M., Joshua, H., Harris, E., Patchett, A., Monaghan, R., Currie, S., Stapley, E., Albers-Schonberg, G., Hensens, O., Hirshfield, J., Hoogsteen, K., Liesch, J., Springer, J., 1980. Mevinolin: a highly potent competitive inhibitor of hydroxymethylglutaryl-coenzyme A reductase and a cholesterol-lowering agent. *Proc. Natl. Acad. Sci.* 77, 3957–3961.

Alresly, Z., Lindequist, U., Lalk, M., Porzel, A., Arnold, N., Wessjohann, L., 2016. Bioactive triterpenes from the fungus *Piptoporus betulinus*. *Rec. Nat. Prod.* 10, 103–108.

Aly, A.H., Debbab, A., Proksch, P., 2011. Fifty years of drug discovery from fungi. *Fungal Divers.* 50, 3–19.

Anke, T., Erkel, G., 2002. Non β-lactam antibiotics, in: Osiewacz, H.D. (Ed.), The Mycota X. Industrial Applications. Springer Verlag, Berlin, Heidelberg, pp. 93–108.

Anke, T., Oberwinkler, F., Steglich, W., Schramm, G., 1977. The strobilurins – New antifungal antibiotics from the basidiomycete *Strobilurus tenacellus*. *J. Antibiot.* 30, 806–810.

Balba, H., 2007. Review of strobilurin fungicide chemicals. *J. Environ. Sci. Health. B* 42, 441–451.

Bartlett, D.W., Clough, J.M., Godfrey, C.R.A., Godwin, J.R., Hall, A.A., Heaney, S.P., Maund, S.J., 2001. Understanding the strobilurin fungicides. *Pestic. Outlook* 12, 143–148.

Capasso, L., 1998. 5300 years ago, the Ice Man used natural laxatives and antibiotics. *Lancet* 352, 1864.

Deacon, J.W., 2006. Introduction: the fungi and fungal activities, in: Fungal Biology. Blackwell Publishing, pp. 1–15.

Dean, R., Van Kan, J.A.L., Pretorius, Z.A., Hammond-Kosack, K.E., Di Pietro, A., Spanu, P.D., Rudd, J.J., Dickmann, M., Kahmann, R., Ellis, J., Foster, G.D., 2012. The Top 10 fungal pathogens in molecular plant pathology. *Mol. Plant Pathol.* 13, 414–430.

Doohan, F., 2011. Fungal pathogens of plants, in: Kavanagh, K. (Ed.), Fungi: Biology and Applications. Wiley Press. Int., London, pp. 313–344.

Estep, L.K., Zala, M., Anderson, N.P., Sackett, K.E., Flowers, M., McDonald, B.A., Mundt, C.C., 2013. First report of resistance to QoI fungicides in North American populations of *Zymoseptoria tritici*, causal agent of septoria tritici blotch of wheat. *Plant Dis.* 97, 1511.

FRAC, 2013. List of plant pathogenic organisms resistant to disease control agents. URL http://www.frac.info/docs/default-source/publications/list-of-resistant-plant-pathogens/list-of-resistant-plant-pathogenic-organisms---february-2013.pdf?sfvrsn=4 (accessed 20th December 2015).

Gams, W., 1971a. *Tolypocladium*, eine Hyphomycetengattung mit geschwollenen Phialiden. *Persoonia* 6, 185–191.

Grove, J.F., MacMillan, J., Mulholland, T.P.C., Rogers, M.A.T., 1952. 762. Griseofulvin. Part IV. Structure. *J. Chem. Soc.* 3977–3987.

Hamad, B., 2010. The antibiotics market. *Nat. Rev. Drug Discov.* 9, 675–676.

Harvey, A., 2000. Strategies for discovering drugs from previously unexplored natural products. *Drug Discov. Today* 5, 294–300.

Hawksworth, D.L., 2001. The magnitude of fungal diversity: the 1.5 million species estimate revisited. *Mycol. Res.* 105, 1422–1432.

Krämer, W., Schirmer, U., Jeschke, P., Witschel, M., 2012. Preface to the Second Edition, in: Krämer, W., Schirmer, U., Jeschke, P., Witschel, M. (Eds.), Modern Crop Protection Compounds. Wiley-VCH, Weinheim, Vol. 1, pp. XXIII–XXIV.

Kupferschmidt, K., 2012. Attack of the Clones. *Science* 337, 636–638.

Martin, M.D., Cappellini, E., Samaniego, J.A., Zepeda, M.L., Campos, P.F., Seguin-Orlando, A., Wales, N., Orlando, L., Ho, S.Y.W., Dietrich, F.S., Mieczkowski, P.A., Heitman, J., Willerslev, E., Krogh, A., Ristaino, J.B., Gilbert, M.T.P., 2013. Reconstructing genome evolution in historic samples of the Irish potato famine pathogen. *Nat. Commun.* 4, 1–7.

Negishi, S., Huang, Z.C., Hasumu, K., Murakawa, S., Endo, A., 1986. Productivity of monacolin K (mevinolin) in the genus *Monascus*. *Hakko Kogaku Kaishi* 64, 584–590.

Pöder, R., 1993. Ice Man's fungi: discussion rekindled. *Science* 262, 1956.

Rüegger, A., Kuhn, M., Lichti, H., Loosli, H.-R., Huguenin, R., Quiquerez, C., von Wartburg, A., 1976. Cyclosporin A, ein immunsuppressiv wirksamer Peptidmetabolit aus *Trichoderma polysporum*. *Helv. Chim. Acta* 59, 1075–1092.

Sauter, H., Earley, F., Rheinheimer, J., Rieck, H., Coqueron, P.-Y., Whittingham, W.G., Walter, H., 2012. Fungicides acting on oxidative phosphorylation, in: Krämer, W., Schirmer, U., Jeschke, P., Witschel, M. (Eds.), Modern Crop Protection Compounds. Wiley-VCH, Weinheim, Vol. 2, pp. 559–691.

Sauter, H., Steglich, W., Anke, T., 1999. Strobilurins: Evolution of a new class of active substances. *Angew. Chemie Int. Ed.* 38, 1328–1349.

Schüffler, A., Anke, T., 2014. Fungal natural products in research and development. *Nat. Prod. Rep.* 31, 1425–1448.

Siah, A., Elbekali, A.Y., Ramdani, A., Reignault, P., Torriani, S.F.F., Brunner, P.C., Halama, P., 2014. QoI resistance and mitochondrial genetic structure of *Zymoseptoria tritici* in Morocco. *Plant Dis.* 98, 1138–1144.

Spiteller, P., 2015. Chemical ecology of fungi. *Nat. Prod. Rep.* 32, 971–993.

Suffert, F., Sache, I., Lannou, C., 2011. Early stages of septoria tritici blotch epidemics of winter wheat: build-up, overseasoning, and release of primary inoculum. *Plant Pathol.* 60, 166–177.

Taher, K., Graf, S., Fakhfakh, M.M., Salah, H.B.H., Yahyaoui, A., Rezgui, S., Nasraoui, B., Stammler, G., 2014. Sensitivity of *Zymoseptoria tritici* isolates from Tunisia to pyraclostrobin, fluxapyroxad, epoxiconazole, metconazole, prochloraz and tebuconazole. *J. Phytopathol.* 162, 442–448.

Talbot, N.J., 2003. On the trail of a cereal killer: Exploring the biology of *Magnaporthe grisea*. *Annu. Rev. Microbiol.* 57, 177–202.

Thind, T.S., 2007. Changing cover of fungicide umbrella in crop protection. *Indian Phytopathol.* 60, 421–433.

Wenger, R.M., 1985. Synthesis of cyclosporine and analogues: Structural requirements for immunosuppressive activity. *Angew. Chemie Int. Ed.* 24, 77–85.

2   General Part

2.1   Peptaibiotics

2.1.1 Definition

According to the definition established by Degenkolb (2003), peptaibiotics are linear, bioactive peptides that (a) have a molecular weight between 500 and 2200 Da with 5–21 residues; (b) show a high content of the C^α-tetrasubstituted amino acids such as α-aminoisobutyric acid (Aib) or its chiral higher homologue isovaline (Iva), and other non-proteinogenic amino acids such as hydroxyproline (Hyp) or pipecolic acid (Pip) (Fig. 2.1); (c) have an acylated *N*-terminus, and (d) possess a *C*-terminal 1,2-amino alcohol, amine, amide, free acid or sugar alcohol.

The recently launched "Peptaibiotics Database" (https://peptaibiotics-database.boku.ac.at/) records over 1350 peptaibiotics sequences (Neumann et al., 2015). The majority of these peptides are **peptaibols** (over 950), in which the *C*-terminus is reduced to an 1,2-amino alcohol while the *N*-terminal amino acid is acetylated. The so-called **lipopeptaibols** exhibit a lipophilic *N*-terminus that is acylated by octanoic, decanoic, or (*Z*)-dec-4-enoic acid (Toniolo et al., 2001). The third subfamily encompasses the **lipoaminopeptaibols** which are characterized by a substitution at the *N*-terminus with long-chain α-methyl fatty acids as well as the the lipoamino acid 2-amino-6-hydroxy-4-methyl-8-oxo-decanoic acid (AHMOD) that is commonly present at amino acid position 2 (Fig. 2.1) (Degenkolb et al., 2003; Gräfe et al., 1995). Peptaibiotics can also be classified according to their chain length as long-chain (17–21 residues), medium-chain (11–16), and short-chain (5–10) peptides (Degenkolb et al., 2007).
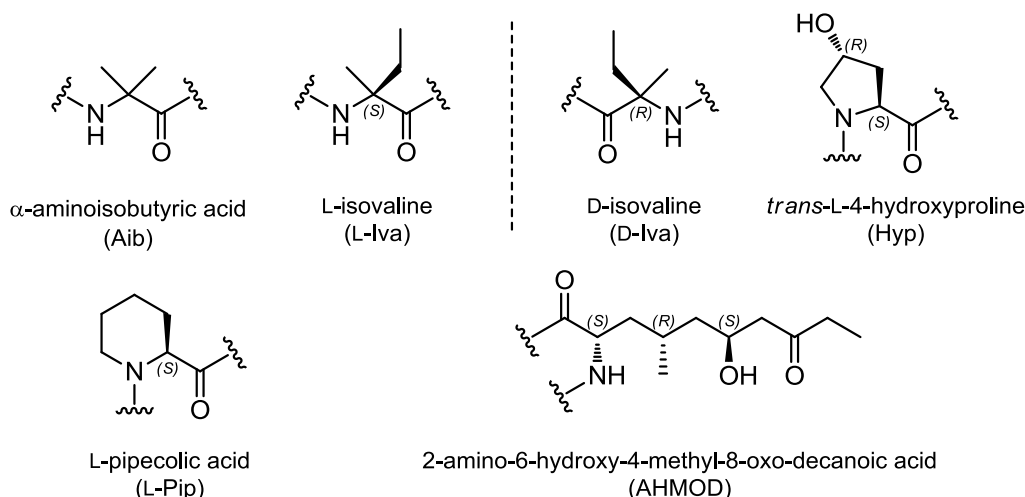

Fig. 2.1. Selected non-proteinogenic amino acids that occur in peptaibiotics.

This heterogeneous class of peptides is biosynthesized by multi-enzyme complexes, called non-ribosomal peptide synthetases (NRPS) *via* the thiotemplate mechanism (Degenkolb et al., 2003). Such synthetases have been characterized from *Sepedonium ampullosporum* (Reiber et al.,

2003) and *Trichoderma virens* (Wiest et al., 2002). Unlike ribosomal peptides, peptaibiotics are insensitive to proteolytic degradation (De Zotti et al., 2009; Yamaguchi et al., 2003).

2.1.2 Peptaibols

The majority of the over 950 published peptaibols are reported from ascomycetous fungi of the family Hypocreaceae, mainly from the genus *Trichoderma*, but also from *Stilbella*, *Acremonium*, *Tolypocladium*, *Gliocladium*, and *Sepedonium* species (Neumann et al., 2015).

The α,α-dialkyl substituents of Aib and Iva residues impose major steric restrictions in peptaibols, thus induce the formation of α-, 3_{10}- or mixed $\alpha/3_{10}$-helical structures (Fig. 2.2A) (Aravinda et al., 2008; Marshall et al., 1990). The α-helical conformation is stabilized by intramolecular hydrogen bridge bonds between the backbone NH and the CO group four residues earlier, leading to a 100° turn (3.6 residues per turn) (Vieira-Pires and Morais-Cabral, 2010). Peptaibols that are extraordinary rich in Aib residues predominantly form a 3_{10}-helix, which is twisted more tightly, resulting in three amino acids per turn (Pike et al., 2014; Toniolo and Benedetti, 1991). The proportions of α- and 3_{10}-helical structures can be estimated *via* circular dichroism (CD) studies by calculating the ratio of the molar ellipticity minima around 207 nm ($\pi \rightarrow \pi^*$ transition) and 222 nm ($n \rightarrow \pi^*$ transition). For α-helical conformations, the ratio of $[\theta]_{222}/[\theta]_{207}$ is typically around 1.0, and about 0.4 for 3_{10}-helical structures (Toniolo et al., 1996).

Their pronounced helical structure and amphipathic nature is likely to be an important feature for their membrane-perturbing properties (Gessmann et al., 2003). There is a controversial discussion about the exact mechanism of action. The most common models for the 19-residue peptaibol alamethicin and the 18-mer trichotoxin A50E are the so-called "barrel-stave" pores (Chugh et al., 2002; Leitgeb et al., 2007). These channels are formed by three to twelve parallel bundles of helical monomers that surround the polar pore lumen (Fig. 2.2B) (Leitgeb et al., 2007).
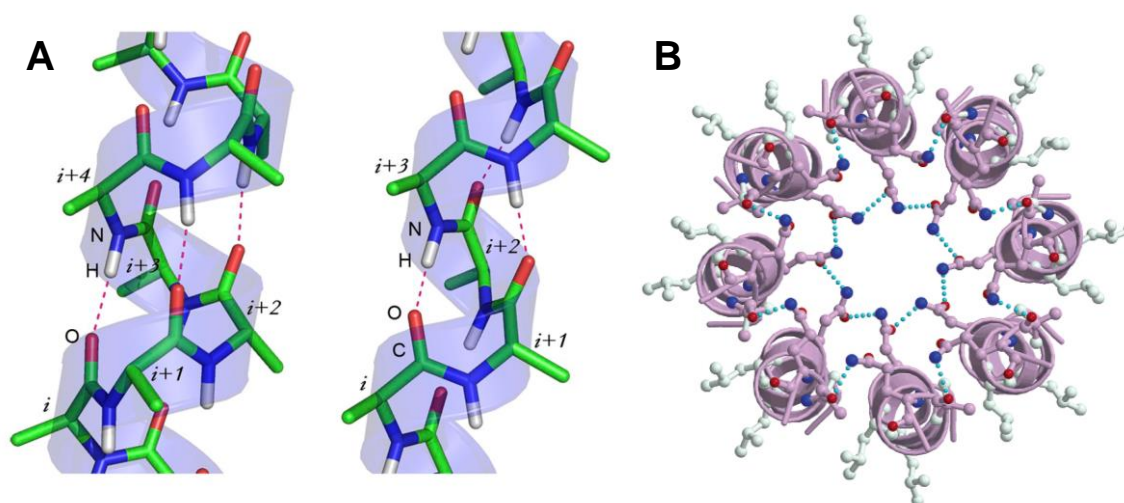
Fig. 2.2. Secondary structures of peptaibols. (A) Structure of α-helical (left) and 3_{10}-helical conformation (right), hydrogen bridge bonds between NH and CO groups are marked by dashed lines (from Vieira-Pires and Morais-Cabral, 2010). (B) Model of an octameric bundle of trichotoxin A50E helices, viewed from top of the *C*-terminus (from Chugh et al., 2002).

The formation of such ion channels in biological membranes cause leakage of cytoplasmic material, leading to cell death (Chugh and Wallace, 2001). Consequently, peptaibols exert a broad spectrum of biological effects including antibiotic (Gräfe et al., 1995; Lee et al., 1999), antiviral (Stadler et al., 2001; Yun et al., 2000), neuroleptic (Kronen et al., 2001; Ritzau et al., 1997), cytotoxic (Ayers et al., 2012; Tavano et al., 2015), antiparasitic (Ayers et al., 2012; Schiell et al., 2001), and antifungal (Berg et al., 1996; Gräfe et al., 1995) activities. In addition, peptaibols are reported as resistance inducers of plants towards phytopathogenic organisms, insects, and nematodes (Jabs et al., 2001).

As peptaibols are peptides, their structural features can be determined in a similar way like peptides by mass spectrometric sequencing. According to the nomenclature by Roepstorff (1984) and Biemann (1992), six diagnostic fragment ion types can be generated by tandem mass spectrometry using collision-induced dissociation (CID) (Degenkolb et al., 2003). The a_n, b_n, and c_n ion series remain their charge at the *N*-terminus, whereas the x_n, y_n, and z_n ions have the charge retained on the *C*-terminal fragment (Fig. 2.3). Low-energy CID, however, commonly produces b_n and y_n type ions as complementary fragments, as the amide bond is the weakest bond (especially for Aib-Pro) within these structures (Sabareesh and Balaram, 2006). Furthermore, v_n (complete side chain loss) and z_n (partial side chain loss) ions are occasionally detected. The y_n series can also be obtained from the negative ion mode that consequently yields negatively charged y_n^- ions (Krause et al., 2006). The mass differences correspond to neutral losses of the respective amino acid residues in their dehydrated forms (see Table B3, Appendix).
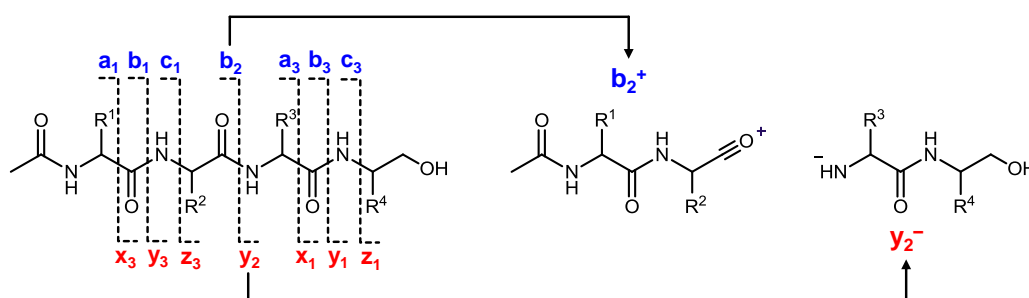
Fig. 2.3. Nomenclature of diagnostic fragment ions in CID tandem mass spectrometry. The x, y, and z ions are *C*-terminal fragments, whereas the a, b, and c ions have the charge retained on the *N*-terminus.

2.1.3 Solid-phase synthesis of peptaibols

Peptaibols can be synthesized *via* classical peptide strategies, either in solution or with solid support. The latter, termed solid-phase peptide synthesis (SPPS), has become the preferred method for the synthesis of small peptides (Hjørringgaard et al., 2009). The synthetic challenges of peptaibols are: (a) efficient coupling of the sterically hindered, poorly reactive α,α-dialkyl amino acids Aib or Iva, especially adjacent Aib-Aib units, (b) lability of the Aib-Pro bond under acidic conditions, and (c) acetylation at the *N*-terminus and incorporation of a *C*-terminal 1,2 amino alcohol. The first difficulty (a) can be overcome by using tetramethylfluoroformamidinium hexafluorophosphate (TFFH) as a coupling reagent, since it is described as especially applicable

for the synthesis of Aib or Iva rich peptaibols (El-Faham and Khattab, 2009). To avoid hydrolytic cleavage of the Aib-Pro bond under acidic conditions, the Boc protection strategy should be omitted, since deprotection must be performed using acids such as TFA. Therefore, the Fmoc strategy was herein applied in which the deprotection is performed under mild basic conditions.

The SPPS of peptaibols follows the cycle illustrated in Fig. 2.4. An amino-protected amino acid is covalently bound to a solid-phase material that is most commonly a polystyrene *resin* cross-linked with 1% divinylbenzene. Then, the Fmoc-protected amino group is deprotected (*deprotection*), the next amino-protected amino acid is reacted with TFFH to form *in situ* an activated acyl fluoride from the carboxylic acid (*activation*), and coupled to the amino group of the resin-bound amino acid (*coupling*). This cycle is repeated until the desired peptide length is achieved. Once all amino acids are coupled to the resin-bound peptide sequence, the *N*-terminus is acetylated using acetanhydride (*acetylation*) followed by final deprotection and *cleavage* from the resin (for details, see Chapters 8 and 9).
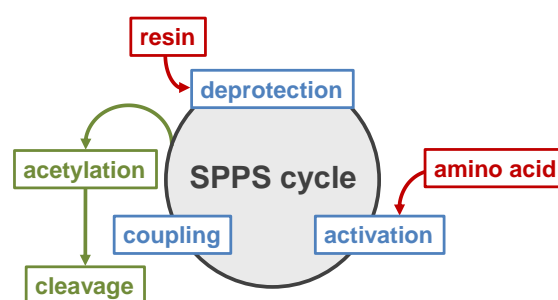
Fig. 2.4. Solid-phase based synthetic cycle of peptaibols (adapted from Kitson, 2014).

2.2   The genus *Hygrophorus* Fr.

2.2.1 Biology and chemistry

In Europe, the genus *Hygrophorus* Fr. (Basidiomycota, Hygrophoraceae) comprises about 60 species (Bon, 1992). The classification on the family level has a complex and controversial history based on different taxonomic approaches. The genus was initially included in the family Hygrophoraceae Lotsy along with genera such as *Hygrocybe* and *Camarophyllus* (Lotsy, 1907). This classification was accepted by several well-known mycologists including Singer (1949), Bresinsky (1967), and Moser (1983) for a long time. In 1990, Cornelis Bas inserted the family Hygrophoraceae as a tribus to Tricholomataceae R. Heim. The recent classification by Lodge et al. (2014) transferred *Hygrophorus* and several other genera back to Hygrophoraceae on the basis of both morphological and phylogenetic studies.

The name *Hygrophorus* (German: Schneckling) originates from the Greek "hygro", meaning moisture, and "phorus" (= bearer), since fruiting bodies of almost all species are particularly characterized by a very slimy to sticky pileus surface. The common English name "waxy caps" reflects the waxy feel or appearance of the lamellae, which are thick, distant, and broadly attached to decurrent. However, the name "waxy cap" is more applicable for the genus *Hygrocybe*, as these basidiocarps actually have waxy caps. The colors of the white-spored *Hygrophorus* fruiting bodies vary from white over yellow-orange-red to (dark) brown, as shown for typical specimens in Fig. 2.5. Species of the genus *Hygrophorus* form obligate ectomycorrhizal symbiosis with deciduous or coniferous trees. Interestingly, field observations revealed that fruiting bodies of

certain *Hygrophorus* species are hardly ever attacked by insect larvae or parasitic fungi (Lübken et al., 2004). The color reaction of the stipe treated with 30% KOH solution is an important taxonomic feature (Lübken et al., 2006). For instance, the stipes of *H. pustulatus*, *H. persoonii*, or *H. agathosmus* turn bright yellow upon application of potassium hydroxide solution. Nevertheless, there is an on-going discussion about the genus, section, and subsection borders.

Fig. 2.5. Selected *Hygrophorus* species. (A) *H. capreolarius*; (B) *H. discoxanthus*; (C) *H. agathosmus*; (D) *H. chrysodon.*

The present classification is based on the systematic and taxonomic approach by Arnolds (1990) in the Flora Agaricina Neerlandica. Arnolds divided the genus *Hygrophorus* into four sections and several subsections primarily based on phenotypic characters like color or viscidity of cap, stipe, and lamellae (Fig. 2.6). Because the Flora Neerlandica considers only 23 species, additional data from Bon (1992) and Lodge (2014) were used to classify the investigated species.
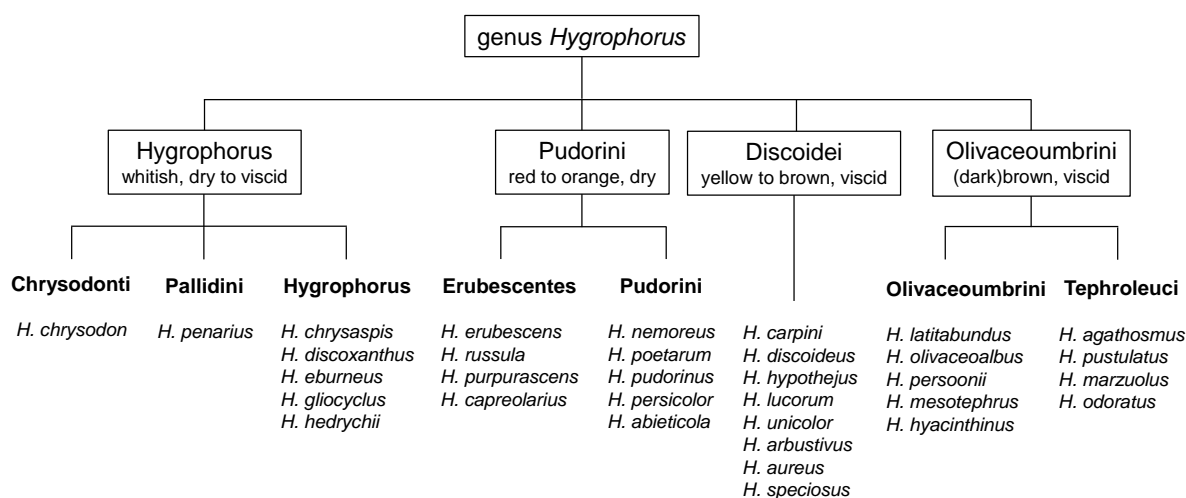
Fig. 2.6. Classification of the genus *Hygrophorus* according to Arnolds (1990), complemented with additional data from Bon (1992) and Lodge (2014).

In one of the first mycochemical studies of *Hygrophorus* spp., Fugmann (1985) isolated the γ-butyrolactone hygrophoric acid (**2.1**) from basidiocarps of *H. lucorum*. Compound **2.1** was further identified in the yellow to orange colored species *H. hypothejus*, *H. aureus*, and *H. speciosus* (all belong to the section Discoidei) (Fugmann, 1985; Gill and Steglich, 1987). Its biosynthesis was proposed by feeding of [α-^{2}H]-caffeic acid to fruiting bodies of *H. lucorum* to start with an enzymatic *ortho* cleavage of caffeic acid and subsequent recyclization to the lactone **2.1** (Gill and Steglich, 1987). In parallel, the dihydroazepin muscaflavin (**2.2**) (main pigment of genus *Hygrocybe*) was detected in basidiocarps of *H. aureus*, *H. hypothejus*, and *H. speciosus* (Fugmann, 1985; Gill and Steglich, 1987) as suggested before by Besl (1975).

Teichert et al. (2008) described the isolation of the β-carboline alkaloids norharmane (**2.3**) and harmane (**2.4**) from basidiocarps of *H. eburneus*. Moreover, *H. hyacinthinus* was found to produce brunnein A (**2.5**) (Teichert et al., 2008), a β-carboline alkaloid that was isolated earlier from fruiting bodies of *Cortinarius brunneus* (Teichert et al., 2007). The occurrence of these β-carboline alkaloids was investigated in 28 species of the genus *Hygrophorus* using LC-MS/MS in the selected reaction monitoring (SRM) mode. While norharmane (**2.3**) and harmane (**2.4**) were found to be ubiquitous in all investigated species, the occurrence of brunnein A (**2.5**) was limited to species of the section Olivaceoumbrini (Teichert et al., 2008). Therefore, brunnein A (**2.5**) was proposed as a chemotaxonomic marker for this section within the genus *Hygrophorus* (Teichert et al., 2008). Furthermore, the ceramide hygrophamide (**2.6**) was isolated and characterized from a Chinese sample of "*H. eburnesus* Fr.*"* (probably *H. eburneus* Fr.) (Qu et al., 2004).
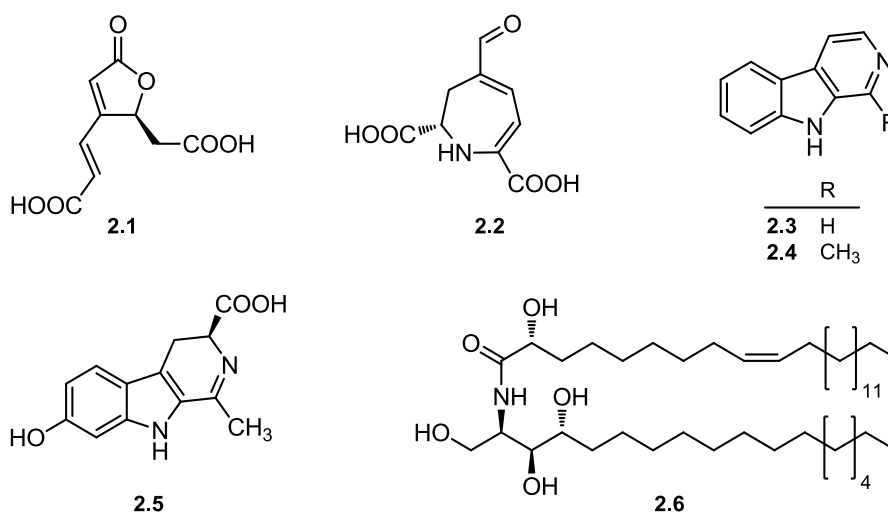
A fungitoxic screening of several *Hygrophorus* spp. extracts revealed activity against the phytopathogenic fungus *Cladosporium cucumerinum* (Teichert et al., 2005a). Subsequently, bioactivity guided isolation yielded eight new fatty acids with a γ-oxocrotonate partial structure (**2.7**–**2.14**) from fruiting bodies of *H. eburneus* (Teichert et al., 2005b). These 4-oxo-2-hexadecenoic and -octadecenoic fatty acids exhibit pronounced biological activity against *C. cucumerinum* and the gram-negative bacterium *Aliivibrio fischeri* (Teichert, 2008). Moreover, compound **2.7** exerts remarkable activity against the oomycete *Phytophthora infestans* (Eschen-Lippold et al., 2009). The antioomycete activity of **2.7** has attracted considerable interest of the

agrochemical industry as a lead structure for the development of new plant protective fungicides (Arnold et al., 2012).
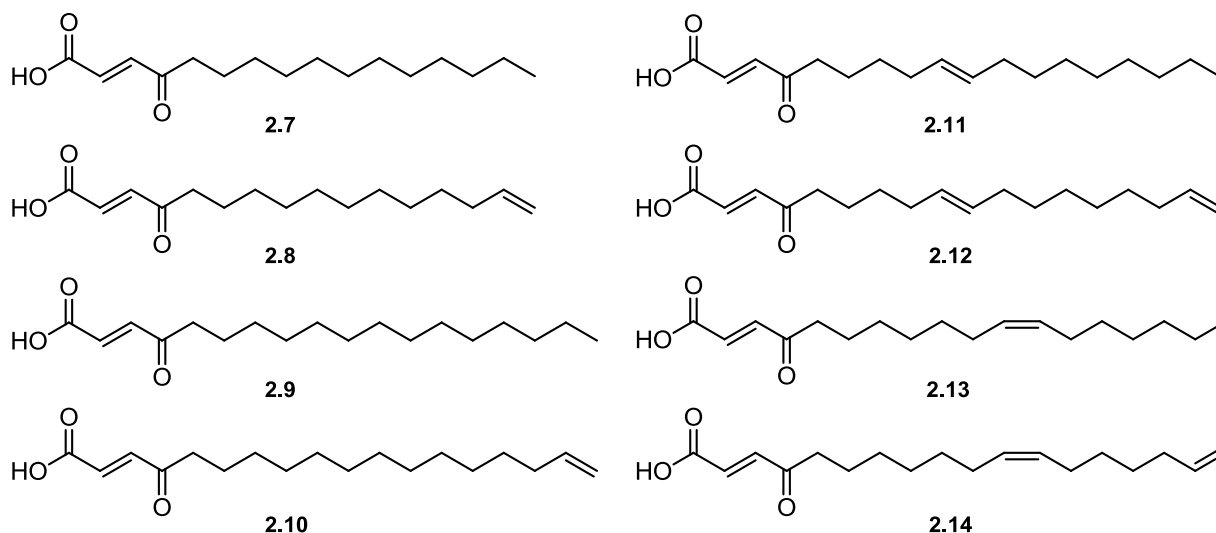
Furthermore, Gilardoni et al. (2006) isolated two 4-oxo-2-alkenoic acid analogues from *H. discoxanthus* with an additional conjugated double bond (**2.15–2.16**) and three oxidized derivatives thereof (**2.17–2.19**) without the α/β-unsaturation. Bioactivity studies revealed that compounds **2.17–2.19** lacking the double bond between position 2 and 3 were devoid of activity against *C. cucumerinum*. Thus, the 2,3-unsaturation seems to be an essential pharmacophoric feature (Teichert, 2008).
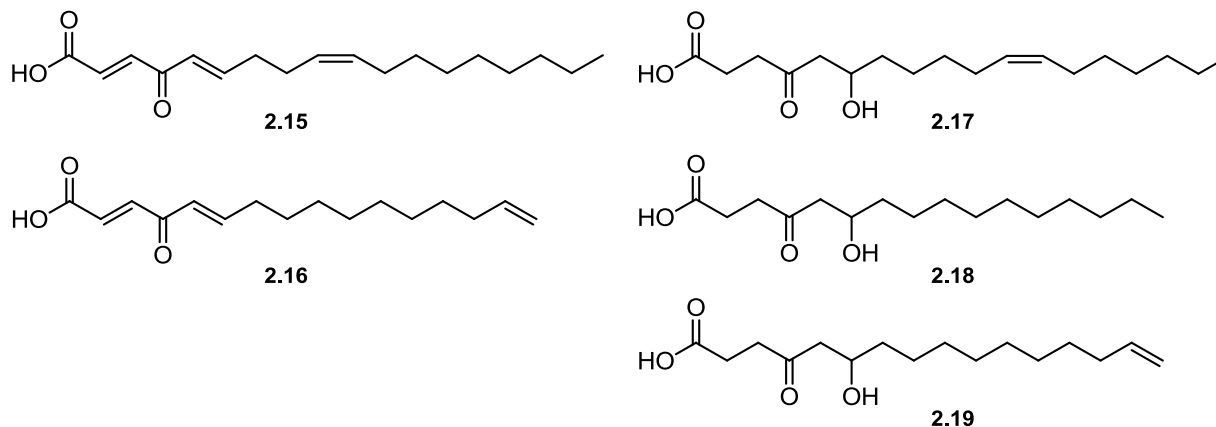
Lübken et al. (2004) isolated 18 novel cyclopentenone derivatives, named hygrophorones A–E (**2.20–2.37**), from fruiting bodies of *H. persoonii*, *H. olivaceoalbus*, *H. pustulatus*, and *H. latitabundus*. Hygrophorones A–D are 2-cyclopentenone derivatives with hydroxyl or acetoxy substituents at C-4 and C-5. An odd numbered alkyl chain ($-C_{11}H_{23}$, $-C_{13}H_{27}$, $-C_{15}H_{31}$, $-C_{17}H_{35}$) is attached to C-5, which is hydroxylated, acetylated, or oxidized to a carbonyl function at C-6. Hygrophorone A- and B-types possess an exocyclic hydroxyl or acetoxy group at C-6, which is oxidized to a carbonyl group in the C and D series. Hygrophorones A and B as well as C and D are diastereomeric pairs: While the endocyclic substituents in hygrophorones A and D possess a *trans* relationship, the B- and C-types are *cis* configured. Hygrophorones of the E series are constitutional isomers of the A/B series, representing a cyclopentene system with an exocyclic

carbonyl function. Additionally, the γ-butyrolactones hygrophorone F[12] (**2.38**) and G[12] (**2.39**) were isolated from basidiocarps of *H. persoonii*.

Hygrophorones exhibit remarkable activity against *C. cucumerinum* and gram-positive bacteria, such as methicillin-resistant *Staphylococcus aureus* (MRSA) and vancomycin-resistant *Enterococcus faecium* (VRE). Among the tested cyclopentenones, 1,4-di-*O*-acetylhygrophorone A[14] (**2.23**) was the most potent compound, exhibiting antibiotic activity comparable to the clinical antibiotics vancomycin, linezolid, and ciprofloxacin. However, hygrophorones are devoid of significant activity against the gram-negative bacteria *Escherichia coli* and *Pseudomonas aeruginosa* (Lübken, 2006).

An ^{1}H NMR based screening of petroleum ether extracts of various *Hygrophorus* spp. revealed the occurrence of hygrophorones additionally in *H. agathosmus*, *H. nemoreus*, *H. discoideus*, and *H. poetarum* (Lübken, 2006). However, a few species, such as *H. abieticola*, were not investigated in these studies. Lübken et al. (2004) postulated that some hygrophorones are responsible for the bright yellow color reaction upon treatment with 30% KOH solution. However, the molecular mechanism of the color reaction remains still unknown. Teichert (2008) suggested that γ-oxocrotonate fatty acids might be biosynthetic precursors of hygrophorones (for details, see Chapter 4).
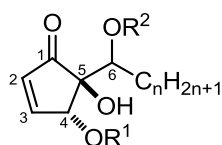
hygrophorone A
(*H. persoonii*)

	R[1]	R[2]	n
2.20	Ac	Ac	12
2.21	Ac	H	12
2.22	H	Ac	12
2.23	Ac	Ac	14
2.24	Ac	H	14
2.25	H	Ac	14
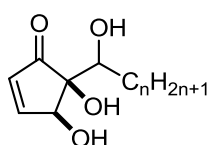
hygrophorone B
(*H. olivaceoalbus*)

	n
2.26	14
2.27	16
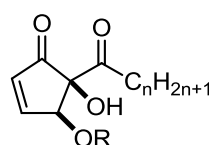
hygrophorone C
(*H. pustulatus*)

	R	n
2.28	Ac	12
2.29	H	12
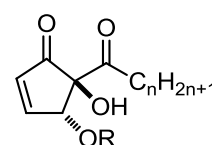
hygrophorone D
(*H. latitabundus*)

	R	n
2.30	Ac	12
2.31	H	12
2.32	Ac	14
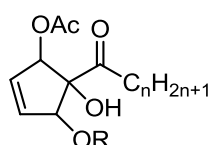
hygrophorone E
(*H. latitabundus*)

	R	n
2.33	Ac	10
2.34	Ac	12
2.35	Ac	14
2.36	H	10
2.37	H	12
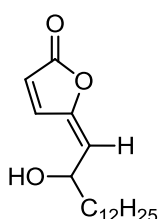
hygrophorone F[12]
(*H. persoonii*)

2.38
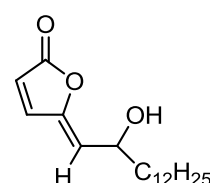
hygrophorone G[12]
(*H. persoonii*)

2.39

In addition, two 2-acylcyclopentene-1,3-dione derivatives, named chrysotriones A (**2.40**) and B (**2.41**), were obtained from fruiting bodies of *H. chrysodon* (Gilardoni et al., 2007). Chrysotriones are structurally related to hygrophorones and can be supposed as oxidation products

thereof (Teichert, 2008). Chrysotrione A (**2.40**) holds a terminal vinyl group at the alkyl side chain, a structural feature that has not been observed in hygrophorones yet. Compounds **2.40** and **2.41** exhibit moderate activity against the phytopathogenic fungus *Fusarium verticillioides* (Gilardoni et al., 2007).
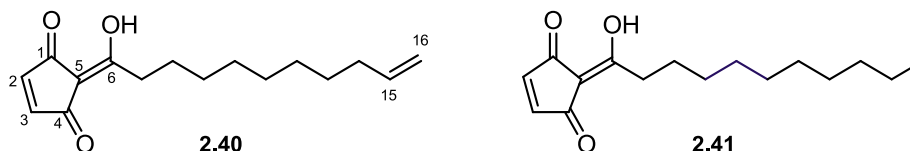
2.2.2 *Hygrophorus abieticola* Krieglst. ex Gröger & Bresinsky

Fruiting bodies of *Hygrophorus abieticola* Krieglsteiner ex Gröger & Bresinsky (German: Weißtannenschneckling) usually grow in clusters under *Abies alba* (silver fir) mainly on calcareous soils (Fig. 2.7A) (Bresinsky, 2008). The yellow to orange colored cap is 5–15 cm in diameter and sticky to viscid in humid environments. The white to yellow-orange stipe is 5–10 cm long and 0.8–2.5 cm thick. The very distant, subdecurrent to adnate, thick lamellae are initially white becoming salmoneous in age. Although considered edible, the resin to turpentine-like taste and smell makes this mushroom not very delicate. Treating the flesh with 30% KOH solution causes no color reaction, whereas the cortex immediately turns bright yellow (Fig. 2.7B). (Krieglsteiner and Gminder, 2001)
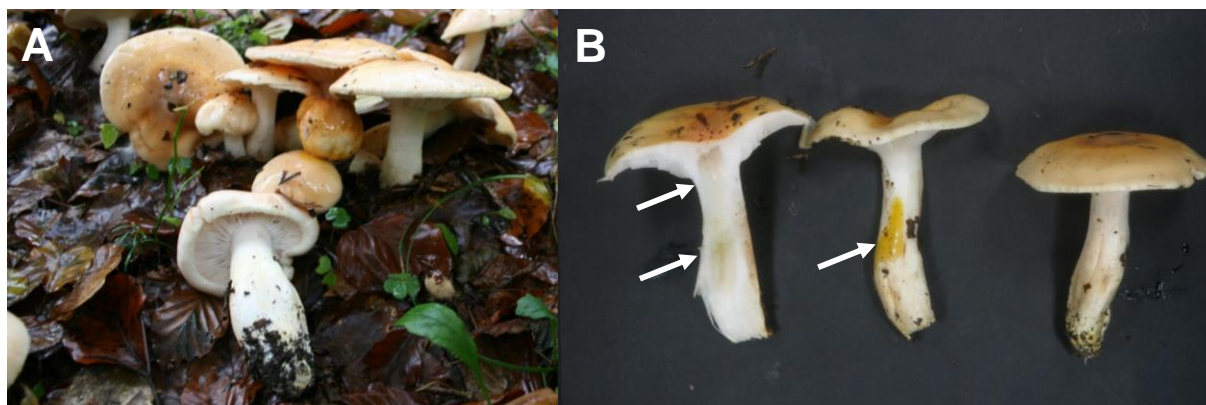
Fig. 2.7. *Hygrophorus abieticola* Krieglst. ex Gröger & Bresinsky – (A) basidiocarps in Paintner Forst near Regensburg; (B) the flesh (left basidiocarp) shows no color reaction after treatment with 30% KOH solution, whereas the cortex turns bright yellow.

The *A. alba* associated *H. abieticola* was separated by Bresinsky (2008) from the strongly related species *H. pudorinus* (Fr.) Fr. The habitat of the latter species was described by Elias Fries (1874) as "in silvis abiegnis montanis" which means, according to Bresinsky (2008), that this species is rather connected to *Picea abies* instead of *Abies alba* (since the silver fir is not present in Sweden at all). Therefore, many collections in herbaria should be reinvestigated and renamed according to their specific mycorrhiza partners.

Larsson and Jacobsson (2014) recently discussed that *H. persicolor* Ricek growing widespread in Sweden in association with *Picea abies* (Hansen and Knudsen, 1992; Ricek, 1974) may be the

species Fries had in mind when he described *H. pudorinus*. Based on ITS sequencing, Lodge et al. (2014) postulated that the type species of *H. pudorinus* Fr. matches that of *H. persicolor* Ricek[1]. Consequently, *H. pudorinus* should be the valid name for the *Picea abies* associated species, while *H. persicolor* is a later synonym (Larsson and Jacobsson, 2014).

2.2.3 *Hygrophorus penarius* Fr.

Fruiting bodies of *Hygrophorus penarius* Fr. (German: Trockener Schneckling) grow solitary or subgregarious in frondose forests mainly on calcareous soils and form ectomycorrhizae with *Quercus* or *Fagus* (Fig. 2.8A). The whitish basidiocarp is 3.5–9 cm in diameter and subviscid but soon dry. The white to ochraceous, dry stipe is 2.8–6 cm long and 0.9–2 cm thick. The subdistant to distant, subdecurrent lamellae are pinkish white. Treatment of the cortex at the stipe base with 30% KOH solution leads to a yellow to orange discoloration (Fig. 2.8B) (Arnolds, 1990).

Although specimens connected either to *Fagus* or to *Quercus* have slight morphological differences, both were interpreted as *H. penarius*. Based on ITS sequencing, Jacobsson and Larsson recently demonstrated that both ecotypes are distinct species. For that reason, the *Quercus* form was described as the new species *Hygrophorus penaroides* Jacobsson & E. Larss. (Jacobsson and Larsson, 2007). The fungal material investigated herein was associated to *Fagus* and therefore assigned as *H. penarius*.

Fig. 2.8. *Hygrophorus penarius* Fr. – (A) basidiocarps in Sperlingsholz near Naumburg (photo: Wolfgang Huth); (B) the stipe of the right fruiting body was treated with 30% KOH solution.

2.3 The genus *Sepedonium* Link

2.3.1 Biology and chemistry

The genus *Sepedonium* Link (Ascomycota, Hypocreaceae) represents the asexual stage (anamorph) of the sexual stage (teleomorph) genus *Hypomyces* (older synonym *Hypocrea*). The sexual ascospores producing perithecia, however, are extremely rarely observed (Sahr et al., 1999). The genus *Sepedonium* comprises mycophilic species, which are parasites on

---

[1] The investigations of Lodge et al. (2014) are doubtful, because the investigated *H. pudorinus* specimens are **not** type material, since they are originated from Canada and USA, respectively.

basidiomycetous fungi of the Boletales sensu lato. The preferred hosts are mushrooms belonging to the genera *Boletus*, *Xerocomus*, and *Paxillus* (Neuhof et al., 2007). The genus also includes highly specialized mycoparasites such as *S. chalcipori* that was hitherto exclusively isolated from the Pepper bolete *Chalciporus piperatus* (Helfer, 1991). *Sepedonium* species live pertophytic, i.e. the infection of the living host results in total necrosis of the mushroom tissue. The dead organic material is then used for their own nutrition (Quang et al., 2010).

Sepedonium species produce two types of asexual spores: On the one hand, hyaline thin-walled phialoconidia are produced directly after infection to maintain a fast reproduction of the organism (Fig. 2.9A). On the other hand, thick-walled, warty ornamented, and often gold-yellow colored aleurioconidia (chlamydospores) are formed in a later infection stage (Fig. 2.9B) (Sahr et al., 1999). The yellow color of the cultures that is causal for the common German name "Goldschimmel" might correspond to the production of the reported (bis)anthraquinones, isoquinoline alkaloids, and tropolones (Neuhof et al., 2007; Quang et al., 2010). It has been shown that aleurioconidia are frost-resistant and therefore may serve as a winter survival form, whereas phialoconidia have been destroyed at –20 °C (Helfer, 1991). In the past, species with yellow, warty aleurioconidia were described as *S. chrysospermum* (Sahr et al., 1999). A modern infrageneric classification of *Sepedonium* has been developed by Rogerson and Samuels (1989) which revealed that *S. chrysospermum* sensu lato was identified as a collective species. Consequently, *S. ampullosporum* (Damon, 1952), *S. chalcipori* (Helfer, 1991), and *S. microspermum* (Besl et al., 1998) were separated from *S. chrysospermum* by morphological and host specificity aspects. In addition, *S. laevigatum* was described as a new species on the basis of phylogenetic analyses (Sahr et al., 1999).

Fig. 2.9. *Sepedonium* infection of *Paxillus involutus* in nature. (A) Early stage infection; the fruiting bodies are partially covered by a white mycelium; (B) late stage infection; the basidiocarps are covered by a gold-yellow mycelium, arising from the production of aleurioconidia (photos: Dr. Norbert Arnold).

Several mycochemical studies of *Sepedonium* species have been performed, many of which were connected to peptaibiotics research (for sequences, see Table B1, Appendix). For instance, the 5-residue peptaibol peptaibolin (**2.42**) was isolated from *Sepedonium* sp. HKI-0117 and *S. ampullosporum* HKI-0053. Compound **2.42** exhibits moderate activity against the gram-

positive bacterium *Bacillus subtilis* and the yeast *Candida albicans* (Hülsmann et al., 1998). Moreover, the strain HKI-0053 also produces a series of 15-mer peptaibols named ampullosporins A–E4 (**2.43**–**2.50**) (Kronen et al., 2001; Ritzau et al., 1997). Ampullosporins A–D (**2.43**–**2.46**) exhibit neuroleptic activity in mice and induce pigment formation of *Phoma destructiva* in a similar way as the immunosuppressant drug cyclosporine A (**1.6**) (Kronen et al., 2001; Ritzau et al., 1997).

The peptaibol chrysaibol (**2.51**) was derived from a New Zealand isolate of *S. chrysospermum* (Mitova et al., 2008). Constituent **2.51** show cytotoxic activity against the P388 murine leukemia cell line as well as antibiotic activity against *B. subtilis*. The 19-residue chrysospermins A–D (**2.52**–**2.55**) isolated from a German *S. chrysospermum* strain also induce pigment formation of *Phoma destructiva* and exhibit antibiotic activity against the gram-positive bacterium *S. aureus* and *B. subtilis* (Dornberger et al., 1995). Furthermore, constituents **2.52**–**2.55** have been patented as nematicidal and anthelminthic agents (Metzger et al., 1994).

Solid-state cultivation of *S. chalcipori* S33 yielded the 15-mer tylopeptins A (**2.56**) and B (**2.57**), which were first described from the putatively contaminated basidiomycete *Tylopilus neofelleus* (Lee et al., 1999; Neuhof et al., 2007). Moreover, two peptaibols, chalciporin A (**2.58**) and B (**2.59**), were isolated and characterized from the strain S33 of *S. chalcipori* (Neuhof et al., 2007). Stadler et al. (2001) isolated eight linear 19-residue peptaibols from *S. microspermum*, named microspermins A–H (**2.60**–**2.67**), which are potent inhibitors of the herpes simplex virus type 1 (HSV-1).

Besides peptaibols, further secondary metabolite classes from *Sepedonium* spp. were reported in the literature. Already in 1965, the yellow tropolone pigments sepedonin (**2.68**) and anhydrosepedonin (**2.69**) were obtained from the culture filtrate of *S. chrysospermum* s.l. (Divekar and Vining, 1964; Divekar et al., 1965). Quang et al. (2010) detected **2.68** and **2.69** in strains of all *Sepedonium* species except *S. brunneum*, *S. chlorinum*, and *S. tulasneanum*. Sepedonin (**2.68**) inhibited the growth of various gram-negative and gram-positive bacteria as well as yeasts and molds (Nagao et al., 2006). Anhydrosepedonin (**2.69**) exhibits antifungal activity against *C. cucumerinum* (Quang et al., 2010).
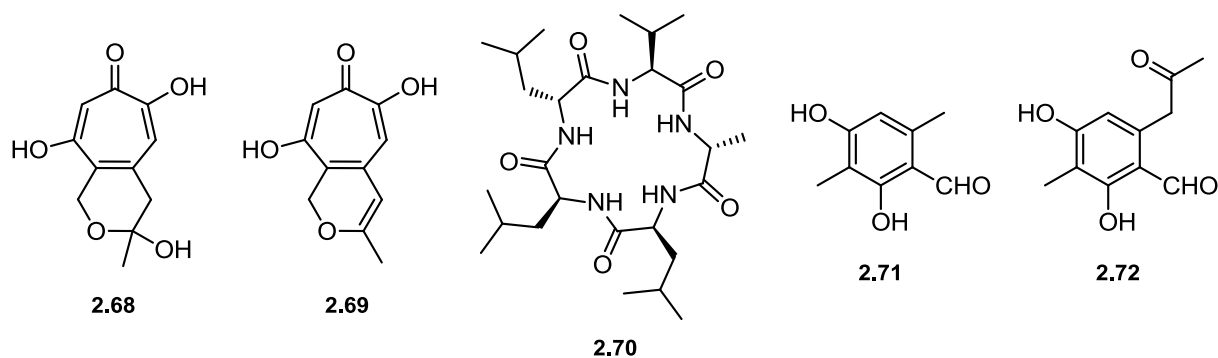
The cyclic pentapeptide chrysosporide (**2.70**) was isolated from a New Zealand strain of *S. chrysospermum* accompanied by 3,6-dimethyl-β-resorcylaldehyde (**2.71**) and 2,4-dihydroxy-3-methyl-6-(2-oxopropyl)benzaldehyde (**2.72**) (Mitova et al., 2006).

The yellow to orange colored (bis)anthraquinone pigments rugulosin (**2.73**), chrysophanol (**2.74**), and skyrin (**2.75**) were obtained from *S. ampullosporum* (Shibata et al., 1957). Metabolite **2.73** is especially active against gram-positive bacteria including methicillin-resistant *S. aureus* (MRSA) (Breen et al., 1955; Yamazaki et al., 2010).

2.73

2.74

2.75
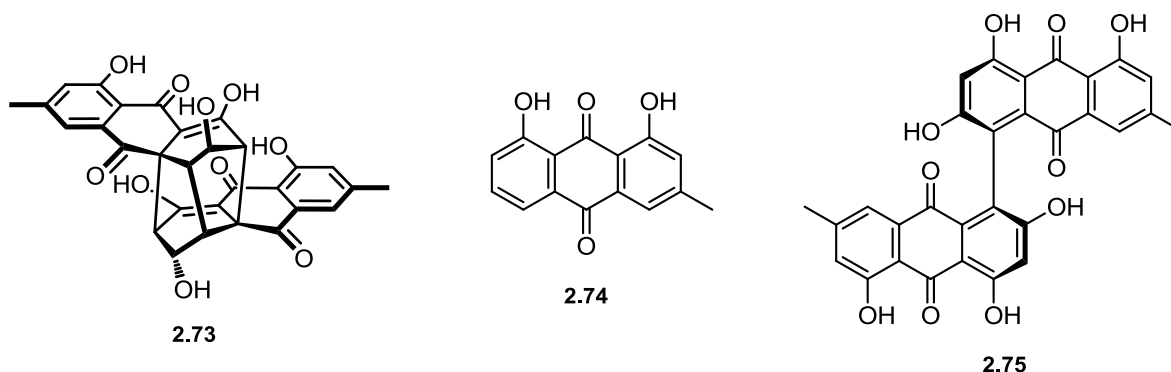
The azaphilone derivative chrysodin (**2.76**) was obtained from *S. chrysospermum* (Closse and Hauser, 1973) and exhibits activity against the yeast *C. albicans* and filamentous fungi such as *Aspergillus niger*, but was devoid of significant effects towards bacteria (Haraguchi et al., 1990). The diterpene compactin (**2.77**), also known as mevastatin, was detected in a strain of *Hypomyces chrysospermus* IFO 7798 (Endo et al., 1986), as isolated earlier from cultures of *Penicillium* spp. (Brown et al., 1976; Endo et al., 1976). Compound **2.77** is a specific, competitive inhibitor of the HMG-CoA reductase (Endo, 1985) (for details, see Chapter 1).

Recently, the yellow isoquinoline alkaloid ampullosine (**2.78**) could be isolated from the culture broth of *S. ampullosporum* (Quang et al., 2010). An LC-MS based screening in the selected reaction monitoring (SRM) mode of different *Sepedonium* spp. demonstrated that **2.78** is produced by almost all species except the phylogenetically more distant species *S. brunneum* and *S. tulasneanum* (Quang et al., 2010). Quang et al. concluded that **2.78** is responsible for the deep yellow color of the *Sepedonium* culture filtrates.

2.76

2.77

2.78
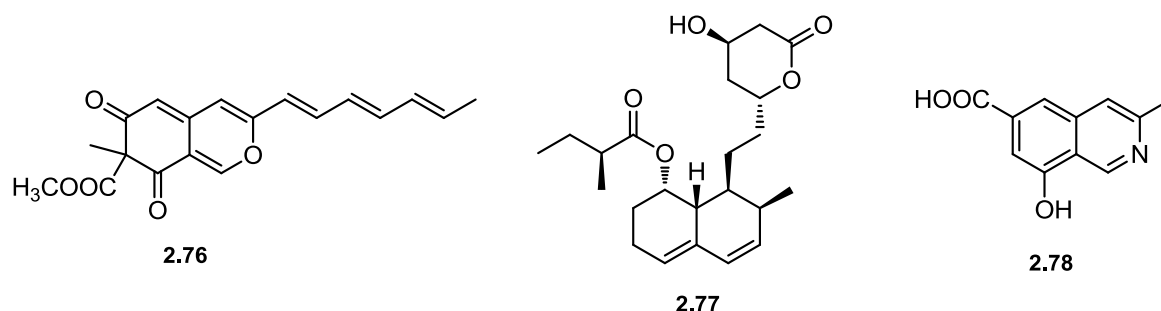
2.3.2 *Sepedonium* strain KSH 883

The Southern Hemisphere offers endemic ectomycorrhiza forming trees from the genus *Nothofagus* (Nothofagaceae), also known as southern beeches. The current distribution pattern of *Nothofagus* spp. in South America, Eastern Australia, New Zealand, and New Guinea indicates that *Nothofagus* existed prior to the break-up of the supercontinent Gondwana, when Antarctica,

Australasia, and South America were connected (Swenson et al., 2001; Zhang, 2011). The ectomycorrhizal associations with *Nothofagus* spp. led to a highly diverse fungal community that is very different from the European one (Garrido, 1988; Horak, 1967; Moser and Horak, 1975; Singer and Digilio, 1952). Several *Nothofagus* associated mushrooms from the order Boletales are commonly colonized by members of the genus *Sepedonium* such as *Boletus loyo* Philippi, *Boletus loyita* Horak, *Paxillus boletinoides* Singer, or *Paxillus statuum* (Speg.) E. Horak (personal observation). During field trips in Chile, the *Sepedonium* strain KSH 883 was isolated from infected fruiting bodies of the endemic mushroom *B. loyo* Phillippi (Boletaceae) (Fig. 2.10).

Fig. 2.10. Occurrence of *Sepedonium* spp. in Chile. (A) Uninfected host mushroom *Boletus loyo*; (B) *B. loyo* colonized by *Sepedonium* strain KSH 883 (photos: Dr. Norbert Arnold).

The fast growing culture of strain KSH 883 produces after about one week yellow, globose aleurioconidia, leading to a brightly yellow color that spreads over the colony (Fig. 2.11A). Initial morphological analyses including scanning electron microscopy of the characteristic aleurioconidia (Fig. 2.11B–D) demonstrated that this strain belongs to the genus *Sepedonium*. Interestingly, the shape and ornamentation of the chlamydospores resembles that of the European species *S. chalcipori* (Jasminovic, 1999). Its phylogenetic position was thus investigated in a polythetic approach based on molecular, chemical, and biological data (for details, see Chapter 8).
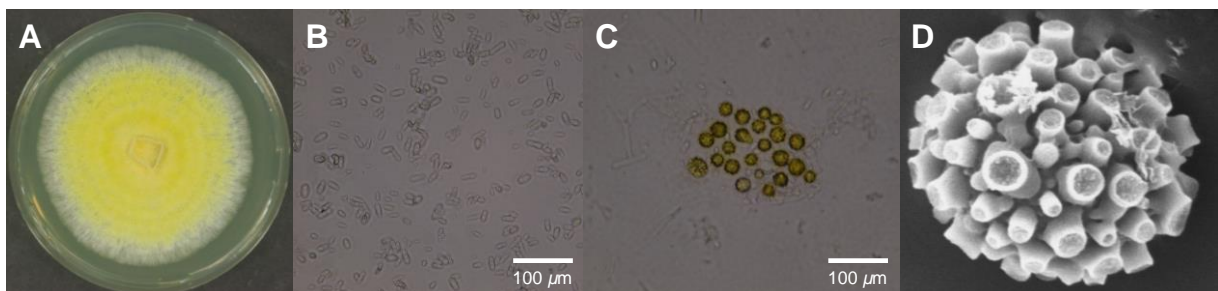
Fig. 2.11. Initial morphological analyses of *Sepedonium* sp. KSH 883. (A) Two week old culture grown on malt peptone agar; (B) hyaline phialoconidia; (C) yellow, globose aleurioconidia; (D) scanning electron micrograph of an aleurioconidium (5000x, photo: Dr. Norbert Arnold/Günter Kolb).

2.3.3 *Sepedonium tulasneanum* (Plowr.) Sacc.

Sepedonium tulasneanum (Plowr.) Sacc. (anamorph: *Hypomyces tulasneanus* Plowr.) was described more than 100 years ago (Saccardo, 1883). The investigated strain KSH 535 was isolated from the Lurid bolete *Boletus luridus*, a common host of this species (Eholzer, 1999). The fast growing culture of strain KSH 535 remains with a flat, white to ochraceous colored mycelium due to the production of hyaline, oval- to lemon-shaped aleurioconidia (Fig. 2.12). Because of these characteristic chlamydospores, *S. tulasneanum* was never confused with yellow colored round-shaped aleurioconidia producing species like *S. chrysospermum* (Sahr et al., 1999).
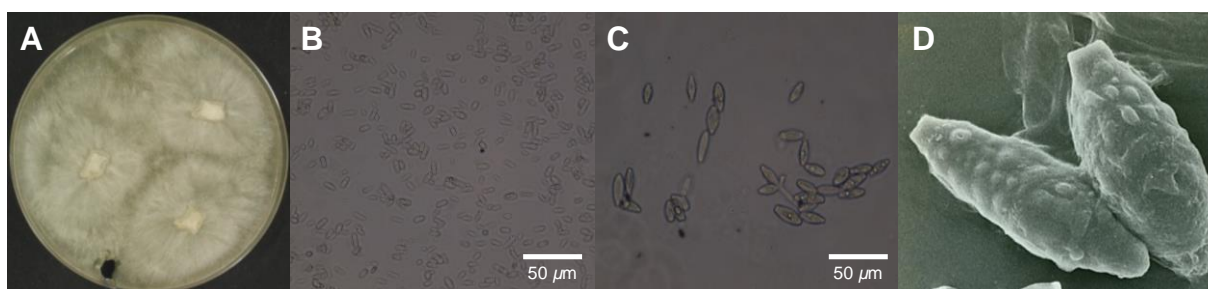
Fig. 2.12. Morphological analyses of *Sepedonium tulasneanum* KSH 535. (A) Three week old culture grown on malt peptone agar; (B) hyaline phialoconidia; (C) hyaline, oval- to lemon-shaped aleurioconidia; (D) scanning electron micrograph of aleurioconidia (3272x, photo from Eholzer, 1999).

2.4   The genus *Gliocladium* Corda

2.4.1 Biology and chemistry

The hyphomycete genus *Gliocladium* Corda (Ascomycota, Hypocreaceae) includes filamentous fungi naturally occurring in soil and plant remains (Domsch et al., 2007). While most of them occur as widespread molds, certain *Gliocladium* species, however, are reported as parasites on fungi and slime molds such as *G. catenulatum* or *G. album* (Helfer, 1991). The strain J1446 of *G. catenulatum* is a commercial biological control agent (BCA) marketed under the name "Prestop Mix" (Verdera, Finland), that exerts a broad spectrum activity against *Fusarium culmorum* on cereals, *Botrytis cinerea*, and *Pythium ultimum* (Lahdenperä, 2006; Mcquilken et al., 2001; Teperi et al., 1998). Colonies of this genus typically grow fast and are characterized by the production of asexual, one-celled hyaline to green pigmented, slimy conidia in conidiophores with phialides (Domsch et al., 2007). As the conidiophores often show penicillate and verticillate branching, *Gliocladium* spp. may be confused with *Penicillium, Verticillium* or *Trichoderma* species (Domsch et al., 2007; Petch, 1939).

The genus *Gliocladium* is known for their production of bioactive and chemically diverse secondary metabolites. For instance, the 16-mer peptaibols antiamoebin I, III, VI, VIII, IX, and XI (**2.79**–**2.84**) were detected in a strain of *G. catenulatum* CBS 511.66 (Jaworski and Brückner, 2000), and the eicosapeptide gliodeliquescin A (**2.85**) was identified in *G. deliquescens* NRRL 3091 (for sequences, see Table B2, Appendix) (Brückner and Przybylski, 1984).

The polyketide glycosides roselipins 1A, 1B, 2A, and 2B (**2.86–2.89**) were obtained from the culture broth of *G. roseum* KF-1040, and identified as selective inhibitors of the diacylglycerol transferase (DGAT), a target for the treatment of obesity (Tomoda et al., 1999).

	R¹ (OH OH, OH)	R²		R¹ (OH OH, OH)	R²
2.86		H	2.88		COCH₃
2.87		H	2.89		COCH₃
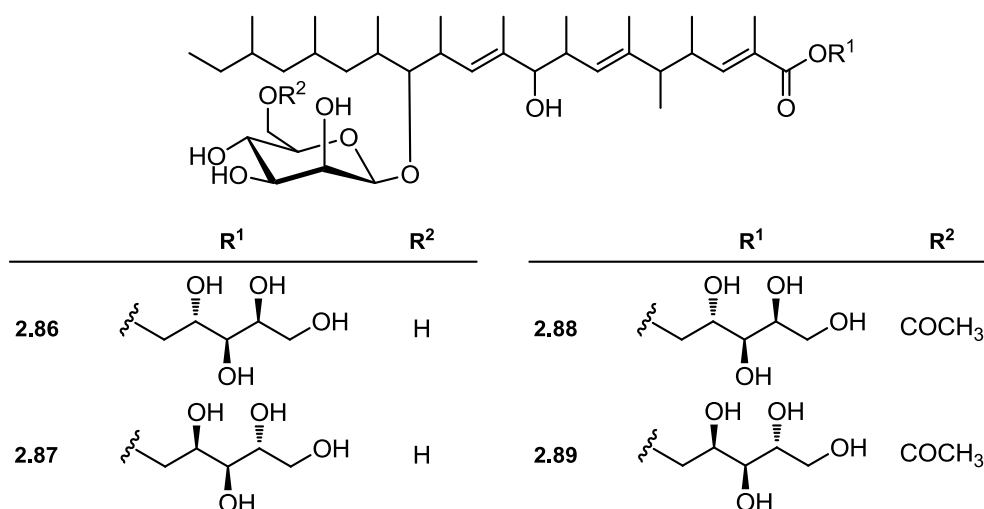
Gliocladium species also produce thiolated and non-thiolated verticillin-type di- and tri-ketopiperazins. For instance, the nematicidal diketopiperazines Sch 52900 (**2.90**) and Sch 52901 (**2.91**) are produced by strains of *Gliocladium* sp. and *G. roseum* 1A (Chu et al., 1995; Dong et al., 2005). The epidithiodiketopiperazines gliocladin A (**2.92**) and B (**2.93**), the atypical non-thiolated triketopiperazine gliocladin C (**2.94**), and the dioxopiperazine glioperazine (**2.95**) were isolated from a strain of *G. roseum* OUPS-N132 (Usami et al., 2004). Gliocladins A–C (**2.92–2.94**) exert significant cytotoxic activity against the lymphocytic leukemia cell line P388 (Usami et al., 2004).

	R
gliocladin A (**2.92**)	OH
gliocladin B (**2.93**)	H

gliocladin C (**2.94**)

	R	x
Sch 52900 (**2.90**)	CH(OH)CH₃	2
Sch 52901 (**2.91**)	CH₂CH₃	2
verticillin A (**2.97**)	CH₃	2
gliocladine A (**2.98**)	CH₃	3
gliocladine B (**2.99**)	CH₃	4

glioperazine (**2.95**)

	R	x
glioclatine (**2.96**)	H	2
gliocladine C (**2.100**)	OH	2
gliocladine D (**2.101**)	OH	3
gliocladine E (**2.102**)	OH	4

3,3'-biindole (**2.103**)
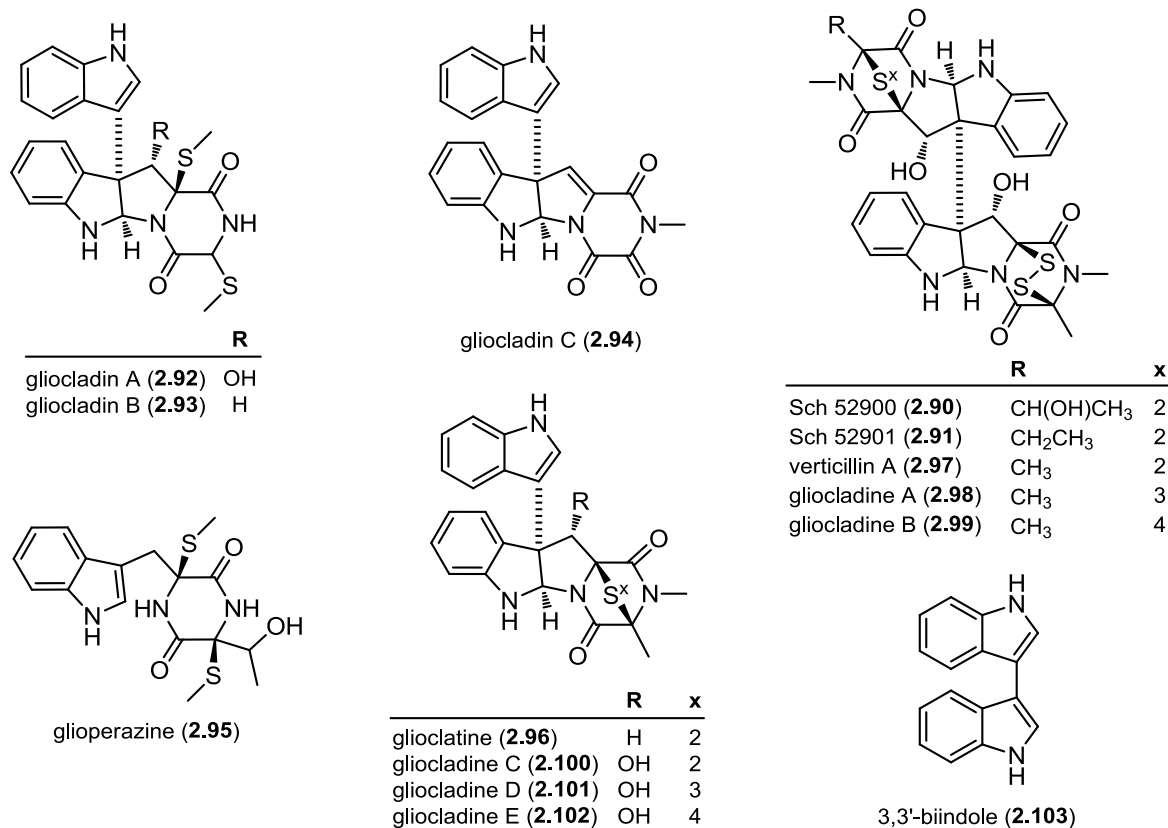
The epidithiodioxopiperazine glioclatine (**2.96**) was obtained from *G. roseum* YMF1.00133 (Dong et al., 2006). Additionally, verticillin A (**2.97**) and gliocladines A–E (**2.98–2.102**) – not to be confused with gliocladins A–C (**2.92–2.94**) – are produced by *G. roseum* 1A (Dong et al., 2005). Gliocladines A (**2.98**) and B (**2.99**) are the penta- and hexasulfide analogues of verticillin A (**2.97**), while gliocladines C–E (**2.100–2.102**) are monomeric piperazines with an indole moiety (Dong et al., 2005). Compounds **2.98–2.102** exert nematicidal activity against *Caenorhabditis elegans* and *Panagrellus redivivus* (Dong et al., 2005). Moreover, Bertinetti reported the isolation of 3,3'-biindole (**2.103**) from *G. catenulatum* BAFC 3584, which may be the biogenetic precursor of the complex functionalized ketopiperazins described above (Bertinetti et al., 2010).

The nonaprenols glisoprenin A (**2.104**) and B (**2.105**) were isolated from *Gliocladium* spec. FO-1513 (Nishida et al., 1992). Compounds **2.104** and **2.105** are potent inhibitors of the acyl-CoA cholesterol acyl transferase (ACAT), a target for the treatment of atherosclerosis (Chang et al., 2009; Nishida et al., 1992). In addition, glisoprenins C, D, and E (**2.106–2.108**) were isolated from submerged cultures of *G. roseum* HA 190-95 and identified as inhibitors of appressorium formation in *Magnaporthe grisea* (Thines et al., 1998).

glisoprenin A (**2.104**)

glisoprenin B (**2.105**)

glisoprenin C (**2.106**)

glisoprenin D (**2.107**)

glisoprenin E (**2.108**)
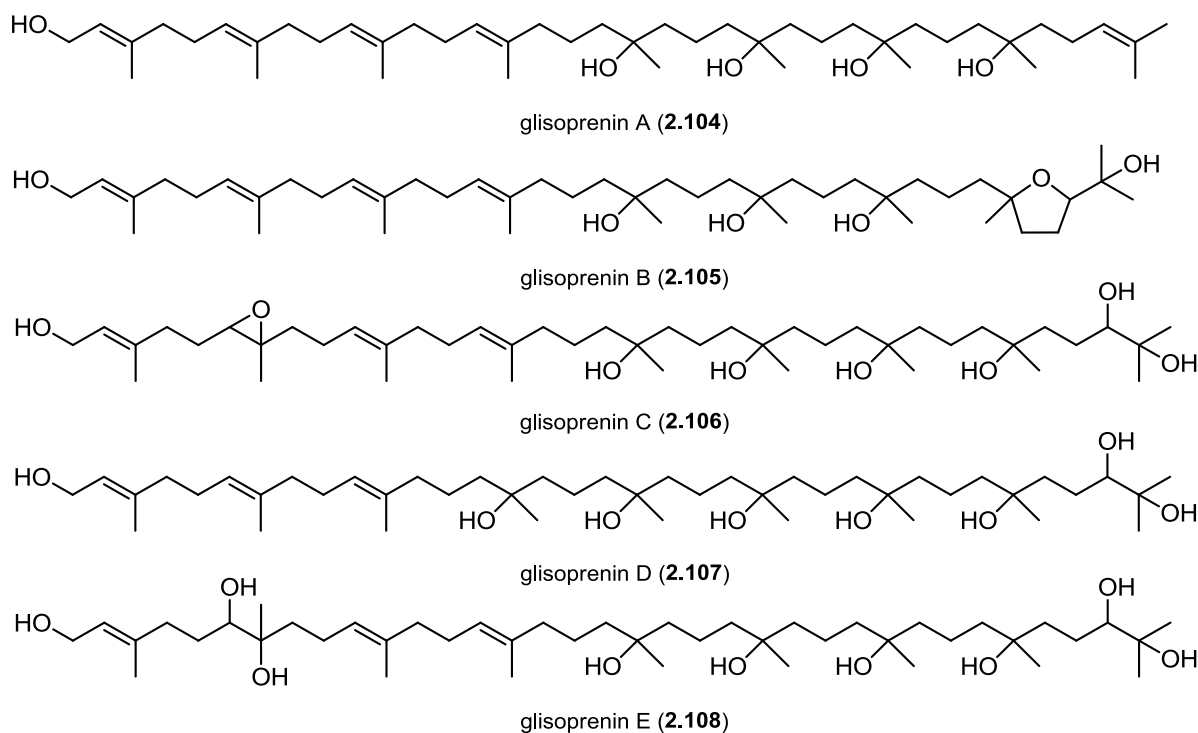
2.4.2 *Gliocladium album* (Preuss) Petch

Gliocladium album (Preuss) Petch parasitizes exclusively on slime molds (Myxomycetes), thus the culture habitat resembles that of *Verticillium rexianum* (Helfer, 1991). The herein investigated strain KSH 719 was isolated from the myxomycete *Fuligo septica*. The strain produces a fast growing culture with a flat, white to cream-colored mycelium and hyaline conidia. According to Petch (1939), this species is separated from *G. penicillioides* by its divergent and more opulent conidiophore branching.

2.5 References

Aravinda, S., Shamala, N., Balaram, P., 2008. Aib residues in peptaibiotics and synthetic sequences: Analysis of nonhelical conformations. *Chem. Biodivers.* 5, 1238–1262.

Arnold, N., Rosahl, S., Westermann, B., Wessjohann, L., Eschen-Lippold, L., Dräger, T., 2012. Antioomycotica. Europäisches Patent, EP2434878 B1.

Arnolds, E., 1990. Tribus Hygrophoraceae (Kühner) Bas et Arnolds, in: Bas, C., Kuyper, T.W., Noordeloos, M.E., Vellinga, E.C. (Eds.), Flora Agaricina Neerlandica. A. A. Balkema, Rotterdam, pp. 115–133.

Ayers, S., Ehrmann, B.M., Adcock, A.F., Kroll, D.J., Carcache de Blanco, E.J., Shen, Q., Swanson, S.M., Falkinham, J.O., Wani, M.C., Mitchell, S.M., Pearce, C.J., Oberlies, N.H., 2012. Peptaibols from two unidentified fungi of the order Hypocreales with cytotoxic, antibiotic, and anthelmintic activities. *J. Pept. Sci.* 18, 500–510.

Bas, C., 1990. Tricholomataceae R. Heim ex Pouz, in: Bas, C., Kuyper, T.W., Noordeloos, M.E., Vellinga, E.C. (Eds.), Flora Agaricina Neerlandica. A. A. Balkema, Rotterdam, pp. 65–70.

Berg, A., Ritzau, M., Ihn, W., Schlegel, B., Fleck, W.F., Heinze, S., Gräfe, U., 1996. Isolation and structure of bergofungin, a new antifungal peptaibol from *Emericellopsis donezkii* HKI 0059. *J. Antibiot.* 49, 817–820.

Bertinetti, B.V, Rodriguez, M.A., Godeas, A.M., Cabrera, G.M., 2010. 1H,1'H-[3,3']biindolyl from the terrestrial fungus *Gliocladium catenulatum*. *J. Antibiot.* 63, 681–683.

Besl, H., Bresinsky, A., Kronawitter, I., 1975. Notizen über Vorkommen und systematische Bewertung von Pigmenten in Höheren Pilzen (1). *Z. Pilzkd.* 41, 81–98.

Besl, H., Hagn, A., Jobst, A., Lange, U., 1998. Der kleinsporige Goldschimmel, *Sepedonium microspermum* – ein Parasit an Röhrlingen der *Xerocomus-chrysenteron*-Gruppe. *Z. Mykol.* 64, 45–52.

Biemann, K., 1992. Mass spectrometry of peptides and proteins. *Annu. Rev. Biochem.* 61, 977–1010.

Bon, M., 1992. Die Grosspilzflora von Europa: Hygrophoraceae. IHW-Verlag, Eching, pp. 1–91.

Breen, J., Dacre, J.C., Raistrick, H., Smith, G., 1955. Studies in the biochemistry of microorganisms. 95. Rugulosin, a crystalline colouring matter of *Penicillium rugulosum* Thom. *Biochem. J.* 60, 618–626.

Bresinsky, A., Huber, J., 1967. Schlüssel für die Gattung "*Hygrophorus*" (Agaricales) nach Exsikkatenmaterial. *Nov. Hedwigia* 14, 143–185.

Bresinsky, A., 2008. Beiträge zu einer Mykoflora Deutschlands (2): Die Gattungen *Hydropus* bis *Hypsizygus* mit Angaben zur Ökologie und Verbreitung der Arten. *Regensburg. Mykol. Schriften* 15, 1–304.

Brown, A.G., Smale, T.C., King, T.J., Hasenkamp, R., Thompson, R.H., 1976. Crystal and molecular structure of compactin, a new antifungal metabolite from *Penicillium brevicompactum*. *J. Chem. Soc. Perkin Trans. 1* 1976, 1165–1170.

Brückner, H., Przybylski, M., 1984. Methods for the rapid detection, isolation and sequence determination of "peptaibols" and other Aib-containing peptides of fungal origin. I. Gliodeliquescin A from *Gliocladium deliquescens*. *Chromatographia* 19, 188–199.

Chang, T.-Y., Li, B.-L., Chang, C.C.Y., Urano, Y., 2009. Acyl-coenzyme A: cholesterol acyltransferases. *AJP Endocrinol. Metab.* 297, E1–E9.

Chu, M., Truumees, I., Rothofsky, M.L., Patel, M.G., Gentile, F., Das, P.R., Puar, M.S., Lin, S.L., 1995. Inhibition of c-fos proto-oncogene induction by Sch 52900 and Sch 52901, novel diketopiperazine produced by *Gliocladium* sp. *J. Antibiot.* 48, 1440–1445.

Chugh, J.K., Brückner, H., Wallace, B.A., 2002. Model for a helical bundle channel based on the high-resolution crystal structure of trichotoxin_A50E. *Biochemistry* 41, 12934–12941.

Chugh, J.K., Wallace, B.A., 2001. Peptaibols: Models for ion channels. *Biochem. Soc. Trans.* 29, 565–570.

Closse, A., Hauser, D., 1973. Isolierung und Konstitutionsermittlung von Chrysodin. *Helv. Chim. Acta* 56, 2694–2698.

Damon, S.C., 1952. Two noteworthy species of *Sepedonium*. *Mycologia* 44, 86–96.

De Zotti, M., Biondi, B., Formaggio, F., Toniolo, C., Stella, L., Park, Y., Hahm, K.S., 2009. Trichogin GA IV: An antibacterial and protease-resistant peptide. *J. Pept. Sci.* 15, 615–619.

Degenkolb, T., Berg, A., Gams, W., Schlegel, B., Gräfe, U., 2003. The occurrence of peptaibols and structurally related peptaibiotics in fungi and their mass spectrometric identification *via* diagnostic fragment ions. *J. Pept. Sci.* 9, 666–678.

Degenkolb, T., Kirschbaum, J., Brückner, H., 2007. New sequences, constituents, and producers of peptaibiotics: An updated review. *Chem. Biodivers.* 4, 1052–1067.

Divekar, P.V., Raistrick, H., Dobson, T.A., Vining, L.C., 1965. Studies in the biochemistry of microorganisms: Part 117. Sepedonin, a tropolone metabolite of *Sepedonium chrysospermum* Fries. *Can. J. Chem.* 43, 1835–1848.

Divekar, P.V., Vining, L.C., 1964. Reaction of anhydrosepedonin with alkali synthesis of a degradation product and some related dimethylhydroxybenzoic acids. *Can. J. Chem.* 42, 63–68.

Domsch, K.H., Gams, W., Anderson, T.-H., 2007. Compendium of soil fungi, Second Edition. IHW-Verlag, Eching, pp. 1–672.

Dong, J.Y., He, H.P., Shen, Y.M., Zhang, K.Q., 2005. Nematicidal epipolysulfanyldioxopiperazines from *Gliocladium roseum*. *J. Nat. Prod.* 68, 1510–1513.

Dong, J.Y., Zhou, W., Li, L., Li, G.H., Liu, Y.J., Zhang, K.Q., 2006. A new epidithiodioxopiperazine metabolite isolated from *Gliocladium roseum* YMF1.00133. *Chinese Chem. Lett.* 17, 922–924.

Dornberger, K., Ihn, W., Ritzau, M., Gräfe, U., Schlegel, B., Fleck, W.F., Metzger, J.W., 1995. Chrysospermins, new peptaibol antibiotics from *Apiocrea chrysosperma* Ap101. *J. Antibiot.* 48, 977–989.

Eholzer, S., 1999. Untersuchungen zur Gattung *Sepedonium*: Neuzugänge in der Pilzkulturen-sammlung Regensburg. Zulassungsarbeit für Lehramt Gymnasium in Bayern, Universität Regensburg.

El-Faham, A., Khattab, S.N., 2009. Utilization of N,N,N,'N'-tetramethylfluoroformamidinium hexafluorophosphate (TFFH) in peptide and organic synthesis. *Synlett* 6, 886–904.

Endo, A., 1985. Compactin (ML-236B) and related compounds as potential cholesterol-lowering agents that inhibit HMG-CoA reductase. *J. Med. Chem.* 28, 401–405.

Endo, A., Hasumi, K., Yamada, A., Shimoda, R., Takeshima, H., 1986. The synthesis of compactin (ML-236B) and monacolin K in fungi. *J. Antibiot.* 39, 1609–1610.

Endo, A., Kuroda, M., Tsujita, Y., 1976. ML-236A, ML-236B, and ML-236C, new inhibitors of cholesterogensis produced by *Penicillium citrinum*. *J. Antibiot.* 29, 1346–1348.

Eschen-Lippold, L., Dräger, T., Teichert, A., Wessjohann, L., Westermann, B., Rosahl, S., Arnold, N., 2009. Antioomycete activity of γ-oxocrotonate fatty acids against *P. infestans*. *J. Agric. Food Chem.* 57, 9607–9612.

Fries, E., 1874. Hymenomycetes europaei sive epicriseos systematis mycologici: Sive. Berling, Uppsala, pp. 1–755.

Fugmann, B., 1985. Neue niedermolekulare Naturstoffe aus Höheren Pilzen (Basidiomyceten). Isolierung, Strukturaufklärung und Synthese. Dissertation, Universität Bonn.

Garrido, N., 1988. Agaricales s.l. und ihre Mykorrhizen in den *Nothofagus*-Wäldern Mittelchiles. *Bibl. Mycol.* 120, 1–528.

Gessmann, R., Brückner, H., Petratos, K., 2003. Three complete turns of a 3_{10}-helix at atomic resolution: The crystal structure of Z-(Aib)$_{11}$-O*t*Bu. *J. Pept. Sci.* 9, 753–762.

Gilardoni, G., Clericuzio, M., Marchetti, A., Finzi, P.V., Zanoni, G., Vidari, G., 2006. New oxidized 4-oxo fatty acids from *Hygrophorus discoxanthus*. *Nat. Prod. Commun.* 1, 1079–1084.

Gilardoni, G., Clericuzio, M., Tosi, S., Zanoni, G., Vidari, G., 2007. Antifungal acylcyclopentenediones from fruiting bodies of *Hygrophorus chrysodon*. *J. Nat. Prod.* 70, 137–139.

Gill, M., Steglich, W., 1987. Pigments of fungi (Macromycetes), in: Herz, W., Grisebach, H., Kirby, G.W., Tamm, C. (Eds.), Progress in the chemistry of organic natural products. Springer Verlag, Wien, New York, Vol. 51, pp. 1–317.

Gräfe, U., Ihn, W., Ritzau, M., Schade, W., Stengel, C., Schlegel, B., Fleck, W.F., Künkel, W., Härtl, A., Gutsche, W., 1995. Helioferins; novel antifungal lipopeptides from *Mycogone rosea*: Screening, isolation, structures and biological properties. *J. Antibiot.* 48, 126–133.

Hansen, L., Knudsen, H., 1992. Nordic Macromycetes, Volume 2. Polyporales, Boletales, Agaricales, Russulales. Nordsvamp, Copenhagen, pp. 1–474.

Haraguchi, H., Taniguchi, M., Motoba, K., Shibata, K., Oi, S., Hashimoto, K., 1990. Chrysodin, an antifungal antimetabolite. *Agric. Biol. Chem.* 54, 2167–2168.

Helfer, W., 1991. Pilze auf Pilzfruchtkörpern: Untersuchungen zur Ökologie, Systematik und Chemie. IHW-Verlag, Eching, pp. 1–157.

Hjørringgaard, C.U., Pedersen, J.M., Vosegaard, T., Nielsen, N.C., Skrydstrup, T., 2009. An automatic solid-phase synthesis of peptaibols. *J. Org. Chem.* 74, 1329–1332.

Horak, E., 1967. Fungi austroamericani, IV. *Darwiniana* 14, 355–2376.

Hülsmann, H., Heinze, S., Ritzau, M., Schlegel, B., Gräfe, U., 1998. Isolation and structure of peptaibolin, a new peptaibol from *Sepedonium* strains. *J. Antibiot.* 51, 1055–1058.

Jabs, T., Ammermann, E., Stierl, R., Lorenz, G., Boland, W., Engelberth, J., 2001. Ionenkanal-bildende Peptaibole als Resistenzinduktoren. Deutsches Patent, DE10013294 A1.

Jacobsson, S., Larsson, E., 2007. *Hygrophorus penarioides*, a new species identified using morphology and ITS sequence data. *Mycotaxon* 99, 337–343.

Jasminovic, A., 1999. Untersuchungen an *Sepedonium*-Stämmen aus Nordamerika und Neuseeland. Zulassungsarbeit für Lehramt Gymnasium in Bayern, Universität Regensburg.

Jaworski, A., Brückner, H., 2000. New sequences and new fungal producers of peptaibol antibiotics antiamoebins. *J. Pept. Sci.* 6, 149–167.

Kitson, S., 2014. Carbon-14 labelled ADCs and peptides. URL http://www.slideshare.net/seankitson/s-kitson-carbon14-labelled-adcs-and-peptides-26feb2014 (accessed 9th September 2015).

Krause, C., Kirschbaum, J., Jung, G., Brückner, H., 2006. Sequence diversity of the peptaibol antibiotic suzukacillin-A from the mold *Trichoderma viride*. *J. Pept. Sci.* 12, 321–327.

Krieglsteiner, G.J., Gminder, A., 2001. Die Großpilze Baden-Württembergs, Band 3: Ständerpilze. Blätterpilze 1. Ulmer, Stuttgart, 1–634.

Kronen, M., Kleinwächter, P., Schlegel, B., Härtl, A., Gräfe, U., 2001. Ampullosporins B, C, D, E1, E2, E3 and E4 from *Sepedonium ampullosporum* HKI-0053: Structures and biological activities. *J. Antibiot.* 54, 175–178.

Lahdenperä, M.-L., 2006. *Gliocladium catenulatum* as an antagonist against grey mould on strawberry. *NJF Report, Nord. Assoc. Agric. Sci.* 2, 15.

Larsson, E., Jacobsson, S., 2014. Vilken vaxskivling var det som Fries beskrev som *Agaricus pudorinus*? *Sven. Mykolgisk Tidskr.* 35, 5–9.

Lee, S.J., Yun, B.S., Cho, D.H., Yoo, I.D., 1999. Tylopeptins A and B, new antibiotic peptides from *Tylopilus neofelleus*. *J. Antibiot.* 52, 998–1006.

Leitgeb, B., Szekeres, A., Manczinger, L., Vágvölgyi, C., Kredics, L., 2007. The history of alamethicin: A review of the most extensively studied peptaibol. *Chem. Biodivers.* 4, 1027–1051.

Lodge, D.J., Padamsee, M., Matheny, P.B., Aime, M.C., Cantrell, S.A., Boertmann, D., Kovalenko, A., Vizzini, A., Dentinger, B.T.M., Kirk, P.M., Ainsworth, A.M., Moncalvo, J.-M., Vilgalys, R., Larsson, E., Lücking, R., Griffith, G.W., Smith, M.E., Norvell, L.L., Desjardin, D.E., Redhead, S.A., Ovrebo, C.L., Lickey, E.B., Ercole, E., Hughes, K.W., Courtecuisse, R., Young, A., Binder, M., Minnis, A.M., Lindner, D.L., Ortiz-Santana, B., Haight, J., Læssøe, T., Baroni, T.J., Geml, J., Hattori, T., 2014. Molecular phylogeny, morphology, pigment chemistry and ecology in Hygrophoraceae (Agaricales). *Fungal Divers.* 64, 1–99.

Lotsy, J.P., 1907. Vorträge über Botanische Stammesgeschichte. Algen und Pilze. Gustav Fischer Verlag, Jena, pp. 1–828.

Lübken, T., 2006. Hygrophorone – Neue antifungische Cyclopentenonderivate aus *Hygrophorus*-Arten (Basidiomycetes). Dissertation, Martin-Luther-Universität Halle-Wittenberg.

Lübken, T., Arnold, N., Wessjohann, L., Böttcher, C., Schmidt, J., 2006. Analysis of fungal cyclopentenone derivatives from *Hygrophorus* spp. by liquid chromatography/electrospray-tandem mass spectrometry. *J. Mass Spectrom.* 41, 361–371.

Lübken, T., Schmidt, J., Porzel, A., Arnold, N., Wessjohann, L., 2004. Hygrophorones A–G: Fungicidal cyclopentenones from *Hygrophorus* species (Basidiomycetes). *Phytochemistry* 65, 1061–1071.

Marshall, G.R., Hodgkin, E.E., Langs, D.A., Smith, G.D., Zabrocki, J., Leplawy, M.T., 1990. Factors governing helical preference of peptides containing multiple alpha,alpha-dialkyl amino acids. *Proc. Natl. Acad. Sci.* 87, 487–491.

Mcquilken, M.P., Gemmell, J., Lahdenperä, M.L., 2001. *Gliocladium catenulatum* as a potential biological control agent of damping-off in bedding plants. *J. Phytopathol.* 149, 171–178.

Metzger, J., Schlegel, B., Fleck, W.F., Dornberger, K., Ihn, W., Schade, W., Gräfe, U., 1994. Chrysospermine, Peptidwirkstoffe aus *Apiocrea chrysosperma* mit pharmakologischer Wirkung, ein Verfahren zu Herstellung und Verwendung derselben. Europäisches Patent, EP0622375 A1.

Mitova, M.I., Murphy, A.C., Lang, G., Blunt, J.W., Cole, A.L.J., Ellis, G., Munro, M.H.G., 2008. Evolving trends in the dereplication of natural product extracts. 2. The isolation of chrysaibol, an

antibiotic peptaibol from a New Zealand sample of the mycoparasitic fungus *Sepedonium chrysospermum*. *J. Nat. Prod.* 71, 1600–1603.

Mitova, M.I., Stuart, B.G., Cao, G.H., Blunt, J.W., Cole, A.L.J., Munro, M.H.G., 2006. Chrysosporide, a cyclic pentapeptide from a New Zealand sample of the fungus *Sepedonium chrysospermum*. *J. Nat. Prod.* 69, 1481–1484.

Moser, M., 1983. Kleine Kryptogamenflora, Band II b/2, Basidiomyceten: Die Röhrlinge und Blätterpilze, Kleine Kryptogamenflora. Gustav Fischer Verlag, Stuttgart, New York, pp. 1–533.

Moser, M., Horak, E., 1975. *Cortinarius* Fr. und nahe verwandte Gattungen in Südamerika. *Beih. zur Nov. Hedwigia* 52, 1–473.

Nagao, K., Yoshida, N., Iwai, K., Sakai, T., Tanaka, M., Miyahara, T., 2006. Production of sepedonin by *Sepedonium chrysospermum* NT-1 in submerged culture. *Environ. Sci.* 13, 251–256.

Neuhof, T., Berg, A., Besl, H., Schwecke, T., Dieckmann, R., von Döhren, H., 2007. Peptaibol production by *Sepedonium* strains parasitizing Boletales. *Chem. Biodivers.* 4, 1103–1115.

Neumann, N.K.N., Stoppacher, N., Zeilinger, S., Degenkolb, T., Brückner, H., Schuhmacher, R., 2015. The Peptaibiotics Database – A comprehensive online resource. *Chem. Biodivers.* 12, 743–751.

Nishida, H., Huang, X.H., Tomoda, H., Omura, S., 1992. Glisoprenins, new inhibitors of acyl-CoA: cholesterol acyltransferase produced by *Gliocladium* sp. FO-1513. II. Structure elucidation of glisoprenins A and B. *J. Antibiot.* 45, 1669–1676.

Petch, T., 1939. *Gliocladium. Trans. Br. Mycol. Soc.* 22, 257–263.

Pike, S.J., Raftery, J., Webb, S.J., Clayden, J., 2014. Conformational analysis of helical aminoisobutyric acid (Aib) oligomers bearing *C*-terminal ester Schellman motifs. *Org. Biomol. Chem.* 12, 4124–4131.

Qu, Y., Zhang, H.-B., Liu, J.-K., 2004. Isolation and structure of a new ceramide from the basidiomycete *Hygrophorus eburnesus* 59, 241–244.

Quang, D.N., Schmidt, J., Porzel, A., Wessjohann, L., Haid, M., Arnold, N., 2010. Ampullosine, a new isoquinoline alkaloid from *Sepedonium ampullosporum* (Ascomycetes). *Nat. Prod. Commun.* 5, 869–872.

Reiber, K., Neuhof, T., Ozegowski, J.H., von Döhren, H., Schwecke, T., 2003. A nonribosomal peptide synthetase involved in the biosynthesis of ampullosporins in *Sepedonium ampullosporum*. *J. Pept. Sci.* 9, 701–713.

Ricek, E.W., 1974. *Hygrophorus persicolor* sp. nov., der Flamingo-Schneckling. *Z. Pilzkd.* 40, 5–8.

Ritzau, M., Heinze, S., Dornberger, K., Berg, A., Fleck, W., Schlegel, B., Hartl, A., Gräfe, U., 1997. Ampullosporin, a new peptaibol-type antibiotic from *Sepedonium ampullosporum* HKI-0053 with neuroleptic activity in mice. *J. Antibiot.* 50, 722–728.

Roepstorff, P., Fohlman, J., 1984. Proposal for a common nomenclature for sequence ions in mass spectra of peptides. *Biol. Mass Spectrom.* 11, 601–601.

Rogerson, C.T., Samuels, G.J., 1989. Boleticolous species of *Hypomyces*. *Mycologia* 81, 413–432.

Sabareesh, V., Balaram, P., 2006. Tandem electrospray mass spectrometric studies of proton and sodium ion adducts of neutral peptides with modified *N*- and *C*-termini: synthetic model peptides and microheterogeneous peptaibol antibiotics. *Rapid Commun. Mass Spectrom.* 20, 618–628.

Saccardo, P.A., 1883. Sylloge fungorum omnium hucusque cognitorum, R. Friedländer & Sohn, Berlin, Vol. II. pp. 1–813.

Sahr, T., Ammer, H., Besl, H., Fischer, M., 1999. Infrageneric classification of the boleticolous genus *Sepedonium*: Species delimitation and phylogenetic relationships. *Mycologia* 91, 935–943.

Schiell, M., Hofmann, J., Kurz, M., Schmidt, F.R., Vértesy, L., Vogel, M., Wink, J., Seibert, G., 2001. Cephaibols, new peptaibol antibiotics with anthelmintic properties from *Acremonium tubakii* DSM 12774. *J. Antibiot.* 54, 220–233.

Shibata, S., Shoji, J., Ohta, A., Watanabe, M., 1957. Metabolic products of fungi. XI. Some observation on the occurrence of skyrin and rugulosin in mold metabolites, with a reference to structural relationship between penicilliopsin and skyrin. *Pharm. Bull.* 5, 380–382.

Singer, R., 1949. The Agaricales (mushrooms) in modern taxonomy. *Lilloa* 22, 5–832.

Singer, R., Digilio, A.P.L., 1952. Pródromo de la flora agaricina Argentina. *Lilloa* 25, 5–462.

Stadler, M., Seip, S., Müller, H., Henkel, T., Lagojda, A., Kleymann, G., 2001. New antiviral peptaibols from the mycoparasitic fungus *Sepedonium microspermum*, in: Book of Abstracts, 13. Irseer Naturstofftage der DECHEMA, Irsee.

Swenson, U., Hill, R.S., McLoughlin, S., 2001. Biogeography of *Nothofagus* supports the sequence of Gondwana break-up. *Taxon* 50, 1025–1041.

Tavano, R., Malachin, G., De Zotti, M., Peggion, C., Biondi, B., Formaggio, F., Papini, E., 2015. The peculiar *N*- and *C*-termini of trichogin GA IV are needed for membrane interaction and human cell death induction at doses lacking antibiotic activity. *BBA - Biomembr.* 1848, 134–144.

Teichert, A., 2008. Chemische und biologische Untersuchungen von Inhaltsstoffen aus Pilzfruchtkörpern der Gattungen *Cortinarius* und *Hygrophorus*. Dissertation, Martin-Luther-Universität Halle-Wittenberg.

Teichert, A., Lübken, T., Kummer, M., Besl, H., Haslberger, H., Arnold, N., 2005a. Bioaktive Sekundärmetaboliten aus der Gattung *Hygrophorus* (Basidiomycetes). *Z. Mykol.* 71, 53–62.

Teichert, A., Lübken, T., Schmidt, J., Kuhnt, C., Huth, M., Porzel, A., Wessjohann, L., Arnold, N., 2008. Determination of β-carboline alkaloids in fruiting bodies of *Hygrophorus* spp. by liquid chromatography/electrospray ionisation tandem mass spectrometry. *Phytochem. Anal.* 19, 335–341.

Teichert, A., Lübken, T., Schmidt, J., Porzel, A., Arnold, N., Wessjohann, L., 2005b. Unusual bioactive 4-oxo-2-alkenoic fatty acids from *Hygrophorus eburneus*. *Z. Naturforsch.* 60b, 25–32.

Teichert, A., Schmidt, J., Porzel, A., Arnold, N., Wessjohann, L., 2007. Brunneins A–C, β-carboline alkaloids from *Cortinarius brunneus*. *J. Nat. Prod.* 70, 1529–1531.

Teperi, E., Keskinen, M., Ketoja, E., Tahvonen, R., 1998. Screening for fungal antagonists of seed-borne *Fusarium culmorum* on wheat using *in vivo* tests. *Eur. J. Plant Pathol.* 104, 243–251.

Thines, E., Eilbert, F., Anke, H., Sterner, O., 1998. Glisoprenins C, D and E, new inhibitors of appressorium formation in *Magnaporthe grisea*, from cultures of *Gliocladium roseum*. 1. Production and biological activities. *J. Antibiot.* 51, 117–122.

Tomoda, H., Ohyama, Y., Abe, T., Tabata, N., Namikoshi, M., Yamaguchi, Y., Masuma, R., Omura, S., 1999. Roselipins, inhibitors of diacylglycerol acyltransferase, produced by *Gliocladium roseum* KF-1040. *J. Antibiot.* 52, 689–694.

Toniolo, C., Benedetti, E., 1991. The polypeptide 3_{10}-helix. *Trends Biochem. Sci.* 16, 350–353.

Toniolo, C., Crisma, M., Formaggio, F., Peggion, C., Epand, R.F., Epand, R.M., 2001. Lipopeptaibols, a novel family of membrane active, antimicrobial peptides. *Cell. Mol. Life Sci.* 58, 1179–1188.

Toniolo, C., Polese, A., Formaggio, F., Crisma, M., Kamphuis, J., 1996. Circular dichroism spectrum of a peptide 3_{10}-helix. *J. Chem. Soc. Chem. Commun.* 118, 2744–2745.

Usami, Y., Yamaguchi, J., Numata, A., 2004. Gliocladins A–C and glioperazine; cytotoxic dioxo- or trioxopiperazine metabolites from a *Gliocladium* sp. separated from a sea hare. *Heterocycles* 63, 1123–1129.

Vieira-Pires, R.S., Morais-Cabral, J.H., 2010. 3_{10} helices in channels and other membrane proteins. *J. Gen. Physiol.* 136, 585–592.

Wiest, A., Grzegorski, D., Xu, B.W., Goulard, C., Rebuffat, S., Ebbole, D.J., Bodo, B., Kenerley, C., 2002. Identification of peptaibols from *Trichoderma virens* and cloning of a peptaibol synthetase. *J. Biol. Chem.* 277, 20862–20868.

Yamaguchi, H., Kodama, H., Osada, S., Kato, F., Jelokhani-Niaraki, M., Kondo, M., 2003. Effect of alpha,alpha-dialkyl amino acids on the protease resistance of peptides. *Biosci. Biotechnol. Biochem.* 67, 2269–2272.

Yamazaki, H., Koyama, N., Omura, S., Tomoda, H., 2010. New rugulosins, anti-MRSA antibiotics, produced by *Penicillium radicum* FKI-3765-2. *Org. Lett.* 12, 1572–1575.

Yun, B.S., Yoo, I.D., Kim, Y.S.H., Kim, Y.S.H., Lee, S.J., Kim, K.S., Yeo, W.H., 2000. Peptaivirins A and B, two new antiviral peptaibols against TMV infection. *Tetrahedron Lett.* 41, 1429–1431.

Zhang, M., 2011. A cladistic scenario of Southern Pacific biogeographical history based on *Nothofagus* dispersal and vicariance analysis. *J. Arid Land* 3, 104–113.

3 Isolation and asymmetric total synthesis of fungal secondary metabolite hygrophorone B^{12}

Front cover (doi: 10.1002/ejoc.201590027)*

Abstract

Hygrophorone B^{12}, a new antifungal constituent from the fruiting bodies of *Hygrophorus abieticola*, has been isolated and subsquently synthesized in enantiomerically pure form. The total synthesis includes a Sharpless asymmetric dihydroxylation protocol as the stereodifferentiating step, followed by two diastereoselective aldol-type reactions. The approach allows the unambiguous control of all three stereogenic centers and, furthermore, the unequivocal determination of the relative and absolute configuration of the antibiotic hygrophorones B for the first time.

3.1 Introduction

Field observations by curious, woodcreeping natural product chemists suggested, that fruiting bodies of the genus *Hygrophorus* (German: Schnecklinge, English: wax caps) are rarely infected by parasitic fungi (Bon, 1992; Lübken et al., 2004). These ecological observations triggered the exploration of a molecular basis for this phenomenon. Petroleum ether extracts of the fruiting bodies of *H. persoonii* and *H. olivaceoalbus,* both of which are characterized by a very slimy pileus surface, revealed a series of structurally related constituents. These include new trihydroxy-functionalized cyclopentenones, termed hygrophorones A^n (**3.1**) and hygrophorones B^n (**3.2**, Fig. 3.1), in which (n) denotes the length of the side chain connected to C-6 (Lübken et al., 2004). The endocyclic diol has a *trans*-relationship in hygrophorones A, and a a *cis*-relationship in hygrophorones B (Lübken et al., 2004; Schmidts et al., 2013). The different aliphatic side chains (n) found for both diastereomers appear to be related to different fatty acids **3.5a–e** as biosynthetic precursors, which also can be isolated from *Hygrophorus* fruiting bodies (Teichert et al., 2005b). Although the biosynthesis has not yet been clarified, it seems to be most likely that the fatty acids **3.5a–e** are connected to the synthesis of the hygrophorones. Very recently, Gryparis et al. (2011) discussed the synthesis of hygrophorones as a product of a singlet-oxygen-mediated oxidation of furans (Montagnon et al., 2008), which may be formed as condensation products of these fatty acids *in vivo*.

The cyclopentenone moieties and the endocyclic diol fragment of the hygrophorones closely resemble the natural products (–)-epipentenomycin (**3.3**) and (–)-pentenomycin (**3.4**) (Aitken et al., 2013; Phutdhawong et al., 2002). But the addition of the lipophilic side chain in the hygrophorones makes these molecules amphiphilic, and creates an additional stereogenic center, which is significant for their pronounced biological activities, especially their fungicidal activities (Lübken et al., 2004).

The biological profile, the densely functionalized headgroup and the ill-defined relative and unknown absolute configuration of these natural products prompted us to perform an asymmetric total synthesis.
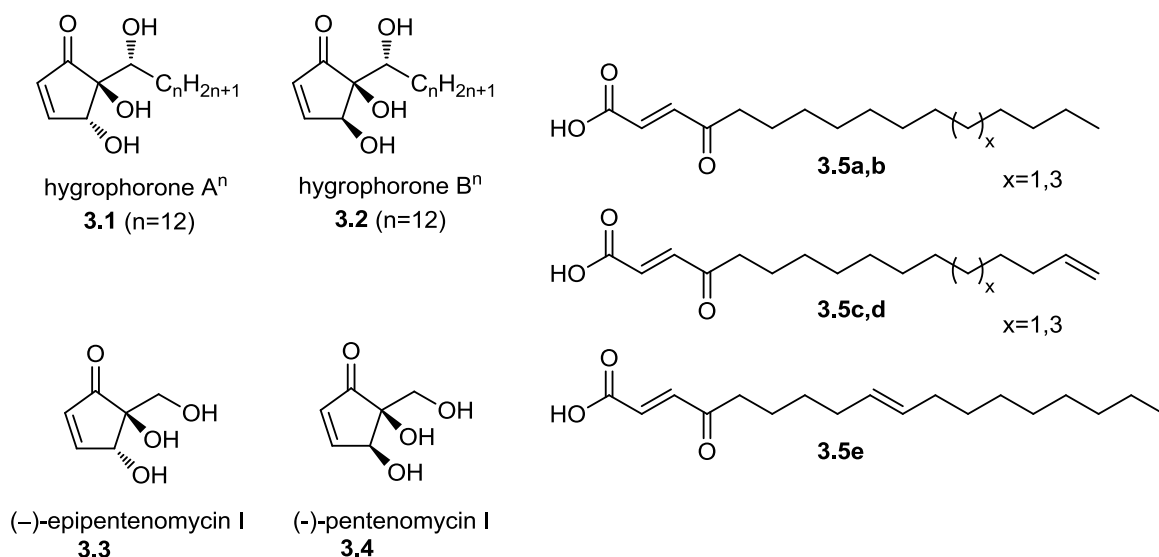
Fig. 3.1. Structures of isolated natural products and related natural antibiotics.

3.2 Results and discussion

3.2.1 Isolation of hygrophorone B[12]

Frozen fruiting bodies of *H. abieticola* were extracted with ethyl acetate. The slightly yellow crude extract was purified by means of adsorption chromatography (silica gel) and size exclusion chromatography (Sephadex LH 20). The final purification was carried out by preparative HPLC to afford pure hygrophorone B[12] (**3.2**) as a colorless powder.

The molecular formula $C_{18}H_{32}O_4$ was determined by HR-FT-ICR-MS (negative ion mode) as *m/z* 311.2224 ([M–H]⁻). The ^1H and ^{13}C NMR spectra of **3.2** are very similar to the spectra of hygrophorones of the B series isolated earlier (Lübken et al., 2004). In contrast to the known hygrophorones B[14] and B[16], the alkyl side chain of **3.2** could be determined as $-C_{12}H_{25}$, which was further confirmed by mass spectrometrical data. Also, $^1H,^1H$ COSY, $^1H,^{13}C$ HMBC and NOE correlations of the cyclic moiety of **3.2** are in agreement with those of other hygrophorones B of the homologous series. Therefore, the structure of **3.2** could be assigned as (+)-*cis*-4,5-dihydroxy-5-(1-hydroxytridecyl)cyclopent-2-enone, and the compound was named hygrophorone B[12] (**3.2**).

3.2.2 Synthesis and stereochemical assignment of hygrophorone B[12]

The very compact functionalization at the cyclopentenone moiety in **3.2** sets some synthetic challenges. The structural elements comprise a 1,2,3-trihydroxy functionalization, with two of the hydroxyl groups at tertiary centers, and the other one at a quaternary center. The relative configuration of the two hydroxy groups attached to the ring is known from structure elucidation of isolated natural products, as described above (Lübken et al., 2004). But the overall relative configuration including the exocyclic hydroxyl group is not known, and nor is the absolute configuration of the three stereogenic centers.

LG leaving group
PG protecting group
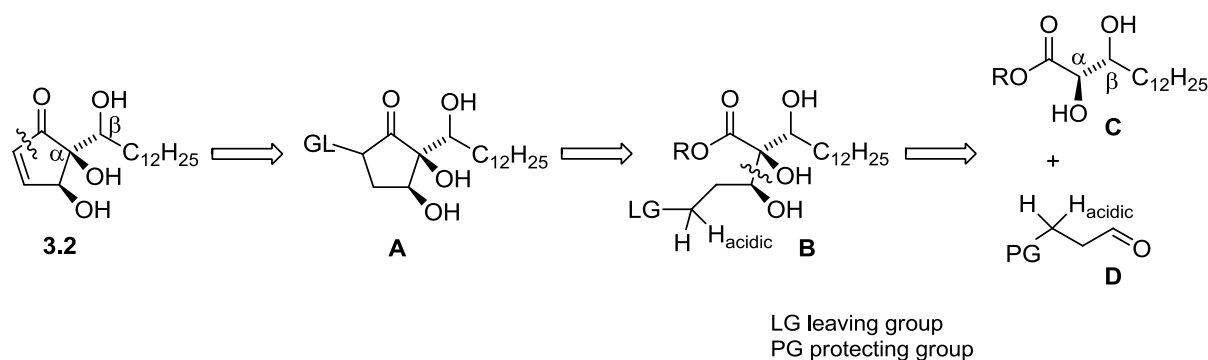
Scheme 3.1. Retrosynthetic analysis of **3.2**.

Cyclopentenones **3.1** and **3.2** have a pronounced lability under certain conditions: the quaternary center α to the carbonyl functionality supports *retro*-Dieckmann type reactions. This must be considered when planning the synthesis. Therefore, in our retrosynthetic approaches, the formation of the cyclopentenone was set to occur at a very late stage by *cis*-elimination from **A** (Scheme 3.1) (Pohmakotr and Popuang, 1991). For the construction of carbocycle **A**, two consecutive aldol-type reactions (starting from **C** and **D**) can be considered. The second, intramolecular, aldol reaction (from intermediate **B**), would be prompted by a functional group conversion.

This retrosynthetic analysis suggests the following sequence in the forward sense: for a partial formation of the 1,2,3-trihydroxylation pattern and to define the absolute configuration of the final product early, a Sharpless asymmetric dihydroxylation (AD) protocol was envisioned as the starting point (Scheme 3.1). Readily available *trans*-olefinic α,β-unsaturated carboxylic esters serve as starting materials, and the absolute stereochemistry of the two newly generated stereocenters in **C** is controlled by the use of the chiral ligands $(DHQ)_2$-PHAL (hydroquinine 1,4-phthalazinediyl diether; AD-mix-α) or $(DHQD)_2$-PHAL (hydroquinidine phthalazine adduct; AD-mix-β) (Zaitsev and Adolfsson, 2006). The first of two subsequent aldol-type reactions establishes the 1,2,3-trihydroxy pattern under regime of self-regenerating stereogenic centers (Seebach et al., 1996). The second one, a Dieckmann-type cyclization, is responsible for the formation of the cyclopentanone scaffold. Overall, it is the exocyclic stereocenter at C-1^β of the final product (β-position in **C**) that controls the stereochemical outcome of the asymmetric synthesis of **3.2**.

Following this plan, the asymmetric total synthesis of hygrophorone B[12] (Scheme 3.2) was begun with the synthesis of *trans*-α,β-unsaturated fatty acid esters **3.6**. To establish the absolute configuration, the double bond was transformed into its dihydroxy congener by Sharpless dihydroxylation (Fernandes et al., 2009). The dihydroxylated esters [i.e., (2R,3S)-(−)-**3.7** and (2S,3R)-(+)-**3.7**] were formed in high chemical yields (98% and 95%, respectively), and with high stereoselectivities. HPLC methods revealed an optical purity >99% ee; no trace of the other enantiomer could be detected in both series, starting either with the AD-mix-α or the AD-mix-β. For brevity, only the synthesis of the AD-mix-α series starting from (−)-**3.7** is described in this Chapter; (+)-**3.7** is redundant (Scheme 3.2).
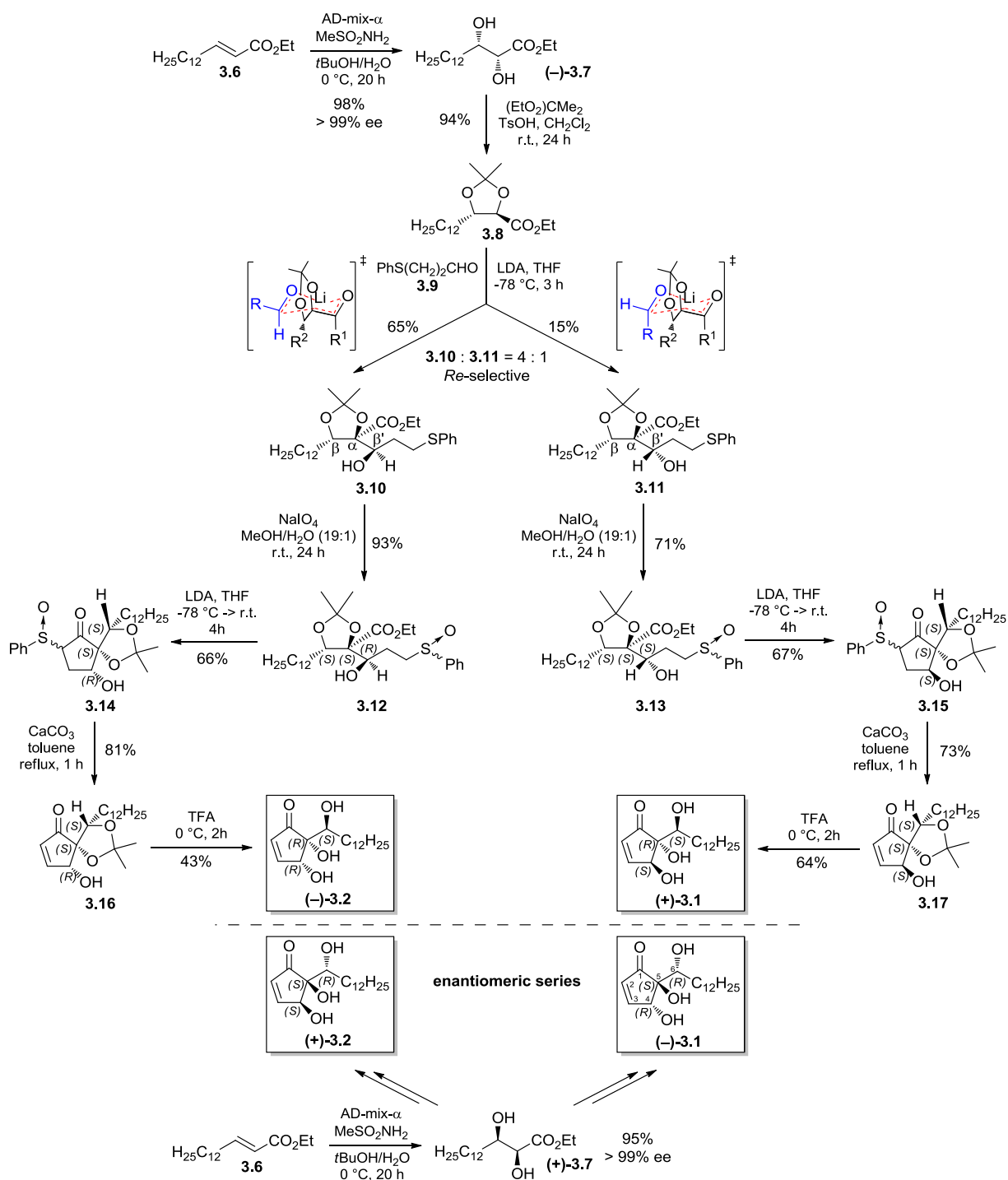
Scheme 3.2. Asymmetric total synthesis of hygrophorones.

To have high diastereoselectivity in subsequent aldol-type reactions, transformation/protection of the acyclic diol into a cyclic acetal was thought to be a prerequisite. Acetalization to **3.8** was carried out with diethoxypropane in order to avoid any transesterified products, leading to the cyclic product in 94% yield. For the aldol reaction, the thiophenol derived aldehyde **3.9** was used (Craig et al., 2010). The formation of the ester enolate from **3.8** by treatment with LDA (lithium diisopropylamide) led to a prochiral sp^2 center at the α-position. The remaining stereocenter at the β-position controls the diastereoselectivity of the aldol-reaction with aldehyde **3.9**. The aldol reaction was diastereoselective, leading to **3.10** and **3.11** in a 4:1 (**3.10**:**3.11**) ratio in an overall

yield of 80%. The aldol products **3.10** and **3.11** could be separated by column chromatography. The three hydroxy groups in the main product (i.e., **3.10**) had an α,β-*anti*, α,β'-*syn* configuration, and the hydroxy groups in the minor diastereomer **3.11** had an α,β-*anti*, α,β'-*anti* conformation. Support for this stereochemical assignment is provided by an X-ray structure from a closely related intermediate with a relative configuration identical to that of the major diastereomer (see Supporting Information). Only two of four possible diastereomers are formed in the aldol reaction, both of which originate from the attack of the *Re* face of the (*E*)-configured ester enolate onto aldehyde **3.9**. A Zimmerman-Traxler transition state predicts that the formation of the diastereomer **3.10** is favoured over **3.11**, which is consistent with the experimental results.

For the following steps, the sulfide moiety had to be changed from a protecting group to a reactive group. This was achieved by altering the oxidation state to a sulfoxide (**3.12** and **3.13**), which enabled this newly transformed functional group to act in two ways: the latent CH-acidity of the neighbouring methylene moiety was unveiled, and most importantly, an elimination was made possible (Chooprayoon et al., 2011; Kambutong et al., 2010). In practical terms, the oxidation of sulfides **3.10** and **3.11** was carried out with sodium periodate to give sulfoxides **3.12** and **3.13** in yields of 93% and 71%, respectively. Subsequently, a Dieckmann-type cyclization of each of the sulfoxides was carried out in the presence of LDA, which led to diastereomeric mixtures of the spirocyclic compounds **3.14** (66%) and **3.15** (67%). In both cases, a 1:1 diastereomeric composition was obtained, with the sulfoxide equally *cis* and *trans* oriented, as determined by NMR studies. Although the diastereomers could be separated by column chromatography for analysis, the diastereomeric mixtures could be used for the next step, since the sulfoxide moiety is eliminated, the stereocenter is destroyed, and both diastereomers give the desired product. This elimination proceeded as expected in toluene under reflux to give the cyclopentenones **3.16** (81%) and **3.17** (73%). Finally, cleavage of the acetals with trifluoroacetic acid led to the hygrophorones (–)-**3.2** (43%) and (+)-**3.1** (64%), respectively. The deprotection must be carried out under solvent-free conditions under ice-cooling, because higher temperatures as well as the use of solvents (e.g. methanol) led to decomposition and side reactions.

NMR spectroscopic analysis revealed a *trans*-relationship for the endocyclic dihydroxy groups of the stereoisomer (+)-**3.1**, and a *cis*-relationship for the same moieties in (–)-**3.2**. Data obtained in earlier isolation studies strongly confirm this result (Lübken et al., 2004). Further evidence for the relative configuration of the hygrophorones is offered by additional X-ray studies. Since no crystals could be obtained from compound (–)-**3.2**, acetyl derivatives were synthesized (Scheme 3.3). Therefore, cyclopentenone **3.16** was acetylated with acetic anhydride and pyridine, and the resulting acetonide **3.18** was deprotected with trifluoroacetic acid to obtain the acetate **3.19** and its acetate migration isomer **3.20** as a regioisomeric mixture in a 2:1 ratio (**3.19**:**3.20**). The regioisomers were separated by preparative HPLC, and crystals of **3.19** suitable for X-ray diffraction analysis were obtained from a solution of the compound in ethyl acetate overlayed with *n*-pentane. The crystal structure of the acetylated hygrophorone **3.19** shows the relative

alignment of the three hydroxyl groups (Fig. 3.2). As deduced from NMR spectroscopic studies, the two endocyclic hydroxyl groups have a *cis*-relationship, whereas the exocyclic hydroxyl group at C-6 has an *anti*-configuration relative to the hydroxy group at C-5. Because the configuration of carbon atom C-6, which carries the exocyclic hydroxy group, being known from the Sharpless dihydroxylation, the absolute configuration of the acetylated hygrophorone **3.19** can be determined as (4*R*,5*R*,6*S*) based on the crystal structure. Thus, it can be concluded that the synthesized hygrophorone (–)-**3.2** has a (4*R*,5*R*,6*S*) configuration, and its enantiomer (+)-**3.2** is (4*S*,5*S*,6*R*) configured.
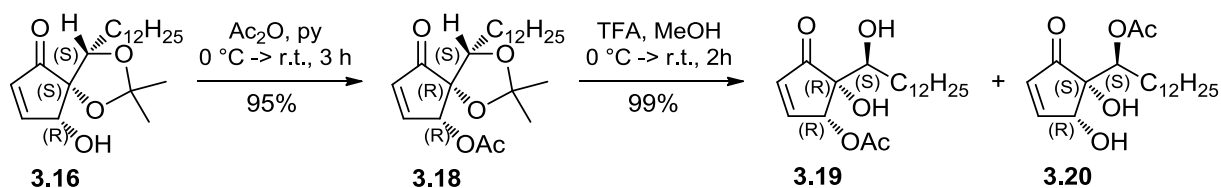
Scheme 3.3. Synthesis of acetylated derivatives of (–)-**3.2**.
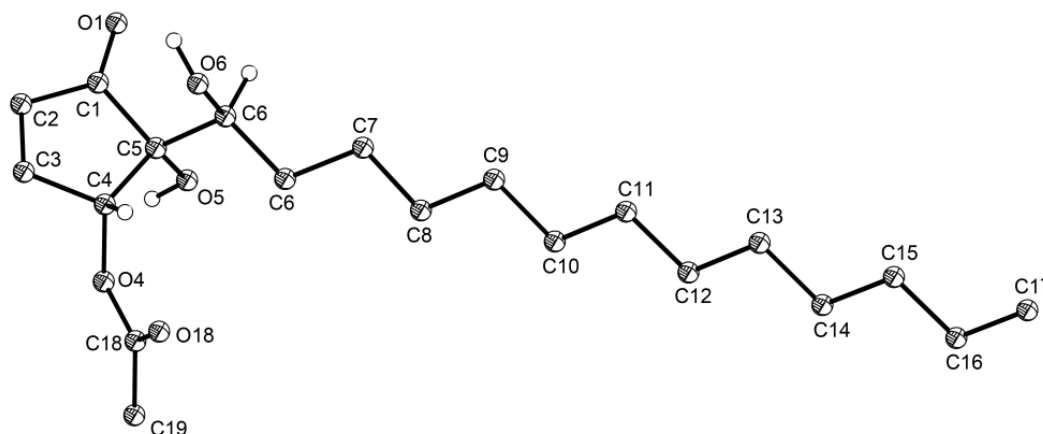
Fig. 3.2. Molecular structure of the acetylated hygrophorone **3.19** from X-ray crystallography.

For the elucidation of the relative configuration of the isolated hygrophorone B[12], the NMR spectra of the synthetic hygrophorones were compared to those of the natural product (Fig. 3.3). This comparison revealed that the ^{1}H and ^{13}C chemical shifts as well as the ^{1}H,^{1}H coupling constants of synthetic (+)-**3.2** and (–)-**3.2** are in good agreement with those of natural hygrophorone B[12]. Nevertheless, for an unambiguous determination of the absolute configuration of hygrophorone B[12], a comparison of the optical rotation values was necessary. The optical rotation value obtained for (+)-**3.2** is in the same range as the corresponding value of the isolated natural product, whereas (–)-**3.2** shows an opposite optical rotation (see also Fig. 3.3). Therefore, it can be concluded that the absolute configuration of natural hygrophorone B[12] is identical to the synthetic hygrophorone (+)-**3.2**, which is (4*S*,5*S*,6*R*) configured.
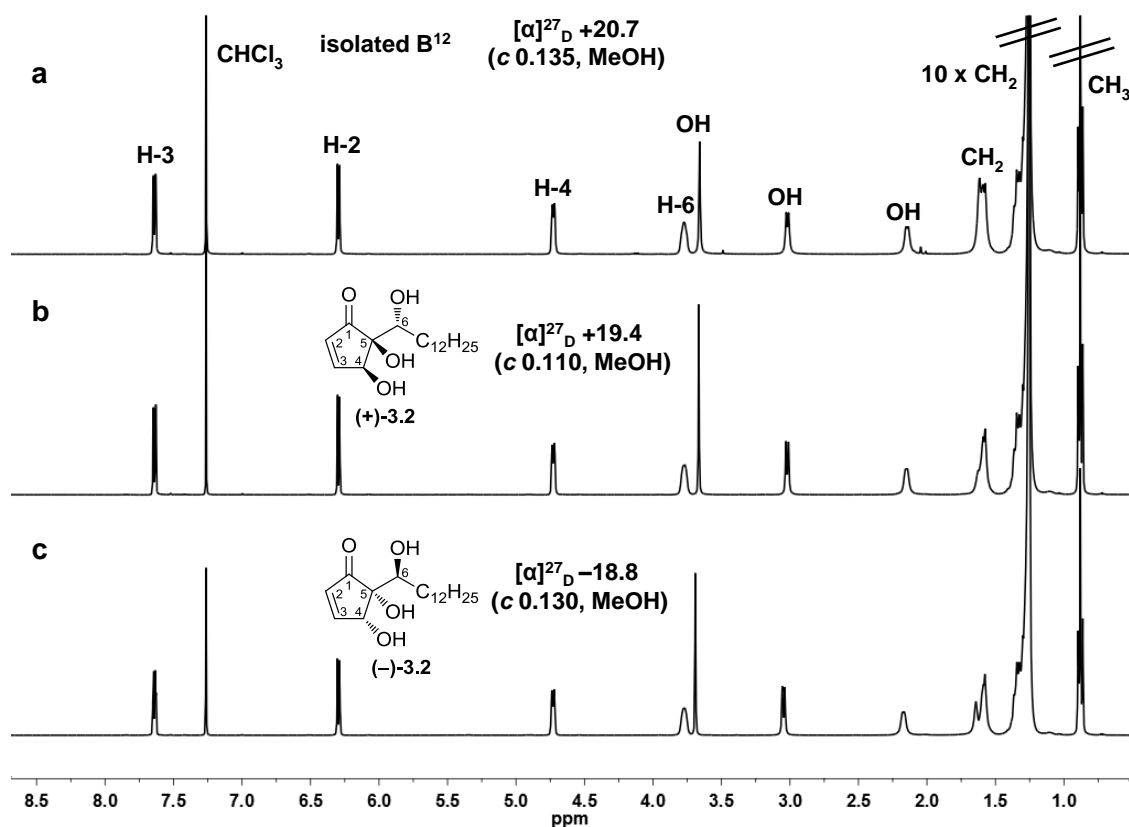
Fig. 3.3. Comparison of ¹H NMR spectra and optical rotation values of isolated hygrophorone B[12] (spectrum a) with synthetic hygrophorones (+)-**3.2** (b) and (–)-**3.2** (c).

3.3 Conclusions

Overall, the novel hygrophorone B^{12} ((+)-**3.2**) could be isolated, and its total synthesis was accomplished in nine steps with an overall yield of 12%. The formation of all of the stereocenters could be controlled by the stereogenic center at the β-position of the starting dihydroxy carboxylate **3.8**, allowing the determination of the relative and absolute configuration of the hygrophorones B for the first time. The approach presented herein offers several other opportunities. The stereodifferentiating step can be carried out with AD-mix-α, leading to (–)-**3.2**, or with AD-mix-β, leading to the corresponding enantiomer (+)-**3.2**. This offers the possibility of accessing both stereoisomers for biological studies. Diastereomers are also formed, and the use of different aldol protocols (open shell) may allow the synthesis of the *trans*-configured dihydroxy congeners as the major diastereomers.

3.4 Experimental Section

General Experimental Procedures. Unless otherwise stated, all chemicals and solvents were obtained commercially and were used without further purification. The ¹H and ¹³C NMR spectra were recorded on a Varian MERCURY-VX 400 system at 400 MHz (¹H) and 100 MHz (¹³C). 2D NMR spectra (HSQC, HMBC, COSY, NOESY) were obtained from an Agilent VNMRS 600

system at 600 MHz (^{1}H) and 150 MHz (^{13}C). Chemical shifts are reported in δ values (ppm) and referenced to tetramethylsilane (TMS) as internal standard (δ 0 ppm, ^{1}H) or CDCl$_3$ (δ 77.0 ppm, ^{13}C). High resolution ESI mass spectra were obtained from a Bruker Apex III Fourier transform ion cyclotron resonance (FT-ICR) mass spectrometer (Bruker Daltonics, Billerica, USA) equipped with an Infinity™ cell, a 7.0 Tesla superconducting magnet (Bruker, Karlsruhe, Germany), an RF-only hexapole ion guide and an external electrospray ion source (Agilent, off axis spray). The sample solutions were introduced continuously *via* a syringe pump with a flow rate of 120 µl h^{-1}. Determinations of melting points were accomplished with a Leica DM LS2 microscope (without correction). The specific optical rotations were determined using a Jasco DIP-2000 Digital Polarimeter. Data for X-ray diffraction analyses of single crystals were collected on a Stoe-IPDS diffractometer at 200 K using Mo Kα radiation (λ = 0.71073 Å, graphite monochromator). Purification of the crude products by column chromatography was performed on silica gel 60 (230–400 mesh, 40–63 µm, Merck) or Sephadex LH 20 (Fluka), while TLC was performed on silica gel coated aluminium foils (silica gel 60 F$_{254}$ with fluorescence indicator, Merck). Preparative HPLC was carried out with a Knauer system equipped with a WellChrom K-1001 pump and a WellChrom K-2501 UV detector using a ODS-A column with fully endcapped C18 phase (5 µm, 150 × 10 mm ID, YMC, USA), using H$_2$O (A) and CH$_3$CN (B) as eluents (linear gradient: 0–20 min, 55–70% B, flow rate 3.5 ml/min).

Fungal Material. Fruiting bodies of *Hygrophorus abieticola* Krieglst. ex Gröger & Bresinsky were collected under *Abies alba* near Kelheim, Bavaria, Germany (October 11, 2007, leg./det. A. Bresinsky). A voucher specimen (coll. 57/07) is deposited at the Leibniz Institute of Plant Biochemistry (IPB), Halle, Germany.

Extraction and isolation of hygrophorone B^{12} ((+)-3.2). Frozen fruiting bodies of *H. abieticola* (2.5 kg) were macerated using a blender and extracted with ethyl acetate (3 × 3 l). The slight yellow solution was evaporated *in vacuo* to dryness. The crude extract (20.2 g) was separated by column chromatography on silica gel (450 × 45 mm) using chloroform/methanol (100:0→0:100) to obtain 10 fractions (A1–A10, each 50 ml). Fraction A6 (3.05 g) was further purified by size exclusion chromatography on Sephadex LH 20 (400 × 40 mm, dichloromethane/methanol 1:1) yielding 7 fractions (B1–B7). Fraction B5 (1.4 g) was further purified by silica gel column chromatography (450 × 45 mm) eluting with *n*-hexane/ethyl acetate 1:1 to afford 230 fractions (each 20 ml). Fractions 173–180 were combined (32.3 mg) and finally purified by preparative HPLC to yield (+)-3.2 as a colorless solid (t$_R$ 14.2 min, 20.1 mg), m.p. 84 °C; TLC R_f 0.29 (*n*-hexane/ethyl acetate 1:1); [α]^{27}$_D$ +20.7 (*c* 0.135, MeOH); ^{1}H NMR (400 MHz, CDCl$_3$) δ = 7.64 (dd, *J* = 6.1, 2.3 Hz, 1H, *H*-3), 6.30 (dd, *J* = 6.1, 1.2 Hz,1H, *H*-2), 4.73 (d, *J* = 6.0 Hz, 1H, *H*-4), 3.78 (m, 1H, *H*-6), 3.66 (s, 1H, 6-O*H*), 3.02 (d, *J* = 7.0 Hz, 1H, 4-O*H*), 2.14 (br d, *J* = 6.6 Hz, 1H, 5-O*H*), 1.65–1.54 (m, 2H, C*H*$_2$), 1.39–1.20 (m, 20H, 10 x C*H*$_2$) 0.88 (t, *J* = 7.0 Hz, 3H, C*H*$_3$) ppm; ^{13}C NMR (100 MHz, CDCl$_3$) δ = 207.2 (*C*-1), 163.5 (*C*-3), 133.5 (*C*-2), 75.9 (*C*-5), 73.3

(C-6), 71.4 (C-4), 31.9, 31.3, 29.6, 29.6, 29.6, 29.6, 29.5, 29.4, 29.3, 26.1, 22.7 (11 x CH_2), 14.1 (C-18); HRMS (ESI) calcd. for $C_{18}H_{31}O_4^-$ 311.2228 [M–H]$^-$, found 311.2224.

Ethyl (2R,3S)-2,3-dihydroxypentadecanoate ((–)-3.7): Potassium osmate(VI) dihydrate (40 mg, 0.11 mmol), hydroquinine 1,4-phthalazinediyl diether (DHQ)$_2$PHAL (169 mg, 0.22 mmol), methanesulfonamide (2.19 g, 23.0 mmol), potassium carbonate (9.55 g, 69.1 mmol), and potassium hexacyanoferrate (III) (22.8 g, 69.1 mmol) were consecutively added to t-BuOH/H$_2$O (150 ml, 1:1) and the resulting mixture was cooled to 0 °C with stirring. Afterwards a solution of Ethyl (2E)-pentadec-2-enoate **3.6** (6.18 g, 23.0 mmol) in t-BuOH/H$_2$O (150 ml, 1:1) was added dropwise and stirring was continued at 0 °C for 20 hours until TLC indicated completion of the reaction (Fernandes and Kumar, 2003, 2002). The reaction was quenched with a saturated aq. sodium sulfite solution (100 ml) and extracted with dichloromethane (5 × 200 ml) after additional 30 min of stirring. The combined organic extracts were dried over sodium sulfate, filtered, evaporated to dryness, and purified *via* column chromatography (petroleum ether/ethyl acetate 1:1) which afforded (–)-**3.7** as a colorless solid (6.82 g, 98%), m.p. 71 °C; TLC R_f 0.67 (petroleum ether/ethyl acetate 2:1); $[\alpha]^{21}_D$ –9.1 (c 1.410, MeOH); ^{1}H NMR (400 MHz, CDCl$_3$) δ = 4.29 (q, J = 7.1 Hz, 2H, OCH_2CH$_3$), 4.08 (d, J = 2.0 Hz, 1H, H-2), 3.88 (td, J = 2.0, 7.1 Hz, 1H, H-3), 3.12 (br s, 1H, OH), 2.03 (br s, 1H, OH), 1.61 (m, 2H, CH_2), 1.46 (m, 2H, H-5), 1.35–1.21 (m, 21 H, 9 x CH_2 + OCH$_2$CH_3), 0.88 (t, J = 6.8 Hz, 3H, CH_3) ppm; ^{13}C NMR (100 MHz, CDCl$_3$): δ = 173.7 (C=O), 73.0 (C-2), 72.5 (C-3), 62.0 (OCH$_2$CH$_3$), 33.8, 31.9, 29.6, 29.6, 29.6, 29.5, 29.5, 29.5, 29.3, 25.7, 22.6 (11 x CH$_2$), 14.1 (OCH$_2$$CH_3$), 14.1 ($CH_3$) ppm; HRMS (ESI) calcd. for $C_{17}H_{34}NaO_4^+$ 325.2349 [M+Na]$^+$, found 325.2348.

Ethyl (2S,3R)-2,3-dihydroxypentadecanoate ((+)-3.7): Potassium osmate(VI) dihydrate (40 mg, 0.11 mmol), hydroquinidine 1,4-phthalazinediyl diether (DHQD)$_2$PHAL (169 mg, 0.22 mmol), methanesulfonamide (2.25 g, 23.7 mmol), potassium carbonate (9.82 g, 71.1 mmol), and potassium hexacyanoferrate (III) (23.4 g, 71.1 mmol) were consecutively added to t-BuOH/H$_2$O (150 ml, 1:1) and the resulting mixture was cooled to 0 °C with stirring. Afterwards a solution of Ethyl (2E)-pentadec-2-enoate 6 (6.36 g, 23.6 mmol) in t-BuOH/H$_2$O (150 ml, 1:1) was added dropwise and stirring was continued at 0 °C for 20 hours until TLC indicated completion of the reaction (Fernandes and Kumar, 2003, 2002). The reaction was quenched with a saturated aq. sodium sulfite solution (100 ml) and extracted with dichloromethane (5 × 200 ml) after additional 30 min of stirring. The combined organic extracts were dried over sodium sulfate, evaporated to dryness and purified *via* column chromatography (petroleum ether/ethyl acetate 1:1) which afforded (+)-**3.7** as a colorless solid (6.830 g, 95%), m.p. 69 °C; TLC R_f 0.67 (petroleum ether/ethyl acetate 2:1); $[\alpha]^{21}_D$ +9.0 (c 0.945, MeOH); ^{1}H NMR (400 MHz, CDCl$_3$) δ = 4.29 (q, J = 7.1 Hz, 2H, OCH_2CH$_3$), 4.08 (d, J = 2.0 Hz, 1H, H-2), 3.88 (t, J = 6.4 Hz, 1H, H-3), 3.11 (d, J = 4.9 Hz, 1H, OH), 1.98 (br s, 1H, OH), 1.60 (m, 2H, CH_2), 1.48 (m, 2H, CH_2), 1.35–1.23 (m, 21 H, 9 x CH_2 + OCH$_2$CH_3), 0.88 (t, J = 6.8 Hz, 3H, CH_3) ppm; ^{13}C NMR (100 MHz, CDCl$_3$)

δ = 173.7 (*C*=O), 73.0 (*C*-2), 72.5 (*C*-3), 62.1 (O*C*H$_2$CH$_3$), 33.8, 31.9, 29.6, 29.6, 29.6, 29.5, 29.5, 29.5, 29.3, 25.7, 22.7 (11 x *C*H$_2$), 14.1 (OCH$_2$*C*H$_3$), 14.1 (*C*H$_3$) ppm; HRMS (ESI) calcd. for C$_{17}$H$_{34}$NaO$_4^+$ 325.2349 [M+Na]$^+$, found 325.2348.

Ethyl (4*R*,5*S*)-2,2-dimethyl-5-dodecyl-1,3-dioxolane-4-carboxylate (3.8): To a solution containing (–)-**3.7** (0.80 g, 2.64 mmol) and 2,2-diethoxypropane (1.7 ml, 10.6 mmol) in dichloromethane (70 ml) was added *p*-toluenesulfonic acid monohydrate (50 mg, 0.26 mmol) and the resulting solution was stirred at room temperature for 24 hours. After TLC indicated completion of the reaction a saturated aq. sodium hydrogen carbonate solution (7 ml) and ethyl acetate (50 ml) were consecutively added, the organic phase was separated and the aqueous layer was extracted twice with ethyl acetate (25 ml). The combined organic extracts were dried over sodium sulfate, filtered and all volatiles were removed under reduced pressure. Purification of the resdiue by column chromatography (petroleum ether/ethyl acetate 5:1) afforded **3.8** as a pale yellow oil (0.85 g, 94%). TLC R_f 0.80 (petroleum ether/ethyl acetate 5:1); [α]$^{21}_D$ –40.4 (*c* 0.056, MeOH); ^{1}H NMR (400 MHz, CDCl$_3$) δ = 4.24 (m, 2H, OC*H$_2$*CH$_3$), 4.11 (m, 2H, *H*-4 + *H*-5), 1.80–1.59 (m, 2H, C*H$_2$*), 1.55–1.36 (m, 2H, C*H$_2$*), 1.47 (s, 3H, C*H$_3$* acetal), 1.44 (s, 3H, C*H$_3$* acetal), 1.36–1.21 (m, 21 H, 9 x C*H$_2$* + OCH$_2$C*H$_3$*), 0.88 (t, *J* = 6.8 Hz, 3H, C*H$_3$*) ppm; ^{13}C NMR (100 MHz, CDCl$_3$) δ = 171.0 (*C*=O), 110.7 (*C*(CH$_3$)$_2$ acetal), 79.2 (*C*-4), 79.1 (*C*-5), 61.2 (O*C*H$_2$CH$_3$), 33.5, 31.9, 29.6 (3 x *C*H$_2$), 29.6 (2 x *C*H$_2$), 29.5, 29.5, 29.5, 29.3 (4 x *C*H$_2$), 27.2 (*C*H$_3$ acetal), 25.7 (*C*H$_3$ acetal), 25.6, 22.7 (2 x *C*H$_2$), 14.1 (OCH$_2$*C*H$_3$), 14.1 (*C*H$_3$) ppm; HRMS (ESI) calcd. for C$_{20}$H$_{38}$NaO$_4^+$ 365.2662 [M+Na]$^+$, found 365.2663.

Aldol reaction of acetal 8 with aldehyde 9 for precursors 3.10 and 3.11. To a solution of diisopropylamine (0.71 ml, 4.96 mmol) in dry THF (150 ml) was added *n*-butyllithium (2.0 ml, 2.5 M in hexane, 4.96 mmol) in *n*-hexane at 0 °C and the mixture was stirred for 30 min. Afterwards the reaction mixture was cooled to –78 °C and stirred for additional 30 min, whereupon acetal **3.8** (851 mg, 2.48 mmol), dissolved in dry THF (2 ml), was added dropwise. After further 30 min of stirring, aldehyde **3.9** (618 mg, 3.72 mmol) in dry THF (2 ml), was slowly added. Stirring was continued for 3 h at –78 °C and then the reaction was quenched with saturated aq. sodium hydrogen carbonate solution (5 ml). Afterwards, ethyl acetate (20 ml) was added, the organic phase was separated and the aqueous layer was extracted with ethyl acetate (3 × 20 ml). The combined organic extracts were dried over sodium sulfate and evaporated to dryness. After purification of the resdiue by column chromatography (dichloromethane) the two diastereomers **3.10** and **3.11** were obtained in a 4:1 ratio.

Ethyl (4*S*,5*S*)-5-dodecyl-4-((*R*)-1-hydroxy-3-(phenylthio)propyl)-2,2-dimethyl-1,3-dioxolane-4-carboxylate (3.10): pale yellow oil (860 mg, 65%); TLC R_f 0.59 (dichloromethane); ^{1}H NMR (400 MHz, CDCl$_3$) δ = 7.37–7.22 (m, 4H, *o*-*H* + *m*-*H* Ph), 7.16 (m, 1H, *p*-*H* Ph), 4.31 (m, 1H, *H*-5), 4.10 (m, 2H, OC*H$_2$*CH$_3$), 4.01 (td, *J* = 10.0, 3.1 Hz, 1H, C*H*OH), 3.23–2.97 (br m, 2H,

CH$_2$CH_2S), 1.96 (d, J = 10.4 Hz, 1H, OH), 1.85–1.72 (m, 2H, CH_2), 1.65–1.48 (m, 2H, CH_2CH$_2$S), 1.59 (s, 3H, CH_3 acetal), 1.40 (s, 3H, CH_3 acetal), 1.37–1.17 (m, 23 H, 10 x CH_2 + OCH$_2$CH_3), 0.88 (t, J = 6.8 Hz, 3H, CH_3) ppm; ^{13}C NMR (100 MHz, CDCl$_3$) δ = 171.1 (C=O), 136.1 (*i-C* Ph), 129.2 + 128.8 (*o-C* + *m-C* Ph), 125.9 (*p-C* Ph), 109.8 (C(CH$_3$)$_2$ acetal), 88.6 (C-4), 79.1 (C-5), 69.7 (COH), 61.2 (OCH$_2$CH$_3$), 32.7, 31.9, 30.6, 30.3, 29.6, 29.6, 29.6, 29.6, 29.5, 29.4, 29.3, 27.0 (12 x CH$_2$), 26.8 (CH$_3$ acetal), 26.6 (CH$_3$ acetal), 22.7 (CH$_2$), 14.1 (OCH$_2$$CH_3$), 14.0 ($CH_3$) ppm; HRMS (ESI) calcd. for C$_{29}$H$_{48}$NaO$_5$S$^+$ 531.3115 [M+Na]$^+$, found 531.3104.

Ethyl (4*S*,5*S*)-5-dodecyl-4-((*S*)-1-hydroxy-3-(phenylthio)propyl)-2,2-dimethyl-1,3-dioxolane-4-carboxylate (3.11): pale yellow oil (191 mg, 15%); TLC R_f 0.21 (dichloromethane); ^{1}H NMR (400 MHz, CDCl$_3$) δ = 7.37–7.23 (m, 4H, *o-H* + *m-H* Ph), 7.16 (m, 1H, *p-H* Ph), 4.26 (m, 2H, OCH_2CH$_3$), 4.09 (dd, J = 10.2, 2.9 Hz, 1H, H-5), 4.01 (t, J = 9.6 Hz, 1H, CHOH), 3.25–3.01 (br m, 2H, CH$_2$CH_2S), 2.32 (d, J = 10.0 Hz, 1H, OH), 2.07–1.44 (br m, 6H, 3 x CH_2), 1.42 (s, 3H, CH_3 acetal), 1.40 (s, 3H, CH_3 acetal), 1.34–1.22 (m, 21 H, 9 x CH_2 + OCH$_2$CH_3), 0.88 (t, J = 6.8 Hz, 3H, CH_3) ppm; ^{13}C NMR (100 MHz, CDCl$_3$) δ = 172.8 (C=O), 136.2 (*i-C* Ph), 128.9 + 128.9 (*o-C* + *m-C* Ph), 125.8 (*p-C* Ph), 109.6 (C(CH$_3$)$_2$ acetal), 86.5 (C-4), 80.9 (C-5), 71.7 (COH), 61.6 (OCH$_2$CH$_3$), 32.4, 31.9, 30.1, 29.7, 29.6, 29.6, 29.6, 29.5, 29.4, 29.3, 29.0, 27.3 (12 x CH$_2$), 26.9 (CH$_3$ acetal), 24.7 (CH$_3$ acetal), 22.7 (CH$_2$), 14.1 (OCH$_2$$CH_3$ + CH$_3$) ppm; HRMS (ESI) calcd. for C$_{29}$H$_{48}$NaO$_5$S$^+$ 531.3115 [M+Na]$^+$, found 531.3102.

Sulfoxidation of 3.10 and 3.11 with sodium periodate. To a solution of the aldol product **3.10** or **3.11** (1 eq.) in methanol/water (10 ml/mmol of **3.10** or **3.11**, 19:1) cooled to 0 °C, sodium periodate (1.1 eq.) was added and the reaction was stirred for 10 min. Afterwards the mixture was warmed to room temperature and stirred for additional 24 hours. After completion of the reaction indicated by TLC analysis the solvent was removed *in vacuo* and the crude product was purified by column chromatography (*n*-hexane/ethyl acetate 2:1) to afford the sulfoxide **3.12** or **3.13**.

Ethyl (4*S*,5*S*)-5-dodecyl-4-((1*R*)-1-hydroxy-3-(phenylsulfinyl)propyl)-2,2-dimethyl-1,3-dioxolane-4-carboxylate (3.12): colorless oil (557 mg, 93%); TLC R_f 0.17 (*n*-hexane/ethyl acetate 2:1); [α]$^{24}_D$ –5.1 (*c* 0.540, MeOH); ^{1}H NMR (400 MHz, CDCl$_3$) δ = 7.61 (m, 2H, *o-H* Ph), 7.51 (m, 3H, *m-H* + *p-H* Ph), 4.38 (m, 1H, H-5), 4.17 (m, 2H, OCH_2CH$_3$), 3.92 (dd, J = 26.3, 8.9 Hz, 1H, CHOH), 3.22–2.87 (br m, 2H, CH$_2$CH_2S), 2.04 (s, 1H, OH), 2.02–1.75 (m, 2H, CH_2), 1.63–1.47 (m, 4H, 2 x CH_2), 1.42 (s, 3H, CH_3 acetal), 1.39–1.20 (m, 24 H, 9 x CH_2 + OCH$_2$CH_3 + CH_3 acetal), 0.88 (t, J = 6.8 Hz, 3H, CH_3) ppm; ^{13}C NMR (100 MHz, CDCl$_3$) δ = 171.5, 171.4 (C=O), 143.2, 142.9 (*i-C* Ph), 131.0, 131.0 (*p-C* Ph), 129.2, 129.2 (*m-C* Ph), 124.2, 124.1 (*o-C* Ph), 109.9, 109.9 (C(CH$_3$)$_2$ acetal), 88.5, 88.4 (C-4), 79.1, 79.0 (C-5), 69.3, 68.9 (COH), 61.3, 61.2 (OCH$_2$CH$_3$), 53.7, 53.2 (CH$_2$$CH_2$S), 31.9, 30.6, 29.6, 29.6, 29.6, 29.5, 29.5, 29.3 (8 x CH$_2$), 26.9, 26.9 (CH$_2$CH$_2$S), 26.8, 26.8 (CH$_3$ acetal), 26.5 (CH$_3$ acetal), 26.4, 25.8, 22.7 (3 x CH$_2$),

14.2, 14.1 (OCH$_2$CH$_3$ + CH$_3$) ppm; HRMS (ESI) calcd. for C$_{29}$H$_{48}$NaO$_6$S$^+$ 547.3064 [M+Na]$^+$, found 547.3064.

Ethyl (4*S*,5*S*)-5-dodecyl-4-((1*S*)-1-hydroxy-3-(phenylsulfinyl)propyl)-2,2-dimethyl-1,3-dioxolane-4-carboxylate (3.13): colorless oil (113 mg, 71%); TLC R_f 0.14 (*n*-hexane/ethyl acetate 2:1); [α]^{24}$_D$ +4.8 (*c* 0.370, MeOH); ^{1}H NMR (400 MHz, CDCl$_3$) δ = 7.61 (m, 2H, *o-H* Ph), 7.52 (m, 3H, *m-H* + *p-H* Ph), 4.25 (m, 2H, OCH$_2$CH$_3$), 4.14 (m, 1H, *H*-5), 3.87 (ddd, *J* = 48.8, 10.2, 1.9 Hz, 1H, C*H*OH), 3.25–2.86 (br m, 2H, CH$_2$CH$_2$S), 2.04 (s, 1H, O*H*), 1.89–1.71 (m, 2H, C*H$_2$*), 1.68–1.42 (m, 4H, 2 x C*H$_2$*), 1.40 (s, 3H, C*H$_3$* acetal), 1.38–1.20 (m, 24 H, 9 x C*H$_2$* + OCH$_2$C*H$_3$* + C*H$_3$* acetal), 0.88 (t, *J* = 6.7 Hz, 3H, C*H$_3$*) ppm; ^{13}C NMR (100 MHz, CDCl$_3$) δ = 172.5, 172.3 (*C*=O), 143.2, 142.5 (*i-C* Ph), 131.0, 131.0 (*p-C* Ph), 129.2, 129.2 (*m-C* Ph), 124.3, 124.1 (*o-C* Ph), 109.6, 109.5 (*C*(CH$_3$)$_2$ acetal), 86.5, 86.4 (*C*-4), 80.8, 80.7 (*C*-5), 71.7, 71.5 (*C*OH), 61.6, 61.5 (O*C*H$_2$CH$_3$), 54.0, 53.3 (*C*H$_2$CH$_2$S), 31.9, 29.7, 29.6, 29.6, 29.5, 29.4, 29.3, 29.2, 29.1 (9 x *C*H$_2$), 27.4, 27.3 (*C*H$_2$CH$_2$S), 27.1, 26.9 (*C*H$_3$ acetal), 26.3, 26.0 (*C*H$_2$), 24.7. 24.7 (*C*H$_3$ acetal), 22.7 (*C*H$_2$), 14.2, 14.1 (OCH$_2$*C*H$_3$ + *C*H$_3$) ppm; HRMS (ESI) calcd. for C$_{29}$H$_{48}$NaO$_6$S$^+$ 547.3064 [M+Na]$^+$, found 547.3068.

Cyclization of 3.12 and 3.13 with LDA. To an ice-cold solution of diisopropylamine (3.2 eq.) in dry THF (5 ml/mmol diisopropylamine) was slowly added a solution of *n*-butyllithium (3.2 eq., 2.5 M in *n*-hexane) and the mixture was stirred for 30 min. After cooling to –78 °C sulfoxide **3.12** or **3.13** (1 eq.) in dry THF (5 ml/mmol of **3.12** or **3.13**), was added dropwise and the resulting mixture was stirred for 2 hours. Afterwards the reaction was slowly warmed to room temperature and stirring was continued for 2 hours. Saturated aq. sodium hydrogen carbonate solution (5 ml/mmol of **3.12** or **3.13**) and ethyl acetate (30 ml/mmol of **3.12** or **3.13**) were consecutively added, the organic phase was separated and the aqueous layer was extracted with ethyl acetate (3x 30 ml/mmol of **3.12** or **3.13**). The combined organic extracts were dried over sodium sulfate, filtered and evaporated to dryness. Purification of the residue by column chromatography (*n*-hexane/ethyl acetate 3:2) afforded the two diastereomers of cyclopentanone **3.14** or **3.15**.

(4*S*,5*S*,9*R*)-4-dodecyl-9-hydroxy-2,2-dimethyl-7-(phenylsulfinyl)-1,3-dioxaspiro [4.4]nonan-6-one (3.14)

Data for first diastereomer of **3.14**: yellow oil (168 mg, 35%); TLC R_f 0.49 (*n*-hexane/ethyl acetate 3:2); [α]^{25}$_D$ –308.7 (*c* 0.990, MeOH); ^{1}H NMR (400 MHz, CDCl$_3$) δ = 7.58 (m, 2H, *o-H* Ph), 7.52 (m, 3H, *m-H* + *p-H* Ph), 4.21 (dd, *J* = 3.9, 2.9 Hz, 1H, *H*-4), 4.12 (m, 1H, *H*-9), 3.48 (t, *J* = 9.5 Hz, 1H, *H*-7), 2.62 (ddd, *J* = 14.4, 10.1, 4.4 Hz, 1H, *H*-8a), 2.04 (s, 1H, O*H*), 1.84 (ddd, *J* = 14.4, 9.0, 2.7 Hz, 1H, *H*-8b), 1.59 (s, 3H, C*H$_3$* acetal), 1.54–1.48 (m, 2H, C*H$_2$*), 1.43 (s, 3H, C*H$_3$* acetal), 1.35–1.21 (m, 20 H, 10 x C*H$_2$*), 0.88 (t, *J* = 6.8 Hz, 3H, C*H$_3$*) ppm; ^{13}C NMR (100 MHz, CDCl$_3$) δ = 207.3 (*C*=O), 141.6 (*i-C* Ph), 131.3 (*p-C* Ph), 129.3 (*m-C* Ph), 123.8 (*o-C* Ph), 111.4 (*C*(CH$_3$)$_2$ acetal), 89.6 (*C*-5), 81.4 (*C*-4), 72.2 (*C*-9), 68.0 (*C*-7), 31.9, 31.0, 29.7, 29.6, 29.6,

29.6, 29.5, 29.3, 29.2 (9 x CH_2), 28.0 (CH_3 acetal), 27.6 (CH_3 acetal), 26.5, 22.7, 21.9 (2 x CH_2 + C-8), 14.1 (CH_3) ppm; HRMS (ESI) calcd. for $C_{27}H_{43}O_5S^+$ 479.2826 $[M+H]^+$, found 479.2823.

Data for second diastereomer of **3.14**: yellow oil (147 mg, 31%); TLC R_f 0.27 (*n*-hexane/ethyl acetate 3:2); $[\alpha]^{25}_D$ +186.4 (*c* 1.270, MeOH); ^{1}H NMR (400 MHz, CDCl$_3$) δ = 7.65 (m, 2H, *o-H* Ph), 7.56 (m, 3H, *m-H* + *p-H* Ph), 4.15–4.03 (m, 2H, *H*-4+*H*-9), 3.40 (dd, *J* = 9.9, 4.5 Hz, 1H, *H*-7), 2.49 (ddd, *J* = 15.7, 7.9, 4.0 Hz, 1H, *H*-8a), 2.19 (ddd, *J* = 15.3, 10.0, 5.0 Hz, 1H, *H*-8b), 2.04 (s, 1H, O*H*), 1.61 (s, 3H, C*H*$_3$ acetal), 1.56–1.48 (m, 2H, C*H*$_2$), 1.46 (s, 3H, C*H*$_3$ acetal), 1.33–1.19 (m, 20 H, 10 x C*H*$_2$), 0.88 (t, *J* = 6.9 Hz, 3H, C*H*$_3$) ppm; ^{13}C NMR (100 MHz, CDCl$_3$) δ = 207.3 (*C*=O), 141.6 (*i-C* Ph), 131.6 (*p-C* Ph), 129.4 (*m-C* Ph), 124.3 (*o-C* Ph), 111.4 (*C*(CH$_3$)$_2$ acetal), 90.5 (*C*-5), 80.5 (*C*-4), 71.1 (*C*-9), 68.3 (*C*-7), 31.9, 31.0, 29.6, 29.6, 29.5, 29.4, 29.4, 29.3 (9 x C*H*$_2$), 27.4 (*C*H$_3$ acetal), 26.5 (*C*H$_3$ acetal), 26.8, 26.0, 22.6 (2 x C*H*$_2$ + *C*-8), 14.1 (*C*H$_3$) ppm; HRMS (ESI) calcd. for $C_{27}H_{43}O_5S^+$ 479.2826 $[M+H]^+$, found 479.2824.

(4*S*,5*S*,9*S*)-4-dodecyl-9-hydroxy-2,2-dimethyl-7-(phenylsulfinyl)-1,3-dioxaspiro[4.4]nonan-6-one (3.15)

Data for first diastereomer of **3.15**: yellow oil (21.0 mg, 32%); TLC R_f 0.76 (*n*-hexane/ethyl acetate 3:2); $[\alpha]^{25}_D$ +128.4 (*c* 0.400, MeOH); ^{1}H NMR (400 MHz, CDCl$_3$) δ = 7.57 (m, 5H, *H* Ph), 4.51 (dd, *J* = 10.9, 3.1 Hz, 1H, *H*-4), 4.04 (d, J = 3.5 Hz, 1H, *H*-9), 3.77 (dd, *J* = 11.0, 2.0 Hz, 1H, *H*-7), 2.55 (ddd, *J* = 15.3, 11.1, 4.0 Hz, 1H, *H*-8a), 2.04 (s, 1H, O*H*), 1.94 (m, 1H, *H*-8b), 1.72–1.60 (m, 2H, C*H*$_2$), 1.60–1.48 (m, 2H, C*H*$_2$), 1.39 (s, 3H, C*H*$_3$ acetal), 1.36–1.20 (m, 21 H, 9 x C*H*$_2$ + C*H*$_3$ acetal), 0.88 (t, *J* = 6.8 Hz, 3H, C*H*$_3$) ppm; ^{13}C NMR (100 MHz, CDCl$_3$) δ = 207.3 (*C*=O), 140.3 (*i-C* Ph), 131.5 (*p-C* Ph), 129.6 (*m-C* Ph), 124.0 (*o-C* Ph), 110.2 (*C*(CH$_3$)$_2$ acetal), 88.0 (*C*-5), 76.6 (*C*-4), 69.0 (*C*-9), 68.1 (*C*-7), 31.9, 31.0, 29.7, 29.6, 29.6, 29.6, 29.6, 29.5, 29.3 (9 x C*H*$_2$), 28.9 (*C*H$_3$ acetal), 26.3 (*C*H$_3$ acetal), 28.1, 26.3, 22.7 (2 x C*H*$_2$ + *C*-8), 14.1 (*C*H$_3$) ppm; HRMS (ESI) calcd. for $C_{27}H_{43}O_5S^+$ 479.2826 $[M+H]^+$, found 479.2817.

Data for second diastereomer of **3.15**: yellow oil (23.5 mg, 35%); TLC R_f 0.45 (*n*-hexane/ethyl acetate 3:2); $[\alpha]^{25}_D$ −306.1 (*c* 0.380, MeOH); ^{1}H NMR (400 MHz, CDCl$_3$) δ = 7.61 (m, 2H, *o-H* Ph), 7.52 (m, 3H, *m-H* + *p-H* Ph), 4.36 (dd, *J* = 10.0, 4.1 Hz, 1H, *H*-4), 4.33 (t, J = 3.4 Hz, 1H, *H*-9), 3.57 (t, *J* = 9.0 Hz, 1H, *H*-7), 2.83 (ddd, *J* = 13.7, 9.4, 4.2 Hz, 1H, *H*-8a), 2.09 (br s, 1H, O*H*), 1.83 (ddd, *J* = 13.9, 8.7, 2.8 Hz, *H*-8b), 1.78–1.67 (m, 2H, C*H*$_2$), 1.62–1.51 (m, 2H, C*H*$_2$), 1.45 (s, 3H, C*H*$_3$ acetal), 1.35 (s, 3H, C*H*$_3$ acetal), 1.32–1.20 (m, 18 H, 9 x C*H*$_2$), 0.88 (t, *J* = 6.8 Hz, 3H, C*H*$_3$) ppm; ^{13}C NMR (100 MHz, CDCl$_3$) δ = 206.8 (*C*=O), 142.5 (*i-C* Ph), 131.3 (*p-C* Ph), 129.2 (*m-C* Ph), 124.2 (*o-C* Ph), 110.5 (*C*(CH$_3$)$_2$ acetal), 86.5 (*C*-5), 77.5 (*C*-4), 72.3 (*C*-9), 68.1 (*C*-7), 31.9, 30.5, 29.6, 29.6, 29.6, 29.6, 29.5, 29.5, 29.3 (9 x C*H*$_2$), 28.8 (*C*H$_3$ acetal), 26.1 (*C*H$_3$ acetal), 26.8, 26.4, 22.7 (2 x C*H*$_2$ + *C*-8), 14.1 (*C*H$_3$) ppm; HRMS (ESI) calcd. for $C_{27}H_{43}O_5S^+$ 479.2826 $[M+H]^+$, found 479.2821.

Elimination of the sulfoxide moiety with calcium carbonate. To a solution containing cyclopentanone **3.14** or **3.15** (1 eq.) in toluene (20 ml/mmol **3.14** or **3.15**) was added calcium

carbonate (1.1 eq.) and the resulting mixture was refluxed for 1 h. After completion of the reaction as indicated by TLC analysis, all volatile material was removed under reduced pressure and the residue was purified by column chromatography (*n*-hexane/ethyl acetate 7:3) to obtain cyclopentenone **3.16** or **3.17**.

(4*S*,5*S*,9*R*)-4-dodecyl-9-hydroxy-2,2-dimethyl-1,3-dioxaspiro[4.4]non-7-en-6-one (3.16):
colorless solid (216 mg, 81%), m.p. 59 °C; TLC R_f 0.71 (*n*-hexane/ethyl acetate 7:3); $[\alpha]^{24}_D$ −39.2 (*c* 0.150, MeOH); ^{1}H NMR (400 MHz, CDCl$_3$) δ = 7.57 (dd, *J* = 6.2, 2.3 Hz, 1H, *H*-8), 6.26 (dd, *J* = 6.2, 1.2 Hz, 1H, *H*-7), 4.47 (d, *J* = 6.9 Hz, 1H, *H*-9), 4.22 (dd, *J* = 9.1, 4.1 Hz, 1H, *H*-4), 2.91 (d, *J* = 7.3 Hz, 1H, O*H*), 1.75 (br m, 2H, C*H*$_2$), 1.60 (s, 3H, C*H*$_3$ acetal), 1.48 (s, 3H, C*H*$_3$ acetal), 1.43–1.15 (m, 20 H, 10 x C*H*$_2$), 0.88 (t, *J* = 6.9 Hz, 3H, C*H*$_3$) ppm; ^{13}C NMR (100 MHz, CDCl$_3$) δ = 202.6 (*C*=O), 161.9 (*C*-8), 134.5 (*C*-7), 111.5 (*C*(CH$_3$)$_2$ acetal), 82.6 (*C*-4), 80.6 (*C*-2), 72.2 (*C*-4), 31.9, 29.6, 29.6, 29.6, 29.5, 29.5, 29.4, 29.3, 29.1 (9 x *C*H$_2$), 27.3 (*C*H$_3$ acetal), 26.6 (*C*H$_2$), 26.2 (*C*H$_3$ acetal), 22.7 (*C*H$_2$), 14.1 (*C*H$_3$) ppm; HRMS (ESI) calcd. for C$_{21}$H$_{36}$NaO$_4$$^+$ 375.2506 [M+Na]$^+$, found 375.2504.

(4*S*,5*S*,9*S*)-4-dodecyl-9-hydroxy-2,2-dimethyl-1,3-dioxaspiro[4.4]non-7-en-6-one (3.17):
colorless oil (48.3 mg, 73%); TLC R_f 0.54 (*n*-hexane/ethyl acetate 7:3); $[\alpha]^{24}_D$ +19.2 (*c* 0.150, MeOH); ^{1}H NMR (400 MHz, CDCl$_3$) δ = 7.43 (dd, *J* = 6.3, 2.0 Hz, 1H, *H*-8), 6.30 (dd, *J* = 6.3, 1.6 Hz, 1H, *H*-7), 4.98 (s, 1H, *H*-9), 4.50 (dd, *J* = 9.8, 2.8 Hz, 1H, *H*-4), 2.26 (s, 1H, O*H*), 1.65 (s, 3H, C*H*$_3$ acetal), 1.46 (s, 3H, C*H*$_3$ acetal), 1.42–1.19 (br m, 22 H, 11 x C*H*$_2$), 0.88 (t, *J* = 6.9 Hz, 3H, C*H*$_3$) ppm; ^{13}C NMR (100 MHz, CDCl$_3$) δ = 203.1 (*C*=O), 159.5 (*C*-8), 134.4 (*C*-7), 109.8 (*C*(CH$_3$)$_2$ acetal), 89.2 (*C*-5), 78.3 (*C*-4), 75.0 (*C*-9), 31.9, 30.3, 29.6, 29.6, 29.6, 29.5, 29.5, 29.4, 29.3 (9 x *C*H$_2$), 27.3 (*C*H$_3$ acetal), 27.0 (*C*H$_2$), 26.5 (*C*H$_3$ acetal), 22.7 (*C*H$_2$), 14.1 (*C*H$_3$) ppm; HRMS (ESI) calcd. for C$_{21}$H$_{36}$NaO$_4$$^+$ 375.2506 [M+Na]$^+$, found 375.2504.

Deprotection of cyclopentenone 3.16 or 3.17 with trifluoroacetic acid. A solution of **3.16** or **3.17** in trifluoracetic acid (2.5 ml/mmol **3.16** or **3.17**) was stirred for 2 hours at 0 °C. Afterwards all volatiles were removed *in vacuo* and the residue was purified by column chromatography (*n*-hexane/ethyl acetate 1:1) which afforded hygrophorones (−)-**3.2** or (+)-**3.1**.

(4*R*,5*R*)-4,5-dihydroxy-5-((*S*)-1-hydroxytridecyl)cyclopent-2-enone ((−)-3.2): colorless solid (55.4 mg, 43%), m.p. 88 °C; TLC R_f 0.29 (*n*-hexane/ethyl acetate 1:1); $[\alpha]^{27}_D$ −18.8 (*c* 0.130, MeOH); ^{1}H NMR (400 MHz, CDCl$_3$) δ = 7.64 (dd, *J* = 6.1, 2.3 Hz, 1H, *H*-3), 6.30 (dd, *J* = 6.1, 1.1 Hz, 1H, *H*-2), 4.73 (d, *J* = 6.4 Hz, 1H, *H*-4), 3.77 (d, 1H, *J* = 4.1 Hz, *H*-6), 3.69 (s, 1H, O*H*), 3.05 (d, *J* = 7.2 Hz, 1H, O*H*), 2.17 (d, *J* = 5.8 Hz, 1H, O*H*), 1.62–1.53 (m, 2H, C*H*$_2$), 1.41–1.20 (m, 20H, 10 x C*H*$_2$), 0.88 (t, *J* = 6.8 Hz, 3H, C*H*$_3$) ppm; ^{13}C NMR (100 MHz, CDCl$_3$) δ = 207.3 (*C*-1), 163.5 (*C*-3), 133.5 (*C*-2), 75.9 (*C*-5), 73.3 (*C*-6), 71.4 (*C*-4), 31.9, 31.2, 29.6, 29.6, 29.6, 29.6, 29.5, 29.4, 29.3, 26.1, 22.7 (11 x *C*H$_2$), 14.1 (*C*H$_3$) ppm; HRMS (ESI) calcd. for C$_{18}$H$_{31}$O$_4$$^-$ 311.2228 [M–H]$^-$, found 311.2225.

(4*S*,5*R*)-4,5-dihydroxy-5-((*S*)-1-hydroxytridecyl)cyclopent-2-enone ((+)-3.1): colorless solid (15.5 mg, 64%), m.p. 69 °C; TLC R_f 0.27 (*n*-hexane/ethyl acetate 1:1); $[\alpha]^{27}_D$ +54.1 (*c* 0.145, MeOH); ^{1}H NMR (400 MHz, CDCl$_3$) δ = 7.59 (dd, *J* = 6.1, 1.9 Hz, 1H, *H*-3), 6.31 (dd, *J* = 6.1, 1.3 Hz, 1H, *H*-2), 4.91 (s, 1H, *H*-4), 4.29 (s, 1H, O*H*), 3.87 (br s, 2H, *H*-6 + O*H*), 3.08 (d, *J* = 6.5 Hz, 1H, O*H*), 1.59–1.47 (m, 2H, C*H*$_2$), 1.39–1.17 (m, 20H, 10 x C*H*$_2$), 0.88 (t, *J* = 6.8 Hz, 3H, C*H*$_3$) ppm; ^{13}C NMR (100 MHz, CDCl$_3$) δ = 205.4 (*C*-1), 162.3 (*C*-3), 132.5 (*C*-2), 83.9 (*C*-5), 79.1 (*C*-6), 73.8 (*C*-4), 31.9, 31.5, 29.7 (3 x *C*H$_2$), 29.6 (2 x *C*H$_2$), 29.6, 29.6, 29.4, 29.3, 26.0, 22.7 (6 x *C*H$_2$),14.1 (*C*H$_3$) ppm; HRMS (ESI) calcd. for C$_{18}$H$_{31}$O$_4^-$ 311.2228 [M–H]$^-$, found 311.2226.

Synthesis of acetylated hygrophorones. Cyclopentenone **3.16** (156 mg, 0.44 mmol) was dissolved in pyridine (6 ml), cooled to 0 °C and acetic anhydride (3 ml) was slowly added. After 10 min the mixture was warmed to room temperature and stirring was continued for 3 hours. All volatiles were removed under reduced pressure and the residue was purified by column chromatography (*n*-hexane/ethyl acetate 5:1) to obtain the acetylated cyclopentenone **3.18** as a colorless oil (165 mg, 95%). To remove the diol protection group, a solution of **3.18** (132 mg, 0.33 mmol) in trifluoroacetic acid/methanol (6 ml, 5:1) was stirred for 30 minutes at 0 °C, warmed to room temperature and stirred for another 2 hours. The reaction mixture was evaporated to dryness and the crude product was purified by column chromatography (*n*-hexane/ethyl acetate 3:2) which afforded the acetylated hygrophorones **3.19** and **3.20** in 2:1 ratio. The regioisomeric mixture could be separated by preparative HPLC (H$_2$O (A) and CH$_3$CN (B) as eluents; linear gradient: 0–15 min, 60–90% B, flow rate 3.5 ml/min).

(4*S*,5*R*,6*R*)-4-dodecyl-2,2-dimethyl-9-oxo-1,3-dioxaspiro[4.4]non-7-en-6-yl acetate (3.18):
colorless oil (165 mg, 95%); TLC R_f 0.44 (*n*-hexane/ethyl acetate 5:1); $[\alpha]^{28}_D$ −6.2 (*c* 0.140, MeOH); ^{1}H NMR (400 MHz, CDCl$_3$) δ = 7.46 (dd, *J* = 6.3, 2.8 Hz, 1H, *H*-3), 6.41 (dd, *J* = 6.3, 1.3 Hz, 1H, *H*-8), 5.65 (dd, *J* = 2.8, 1.3 Hz, 1H, *H*-6), 4.39 (dd, *J* = 9.4, 3.2 Hz, 1H, *H*-4), 2.15 (s, 3H, C*H*$_3$ OAc), 1.62 (s, 3H, C*H*$_3$ acetal), 1.51 (m, 2H, C*H*$_2$), 1.36 (s, 3H, C*H*$_3$ acetal), 1.33–1.20 (m, 20 H, 10 x C*H*$_2$), 0.88 (t, *J* = 6.9 Hz, 3H, C*H*$_3$) ppm; ^{13}C NMR (100 MHz, CDCl$_3$) δ = 203.9 (*C*=O), 170.3 (*C*=O OAc), 156.3 (*C*-7), 136.9 (*C*-8), 111.3 (*C*(CH$_3$)$_2$ acetal), 82.8 (*C*-5), 81.8 (*C*-4), 73.2 (*C*-6), 31.9, 29.6, 29.6, 29.6, 29.5, 29.5, 29.4, 29.3, 29.3 (9 x *C*H$_2$), 27.4 (*C*H$_3$ acetal), 26.7 (*C*H$_2$), 25.7 (*C*H$_3$ acetal), 22.7 (*C*H$_2$), 20.6 (*C*H$_3$ OAc), 14.1 (*C*H$_3$) ppm; HRMS (ESI) calcd. for C$_{23}$H$_{38}$NaO$_5^+$ 417.2611 [M+Na]$^+$, found 417.2611.

(4*R*,5*R*)-5-hydroxy-5-((*S*)-1-hydroxytridecyl)-4-oxocyclopent-2-en-4-yl acetate (3.19):
white solid (78.6 mg, 67%), m.p. 99 °C; TLC R_f 0.35 (*n*-hexane/ethyl acetate 3:2); $[\alpha]^{27}_D$ −16.4 (*c* 0.130, MeOH); ^{1}H NMR (400 MHz, CDCl$_3$) δ = 7.58 (dd, *J* = 6.1, 2.7 Hz, 1H, *H*-3), 6.43 (dd, *J* = 6.2, 1.2 Hz, 1H, *H*-2), 5.73 (dd, *J* = 2.6, 1.3 Hz, 1H, *H*-4), 3.82 (m, 1H, *H*-6), 3.20 (s, 1H, O*H*), 2.24 (d, *J* = 7.7 Hz, 1H, O*H*), 2.16 (s, 3H, O*Ac*), 1.61–1.45 (m, 2H, *H*-7), 1.39–1.19 (m,

20H, 10 x CH_2), 0.88 (t, J = 6.8 Hz, 3H, CH_3) ppm; ^{13}C NMR (100 MHz, CDCl$_3$) δ = 206.6 (*C*-1), 170.1 (*C*=O OAc), 158.2 (*C*-3), 135.9 (*C*-2), 77.0 (*C*-5), 73.9 (*C*-6), 73.0 (*C*-4), 31.9, 31.2, 29.6, 29.6, 29.6, 29.5, 29.5, 29.4, 29.3, 26.1, 22.7 (11 x CH_2), 20.7 (CH_3 OAc), 14.1 (CH_3) ppm; HRMS (ESI) calcd. for C$_{20}$H$_{34}$NaO$_5^+$ 377.2298 [M+Na]$^+$, found 377.2297.

(4R,5S)-5-hydroxy-5-((S)-1-(acetyloxy)tridecyl)-1-oxocyclopent-2-enone (3.20): colorless oil (38.5 mg, 33%); TLC R_f 0.35 (*n*-hexane/ethyl acetate 3:2); [α]$^{28}_D$ −16.6 (*c* 0.140, MeOH); ^{1}H NMR (400 MHz, CDCl$_3$) δ = 7.64 (dd, J = 6.1, 2.4 Hz, 1H, *H*-3), 6.29 (dd, J = 6.1, 1.2 Hz, 1H, *H*-2), 5.19 (dd, J = 10.1, 2.8 Hz, 1H, *H*-6), 4.80 (d, 6.0 Hz, 1H, *H*-4), 3.39 (s, 1H, O*H*), 2.99 (d, J = 7.2 Hz, 1H, O*H*), 1.99 (s, 3H, O*Ac*), 1.85 (m, 1H, *H*-7A), 1.62 (m, 1H, *H*-7B), 1.37–1.20 (m, 20H, 10 x CH_2), 0.88 (t, J = 6.9 Hz, 3H, CH_3) ppm; ^{13}C NMR (100 MHz, CDCl$_3$) δ = 205.1 (*C*-1), 170.0 (*C*=O OAc), 162.9 (*C*-3), 133.0 (*C*-2), 75.5 (*C*-5), 73.7 (*C*-6), 71.5 (*C*-4), 31.9, 29.6, 29.6, 29.6, 29.5, 29.4, 29.4, 29.3, 29.2, 25.8, 22.7 (11 x CH_2), 20.8 (CH_3 OAc), 14.1 (CH_3) ppm; HRMS (ESI) calcd. for C$_{20}$H$_{34}$NaO$_5^+$ 377.2298 [M+Na]$^+$, found 377.2296.

3.5 References

Aitken, D., Eijsberg, H., Frongia, A., Ollivier, J., Piras, P., 2013. Recent progress in the synthetic assembly of 2-cyclopentenones. *Synthesis* 46, 1–24.

Bon, M., 1992. Die Grosspilzflora von Europa: Hygrophoraceae. IHW-Verlag, Eching, pp. 1–91.

Chooprayoon, S., Kuhakarn, C., Tuchinda, P., Reutrakul, V., Pohmakotr, M., 2011. Asymmetric total synthesis of (+)-swainsonine. *Org. Biomol. Chem.* 9, 531–537.

Craig, D., Lu, P., Mathie, T., Tholen, N.T.H., 2010. Directed addition of sulfur-stabilised carbanions to 1,2,3-trisubstituted aziridines. *Tetrahedron* 66, 6376–6382.

Fernandes, R.A., Ingle, A.B., Chavan, V.P., 2009. Synthesis of β,γ-disubstituted-γ-lactones through a Johnson–Claisen rearrangement: a short route to xylobovide, nor-canadensolide, canadensolide, sporothriolide and santolinolide. *Tetrahedron: Asymmetry* 20, 2835–2844.

Fernandes, R.A., Kumar, P., 2003. Enantioselective syntheses of xylo-C18-phytosphingosines using double stereodifferentiation. *Synthesis* 129–135.

Fernandes, R.A., Kumar, P., 2002. Asymmetric dihydroxylation and one-pot epoxidation routes to (+)- and (−)-posticlure: a novel trans-epoxide as a sex pheromone component of *Orgyia postica* (Walker). *Tetrahedron* 58, 6685–6690.

Gryparis, C., Lykakis, I.N., Efe, C., Zaravinos, I.-P., Vidali, T., Kladou, E., Stratakis, M., 2011. Functionalized 3(2*H*)-furanones *via* photooxygenation of (β-keto)-2-substituted furans: Application to the biomimetic synthesis of merrekentrone C. *Org. Biomol. Chem.* 9, 5655–5658.

Kambutong, S., Kuhakarn, C., Tuchinda, P., Pohmakotr, M., 2010. Synthesis of (+)-4-Desoxypentenomycin and Analogues. *Synthesis* 2010, 1453–1458.

Lübken, T., Schmidt, J., Porzel, A., Arnold, N., Wessjohann, L., 2004. Hygrophorones A–G: Fungicidal cyclopentenones from *Hygrophorus* species (Basidiomycetes). *Phytochemistry* 65, 1061–1071.

Montagnon, T., Tofi, M., Vassilikogiannakis, G., 2008. Using singlet oxygen to synthesize polyoxygenated natural products from furans. *Acc. Chem. Res.* 41, 1001–1011.

Phutdhawong, W., Pyne, S.G., Baramee, A., Buddhasukh, D., Skelton, B.W., White, A.H., 2002. Synthesis of (±) epipentenomycin I and III. *Tetrahedron Lett.* 43, 6047–6049.

Pohmakotr, M., Popuang, S., 1991. Intramolecular acylation of α-sulfinyl carbanion: a facile synthesis of (±)-pentenomycin I and (±)-epipentenomycin I. *Tetrahedron Lett.* 32, 275–278.

Schmidts, V., Fredersdorf, M., Lübken, T., Porzel, A., Arnold, N., Wessjohann, L., Thiele, C.M., 2013. RDC-based determination of the relative configuration of the fungicidal cyclopentenone 4,6-diacetylhygrophorone A[12]. *J. Nat. Prod.* 76, 839–844.

Seebach, D., Sting, A.R., Hoffmann, M., 1996. Self-regeneration of stereocenters (*SRS*) – Applications, limitations, and abandonment of a synthetic principle. *Angew. Chemie Int. Ed.* 35, 2708–2748.

Teichert, A., Lübken, T., Schmidt, J., Porzel, A., Arnold, N., Wessjohann, L., 2005b. Unusual bioactive 4-oxo-2-alkenoic fatty acids from *Hygrophorus eburneus*. *Z. Naturforsch.* 60b, 25–32.

Zaitsev, A., Adolfsson, H., 2006. Recent developments in asymmetric dihydroxylations. *Synthesis* 2006, 1725–1756.

3.6 Supporting Information

Supplementary data associated with this article (asymmetric total synthesis of hygrophorones (+)-**3.2** and (–)-**3.1**; X-ray structure of aldol product **3.30** (related intermediate to **3.11**); NMR spectra of intermediates and final products) can be found at http://dx.doi.org/10.1002/ejoc.201403455.

4 A study on the biosynthesis of hygrophorone B^{12} in the mushroom *Hygrophorus abieticola* reveals an unexpected labelling pattern in the cyclopentenone moiety
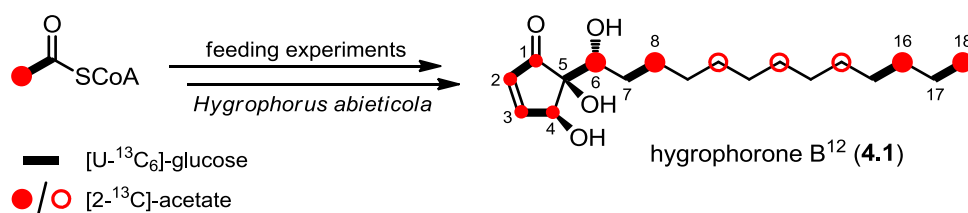
Abstract

The hitherto unknown natural formation of hygrophorones, antibacterial and antifungal cyclopentenone derivatives from mushrooms, was investigated for hygrophorone B^{12} in *Hygrophorus abieticola* Krieglst. ex Gröger & Bresinsky by feeding experiments in the field using ^{13}C labelled samples of D-glucose and sodium acetate. The incorporation of ^{13}C isotopes was extensively studied using 1D and 2D NMR spectroscopy as well as ESI-HRMS analyses. In the experiment with [U-^{13}C$_6$]-glucose, six different ^{13}C$_2$ labelled isotopomers were observed in the 2D INADEQUATE spectrum due to incorporation of [1,2-^{13}C$_2$]-acetyl-CoA. This labelling pattern demonstrated that hygrophorone B^{12} is derived from a fatty acid-polyketide route instead of a 1,4-α-D-glucan derived anhydrofructose pathway. The experiment with [2-^{13}C]-acetate revealed an unexpected incorporation pattern in the cyclopentenone functionality of hygrophorone B^{12}. Four single-labelled isotopomers, in particular [1-^{13}C]-, [2-^{13}C]-, [3-^{13}C]-, and [4-^{13}C]-hygrophorone B^{12}, were detected that showed only half enrichment in comparison to the respective labelled alkyl side chain carbons. This labelling pattern indicates the formation of a symmetrical intermediate during hygrophorone B^{12} biosynthesis. Based on these observations, a biogenetic route *via* a 4-oxo fatty acid and a chrysotrione B homologue is discussed.

4.1 Introduction

Fungal fruiting bodies of the basidiomycetous genus *Hygrophorus* (Hygrophoraceae, Agaricales) are an exceptional source for chemically diverse secondary metabolites, such as γ-butyrolactones (Gill and Steglich, 1987; Lübken et al., 2004), a dihydroazepine (Gill and Steglich, 1987), a ceramide (Qu et al., 2004), (nor-)sesquiterpenes (Otto et al., 2014), 4-oxo fatty acids (Teichert et al., 2005a; Gilardoni et al., 2006), cyclopentenediones (Gilardoni et al., 2007), and cyclopentenones (Lübken et al., 2004; Bette et al., 2015). The latter compound class, named hygrophorones A–E, represents 2-cyclopentenones with hydroxy or acetoxy substituents at C-4 and C-5, to which an odd-numbered 1'-oxidized alkyl chain (C_{11}, C_{13}, C_{15}, C_{17}) is attached (Lübken et al., 2004; Schmidts et al., 2013).

Very recently, the metabolite hygrophorone B^{12} (**4.1**) was isolated from fruiting bodies of *Hygrophorus abieticola* Krieglst. ex Gröger & Bresinsky and subsequently synthesized in an enantiomerically pure form, allowing for an unambiguous determination of the absolute configuration (Bette et al., 2015). Despite synthetic examinations, the *in vivo* formation of hygrophorones remains yet to be investigated. Biogenetic pathways can be studied by feeding experiments using stable-isotope labelled precursors (e.g. ^2H, ^{13}C, ^{15}N) in combination with an NMR-based analysis of incorporation patterns.

In theory, the biogenesis of hygrophorones, in particular hygrophorone B^{12} (**4.1**), might follow one of the two pathways shown in Scheme 4.1. Due to its structural similarity to oxidized fatty acids, **4.1** may be biosynthesized *via* an acetyl-CoA derived fatty acid-polyketide metabolism (pathway A). Another possible biogenesis of **4.1** includes the separate formation of a cyclopentenone unit followed by stereospecific alkylation at C-5 (pathway B).
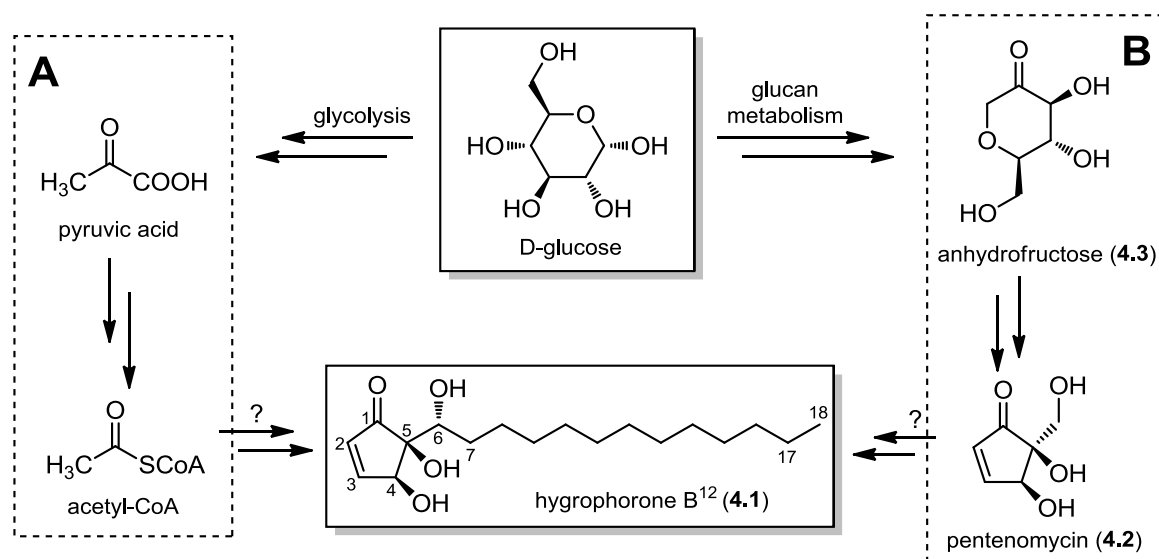
Scheme 4.1. Possible biogenetic pathways to hygrophorone B^{12} (**4.1**) starting from D-glucose. (A) glycolysis to acetyl-CoA and subsequent fatty acid-polyketide biosynthesis; (B) 1,4-α-D-glucan metabolism to anhydrofructose (**4.3**) and pentenomycin (**4.2**) followed by a stereospecific alkylation.

In this case, pentenomycin (**4.2**) may serve as precursor (Umino et al., 1973), which could be formed from 1,4-α-D-glucans over anhydrofructose (**4.3**) (Baute et al., 1988), similarly to its diastereomer epipentenomycin in the ascomycete *Peziza echinospora* (Baute et al., 1991). The latter pathway B is supported by identification in fungi with structurally very similar compounds, while pathway A is supported by our finding of fatty acids with a 4-oxo-crotonate moiety as potential intermediates (Teichert et al., 2005b).

The present study describes *in vivo* feeding experiments on fruiting bodies of *H. abieticola* using ^{13}C labelled samples of D-glucose and sodium acetate in order to investigate the hitherto unknown biosynthesis of hygrophorone B[12] (**4.1**).

4.2   Results and discussion

Feeding experiments on *H. abieticola* were performed in the field allowing the mushrooms to grow under natural conditions. To guarantee an efficient incorporation of labelled precursors into **4.1**, young fruiting bodies were selected due to their high rate of secondary metabolic activity. For this purpose, aqueous solutions of [U-^{13}C$_6$]-glucose, [1-^{13}C]-glucose, or [2-^{13}C]-acetate were injected separately *via* a syringe into the caps and stems of fruiting bodies of *H. abieticola* and harvested seven to nine days after feeding.

To investigate the biosynthesis of hygrophorone B[12] (**4.1**) with special focus on the cyclopentenone functionality, [U-^{13}C$_6$]-glucose can be used as a precursor for both possible biogenetic routes described in Scheme 4.1. Both pathways will consequently generate different incorporation patterns in the cyclopentenone moiety, leading to different NMR signatures (Fig. 4.1).
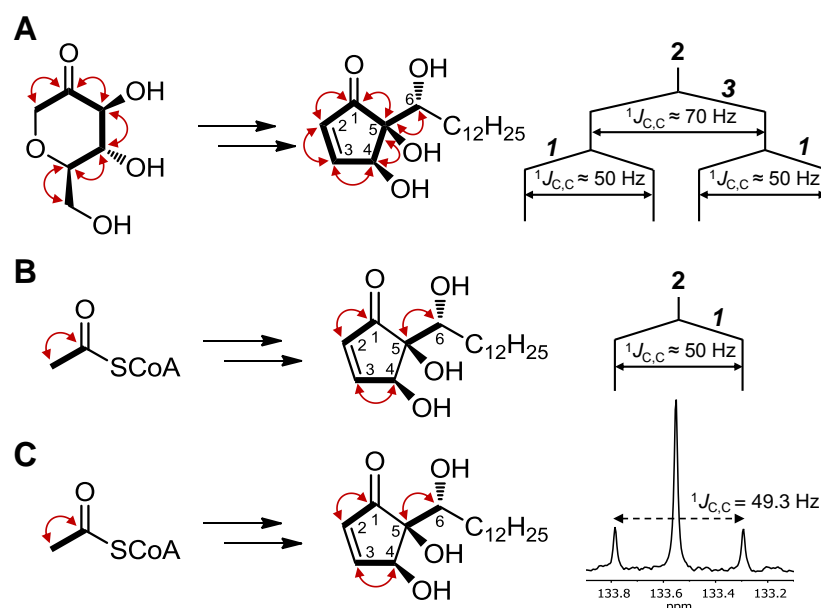
Fig. 4.1. Predicted and observed ^{13}C labelling patterns of the cyclopentenone moiety in **4.1** after incorporation of [U-^{13}C$_6$]-glucose and resulting NMR signatures exemplified for C-2 (right side). ^{13}C-^{13}C couplings are indicated by arrows and bold bonds. (A) predicted for anhydrofructose pathway; (B) predicted for acetyl-CoA derived biogenesis; (C) observed labelling pattern.

Thus, a putative formation of **4.1** following the anhydrofructose route would result in an uniformly ^{13}C labelled ring system leading to a double doublet (dd) NMR signal due to [13]C-^{13}C coupling between adjacent ^{13}C nuclei. In turn, a fatty acid-polyketide biogenesis would lead to an [13]C$_2$ isotopomeric labelling pattern in the cyclopentenone moiety of **4.1** arising from incorporation of [1,2-[13]C$_2$]-acetyl-CoA at the various positions, along with biogenic unlabelled acetyl-CoA. As a result, a doublet (d) signal splitting is observed.

To examine these putative biogenetic pathways, each of five basidiocarps of *H. abieticola* were fed with 100 mg of [U-[13]C$_6$]-glucose. Hygrophorone B[12] (**4.1**) was isolated from the EtOAc extract of *H. abieticola* fruiting bodies by repeated sequential fractionation on silica gel SPE cartridges followed by preparative HPLC (see Chapter 4.4). Up to 6 mg of hygrophorone B[12] (**4.1**) can be obtained from a single fruiting body. The 1D NMR and ESI-HRMS data of **4.1** were in accordance with those reported recently in the literature (Bette et al., 2015).

The proton-decoupled ^{13}C NMR spectrum of hygrophorone B[12] (**4.1**) after feeding of [U-[13]C$_6$]-glucose revealed an efficient incorporation of [13]C$_2$ units as predicted for an acetyl-CoA based pathway (Fig. 4.2). All ^{13}C signals were segregated into doublets caused by [1]$J_{C,C}$ coupling between neighbored ^{13}C isotopes at high intensities of approximately 52% in comparison to the global singlet signals (Table 4.1). Coupling carbon pairs were suggested from satellite signals with similar coupling constants. Both the cyclopentenone ring and the alkyl side chain carbon atoms of **4.1** were equally labelled exhibiting an average absolute ^{13}C enrichment of 0.56% per carbon atom (see S2, Supporting Information).
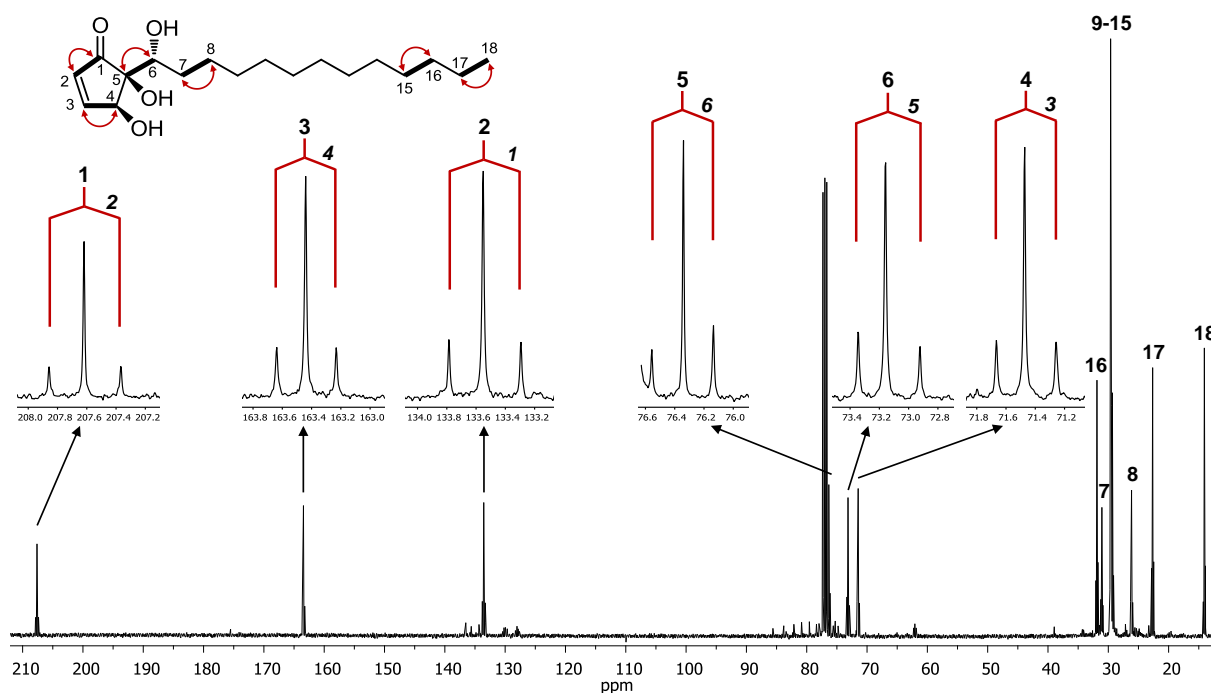
Fig. 4.2. Proton-decoupled ^{13}C NMR spectrum (100 MHz, CDCl$_3$) of hygrophorone B[12] (**4.1**) isolated from fruiting bodies of *H. abieticola* fed with [U-[13]C$_6$]-glucose. Signals of the cyclopentenone functionality as well as C-6 are expanded. Doublet signals indicate [1]$J_{C,C}$ coupling between adjacent carbons, marked by arrows and bold bonds.

Table 4.1. Incorporation of [U-$^{13}C_6$]-glucose, [1-^{13}C]-glucose, and [2-^{13}C]-acetate into hygrophorone B[12] (**4.1**) based on ^{13}C NMR spectroscopic data (solvent CDCl$_3$). Distinct single-labelled signals are marked in bold type.

| Pos. | δ$_C$ (ppm)[a] | [U-$^{13}C_6$]-glucose | | | [1-^{13}C]-glucose | [2-^{13}C]-acetate |
		INADEQUATE correlation[b]	$^1J_{C,C}$ (Hz)	satellite intensity (%)[c]	relative ^{13}C enrichment[d]	relative ^{13}C enrichment[d]
1	207.6	2	49.3	52.6	1.05	**1.33**
2	133.6	1	49.3	48.3	1.06	**1.43**
3	163.5	4	41.1	51.4	1.05	**1.36**
4	71.5	3	41.1	53.0	1.07	**1.36**
5	76.4	6	42.3	56.6	0.95	1.02
6	73.2	5	42.3	52.9	1.09	**1.70**
7	31.1	8	35.2	55.2	1.00	1.00
8	26.2	7	35.2	55.0	1.09	**1.82**
9–15	29.7–29.3	---[e]	---[e]	---[e]	---[e]	---[e]
16	31.9	15	34.6	51.0	1.10	**1.78**
17	22.7	18	34.7	49.3	0.99	1.02
18	14.1	17	34.7	51.6	1.08	**1.82**

[a] Recorded at 100 MHz. [b] Recorded at 150 MHz. [c] Percentage ratio of the ^{13}C-^{13}C satellite area to the global NMR signal area of the corresponding carbon atom. [d] ^{13}C signal area of each peak in the labelled **4.1** divided by that of the corresponding resonance integral in the unlabelled **4.1**, normalized to the unenriched peak of C-7. [e] Not assignable due to overlapping signals.

The incorporation of $^{13}C_2$ units was corroborated by ESI-HRMS measurements showing a significant enrichment of the [M+2] and [M+4] ion abundances (Table 4.2). The slightly increased intensity of the [M+1] ion, however, may be explained by indirect metabolism of glucose *via* several pathways, yielding single-labelled acetyl-CoA.

Table 4.2. ESI-HRMS analyses of hygrophorone B[12] (**4.1**) labelled with [U-$^{13}C_6$]-glucose, [1-^{13}C]-glucose, and [2-^{13}C]-acetate.

| ion | | unlabelled control | [U-$^{13}C_6$]-glucose | [1-^{13}C]-glucose | [2-^{13}C]-acetate |
		m/z, relative intensity (%)			
$^{12}C_{18}H_{32}O_4Na^+$	[M]	335.2189, **100.0**	335.2186, **100.0**	335.2194, **100.0**	335.2199, **100.0**
$^{12}C_{17}^{13}C_1H_{32}O_4Na^+$	[M+1]	336.2223, **18.9**	336.2220, **22.5**	336.2228, **20.6**	336.2233, **23.0**
$^{12}C_{16}^{13}C_2H_{32}O_4Na^+$	[M+2]	337.2252, **0.7**	337.2254, **5.8**	337.2256, **0.8**	337.2262, **3.6**
$^{12}C_{15}^{13}C_3H_{32}O_4Na^+$	[M+3]	*n.d.*	*n.d.*	*n.d.*	338.2297, **0.8**
$^{12}C_{14}^{13}C_4H_{32}O_4Na^+$	[M+4]	*n.d.*	339.2316, **0.4**	*n.d.*	339.2331, **0.3**

n.d. = not detected

For an unambiguous confirmation of enriched carbon atom pairs in hygrophorone B[12] (**4.1**) after feeding of [U-$^{13}C_6$]-glucose, a two-dimensional INADEQUATE experiment was performed. As depicted in Fig. 4.3, this ^{13}C homonuclear correlation experiment allowed the identification of $^1J_{C,C}$ couplings as pairs of antiphase doublet peaks along a horizontal line (Hull, 1994). The distance between these antiphase doublets reveals the coupling constant of the respective ^{13}C-^{13}C coupling. In total, six different $^{13}C_2$ labelled isotopomers, namely [1,2-$^{13}C_2$]-, [3,4-$^{13}C_2$]-, [5,6-

[$^{13}C_2$]-, [7,8-$^{13}C_2$]-, [15,16-$^{13}C_2$]-, and [17,18-$^{13}C_2$]-**4.1**, were detected (Fig. 4.3). As a result of signal overlap of C-9 to C-15 resonating around δ_c 30, coupling pairs for these carbons could not be assigned. Based on the observed labelling pattern of the other alkyl chain carbons, however, it is proposed that the carbons C-9 to C-15 are labelled as well. The ^{13}C NMR data including INADEQUATE correlations and $^1J_{C,C}$ coupling constants of **4.1** after feeding of [U-$^{13}C_6$]-glucose are summarized in Table 4.1. The incorporation pattern of $^{13}C_2$ units into hygrophorone B^{12} (**4.1**) is in agreement with a [1,2-$^{13}C_2$]-acetyl-CoA derived fatty acid-polyketide metabolic origin as proposed in Fig. 4.1. Thus, a pentenomycin (**4.2**) biosynthetic pathway *via* anhydrofructose (**4.3**) can be excluded.

Additionally, labelling experiments using [1-^{13}C]-glucose as precursor for single-labelled [2-^{13}C]-acetyl-CoA were performed to investigate the biosynthetic cyclization process of the cyclopentenone function in hygrophorone B^{12} (**4.1**). Therefore, each of five basidiocarps were fed with 100 mg of [1-^{13}C]-glucose, and **4.1** was purified using the solid-phase extraction method described above. As a result of different relaxation times as well as NOE effects of carbon nuclei, resonances with unequal signal intensities are typically observed under standard ^{13}C NMR conditions. To compare signal areas between putatively enriched and naturally abundant carbon resonances in **4.1**, however, almost quantitative ^{13}C NMR spectra were recorded using the inverse-gated-decoupling pulse sequence and a longer relaxation delay (Giraudeau and Baguet, 2006).
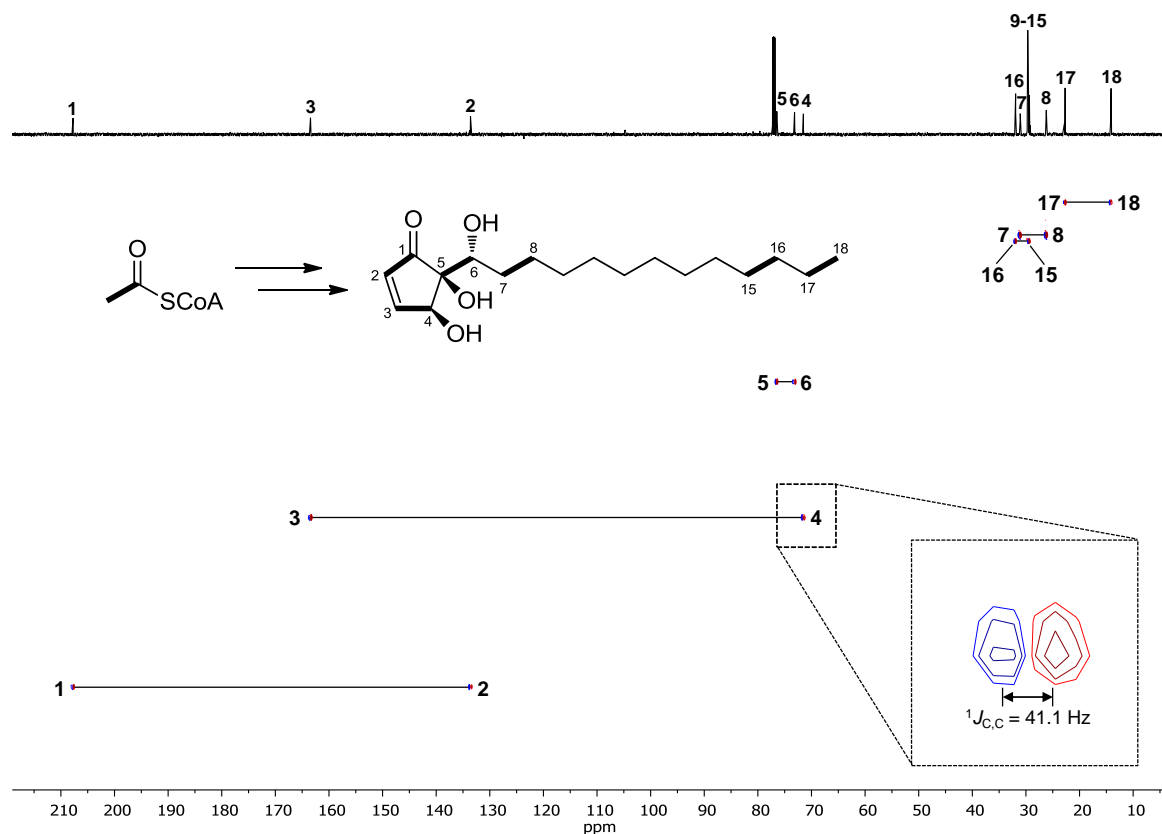
Fig. 4.3. Two-dimensional INADEQUATE spectrum (150 MHz, CDCl$_3$) of hygrophorone B^{12} (**4.1**) labelled with [U-$^{13}C_6$]-glucose. Correlating carbons are marked by horizontal lines (spectrum) and bold bonds (structure), respectively. The one-dimensional ^{13}C NMR spectrum is shown on top.

Surprisingly, the spectrum of **4.1** after feeding of [1-^{13}C]-glucose was devoid of any significantly enriched ^{13}C signals (Table 4.1). This was supported by ESI-HRMS investigations revealing no distinct isotope clusters that would indicate ^{13}C enrichment in **4.1** (Table 4.2). An upregulated pentose phosphate pathway (PPP) in the [1-^{13}C]-glucose fed fruiting bodies of *H. abieticola* may explain this observation. Such an upregulation results in a low level conversion of [1-^{13}C]-glucose to [2-^{13}C]-acetyl-CoA (see S13, Supporting Information), because [1-^{13}C]-glucose is decarboxylated at C-1 during the oxidative stage of the PPP, leading to unlabelled acetyl-CoA (Dunstan et al., 1990).

To obtain an efficient incorporation of [2-^{13}C]-acetyl-CoA, however, additional feeding experiments using its direct precursor [2-^{13}C]-acetate were performed (100 mg per mushroom). HRMS analyses revealed significantly increased [M+1], [M+2], [M+3], and [M+4] ion abundances (Table 4.2). In fact, the inverse-gated decoupled ^{13}C NMR spectra of **4.1** displayed a distinct enrichment of ^{13}C signals corresponding to C-6, C-8, C-16, and C-18 (Fig. 4.4, Table 4.1). This observation unambiguously confirmed that the chain elongation proceeds in the C-18→C-6 direction. As described above, specifically labelled carbons between C-9 and C-15 could not be assigned due to signal overlap. However, based on the observed ^{13}C incorporation of solely even-numbered alkyl side chain atoms, it is assumed that carbons C-10, C-12, and C-14 are ^{13}C enriched as well.
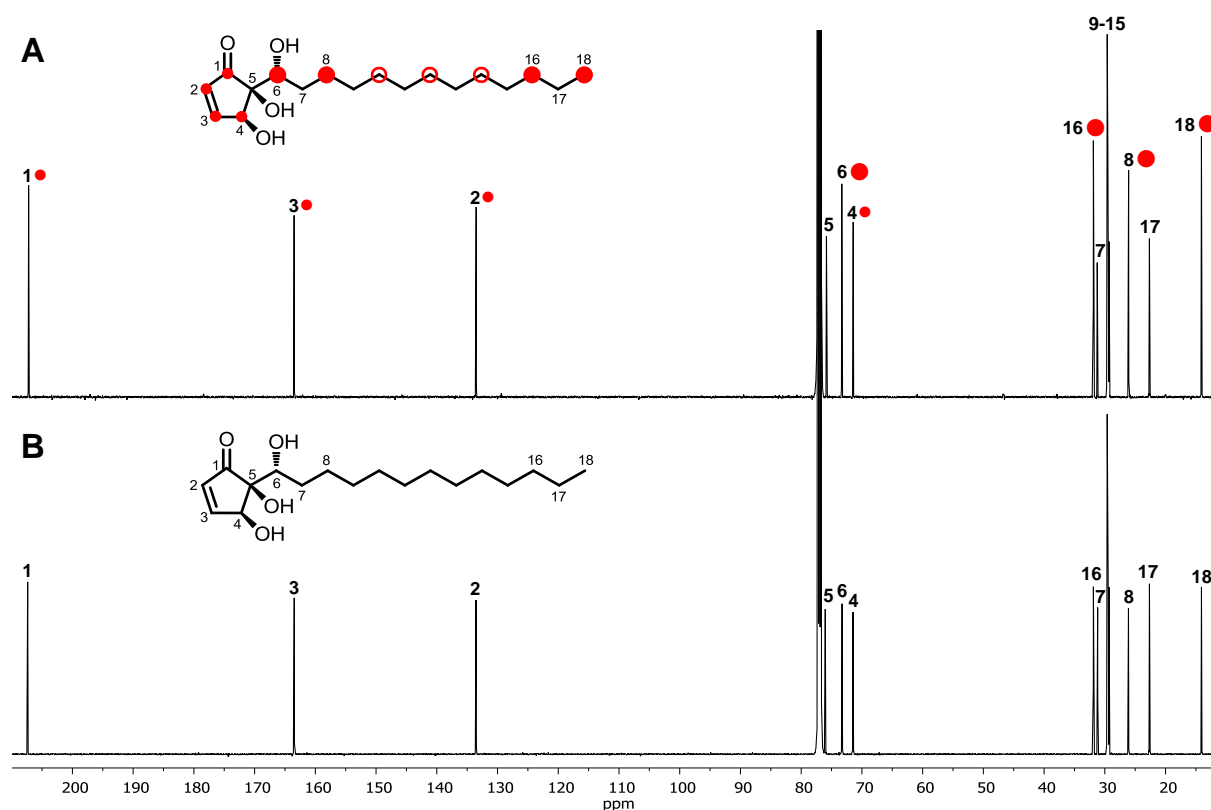
Fig. 4.4. Inverse-gated decoupled ^{13}C NMR spectra (150 MHz, CDCl$_3$) of hygrophorone B[12] (**4.1**) labelled with [2-^{13}C]-acetate (A) and with natural ^{13}C isotopic abundance isolated from unlabelled basidiocarps (B). ^{13}C enriched carbons are indicated by scaled red dots (●) according to their rate of enrichment. Due to signal overlap of C-9 to C-15, incorporation could not be assigned to a specific carbon atom. The assumed labelling positions are marked by red circles (○).

Surprisingly, the cyclopentenone moiety in **4.1** displayed an unusual ^{13}C incorporation pattern. Four single-labelled isotopomers, namely [1-^{13}C]-, [2-^{13}C]-, [3-^{13}C]-, and [4-^{13}C]-**4.1**, were detected that showed equally enriched ^{13}C abundances with about half enrichment in comparison to the respective labelled, even-numbered alkyl side chain carbons (Fig. 4.4, Table 4.1). This observation was corroborated by quantitative ^{1}H NMR investigations displaying a twofold higher abundant ^{13}C satellite signal of H[3]-18 compared to the cyclopentenone resonances of H-2, H-3, and H-4 (see S9–11, Supporting Information).

The above results confirm that **4.1** labelled with [2-^{13}C]-acetate is a 1:1 mixture of two differently labelled cyclopentenone species, in particular [1-^{13}C]- and [3-^{13}C]-**4.1** as well as [2-^{13}C]- and [4-^{13}C]-**4.1** (Fig. 4.4). This labelling pattern indicates that the biosynthesis of **4.1** includes the formation of a symmetrical intermediate (Scheme 4.2). It is conceivable that the cyclization of 4-oxo fatty acids such as 4-oxooctadec-2-enoic acid (**4.4**) may afford the β,β'-triketone **4.5**, which resembles the structure of chrysotrione B (cf. structure **4.5**) by having two additional methylene groups in the alkyl side chain (Gilardoni et al., 2007). Interestingly, chrysotrione B was isolated earlier from fruiting bodies of *H. chrysodon* (Batsch.: Fr.) Fr., and its biogenesis was hypothesized *via* a 4-oxo fatty acid intermediate as well (Gilardoni et al., 2007). Acylcyclopentenediones of type **4.5** show an interesting series of keto-enol tautomerism as extensively studied by Forsen and Nilsson (1970) on the basis of NMR experiments. The enolization equilibrium includes the tautomeric enols **4.5a** and **4.5b**, which are stabilized by intramolecular hydrogen bonding (Scheme 4.2). The interconversion of the tautomers **4.5a** and **4.5b** explains the observed equal distribution of ^{13}C isotopes at C-1, C-2, C-3, and C-4 with only half of the enrichment detected in the labelled, even-numbered alkyl chain carbons (Table 4.1).
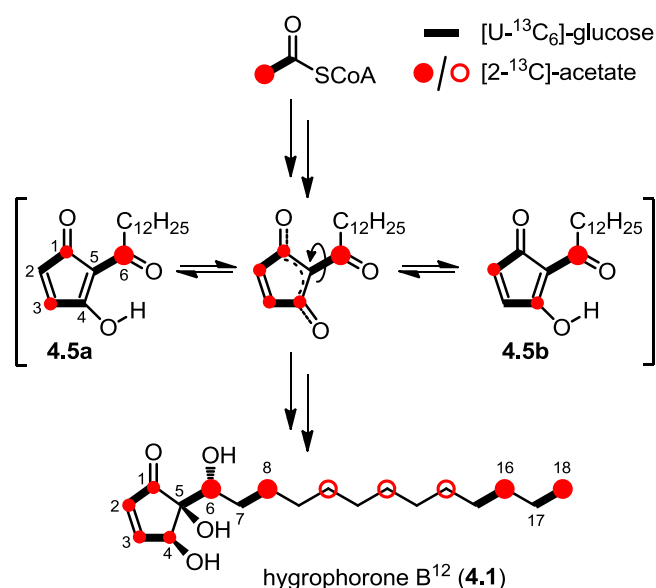
Scheme 4.2. Proposed key step in the biosynthesis of hygrophorone B[12] (**4.1**). The labelling patterns in **4.1** from feeding experiments with [U-[13]C[6]]-glucose (▬) and [2-^{13}C]-acetate (● observed; ○ assumed, see Fig. 4.4) are shown on bottom. The size of the dots corresponds to their rate of enrichment. The interconversion of the tautomers **4.5a** and **4.5b** may explain the observed equal distribution of ^{13}C isotopes at C-1, C-2, C-3, and C-4 with about half enrichment in comparison to the even-numbered alkyl side chain carbons.

4.3   Conclusions

In summary, after feeding of [U-^{13}C$_6$]-glucose, six different ^{13}C$_2$ labelled isotopomers were detected in the 2D INADEQUATE spectrum of **4.1** due to incorporation of [1,2-^{13}C$_2$]-acetyl-CoA. This labelling pattern unambiguously demonstrated that hygrophorone B^{12} (**4.1**) is derived from a fatty acid-polyketide route instead of a 1,4-α-D-glucan derived anhydrofructose pathway. In addition, the cyclization process of the cyclopentenone unit in **4.1** was investigated using precursors for single-labelled acetyl-CoA. While [1-^{13}C]-glucose caused no significant incorporation into **4.1**, the feeding of [2-^{13}C]-acetate revealed an unexpected incorporation pattern in the cyclopentenone system. The fact that the four carbon atoms C-1, C-2, C-3, and C-4 were equally labelled and the even-numbered alkyl side chain carbons showed a two-fold ^{13}C enrichment in comparison to the cyclopentenone carbons suggests the formation of a symmetrical intermediate during the biosynthesis of **4.1**. Based on the above evidences, the biogenetic formation of **4.1** *via* (*E*)-4-oxooctadec-2-enoic acid (**4.4**) is proposed as illustrated in Scheme 4.3.
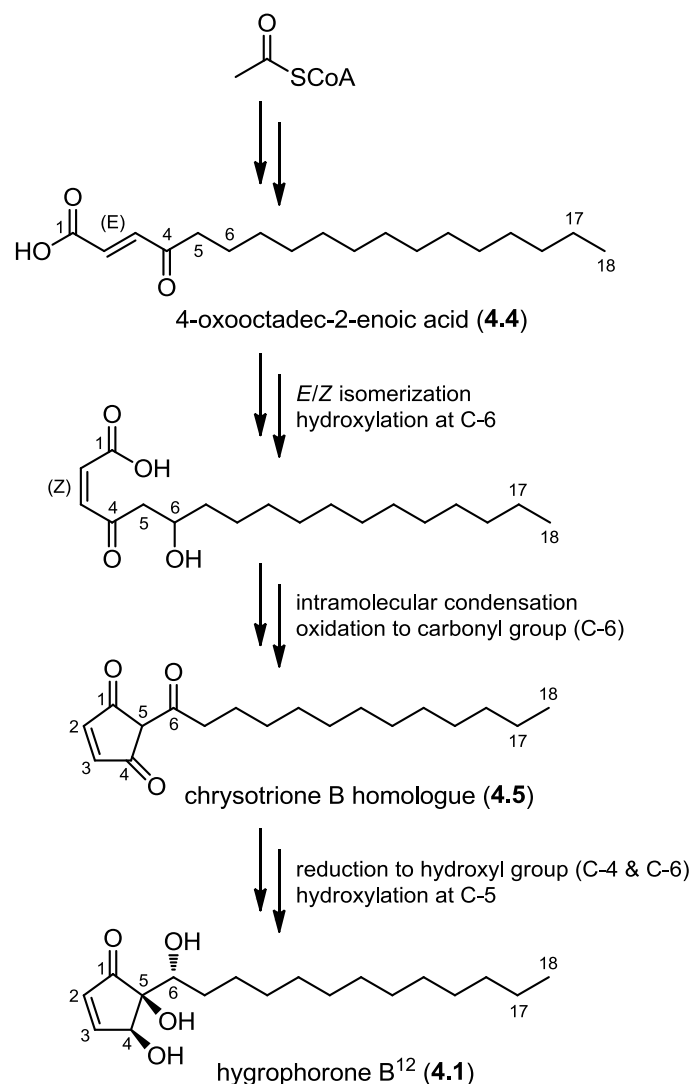
Scheme 4.3. Suggested biosynthesis of hygrophorone B^{12} (**4.1**) *via* 4-oxooctadec-2-enoic acid (**4.4**) and a chrysotrione B homologue (**4.5**), considering the proposals of Teichert et al. (2005b) and Gilardoni et al. (2007).

After *E/Z* isomerization and hydroxylation of **4.4**, an intramolecular cyclization, such as an aldol-type or lactonization reaction, may eventually afford the cyclic β,β'-triketone **4.5**, which resembles the structure of its shorter-chain homologue chrysotrione B (cf. structure **4.5**). Finally, stereospecific carbonyl group reduction at C-4 and C-6, and subsequent hydroxylation at C-5 in **4.5**, or vice versa, would yield hygrophorone B[12] (**4.1**). It can be assumed that the biosynthesis of other cyclopentenone type hygrophorones in fruiting bodies of *Hygrophorus* spp. (Lübken et al., 2004) might follow an analogous pathway *via* oxidized fatty acids.

4.4 Experimental Section

General Experimental Procedures. Chromabond® silica gel SPE cartridges (3 ml, 500 mg) were purchased from Macherey-Nagel (Germany). Analytical TLC was performed on precoated silica gel 60 F_{254} plates (Merck) using *n*-hexane/EtOAc (1:1) as mobile phase. Spots of hygrophorone B[12] were visualized under UV light at 254 nm or by spraying with a 0.5% solution of vanillin in $H_2SO_4/CH_3COOH/MeOH$ (1:2:20, v/v/v) followed by heating at 110 °C. Preparative HPLC was performed on a Knauer system equipped with a WellChrom K-1001 pump and a WellChrom K-2501 UV detector using an ODS-A column (5 μm, 120 Å, 150 × 10 mm ID, YMC, USA) and eluting with H_2O (A) and CH_3CN (B) at a flow rate of 3.5 ml·min^{-1}.

Chemicals. The precursors [1-^{13}C]-D-glucose and [U-$^{13}C_6$]-D-glucose (both 99% ^{13}C abundance) were purchased from Deutero GmbH (Germany), while sodium [2-^{13}C]-acetate (99% ^{13}C abundance) was obtained from Sigma Aldrich (Germany).

Feeding experiments. Feeding experiments on fruiting bodies of *H. abieticola* Krieglst. ex Gröger & Bresinsky growing in Paintner Forst near Kelheim, Germany (leg./det. A. Otto/N. Arnold) were performed in October 2013 and November 2014. For this purpose, 100 mg of the respective precursor was solved in 200 μl water and injected *via* a syringe into the caps and stems of young fruiting bodies of *H. abieticola*. Mushroom growth was analyzed by measuring the cap diameter at the beginning and the end of the respective feeding experiment (Table 4.3). The fruiting bodies were harvested after seven to nine days, immediately frozen in liquid nitrogen, and stored at –20 °C until work-up. Unlabelled basidiocarps were used as control.

Isolation procedure of hygrophorone B^{12} (4.1). Frozen fruiting bodies fed with the respective precursor were macerated using a blender and exhaustively extracted with *n*-hexane (3 × 2 l) and EtOAc (3 × 2 l). The extracts were combined after TLC analysis and concentrated *in vacuo* to dryness. The resulting yellow crude extract was purified by sequential fractionation on Chromabond® silica gel SPE cartridges (3 ml, 500 mg, Macherey-Nagel) eluting with *n*-hexane/EtOAc (100:0→0:100) to yield 11 fractions (A1–11). Fractions A4–7 (70:30 to 30:70 eluates) containing compound **4.1** (R_f 0.30, *n*-hexane/EtOAc 1:1) were combined. Repeated SPE

fractionation on silica gel using the same gradient system afforded fractions B1–11. The 60:40 eluate (fraction B5) was finally purified by preparative HPLC (0–24 min, 55–75% B) to yield pure **4.1** (t_R 14.2 min). Further experimental details are given in Table 4.3.

NMR spectroscopy. NMR spectra were obtained from an Agilent DD2 400 and VNMRS 600 system, respectively. Hygrophorone B[12] was measured in $CDCl_3$ as solvent, and chemical shifts were referenced to internal TMS (δ_H 0 ppm, ^1H) and $CDCl_3$ (δ_C 77.0 ppm, ^{13}C). Quantitative ^1H spectra were recorded at 599.83 MHz using an acquisition time of 6.82 s and a relaxation delay of 13.18 s. Absolute ^{13}C abundances were determined from proton signals *via* the ^{13}C-coupled satellites. The 2D INADEQUATE spectrum was measured at 150.84 MHz and optimized for a ^{13}C-^{13}C coupling constant of 55 Hz. The non-quantitative ^1H decoupled ^{13}C NMR spectra were recorded at 100.54 MHz. The inverse-gated decoupled ^{13}C NMR spectra of labelled and naturally ^{13}C abundant samples were measured at 150.84 MHz under identical spectroscopic conditions (acquisition time 7.55 s, relaxation delay 22.45 s). This standardization considers different relaxation behavior of carbon atoms to prevent false quantification of ^{13}C abundances. The relative ^{13}C incorporation rates of single-labelled, individual carbon atoms were determined by comparing the signal areas of biosynthetic samples with the signals of samples with natural ^{13}C abundance. Multiple-labelled isotopomers displaying ^{13}C-^{13}C couplings were quantified from the corresponding satellite signals in the ^{13}C NMR spectra. The integrals of the respective satellite pair were referenced to the total signal area of a given carbon atom.

Table 4.3. Experimental details of labelling studies and purification of hygrophorone B[12] (**4.1**).

precursor	feeding experiments			weight of		
	number of fruit bodies	days to harvest	growth (cm)	fruiting bodies	crude extract	purified **4.1**
[U-$^{13}C_6$]-glucose	4	9	3.5–4.5	180 g	1.48 g	26.9 mg
[1-^{13}C]-glucose	5	9	3.0–4.5	230 g	1.91 g	32.1 mg
[2-^{13}C]-acetate	2	7	3.0–6.5	78 g	0.55 g	6.5 mg

Mass spectrometry. The positive ion high resolution ESI mass spectra were obtained from an Orbitrap Elite mass spectrometer (Thermo Fisher Scientific, Germany) equipped with an HESI electrospray ion source (spray voltage 4.5 kV, capillary temperature 275 °C, source heater temperature 40 °C, FTMS resolution 60.000). Nitrogen was used as sheath gas. The sample solutions were introduced continuously *via* a 500 μl Hamilton syringe pump with a flow rate of 5 μl·min^{-1}. The instrument was externally calibrated by the Pierce LTQ Velos ESI positive ion calibration solution (product no. 88323) from Thermo Fisher Scientific. The data were evaluated by using the Xcalibur software 2.7 SP1.

4.5 References

Baute, M.-A., Baute, R., Deffieux, G., 1988. Fungal enzymatic activity degrading 1,4-D-glucans to 1,5-D-anhydrofructose. *Phytochemistry* 27, 3401–3403.

Baute, M.-A., Deffieux, G., Baute, R., Badoc, A., Vercauteren, J., Léger, J.-M., Neveu, A., 1991. Fungal enzymic activity degrading 1,4-D-glucans to echinosporin (5-epipentenomycin I). *Phytochemistry* 30, 1419–1423.

Bette, E., Otto, A., Dräger, T., Merzweiler, K., Arnold, N., Wessjohann, L., Westermann, B., 2015. Isolation and asymmetric total synthesis of fungal secondary metabolite hygrophorone B^{12}. *Eur. J. Org. Chem.* 2015, 2357–2365.

Dunstan, R.H., Greenaway, W., Whatley, F.R., 1990. Discrimination by paracoccus denitrificans between (6-^{13}C)glucose and (1-^{13}C)glucose as carbon substrates for growth: An investigation using gas chromatography/mass spectrometry. *Biol. Mass Spectrom.* 19, 369–381.

Forsen, S., Nilsson, M., 1970. Enolization, in: Zabicky, J. (Ed.), The chemistry of the carbonyl group, John Wiley & Sons, London, Vol. 2, pp. 157–241.

Gilardoni, G., Clericuzio, M., Marchetti, A., Finzi, P.V., Zanoni, G., Vidari, G., 2006. New oxidized 4-oxo fatty acids from *Hygrophorus discoxanthus*. *Nat. Prod. Commun.* 12, 1079–1084.

Gilardoni, G., Clericuzio, M., Tosi, S., Zanoni G., Vidari, G., 2007. Antifungal acylcyclopentenediones from fruiting bodies of *Hygrophorus chrysodon*. *J. Nat. Prod.* 70, 137–139.

Gill, M., Steglich, W., 1987. Pigments of fungi (Macromycetes), in: Herz, W., Grisebach, H., Kirby, G.W., Tamm, C. (Eds.), Progress in the chemistry of organic natural products. Springer Verlag, Wien, New York, Vol. 51, pp. 1–317.

Giraudeau, P., Baguet, E., 2006. Improvement of the inverse-gated-decoupling sequence for a faster quantitative analysis of various samples by ^{13}C NMR spectroscopy. *J. Magn. Reson.* 180, 110–117.

Hull, W.E., 1994. Experimental aspects of two-dimensional NMR, in: Croasmun, W.R., Carlson R.M.K. (Eds.), Two-dimensional NMR spectroscopy: Applications for Chemists and Biochemists. Wiley-VCH, Weinheim, pp. 67–456.

Lübken, T., Schmidt, J., Porzel, A., Arnold, N., Wessjohann, L., 2004. Hygrophorones A–G: fungicidal cyclopentenones from *Hygrophorus* species (Basidiomycetes). *Phytochemistry* 65, 1061–1071.

Otto A., Porzel A., Schmidt J., Wessjohann L., Arnold N., 2014. Penarines A–F, (nor-) sesquiterpene carboxylic acids from *Hygrophorus penarius* (Basidiomycetes). *Phytochemistry* 108, 229–233.

Qu, Y., Zhang, H., Liu, J., 2004. Isolation and structure of a new ceramide from the basidiomycete *Hygrophorus eburnesus*. *Z. Naturforsch.* 59b, 241–244.

Schmidts, V., Fredersdorf, M., Lübken, T., Porzel, A., Arnold, N., Wessjohann, L., Thiele, C. M., 2013. RDC-based determination of the relative configuration of the fungicidal cyclopentenone 4,6-diacetylhygrophorone A^{12}. *J. Nat. Prod.* 76, 839–844.

Teichert, A., Lübken, T., Schmidt, J., Porzel, A., Arnold, N., Wessjohann, L., 2005a. Unusual bioactive 4-oxo-2-alkenoic fatty acids from *Hygrophorus eburneus*. *Z. Naturforsch.* 60b, 25–32.

Teichert, A., Lübken, T., Kummer, M., Besl, H., Haslberger, H., Arnold, N., 2005b. Bioaktive Sekundärmetaboliten aus der Gattung *Hygrophorus* (Basidiomycetes). *Z. Mykol.* 71, 53–62.

Umino, K., Furumai, T., Matsuzawa, N., Awataguchi, Y., Ito, Y., 1973. Studies on pentenomycins. I. Production, isolation and properties of pentenomycins I and II, new antibiotics from *Streptomyces eurythermus* MCRL 0738. *J. Antibiot.* 26, 506–512.

4.6 Supporting Information

Supplementary data associated with this article can be found at http://dx.doi.org/10.1016/j.phytochem.2015.08.018.

5 Structure and absolute configuration of pseudohygrophorones A[12] and B[12], alkyl cyclohexenone derivatives from *Hygrophorus abieticola* (Basidiomycetes)
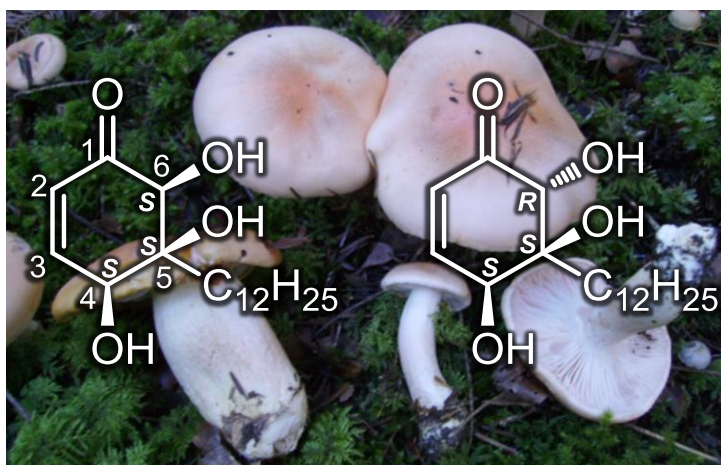
Abstract

Pseudohygrophorones A[12] (**5.1**) and B[12] (**5.2**), the first naturally occurring alkyl cyclohexenones from a fungal source, and the recently reported hygrophorone B[12] (**5.3**) have been isolated from fruiting bodies of the basidiomycete *Hygrophorus abieticola* Krieglst. ex Gröger & Bresinsky. Their structures were assigned on the basis of extensive one and two dimensional NMR spectroscopic analyses as well as ESI-HRMS measurements. The absolute configuration of the three stereogenic centers in the diastereomeric compounds **5.1** and **5.2** was established with the aid of $^3J_{H,H}$ and $^4J_{H,H}$ coupling constants, NOE interactions, and conformational analyses in conjunction with quantum chemical CD calculations. It was concluded that pseudohygrophorone A[12] (**5.1**) is 4*S*,5*S*,6*S* configured, while pseudohygrophorone B[12] (**5.2**) was identified as the C-6 epimer of **5.1**, corresponding to the absolute configuration 4*S*,5*S*,6*R*. In addition, the mass spectrometric fragmentation behavior of **5.1**–**5.3** obtained by the higher-energy collisional dissociation (HCD) method allows a clear distinction between the pseudohygrophorones (**5.1** and **5.2**) and hygrophorone B[12] (**5.3**). The isolated compounds **5.1**–**5.3** exhibited pronounced biological activity against phytopathogenic organisms.

5.1 Introduction

Fungal basidiocarps are responsible for the production of sexual spores, which are the fundamental dispersal units of such organisms. It is therefore not surprising that certain fungal species have evolved secondary metabolites to protect their fruiting bodies, e.g. against infections by widespread parasitic moulds, to ensure full development and distribution of their spores.

Field observations revealed that fruiting bodies of certain species of the genus *Hygrophorus* (Hygrophoraceae, Agaricales) are hardly ever attacked by mycophilic fungi (Lübken et al., 2004). Consequently, several novel compound classes with pronounced biological activity were isolated from *Hygrophorus* spp. such as hygrophorones (Lübken et al., 2004), 4-oxo fatty acids (Gilardoni et al., 2006; Teichert et al., 2005b), or chrysotriones (Gilardoni et al., 2007). Additionally, rare ventricosane-type (nor-)sesquiterpenes were characterized from *H. penarius* (Otto et al., 2014). The relative configuration of the cyclopentenone derivative 1,4-di-*O*-acetylhygrophorone A[12] was elucidated earlier based on residual dipolar couplings (RDCs) (Schmidts et al., 2013). Recently, hygrophorone B[12] (**5.3**) has been isolated from fruiting bodies of *Hygrophorus abieticola* Krieglst. ex Gröger & Bresinsky, and subsequently synthesized in an enantiomerically pure form, allowing for an unambiguous determination of the relative and absolute configuration (Bette et al., 2015). Moreover, the biosynthesis of **5.3** was investigated by feeding of ^{13}C labelled precursors to basidiocarps of *H. abieticola* (Otto et al., 2015b).

Fruiting bodies of *H. abieticola* usually grow in clusters under *Abies alba* mainly on calcareous soils (Bresinsky, 2008). The yellow to orange colored cap is 5–15 cm in diameter and characterized by a sticky to viscid surface in humid environments. The white to yellow-orange stipe is 5–10 cm long and 0.8–2.5 cm thick. The very distant, subdecurrent to adnate, thick lamellae are initially white, becoming salmoneous in age. The resin- to turpentine-like taste and smell makes this principally edible mushroom not very delicious (Krieglsteiner and Gminder, 2001).

The present paper describes the isolation and structural elucidation of two previously unknown cyclohexenone derivatives, named pseudohygrophorones A[12] (**5.1**) and B[12] (**5.2**), together with the known hygrophorone B[12] (**5.3**) from the EtOAc extract of *H. abieticola*. The isolated compounds **5.1**–**5.3** were tested against the phytopathogenic fungi *Botrytis cinerea* Pers. and *Septoria tritici* Desm. as well as the oomycete *Phytophthora infestans* (Mont.) de Bary.

5.2 Results and discussion

5.2.1 Isolation and structural elucidation

Repeated column chromatography on silica gel, Sephadex LH 20, and preparative RP18 HPLC yielded compounds **5.1**–**5.3** (see Chapter 5.4).
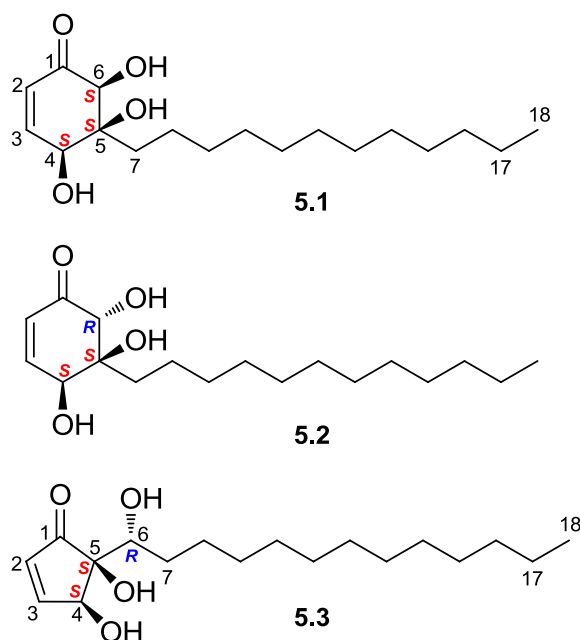
Fig. 5.1. Chemical structures of compounds **5.1–5.3**.

Compound **5.1** was isolated as an optically active, white, amorphous solid. The molecular formula $C_{18}H_{32}O_4$ was determined by ESI-HRMS measurements of the molecular ion at *m/z* 311.2237 ([M–H]⁻, calcd for $C_{18}H_{31}O_4^-$, 311.2228), corresponding to three degrees of unsaturation. The ^{1}H NMR spectrum (Table 5.1) of **5.1** displayed two olefinic signals at δ_H 6.151 (1H, dd, *J* = 10.2/2.5 Hz) and δ_H 6.833 (1H, dd, *J* = 10.2/2.1 Hz), indicating an endocyclic double bond. This was supported by ^{13}C resonances at δ_C 125.1 (C-2) and δ_C 151.0 (C-3), respectively (Table 5.1). The presence of a conjugated ketone was evidenced by a carbon signal at δ_C 198.3. Furthermore, deshielded methine proton resonances at δ_H 4.159 (1H, d, *J* = 1.8 Hz) and δ_H 4.496 (1H, br d, $^3J_{H4\text{-}OH4}$ = 11.0 Hz) as well as an oxygenated tertiary carbon signal at δ_C 81.5 were assigned to three hydroxy functionalities. A broad overlapping multiplet between δ_H 1.23 and δ_H 1.33, accompanied by a triplet at δ_H 0.882 (3H, *J* = 7.2 Hz) was evident for a saturated *n*-alkyl chain (-$C_{12}H_{25}$).

Thus, the structural features of constituent **5.1** arising from its 1D NMR spectra were similar to those of the cyclopentenone derivative hygrophorone B[12] (**5.3**) (Bette et al., 2015). In contrast to **5.3**, compound **5.1** exhibited a considerably larger $^3J_{H2\text{-}H3}$ coupling constant of 10.1 Hz (**5.3**: 6.0 Hz), suggesting the presence of a cyclohexenone system (Queiroz et al., 2003). Interpretation of HMBC correlations (Fig. 5.2) indicated that the six-membered ring of **5.1** was formed by one endocyclic double bond (C-2, C-3), one keto group (C-1) and three oxygenated carbon atoms (C-4, C-5, C-6).
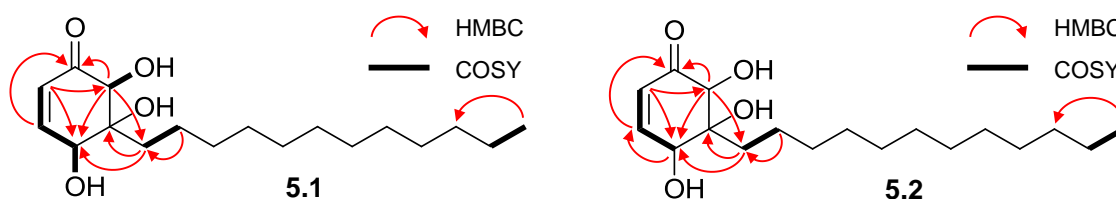
Fig. 5.2. Key HMBC (H to C) and COSY correlations of pseudohygrophorones A[12] (**5.1**) and B[12] (**5.2**).

The absent COSY spin system between H-4 (δ_H 4.496) and H-6 (δ_H 4.159) as well as HMBC correlations of the alkyl chain protons H_A-7/H_B-7 to C-4 (δ_C 68.7), C-5 (δ_C 81.5), and C-6 (δ_C 75.3) unambiguously confirmed that the *n*-dodecyl side chain is attached to C-5. Based on the above data, the constitution of **5.1** was assigned as 4,5,6-trihydroxy-5-dodecyl-2-cyclohexenone (Fig. 5.1), and trivially named pseudohygrophorone A[12] (**5.1**) due to its close structural relationship to hygrophorones (Lübken et al., 2004).

Table 5.1. ^{1}H and ^{13}C NMR data of pseudohygrophorones A[12] (**5.1**) and B[12] (**5.2**) including HMBC (H to C) and NOE correlations (600/150 MHz, CDCl$_3$, δ in ppm).

Pos.	pseudohygrophorone A[12] (**5.1**)				pseudohygrophorone B[12] (**5.2**)			
	δ_C	δ_H, mult. (*J* in Hz)	HMBC	NOE	δ_C	δ_H, mult. (*J* in Hz)	HMBC	NOE
1	198.3	---	---	---	198.1	---	---	---
2	125.1	6.151 dd (10.2/2.5)	4, 6	3	128.6	6.205 d (10.1)	4, 6	3
3	151.0	6.833 dd (10.2/2.1)	1, 5	2, 4	145.2	6.972 dd (10.1/5.7)	1, 4, 5	2, 4
4	68.7	4.496 br d (11.0)	---	3, 6, 8	68.1	4.442 d (5.9)	2, 3, 6, 7	3, 8B, 7B w
OH-4	---	2.705 d (11.0)	---	---	---	*n.d.*	---	---
5	81.5	---	---	---	76.8	---	---	---
OH-5	---	2.064 br s	4, 5	---	---	*n.d.*	---	---
6	75.3	4.159 d (1.8)	1, 2, 4, 7	4, 8	76.7	4.694 s	1, 4, 5, 7	---
OH-6	---	3.713 d (1.8)	1, 5, 6	---	---	*n.d.*	---	---
7A	35.0	1.94[a]	4, 5, 6, 8, 9	7B, 8	31.0	1.709 m	4, 5, 6, 8, 9	7B, 8B
7B		1.75[a]	4, 5, 6, 8, 9	7A, 8		1.147 m	4, 5, 6, 8, 9	7A, 4 w
8A	25.1	1.43[a]	7, 9	4, 6, 7A, 7B	23.0	1.46[a]	7, 9	8B
8B						1.22[a]	9	4, 7A, 8A
9	29.9	1.35[a]	---[b]	---[b]	30.1	1.24[a]	---[b]	---[b]
10–15	29.64[c] 29.62[c] 29.61[c] 29.54[c] 29.51[c] 29.3	1.33 – 1.23[a]	---[b]	---[b]	29.63[c] 29.61[c] 29.59[c] 29.52[c] 29.46[c] 29.3	1.33 – 1.20[a]	---[b]	---[b]
16	31.9	1.25[a]	---[b]	---[b]	31.9	1.24[a]	---[b]	---[b]
17	22.7	1.28[a]	---[b]	---[b]	22.7	1.28[a]	---[b]	---[b]
18	14.1	0.882 t 7.2	16, 17	17	14.1	0.880 t 7.2	16, 17	17

n.d. = not detected. [a] Overlapping signals; chemical shifts were determined from ^{1}H,^{13}C-HSQC correlation peaks. [b] Not assignable due to overlapping signals. [c] Two decimals are given to assign resolved ^{13}C alkyl chain signals.

Pseudohygrophorone B[12] (**5.2**) was isolated as a colorless oil. ESI-HRMS measurements of **5.2** afforded a pseudomolecular ion at *m/z* 311.2236 ([M–H]$^-$, calcd for $C_{18}H_{31}O_4^-$, 311.2228), demonstrating the same molecular formula as pseudohygrophorone A[12] (**5.1**). In addition, the ^{1}H NMR spectrum of **5.2** was very similar to that of **5.1** (Table 5.1). Two signals at δ_H 6.205 (1H, d, *J* = 10.1 Hz, H-2) and δ_H 6.972 (1H, dd, *J* = 10.1/5.7 Hz, H-3) confirmed the presence of olefinic protons with corresponding ^{13}C resonances at δ_C 128.6 (C-2) and δ_C 145.2 (C-3), respectively. Extensive analyses of HMBC and COSY correlations (Fig. 5.2) revealed that pseudo-hygrophorone B[12] (**5.2**) is a diastereomer of **5.1** (Fig. 5.1).

Compound **5.3** was isolated as a white, amorphous solid and identified as the known cyclopentenone derivative hygrophorone B[12] (**5.3**) by comparing its spectroscopic data (1D NMR and ESI-HRMS) with those reported recently in the literature (Bette et al., 2015).

5.2.2 Assignment of the absolute configuration

The cyclohexenone derivatives **5.1** and **5.2** contain three asymmetric centers, corresponding to eight possible stereoisomers. The stereochemical assignment of compounds **5.1** and **5.2** was deduced from $J_{H,H}$ and NOE investigations combined with conformational analyses and quantum chemical calculations of CD spectra. Computational studies of structurally related cyclohexenone-*cis*-diols including conformational analyses and calculations of CD spectra have been reported by Kwit and co-workers (Kwit et al., 2010). The most striking difference between the experimental CD spectra of **5.1** and **5.2** was their opposite sign of the *n*-π* Cotton effect (CE) around 300 nm (Figs. 5.4 and 5.5).

Based on the small $^3J_{H3-H4}$ (2.1 Hz), but large $^4J_{H2-H4}$ (2.5 Hz) coupling constant in **5.1**, a perpendicular orientation of the allylic proton H-4 was suggested (Fig. 5.3) (Garbisch, 1964). This was supported by absent HMBC correlation peaks of H-4, since three-bond carbon-proton couplings also follow the Karplus relationship, exhibiting a minimum at dihedral angles around 90 degrees (Sahu et al., 2008). NOE cross peaks between H-4 and H-6 revealed a mutual *cis* geometry of H-4/H-6 (Fig. 5.4), indicative of four possible stereoisomers as two pairs of enantiomers (4*S*,5*R*,6*S* and 4*R*,5*S*,6*R* as well as 4*R*,5*R*,6*R* and 4*S*,5*S*,6*S*).

	expected	observed
$^3J_{H3-H4}$	small	2.1 Hz
$^4J_{H2-H4}$	medium	2.5 Hz

5.1

	expected	observed
$^3J_{H3-H4}$	large	5.7 Hz
$^4J_{H2-H4}$	small	---

5.2
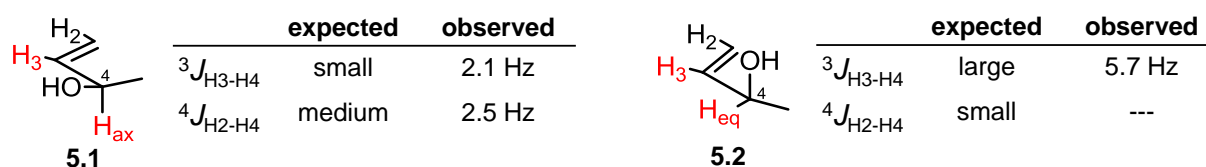
Fig. 5.3. $J_{H,H}$-based orientation assignment of the allylic proton H-4 in compounds **5.1** (axial) and **5.2** (equatorial).

To assign the absolute configuration of structure **5.1**, energy minimization on the BP86/def2-TZVPP level of the four possible *cis*-H-4/H-6 configured stereoisomers was performed. To take into account the different conformations the molecules might adopt, the low energy conformers were calculated on the basis of the favored (C-5)-sofa structure (Kwit et al., 2010) with almost ideal equatorial and axial orientations of the substituents at C-4, C-5, and C-6, different torsion angles of the 4-5-7-8 plane (minus gauche, plus gauche, and anti), and the *n*-alkyl side chain in an all-*trans* conformation. The (C-5)-sofa structure is characterized by *M* or *P* helicity as well as a planar enone chromophore (O=C1–C2=C3) (Kwit et al., 2010).

The conformational analysis of **5.1** yielded three relevant conformers for each stereoisomer within an energetical range of 3 kcal/mol above the global minimum (Fig. S27; Table S1, Supporting Information), all of which are characterized by orientations in which the 6-hydroxy function can form a hydrogen bond with the 1-oxo group. In addition, the energetically favored

axial geometry of the allylic proton H-4 correlated with the results from proton coupling constant analyses (Fig. 5.3). For each of the conformers thus identified, quantum chemical calculations on the TDCAM-B3LYP/def2-TZVP level were performed, providing single UV and CD spectra. The simulated CD curves were then weighted according to their Boltzmann statistics. While *RRR*- and *RSR*-**5.1** gave CD curves opposite to the experimental spectrum (Fig. S9, Supporting Information), the calculated CD spectra of both *SSS* and *SRS* stereoisomers nicely matched the curve of **5.1**, showing a positive *n-π** CE at approx. 300 nm along with negative and positive CEs around 200 and 235 nm, respectively (Fig. 5.4).
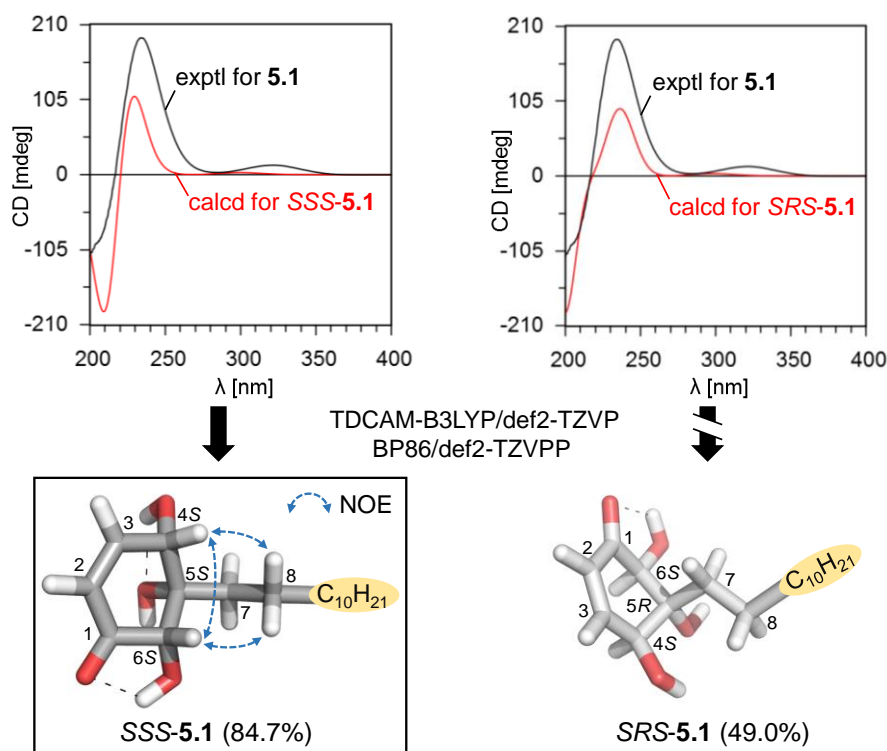
Fig. 5.4. Comparison of the Boltzmann weighted CD spectra of *SSS*-**5.1** and *SRS*-**5.1** (both 5 nm shift) with the experimental spectrum of pseudohygrophorone A[12] (**5.1**). The molecular structures of the BP86/def2-TZVPP-optimized main conformers (with respective Boltzmann population percentages in parentheses) are given below. The observed NOE interactions could be reconstructed only for the lowest energy conformer of *SSS*-**5.1**.

For a final assignment of the absolute configuration as either *SSS* or *SRS* in pseudo-hygrophorone A[12] (**5.1**), the significantly populated conformations of both epimers were analyzed to reveal spatial adjacent protons. The NOE correlation peaks between H-4, H-6, and the geminal protons at C-8 (and neither to H_A-7 nor H_B-7) indicated that the dodecyl side chain attached at C-5 is in the same plane as the *cis*-oriented protons H-4 and H-6 (Fig. 5.4). In fact, the observed NOE interactions could only be reconstructed for the low energy conformers of *SSS*-**5.1** (all relevant distances below 3 Å), since the axial oriented alkyl side chain in the energy minimized structures of the *SRS* isomer is antiperiplanar to H-4 and H-6, resulting in large spatial distances (Fig. 5.4; Table S1, Supporting Information). Based on these results, the absolute configuration of pseudohygrophorone A[12] (**5.1**) is with high probability 4*S*,5*S*,6*S* (Fig. 5.1).

The ^{1}H NMR spectrum of pseudohygrophorone B[12] (**5.2**) revealed, in contrast to its diastereomer **5.1**, a fairly large $^3J_{H3-H4}$ coupling constant of 5.7 Hz and absence of a $^4J_{H2-H4}$ coupling, corresponding to an equatorial geometry of H-4 in **5.2** (Fig. 5.3) (Garbisch, 1964). Deduced from absent NOE correlation peaks between H-4 and H-6, the orientation of these protons was proposed as *trans* (Fig. 5.5).
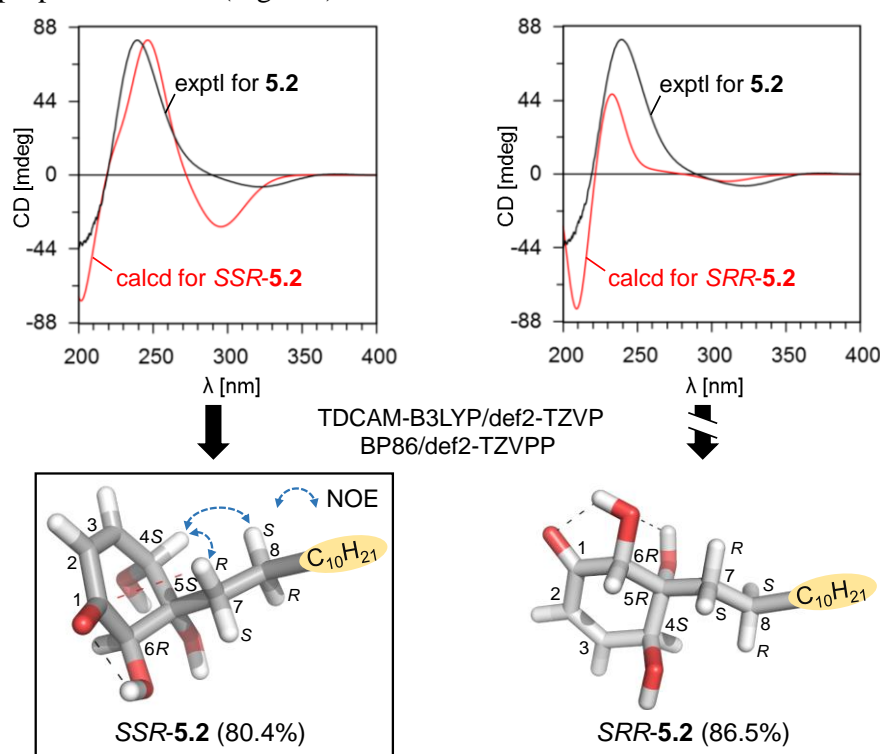
Fig. 5.5. Comparison of the Boltzmann weighted CD spectra of *SSR*-**5.2** (–5 nm shift) and *SRR*-**5.2** (11 nm shift) with the experimental spectrum of pseudohygrophorone B[12] (**5.2**). The molecular structures of the BP86/def2-TZVPP-optimized main conformers (with respective Boltzmann population percentages in parentheses) are given below. The observed NOE interactions could be reconstructed only for the lowest energy conformer of *SSR*-**5.2**.

Thus, energy optimized conformers of the four possible *trans*-H-4/H-6 configured isomers of **5.2** (*SRR* and *RSS* as well as *SSR* and *RRS*) were calculated, and their CD curves were simulated followed by Boltzmann weighting. While the calculated CD spectra of the *RSS* and *RRS* isomers were mirror-imaged to the experimental curve of **5.2** (Fig. S20, Supporting Information), the CD spectra of both *SSR*- and *SRR*-**5.2** fitted well to the spectrum of **5.2** (Fig. 5.5).

The absolute configuration in **5.2** was finally assigned similarly to that described above for compound **5.1**. The BP86/def2-TZVPP-optimized conformations of both epimers show an equatorially oriented allylic proton H-4 in their most stable conformations (Fig. S28, Supporting Information), fitting to the NMR data (Fig. 5.3). The experimental NOE interactions solely matched the most populated conformer of *SSR*-**5.2**, showing spatial proximity (< 3 Å) between H-4/H$_{pro-R}$-7 and H-4/H$_{pro-S}$-8 (Fig. 5.5; Table S2, Supporting Information). In addition to these observations, the signal of H$_{pro-R}$-7, which exhibits an NOE correlation to H-4, is shifted to high field (δ_H 1.147). The shielding of this proton may be explained by the magnetic anisotropy of the C=O function that is present in the cyclohexenone system of **5.2**. In fact, a spatial proximity of

H$_{pro-R}$-7 to the shielding cone of the carbonyl function (2.7 Å) was detected only in the energetically most stable conformer of *SSR*-**5.2** (Fig. 5.6). In turn, the faraway proton H$_{pro-S}$-7 is shifted downfield, resonating at δ$_H$ 1.709. On the basis of the aforementioned evidence, pseudohygrophorone B[12] (**5.2**) was identified as the C-6 epimer of **5.1**, corresponding to the absolute configuration 4*S*,5*S*,6*R* (Fig. 5.1).
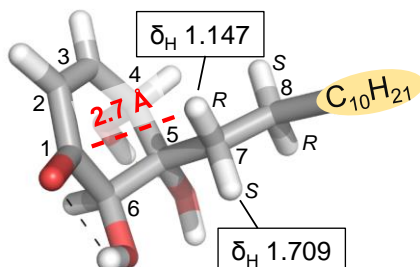
Fig. 5.6. Magnetic anisotropy effect of the C=O function to H$_{pro-R}$-7 in the main conformer of pseudohygrophorone B[12] (**5.2**). The spatial proximity of H$_{pro-R}$-7 to the shielding cone of the carbonyl group leads to a high field shift, whereas the faraway proton H$_{pro-S}$-7 is shifted downfield.

5.2.3 Higher-energy collisional dissociation (HCD) fragmentation studies

The MS fragmentation behavior of pseudohygrophorones A[12] (**5.1**) and B[12] (**5.2**) was investigated under negative ion ESI-HCD conditions and compared with that of hygrophorone B[12] (**5.3**). Tandem mass spectrometric data of hygrophorones under ESI-CID-MS conditions using both a triple quadrupole and a QqTOF system were reported earlier (Lübken et al., 2006).

Scheme 5.1. Negative ion ESI-HCD fragmentation behavior of compounds **5.1–5.3**.
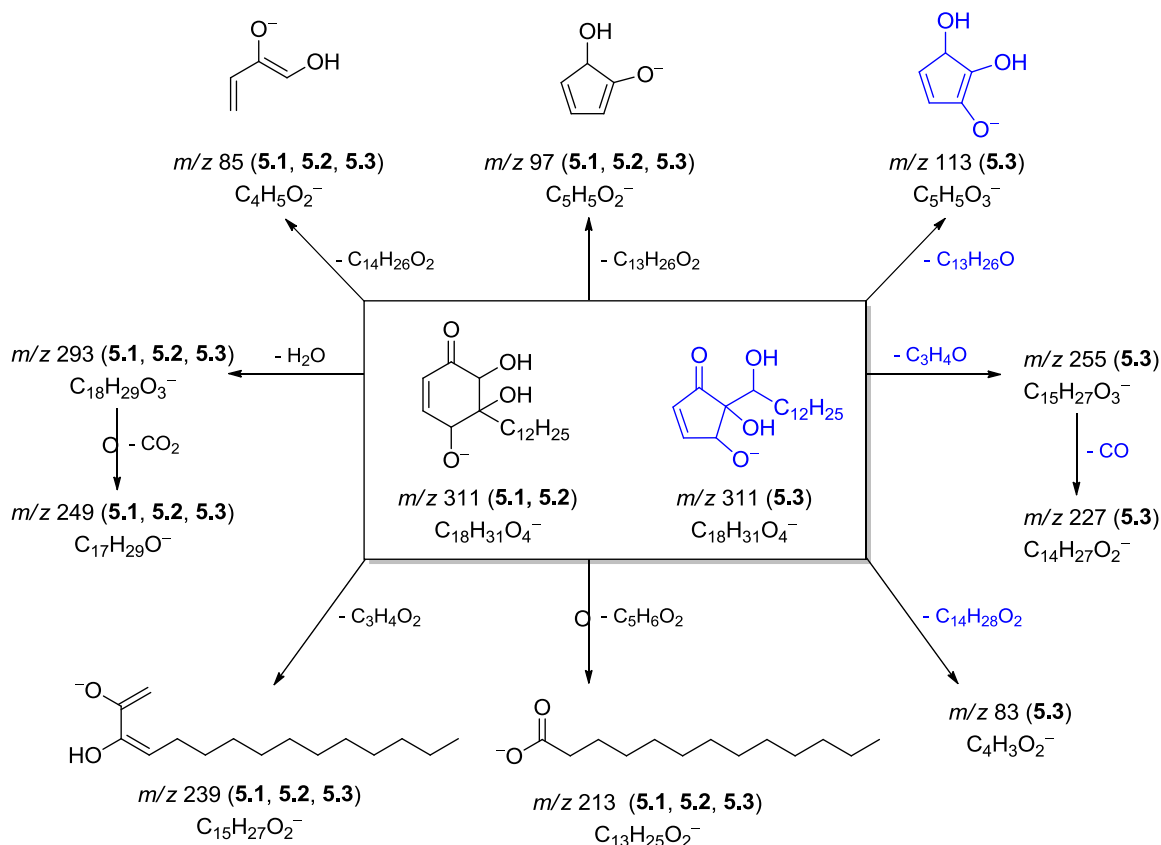
While the HCD spectra of the cyclohexenone derivatives **5.1** and **5.2** were almost identical, they showed both differences and similarities to that of the cyclopentenone derivative **5.3** (Scheme 5.1). For instance, ions indicative of the length of the alkyl side chain at *m/z* 293 ([M–H–H_2O]$^-$), 239, and 213 were detected equally in **5.1**–**5.3**. In contrast, the fragment ions at *m/z* 249 ([M–H–H_2O–CO_2]$^-$), and 97 appeared very abundant in **5.3**, but only weakly in **5.1** and **5.2**. Interestingly, the mass spectrum of hygrophorone B[12] (**5.3**) displayed fragment ions at *m/z* 83, 113, 227, and 255, which were not detected in the spectra of the cyclohexenones **5.1** and **5.2**. The HCD spectra of pseudohygrophorones **5.1** and **5.2**, on the contrary, exhibited a dominant key ion at *m/z* 85 that was only weakly abundant from hygrophorone B[12] (**5.3**). Consequently, the above discussed key ions and significant differences in the abundance ratio *m/z* 85 to *m/z* 97 allow a clear distinction between the pseudohygrophorones (**5.1**, **5.2**) and hygrophorone B[12] (**5.3**) on the basis of their HCD mass spectra.

5.2.4 Biological evaluation against phytopathogenic organisms

The isolated (pseudo-)hygrophorones **5.1**–**5.3** were examined towards their activity against the plant pathogenic fungi *Botrytis cinerea* (grey mold pathogen on many crops including strawberries and wine grapes) and *Septoria tritici* (causes septoria leaf blotch of wheat) as well as the oomycete *Phytophthora infestans* (causal agent of the late blight disease on potato and tomato) using a 96 well microtiter plate assay (Table 5.2). The commercially used fungicides dodine and pyraclostrobin were used as reference compounds.

Pseudohygrophorones A[12] (**5.1**) and B[12] (**5.2**) showed remarkable effects against *P. infestans*, and moderate activity towards *B. cinerea* and *S. tritici*, while hygrophorone B[12] (**5.3**) exhibited outstanding activity against all organisms tested (Table 5.2). Their activity is similar to that of the commercial fungicide dodine. Since both dodine and (pseudo-)hygrophorones are amphiphilic compounds, it is likely that some or all activity is related to membrane activity, an antibiotic mechanism that commonly is not prone to resistance formation in contrast to the selective and thus highly active protein inhibitors such as strobilurins.

Table 5.2. Antiphytopathogenic activity of compounds **5.1**–**5.3** against *B. cinerea*, *S. tritici*, and *P. infestans* (IC$_{50}$, µM).

compound	*B. cinerea*	*S. tritici*	*P. infestans*
5.1	18.0 ± 2.6	17.5 ± 2.6	7.6 ± 0.5
5.2	19.0 ± 1.2	24.5 ± 3.2	4.3 ± 0.4
5.3	4.9 ± 0.7	5.9 ± 0.7	1.6 ± 0.3
pyraclostrobin[a]	< 0.0052	< 0.0052	0.018 ± 0.002
dodine[a]	9.4 ± 0.6	2.8 ± 0.2	43.8 ± 5.6

[a] Used as reference compounds.

5.3 Conclusions

In summary, two new alkyl cyclohexenones, named pseudohygrophorones A[12] (**5.1**) and B[12] (**5.2**), along with the recently reported hygrophorone B[12] (**5.3**) were isolated from fruiting bodies of *H. abieticola*. Their structures were unambiguously established on the basis of extensive 1D and 2D NMR spectroscopic analyses as well as ESI-HRMS experiments. The absolute configuration of **5.1** and **5.2** was deduced from $^3J_{H,H}$ and $^4J_{H,H}$ coupling constants, NOE interactions, and conformational analyses in combination with quantum chemical CD calculations. In addition, the ESI-HCD fragmentation behavior of **5.1**–**5.3** was investigated and identified as a valuable technology to distinguish between pseudohygrophorones (**5.1**, **5.2**) and a corresponding hygrophorone (B[12], **5.3**).

To the best of our knowledge, this rare group of alkyl cyclohexenones is hitherto exclusively reported from plants of the family Anacardiaceae such as *Lannea edulis* Engl. (Queiroz et al., 2003), *Lannea welwitschii* (Hiern) Engl. (Groweiss et al., 1997), *Tapirira obtusa* (Benth) J.D. Mitchel (Correia et al., 2001), and *Tapirira guianensis* Aubl (David et al., 1998; Roumy et al., 2009). Thus, pseudohygrophorones **5.1** and **5.2** represent the first examples of this group of secondary metabolites not only from basidiocarps of the genus *Hygrophorus*, but from the entire fungal kingdom. The isolated metabolites **5.1**–**5.3** exhibited pronounced activity against the phytopathogenic fungi *Septoria tritici* and *Botrytis cinerea* as well as the oomycete *Phytophthora infestans*. Compounds **5.1**–**5.3** thus may serve as lead structures for the development of novel fungicidal plant protection agents.

5.4 Experimental Section

General Experimental Procedures. Column chromatography was performed on silica gel (40–63 μm, Merck, Germany) and Sephadex LH 20 (Fluka, Germany), while analytical TLC was performed on precoated silica gel F$_{254}$ plates (Merck, Germany). The compound spots were detected by their UV absorbance at λ 254 nm and/or by spraying of the TLC plates with vanillin-sulfuric acid reagent followed by heating in a hot air stream. The given R_f values are uncorrected. IR spectra were obtained from a Thermo Nicolet 5700 FT-IR spectrometer. UV spectra were measured with a Jasco V-560 UV/Vis spectrophotometer, whereas CD spectra were acquired on a Jasco J-815 CD spectrophotometer. The specific rotation was measured with a Jasco P-2000 polarimeter.
1D (^{1}H, ^{13}C) and 2D (^{1}H,^{13}C HSQC, ^{1}H,^{13}C HMBC, ^{1}H,^{1}H COSY, ^{1}H,^{1}H ROESY) NMR spectra were obtained from an Agilent VNMRS 600 system. The spectra were recorded at 600 MHz (^{1}H) and 150 MHz (^{13}C), respectively. Chemical shifts were referenced to internal TMS (δ_H 0, ^{1}H) or CDCl$_3$ (δ_C 77.0, ^{13}C). The mixing time for the ^{1}H,^{1}H ROESY experiments was set to 0.4 s. The negative ion high resolution ESI mass spectra were obtained from an Orbitrap Elite mass spectrometer (Thermo Fisher Scientific, Germany) equipped with an HESI electrospray ion source

(spray voltage 3.5 kV, capillary temperature 275 °C, source heater temperature 40 °C, FTMS resolution 60.000). Nitrogen was used as sheath gas. The sample solutions were introduced continuously *via* a 500 µl Hamilton syringe pump with a flow rate of 5 µl min^{-1}. The instrument was externally calibrated by the Pierce LTQ Velos ESI negative ion calibration solution (product no. 88324) from Thermo Fisher Scientific. The data were evaluated by the Xcalibur software 2.7 SP1. The negative ion ESI higher-energy collisional dissociation (HCD) mass spectra were recorded at a normalized collision energy (NCE) of 50% (corresponding to 15 eV) using nitrogen as collision gas.

Preparative HPLC was performed on a Knauer system equipped with a WellChrom K-1001 pump and a WellChrom K-2501 UV detector using an ODS-A column (5 µm, 120 Å, 150 × 10 mm ID, YMC, USA) eluting with H_2O (A) and CH_3CN (B) at a flow rate of 3.5 ml/min.

Fungal Material. Fruiting bodies of *Hygrophorus abieticola* Krieglst. ex Gröger & Bresinsky were collected under *Abies alba* Mill. in Paintner Forst near Kelheim, Bavaria, Germany (October 11, 2007, leg./det. A. Bresinsky). A voucher specimen (coll. 57/07) is deposited at the Leibniz Institute of Plant Biochemistry (IPB), Halle, Germany.

Extraction and isolation. Frozen fruiting bodies of *H. abieticola* (2.5 kg) were macerated using a blender and extracted with EtOAc (3 × 3 l). The slightly yellow solution was evaporated *in vacuo* to dryness. The crude extract (20.2 g) was subjected to silica gel column chromatography (CC, 450 × 45 mm) eluting with $CHCl_3$/MeOH (100:0→0:100) to obtain 10 fractions (A1–10, each 50 ml). Fraction A6 (3.05 g) was further purified by size exclusion CC on Sephadex LH 20 (400 × 40 mm, eluent CH_2Cl_2/MeOH 1:1), yielding 7 fractions (B1–7, each 50 ml). Fraction B5 (1.40 g) was further purified by silica gel CC (450 × 45 mm) eluting with *n*-hexane/EtOAc (1:1) to afford 230 fractions (each 20 ml). Fraction 79 (5.2 mg) was purified by preparative RP18 HPLC (0–19 min, 55–80% B) to yield **5.1** (t$_R$ 12.4 min, 0.9 mg). Final purification of fractions 95–105 (21.3 mg) by preparative RP18 HPLC (0–19 min, 60–70% B) afforded **5.2** (t$_R$ 11.3 min, 1.2 mg). Fractions 173–180 (32.3 mg) were finally purified by preparative HPLC (0–24 min, 55–75% B) to obtain **5.3** (t$_R$ 14.2 min, 20.1 mg).

Pseudohygrophorone A[12] (5.1): white, amorphous solid; TLC R_f 0.31 (*n*-hexane/EtOAc 1:1); $[\alpha]^{24}_D$ +87.9 (*c* 0.070, CHCl$_3$); UV (MeOH) λ_{max} (log ε) 218 nm (3.72); CD (MeOH) $[\theta]_{195}$ −10536, $[\theta]_{234}$ +13682, $[\theta]_{322}$ +952 °×cm^2×dmol^{-1}; IR (ATR) υ_{max} 3510 (br, w), 3402 (br, w), 2916 (s), 2849 (s), 1716 (s), 1694 (s), 1471 (m), 1398 (w), 1355 (w), 1251 (w), 1214 (w), 1155 (m), 1073 (m), 1001 (m), 961 (w), 931 (w), 842 (m), 796 (w), 719 (w), 686 (w) cm^{-1}; ^{1}H NMR and ^{13}C NMR see Table 5.1; ESI-HRMS *m/z* 311.2237 ([M–H]$^-$, calcd for $C_{18}H_{31}O_4^-$, 311.2228); ESI-HCD-HRMS *m/z* (rel. int. in %, molecular formula, error in ppm) 311.2231 (100, $C_{18}H_{31}O_4^-$, 1.1), 293.2125 (25, $C_{18}H_{29}O_3^-$, 0.9), 249.2227 (4, $C_{17}H_{29}O^-$, 1.3), 239.2020 (39, $C_{15}H_{27}O_2^-$, 1.3), 213.1863 (5, $C_{13}H_{25}O_2^-$, 1.2), 97.0298 (4, $C_5H_5O_2^-$, 2.7), 85.0298 (33, $C_4H_5O_2^-$, 3.4).

Pseudohygrophorone B[12] (5.2): colorless oil; TLC R_f 0.30 (*n*-hexane/EtOAc 1:1); $[\alpha]^{24}_D$ +19.7 (*c* 0.120, CHCl$_3$); UV (MeOH) λ_{max} (log ε) 214 nm (3.71); CD (MeOH) $[\theta]_{200}$ −3585, $[\theta]_{239}$ +6699, $[\theta]_{323}$ −587 °×cm^2×dmol^{-1}; IR (ATR) υ_{max} 3402 (br, w), 2916 (s), 2845 (s), 2356 (w), 1692 (s), 1464 (m), 1377 (w), 1243 (w), 1096 (m), 1054 (m), 1032 (m), 951 (w), 926 (w), 905 (w), 849 (m), 776 (w), 718 (w), 676 (w) cm^{-1}; ^{1}H NMR and ^{13}C NMR see Table 5.1; ESI-HRMS *m/z* 311.2236 ([M–H]$^-$, calcd for $C_{18}H_{31}O_4^-$, 311.2228); ESI-HCD-HRMS *m/z* (rel. int. in %, molecular formula, error in ppm) 311.2232 (100, $C_{18}H_{31}O_4^-$, 1.3), 293.2125 (23, $C_{18}H_{29}O_3^-$, 1.0), 249.2227 (5, $C_{17}H_{29}O^-$, 1.2), 239.2020 (33, $C_{15}H_{17}O_2^-$, 1.3), 213.1863 (13, $C_{13}H_{25}O_2^-$, 1.5), 97.0298 (7, $C_5H_5O_2^-$, 2.9), 85.0298 (27, $C_4H_5O_2^-$, 3.5).

Hygrophorone B[12] (5.3): white solid; TLC R_f 0.31 (*n*-hexane/EtOAc 1:1); $[\alpha]^{24}_D$ +11.3 (*c* 1.850, CHCl$_3$); IR (ATR) υ_{max} 3510 (br, w), 3401 (w), 2916 (s), 2850 (s), 1715 (s), 1694 (s), 1594 (w), 1470 (m), 1397 (w), 1356 (w), 1251 (w), 1214 (w), 1115 (m), 1071 (m), 1001 (m), 961 (m), 930 (w), 875 (w), 843 (m), 794 (w), 720 (w), 686 (w) cm^{-1}; ^{1}H NMR, ^{13}C NMR, and ESI-HRMS in agreement with Bette et al. (2015); ESI-HCD-HRMS *m/z* (rel. int. in %, molecular formula, error in ppm) 311.2231 (100, $C_{18}H_{31}O_4^-$, 1.1), 293.2124 (52, $C_{18}H_{29}O_3^-$, 0.6), 255.1968 (26, $C_{15}H_{27}O_3^-$, 1.0), 249.2227 (32, $C_{17}H_{29}O^-$, 1.2), 239.2020 (14, $C_{15}H_{27}O_2^-$, 1.3), 227.2019 (22, $C_{14}H_{27}O_2^-$, 1.1), 213.1862 (97, $C_{13}H_{25}O_2^-$, 0.8), 113.0247 (11, $C_5H_5O_3^-$, 2.6), 97.0297 (83, $C_5H_5O_2^-$, 2.5), 85.0297 (4, $C_4H_5O_2^-$, 2.7), 83.0141 (22, $C_4H_3O_2^-$, 3.3).

Computational details. The initial conformational analyses of the four diastereomers (4*S*,5*S*,6*S*, 4*S*,5*R*,6*S*, 4*S*,5*R*,6*R*, and 4*S*,5*S*,6*R*) and their enantiomers was performed using the MMFF94 molecular mechanics force field (Halgren, 1999), with the aid of the Molecular Operating Environment (MOE, 2014) program package (for the results, see Tables S1 and S2). For all structures, a (C-5)-sofa conformation with nearly ideal equatorial and axial orientations of the substituents at C-4, C-5, and C-6 was the most stable one. The rotation around the C-7/C-8 bond out of *trans* was energetically unfavored, thus in all cases the conformation of the alkyl side chain carbons (C-7 to C-18) was fixed to all *trans* in the subsequent DFT calculations. Conformational rotation of the alkyl side chain around the C-5/C-7 bond resulted in three relevant conformations (anti, plus gauche, minus gauche). The force field minimum energy conformers thus obtained were subsequently optimized by applying the density functional theory (DFT) using the BP86 functional with the def2-TZVPP basis set (Becke, 1988; Karton et al., 2008; Perdew, 1986; Schäfer et al., 1992; Weigend and Ahlrichs, 2005) implemented in the *ab initio* ORCA 3.0.3 program package (Neese, 2012). The DFT calculations were carried out in MeOH using the COSMO model (Sinnecker et al., 2006) to include any influence of the solvent. The structures of all DFT-computed conformers can be found in the Supporting Information.

The quantum chemical simulation of the UV and CD spectra was also carried out with ORCA (Neese, 2012). Time-dependent (TD)-DFT calculations of the first 50 excited states of each conformer were performed in MeOH using the long-range corrected hybrid functional CAM-

B3LYP (Yanai et al., 2004) with the def2-TZVP(-f) and def2-TZVP/J basis sets (Karton et al., 2008; Schäfer et al., 1992; Weigend and Ahlrichs, 2005). The CD curves were obtained with the help of the software SpecDis 1.62 (Bruhn et al., 2013, 2014) from the calculated rotatory strength values using a Gaussian distribution function at a half bandwidth of $\sigma = 0.3$ eV. The single spectra of the individual conformers were summed up according to their contribution to Boltzmann-statistical weighting (as derived from the single-point energy calculations), wavelength shifted, and compared with the experimental spectra.

Antiphytopathogenic bioassay. Pure compounds were tested in a 96-well microtiter plate assay against *Botrytis cinerea* Pers., *Septoria tritici* Desm. and *Phytophthora infestans* (Mont.) de Bary according to the fungicide resistance action committee (FRAC) with minor modifications (Stammler and Semar, 2011; Stammler and Speakman, 2006; Stammler, 2006): Crude extracts and fractions were examined at a final concentration of 125 μg/ml, while pure compounds were tested in a serial dilution, ranging from 100 μM to 0.1 μM. The solvent DMSO was used as negative control (max. concentration 2.5%), and the commercially used fungicides dodine and pyraclostrobin (Sigma Aldrich, Germany) served as positive controls. Seven days after inoculation, the pathogen growth was evaluated by measurement of the optical density (OD) at λ 405 nm with a Tecan GENios Pro microplate reader (5 measurements per well using multiple reads in a 3×3 square). Each experiment was carried out in triplicates. IC$_{50}$ values were calculated from dose-response curves on the basis of sigmoidal curve fitting (four parameter logistic) using the software SigmaPlot 12.0.

5.5   References

Becke, A.D., 1988. Density-functional exchange-energy approximation with correct asymptotic behavior. *Phys. Rev. A* 38, 3098–3100.

Bette, E., Otto, A., Dräger, T., Merzweiler, K., Arnold, N., Wessjohann, L., Westermann, B., 2015. Isolation and asymmetric total synthesis of fungal secondary metabolite hygrophorone B[12]. *Eur. J. Org. Chem.* 2015, 2357–2365.

Bresinsky, A., 2008. Beiträge zu einer Mykoflora Deutschlands (2): Die Gattungen *Hydropus* bis *Hypsizygus* mit Angaben zur Ökologie und Verbreitung der Arten. *Regensburg. Mykol. Schriften* 15, 1–304.

Bruhn, T., Schaumlöffel, A., Hemberger, Y., Bringmann, G., 2014. SpecDis version 1.62, University of Würzburg, Germany.

Bruhn, T., Schaumlöffel, A., Hemberger, Y., Bringmann, G., 2013. SpecDis: Quantifying the comparison of calculated and experimental electronic circular dichroism spectra. *Chirality* 25, 243–249.

Correia, S.D.J., David, J.M., David, J.P., Chai, H.B., Pezzuto, J.M., Cordell, G.A., 2001. Alkyl phenols and derivatives from *Tapirira obtusa*. *Phytochemistry* 56, 781–784.

David, J.M., Chavez, J.P., Chai, H.B., Pezzuto, J.M., Cordell, G.A., 1998. New cytotoxic compounds from *Tapirira guianensis*. *J. Nat. Prod.* 61, 287–289.

Garbisch, E.W., 1964. Conformations. VI. Vinyl-allylic proton spin couplings. *J. Am. Chem. Soc.* 86, 5561–5564.

Gilardoni, G., Clericuzio, M., Marchetti, A., Finzi, P.V., Zanoni, G., Vidari, G., 2006. New oxidized 4-oxo fatty acids from *Hygrophorus discoxanthus*. *Nat. Prod. Commun.* 1, 1079–1084.

Gilardoni, G., Clericuzio, M., Tosi, S., Zanoni, G., Vidari, G., 2007. Antifungal acylcyclopentenediones from fruiting bodies of *Hygrophorus chrysodon*. *J. Nat. Prod.* 70, 137–139.

Groweiss, A., Cardellina, J.H., Pannell, L.K., Uyakul, D., Kashman, Y., Boyd, M.R., 1997. Novel cytotoxic, alkylated hydroquinones from *Lannea welwitschii*. *J. Nat. Prod.* 60, 116–121.

Halgren, T.A., 1999. MMFF VI. MMFF94s option for energy minimization studies. *J. Comp. Chem.* 20, 720–729.

Karton, A., Tarnopolsky, A., Lamère, J.F., Schatz, G.C., Martin, J.M.L., 2008. Highly accurate first-principles benchmark data sets for the parametrization and validation of density functional and other approximate methods. Derivation of a robust, generally applicable, double-hybrid functional for thermochemistry and thermochemical kinetics. *J. Phys. Chem. A* 112, 12868–12886.

Krieglsteiner, G.J., Gminder, A., 2001. Die Großpilze Baden-Württembergs, Band 3: Ständerpilze. Blätterpilze 1. Ulmer, Stuttgart, 1–634.

Kwit, M., Gawronski, J., Boyd, D.R., Sharma, N.D., Kaik, M., 2010. Circular dichroism, optical rotation and absolute configuration of 2-cyclohexenone-cis-diol type phenol metabolites: redefining the role of substituents and 2-cyclohexenone conformation in electronic circular dichroism spectra. *Org. Biomol. Chem.* 8, 5635–5645.

Lübken, T., Arnold, N., Wessjohann, L., Böttcher, C., Schmidt, J., 2006. Analysis of fungal cyclopentenone derivatives from *Hygrophorus* spp. by liquid chromatography/electrospray-tandem mass spectrometry. *J. Mass Spectrom.* 41, 361–371.

Lübken, T., Schmidt, J., Porzel, A., Arnold, N., Wessjohann, L., 2004. Hygrophorones A–G: Fungicidal cyclopentenones from *Hygrophorus* species (Basidiomycetes). *Phytochemistry* 65, 1061–1071.

Molecular Operating Environment (MOE) 2014.09, 2014. Chemical Computing Group Inc.: Montreal, QC, Canada.

Neese, F., 2012. The ORCA program system. *Wiley Interdiscip. Rev.: Comput. Mol. Sci.* 2, 73–78.

Otto, A., Porzel, A., Schmidt, J., Wessjohann, L., Arnold, N., 2015b. A study on the biosynthesis of hygrophorone B[12] in the mushroom *Hygrophorus abieticola* reveals an unexpected labelling pattern in the cyclopentenone moiety. *Phytochemistry* 118, 174–180.

Otto, A., Porzel, A., Schmidt, J., Wessjohann, L., Arnold, N., 2014. Penarines A–F, (nor-) sesquiterpene carboxylic acids from *Hygrophorus penarius* (Basidiomycetes). *Phytochemistry* 108, 229–233.

Perdew, J.P., 1986. Density-functional approximation for the correlation energy of the inhomogeneous electron gas. *Phys. Rev. B* 33, 8822–8824.

Queiroz, E.F., Kuhl, C., Terreaux, C., Mavi, S., Hostettmann, K., 2003. New dihydroalkylhexenones from *Lannea edulis*. *J. Nat. Prod.* 66, 578–580.

Roumy, V., Fabre, N., Portet, B., Bourdy, G., Acebey, L., Vigor, C., Valentin, A., Moulis, C., 2009. Four anti-protozoal and anti-bacterial compounds from *Tapirira guianensis*. *Phytochemistry* 70, 305–311.

Sahu, N.P., Banerjee, S., Mondal, N.B., Mandal, D., 2008. Steroidal saponins, in: Kinghorn, A.D., Falk, H., Kobayashi, J. (Eds.), Fortschritte der Chemie organischer Naturstoffe / Progress in the Chemistry of Organic Natural Products. Springer Verlag, Wien, pp. 45–141.

Schäfer, A., Horn, H., Ahlrichs, R., 1992. Fully optimized contracted gaussian-basis sets for atoms Li to Kr. *J. Chem. Phys.* 97, 2571–2577.

Schmidts, V., Fredersdorf, M., Lübken, T., Porzel, A., Arnold, N., Wessjohann, L., Thiele, C.M., 2013. RDC-based determination of the relative configuration of the fungicidal cyclopentenone 4,6-diacetylhygrophorone A[12]. *J. Nat. Prod.* 76, 839–844.

Sinnecker, S., Rajendran, A., Klamt, A., Diedenhofen, M., Neese, F., 2006. Calculation of solvent shifts on electronic g-tensors with the conductor-like screening model (COSMO) and its self-consistent generalization to real solvents (direct COSMO-RS). *J. Phys. Chem. A* 110, 2235–2245.

Stammler, G., 2006. *Phytophthora infestans* microtiter method with sporangia. URL http://www.frac.info/docs/default-source/monitoring-methods/approved-methods/phytin-microtiter-method-sporangia-basf-2006-v1.pdf?sfvrsn=4 (accessed 24th October 2015).

Stammler, G., Semar, M., 2011. Sensitivity of *Mycosphaerella graminicola* (anamorph: *Septoria tritici*) to DMI fungicides across Europe and impact on field performance. *EPPO Bull.* 41, 149–155.

Stammler, G., Speakman, J., 2006. Microtiter method to test the sensitivity of *Botrytis cinerea* to boscalid. *J. Phytopathol.* 154, 508–510.

Teichert, A., Lübken, T., Schmidt, J., Porzel, A., Arnold, N., Wessjohann, L., 2005b. Unusual bioactive 4-oxo-2-alkenoic fatty acids from *Hygrophorus eburneus*. *Z. Naturforsch.* 60b, 25–32.

Weigend, F., Ahlrichs, R., 2005. Balanced basis sets of split valence, triple zeta valence and quadruple zeta valence quality for H to Rn: Design and assessment of accuracy. *Phys. Chem. Chem. Phys.* 7, 3297–3305.

Yanai, T., Tew, D.P., Handy, N.C., 2004. A new hybrid exchange-correlation functional using the Coulomb-attenuating method (CAM-B3LYP). *Chem. Phys. Lett.* 393, 51–57.

5.6   Supporting Information

Supplementary data associated with this article (1D NMR and ESI-HRMS spectra of compounds **5.1**–**5.3**; 2D NMR, UV, CD, IR spectra, and additional computational data of compounds **5.1** and **5.2**) can be found at http://pubs.acs.org/doi/10.1021/acs.jnatprod.5b00675.

6 Structural and stereochemical elucidation of new hygrophorones from *Hygrophorus abieticola* (Basidiomycetes)
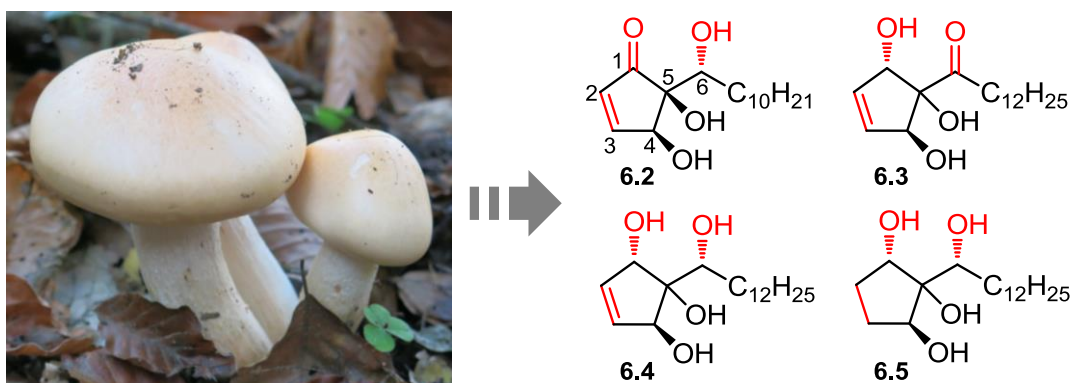
Abstract

Four new hygrophorones (**6.2–6.5**) have been isolated from fruiting bodies of the basidiomycete *Hygrophorus abieticola* Krieglst. ex Gröger & Bresinsky. Their structures were assigned on the basis of extensive one and two dimensional NMR spectroscopic analyses as well as ESI-HRMS measurements. Among these compounds, two previously undescribed hygrophorone types, named hygrophorone H^{12} (**6.4**) and 2,3-dihydrohygrophorone H^{12} (**6.5**), were identified. The absolute configuration of hygrophorone E^{12} (**6.3**) is suggested based on quantum chemical CD calculations, while a semisynthetic approach in conjunction with computational studies and analysis of NOE interactions allowed the stereochemical assignment of compounds **6.4** and **6.5**. Additionally, semisynthetic derivatives of hygrophorone B^{12} (**6.1**) were generated by acetylation of the hydroxyl groups. The biological activity of the natural and semisynthetic hygrophorones was evaluated against phytopathogenic organisms, revealing that the α,β-unsaturated carbonyl functionality is likely to be an essential structural feature. Hygrophorone B^{12} (**6.1**) was identified as the most active compound, acting against both ascomycetous fungi and oomycetes. Additionally, it could be shown that hygrophorone B^{12} (**6.1**) efficiently reacts with ʟ-cysteine in a nucleophilic addition reaction (Michael reaction). The activity of the tested hygrophorones may be thus contributed to the α,β-unsaturated carbonyl group reacting *in vivo* with biological nucleophiles.

6.1 Introduction

Field observations revealed that fruiting bodies of certain species of the genus *Hygrophorus* (Hygrophoraceae, Agaricales) are hardly ever attacked by mycophilic fungi (Lübken et al., 2004). Consequently, novel compound classes with antifungal activity were isolated from *Hygrophorus* spp. such as 4-oxo fatty acids (Gilardoni et al., 2006; Teichert et al., 2005b), chrysotriones (Gilardoni et al., 2007), and hygrophorones (Lübken et al., 2006, 2004; Schmidts et al., 2013). In addition, rare ventricosane-type (nor-)sesquiterpenes were obtained from fruiting bodies of *H. penarius* (Otto et al., 2014).

Recently, two yet unknown cyclohexenone derivatives, named pseudohygrophorones A[12] (**5.1**) and B[12] (**5.2**), together with hygrophorone B[12] (**6.1**) have been isolated from fruiting bodies of *Hygrophorus abieticola* Krieglst. ex Gröger & Bresinsky (Bette et al., 2015; Otto et al., 2016a). Hygrophorone B[12] (**6.1**) was subsequently synthesized in an enantiomerically pure form, allowing for an unambiguous determination of the relative and absolute configuration (Bette et al., 2015). Moreover, the biosynthesis of **6.1** was investigated by feeding of ^{13}C labelled precursors to basidiocarps of *H. abieticola* (Otto et al., 2015b).

The medium-sized to large fruiting bodies of *H. abieticola* are obligate mycorrhizal symbionts with *Abies alba* (silver fir), growing usually in clusters on calcareous soils (Bresinsky, 2008). The yellow to orange colored basidiocarps are characterized by a sticky to viscid surface in humid atmosphere. Although considered edible, the resin to turpentine-like taste and smell makes this mushroom not very delicate (Krieglsteiner and Gminder, 2001).

The present study describes the isolation and structural elucidation of four new hygrophorones (**6.2–6.5**) from fruiting bodies of the basidiomycete *Hygrophorus abieticola* Krieglst. ex Gröger & Bresinsky. Additionally, the semisynthetic derivatives **6.1a–6.1d** were generated by acetylation of hygrophorone B[12] (**6.1**). The biological activity of the compounds **6.1–6.5** was evaluated against phytopathogenic organisms as well as clinical isolates of multi-resistant bacteria.

6.2 Results and discussion

6.2.1 Isolation and structural elucidation

Repeated column chromatography on silica gel, Sephadex LH 20, and preparative RP18 HPLC yielded compounds **6.1–6.5** (see Chapter 6.4).

Compound **6.1**, isolated as a white solid, was identified as the known cyclopentenone derivative hygrophorone B[12] (**6.1**) by comparing its optical and spectroscopic data ($[\alpha]_D$, IR, 1D NMR, and ESI-HRMS) with those reported recently in the literature (Bette et al., 2015; Otto et al., 2016a).

Compound **6.2** was isolated as a colorless oil. The molecular formula $C_{16}H_{28}O_4$ was determined by HRMS measurements of the molecular ion at *m/z* 319.1680 ([M+Cl]⁻, calculated

for $C_{16}H_{28}O_4Cl^-$ 319.1682), corresponding to three degrees of unsaturation. The ^1H and ^{13}C NMR spectra (Table 6.1) of **6.2** were almost identical to those of hygrophorone B[12] (**6.1**). In contrast to **6.1**, the ^{13}C NMR spectrum of **6.2** lacked two aliphatic ^{13}C signals corresponding to the side chain, which was further confirmed by the ESI-HRMS data. The alkyl chain of **6.2** connected to C-6 was therefore determined as $-C_{10}H_{21}$. On the basis of these data, **6.2** was identified as a homologue of **6.1** lacking two methylene groups in the alkyl side chain. The absolute configuration of **6.2** was identified to be identical to that of hygrophorone B[12] (**6.1**) due to the fact that the optical rotation of both **6.1** and **6.2** showed a positive value. Therefore, **6.2** was assigned as the new (4*S*,5*S*)-dihydroxy-5-((*R*)-1-hydroxyundecyl)-cyclopent-2-enone (IUPAC name), and consequently named hygrophorone B[10] (**6.2**) (Fig. 6.1).
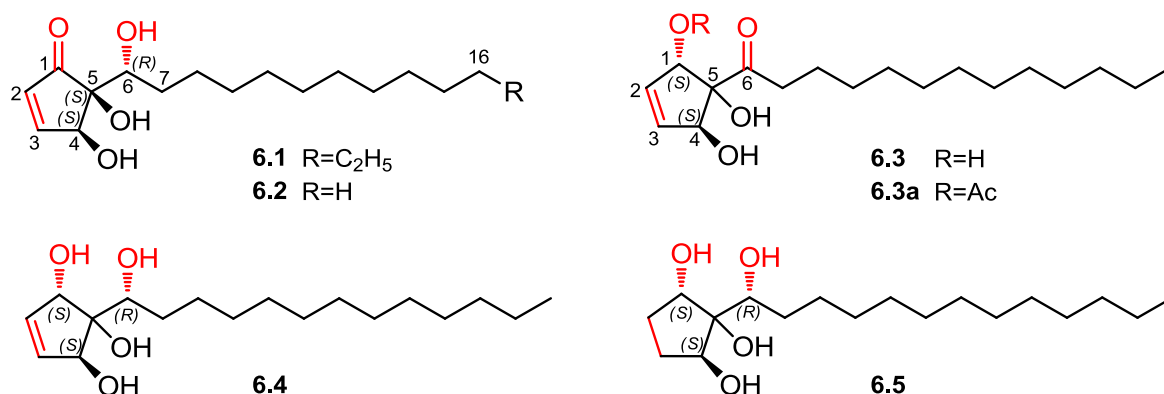
Fig. 6.1. Chemical structures of compounds **6.1–6.5**.

Compound **6.3** was isolated as a colorless oil. HRMS measurements revealed the molecular formula as $C_{18}H_{32}O_4$ (*m/z* 311.2231, [M–H]$^-$, calculated for $C_{18}H_{31}O_4^-$ 311.2228), equal to that of hygrophorone B[12] (**6.1**). The ^{13}C NMR spectrum (Table 6.1) exhibited two olefinic ^{13}C signals (δ_C 136.0 and 135.7), three oxygenated carbon atoms (δ_C 76.3, 84.1, and 85.5) as well as aliphatic alkyl side chain carbons (δ_C 14.1–39.0), disclosing similar structural features as compounds **6.1** and **6.2**. A strong IR absorption band at 1703 cm^{-1} as well as ^{13}C resonance signal at δ_C 212.1 corresponded to a non-conjugated carbonyl functionality. The ^1H NMR spectrum of **6.3** (Table 6.1) displayed resonances of two oxygenated, low field shifted methine protons at δ_H 4.947 (1H, br s, H-1) and δ_H 4.856 (1H, br s, H-4), of which both signals exhibited HMBC correlations to the olefinic carbon resonances. The endocyclic double bond proton signals at δ_H 6.078 (1H, ddd, $J = 6.1/1.8/0.8$ Hz, H-2) and δ_H 6.060 (1H, ddd, $J = 6.1/1.9/0.9$ Hz, H-3) were in the same COSY spin system with the oxygenated methine signals H-1 and H-4, but were devoid of HMBC correlation peaks to the CO group resonating at δ_C 212.1. The presence of a five membered ring system was deduced from the $^3J_{H2-H3}$ coupling constant of 6.1 Hz (Lübken et al., 2004). These observations gave evidence, that **6.3** possessed a cyclopentene system missing the endocyclic carbonyl function. In fact, deshielded ^1H signals resonating at δ_H 2.796 (1H, dt, $J = 17.9/7.5$ Hz, H$_A$-7) and δ_H 2.589 (1H, dt, $J = 17.9/7.5$ Hz, H$_B$-7) as well as HMBC correlation peaks between H$_2$-8 and δ_C 212.1 corresponded to an exocyclic carbonyl group at C-6 directly adjacent to the

alkyl side chain. The constitution was fully supported by HMBC and COSY correlation analyses (Fig. 6.2). Based on the above spectroscopic data, **6.3** was assigned as the new 1-(1,2,5-trihydroxy-cyclopent-3-enyl)-tridecanone (according to IUPAC). The constitution of **6.3** was therefore found to be similar to that of E series hygrophorones isolated earlier from fruiting bodies of *H. latitabundus*, but exclusively as mono-*O*- or di-*O*-acetylated derivatives such as 1,4-di-*O*-acetylhygrophorone E^{12} (**6.3a**) (Lübken et al., 2004).
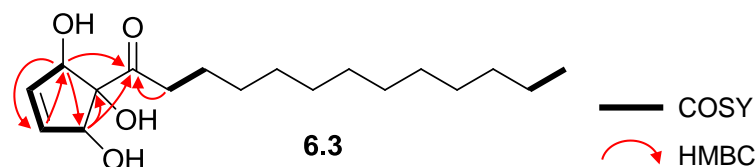
Fig. 6.2. Key HMBC and COSY correlations of hygrophorone E^{12} (**6.3**).

To clarify whether compound **6.3** possesses the same stereochemistry as E-type hygrophorones isolated from *H. latitabundus*, **6.3** was acetylated with an excess of acetic anhydride in pyridine to obtain **6.3a** or its diastereomer (Scheme S1, Supporting Information). In fact, the ^{1}H and ^{13}C NMR spectra as well as optical rotation value of the diacetylated derivative of **6.3** were in accordance with that of **6.3a** reisolated from *H. latitabundus*, concluding that the di-*O*-acetylated derivative of **6.3** is identical to 1,4-di-*O*-acetylhygrophorone E^{12} (**6.3a**). Therefore, the structure of compound **6.3** was identified as a new natural product and consequently named hygrophorone E^{12} (Fig. 6.1).

Compound **6.4** was isolated as a colorless oil. Based on ESI-HRMS measurements, the molecular formula of **6.4** was determined as $C_{18}H_{34}O_4$, suggesting two atomic mass units more than that of hygrophorone E^{12} (**6.3**). The ^{13}C NMR spectrum (Table 6.1) of compound **6.4** solely differed from **6.3** by an additional oxygenated carbon signal (in total four), while the carbonyl group resonance was absent, indicative for a tetrahydroxylated hygrophorone derivative. This was supported by the IR spectrum that lacked the characteristic carbonyl absorption band around 1700 cm^{-1}. Instead, the ^{1}H NMR spectrum (Table 6.1) displayed an additional hydroxylated methine proton signal at δ_H 3.952 (1H, dd, J = 9.9/1.5 Hz), exhibiting a HSQC correlation peak to the ^{13}C resonance at δ_C 75.3.
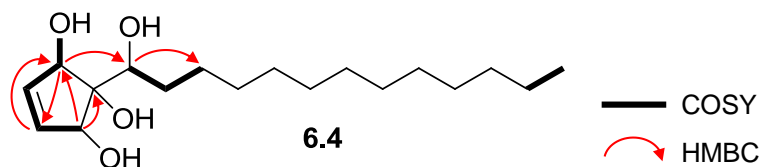
Fig. 6.3. Key HMBC and COSY correlations of hygrophorone H^{12} (**6.4**).

Based on the observed HMBC and COSY correlations (Fig. 6.3), compound **6.4** was assigned as 2-(1-hydroxytridecyl)cyclopent-4-ene-1,2,3-triol (IUPAC name) and identified as a novel tetrahydroxylated hygrophorone type, given the name hygrophorone H^{12} (Fig. 6.1).

Table 6.1. ^{1}H and ^{13}C NMR data of compounds **6.2–6.5** (600/150 MHz, CDCl$_3$, δ in ppm).

Pos.	6.2 δ$_H$, mult. *J* (Hz)	6.2 δ$_C$	6.3 δ$_H$, mult. *J* (Hz)	6.3 δ$_C$	6.4 δ$_H$, mult. *J* (Hz)	6.4 δ$_C$	6.5 δ$_H$, mult. *J* (Hz)	6.5 δ$_C$
1	---	207.1	4.947 br s	76.3	5.025 br s	78.4	4.452 dd (8.1/7.7)	75.9
OH-1	---	---	*n.d.*	---	2.512 br s	---	*n.d.*	---
2	6.300 dd (6.0/1.3)	133.5	6.078 ddd (6.1/1.8/0.8)	136.0	5.956 dd (5.9/1.5)	136.7	2.22[a]; 1.60[a]	29.1
3	7.639 dd (6.0/2.3)	163.5	6.060 ddd (6.1/1.9/0.9)	135.7	6.025 ddd (5.9/2.5/1.9)	134.5	2.28[a]; 1.445 m	31.1
4	4.721 dd (2.3/1.3)	71.5	4.856 br s	84.1	4.599 br s	82.2	4.080 dd (5.3/2.5)	78.3
OH-4	*n.d.*	---	*n.d.*	---	2.283 br s[b]	---	*n.d.*	---
5	---	76.5	---	85.5	---	79.3	---	80.7
OH-5	*n.d.*	---	4.323 br s	---	3.244 s	---	*n.d.*	---
6	3.772 br d (10.3)	73.4	---	212.1	3.952 dd (9.9/1.5)	75.3	3.949 dd (9.5/2.6)	75.4
OH-6	*n.d.*	---	---	---	1.841 br s[b]	---	*n.d.*	---
7A	1.57[a]	31.3	2.796 dt (17.9/7.5)	39.0	1.739 m	31.3	1.62[a]	31.4
7B	1.34[a]		2.589 dt (17.9/7.5)		1.57[a]		1.62[a]	
8	1.57[a]; 1.32[a]	26.1	1.605 m	23.3	1.57[a]; 1.37[a]	26.1	1.54[a]; 1.35[a]	25.9
9–15	1.38 – 1.20[a]	29.56[c] 29.56[c] 29.50[c] 29.41[c] 29.31[c] 31.9 22.7	1.33 – 1.21[a]	29.64[c] 29.62[c] 29.60[c] 29.47[c] 29.43[c] 29.3 29.2	1.34 – 1.21[a]	29.68[c] 29.66[c] 29.65[c] 29.62[c] 29.4 *	1.35 – 1.20[a]	29.67[c] 29.66[c] 29.64[c] 29.4 *
16	0.881 t (7.0)	14.1	1.25[a]	31.9	1.25[a]	31.9	1.26[a]	31.9
17	---	---	1.28[a]	22.7	1.28[a]	22.7	1.27[a]	22.7
18	---	---	0.881 t (7.0)	14.1	0.881 t (7.0)	14.1	0.881 t (7.0)	14.1

n.d. = not detected [a] Overlapping signals; chemical shifts were determined from ^{1}H,^{13}C HSQC correlation peaks. [b] Assignments may be interchanged. [c] Two decimals are given to assign resolved ^{13}C alkyl chain signals. * Partially unresolved CH$_2$ signals missing.

Compound **6.5** was isolated as a white powder. HRMS measurements of the ion at *m/z* 315.2551 ([M–H]$^-$, calculated for C$_{18}$H$_{35}$O$_4$$^-$ 315.2541) revealed a molecular formula of C$_{18}$H$_{36}$O$_4$ indicating the 2,3-dihydro derivative of **6.4**. In fact, the existence of a functionalized cyclopentane system was verified by ^{1}H and ^{13}C NMR spectra (Table 6.1), which were devoid of characteristic signals of the endocyclic double bond. Instead, aliphatic proton signals between δ$_H$ 1.42 and δ$_H$ 2.28 (H$_2$-2 and H$_2$-3) were detected, exhibiting COSY correlation peaks to oxygenated methine signals at δ$_H$ 4.452 (1H, dd, *J* = 8.1/7.7 Hz, H-1) and δ$_H$ 4.080 (1H, dd, *J* = 5.3/2.5 Hz, H-4). The observed HMBC and COSY correlations of **6.5** (Fig. 6.4) were consistent with the 2,3-dihydro derivative of **6.4**. Therefore, compound **6.5** was assigned as 2-(1-hydroxytridecyl)cyclopentane-1,2,3-triol, and consequently named 2,3-dihydrohygrophorone H^{12} (Fig. 6.1).

85
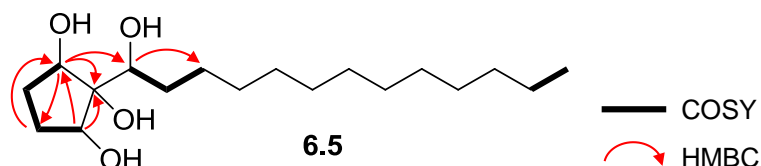
Fig. 6.4. Key HMBC and COSY correlations of 2,3-dihydrohygrophorone H[12] (**6.5**).

6.2.2 Semisynthetic derivatives for biological evaluation

For initial structure-activity relationship (SAR) studies, acetyl derivatives of hygrophorone B[12] (**6.1**) were generated through acetylation of **6.1** with acetic anhydride in pyridine. Depending on the reaction time and reagent excess, the regioisomers 4-*O*-acetylhygrophorone B[12] (**6.1a**) and 6-*O*-acetylhygrophorone B[12] (**6.1b**) as well as 4,6-di-*O*-acetylhygrophorone B[12] (**6.1c**) were obtained, but no triacetylated derivative **6.1d** due to the low reactivity of the tertiary alcohol function at C-5 (Scheme 6.1). The desired 4,5,6-tri-*O*-acetylhygrophorone B[12] (**6.1d**) was exclusively formed after addition of catalytic amounts of 4-dimethylaminopyridine (DMAP) to the reaction mixture.
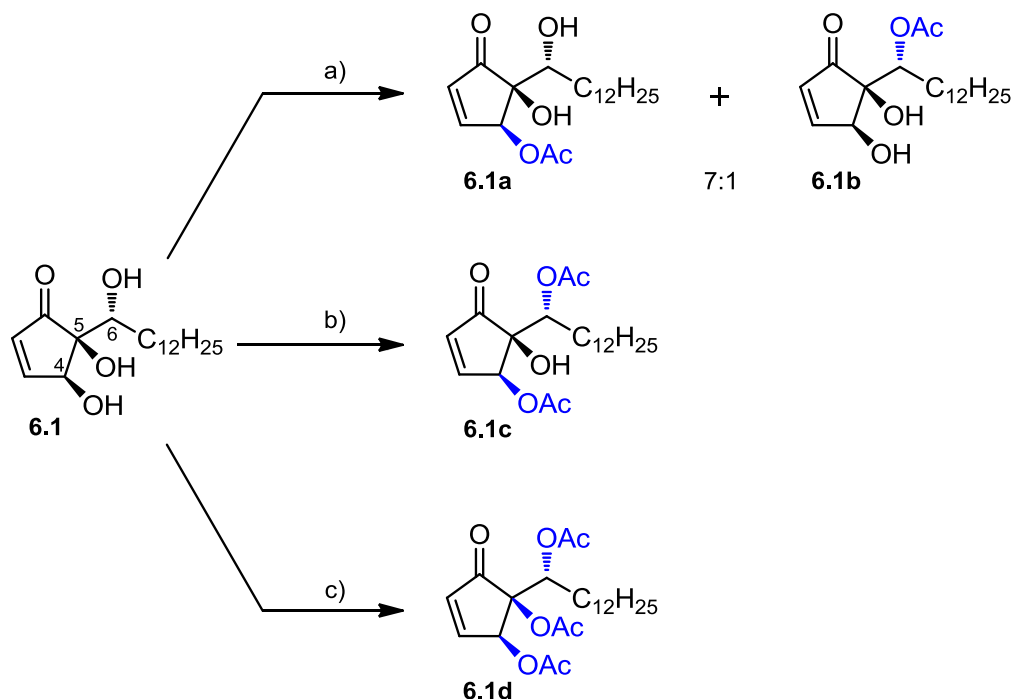
Scheme 6.1. Acetylation of hygrophorone B[12] (**6.1**). (a) Ac$_2$O, pyridine, 2 h, r.t.; (b) Ac$_2$O, pyridine, 15 h, r.t.; (c) Ac$_2$O, pyridine, DMAP, 50 h, r.t.

The acetoxy derivatives **6.1a–d** were purified by preparative HPLC and characterized by 1D NMR and ESI-HRMS analyses. The spectroscopic data (Table 6.2) were in accordance with those of structurally similar hygrophorone B[14] acetyl derivatives reported earlier (Lübken et al., 2004). These data show the expected downfield shift of the proton signals H-4 and/or H-6 due to acetylation and the presence of acetyl groups.

Table 6.2. ^{1}H and ^{13}C NMR data of hygrophorone B[12] acetyl derivatives **6.1a–d** (400/100 MHz, CDCl$_3$, δ in ppm).

Pos.	6.1a δ_H, mult. J (Hz)	6.1a δ_C	6.1b δ_H, mult. J (Hz)[b]	6.1b δ_C[c]	6.1c δ_H, mult. J (Hz)	6.1c δ_C	6.1d δ_H, mult. J (Hz)	6.1d δ_C
1	---	206.6	---	204.9	---	204.1	---	200.3
2	6.434 dd (6.1/1.3)	135.9	6.300 dd (6.1/1.2)	133.0	6.434 dd (6.2/1.2)	135.5	6.465 dd (6.3/1.4)	135.7
3	7.585 dd (6.1/2.7)	158.2	7.637 dd (6.1/2.4)	162.7	7.546 dd (6.2/2.8)	157.2	7.428 dd (6.3/2.8)	154.7
4	5.725 dd (2.7/1.3)	73.0	4.790 dd (2.4/1.2)	71.5	5.785 dd (2.8/1.2)	72.6	5.965 dd (2.8/1.4)	70.8
OH-4	---	---	*n.d.*	---	---	---	---	---
CO-CH$_3$-4	2.162 s	20.7	---	---	2.148 s	20.7	2.099 s	20.7
CO-CH$_3$-4	---	170.1	---	---	---	169.8	---	169.2
5	---	77.2	---	75.5	---	77.2	---	73.1
OH-5	3.132 br s	---	*n.d.*	---	2.704 br s	---	---	---
CO-CH$_3$-5	---	---	---	---	---	---	1.999 s	20.2
CO-CH$_3$-5	---	---	---	---	---	---	---	168.7
6	3.814 m	74.0	5.167 dd (10.2/2.8)	73.2	5.083 dd (9.8/3.4)	73.9	5.225 dd (10.0/2.8)	79.3
OH-6	*n.d.*	---	---	---	---	---	---	---
CO-CH$_3$-6	---	---	2.000 s	20.8	2.058 s	20.8	2.091 s	20.7
CO-CH$_3$-6	---	---	---	169.9	---	170.4	---	169.6
7	1.51[a]; 1.30[a]	31.2	1.85[a]; 1.63[a]	29.2	1.69[a]	28.8	1.82[a]; 1.68[a]	29.2
8	1.55[a]; 1.31[a]	26.1	1.32[a]	25.7	1.25[a]	25.6	1.27[a]	25.7
9–15	1.39 – 1.20[a]	29.7 – 29.3	1.36 – 1.19[a]	29.7 – 29.3	1.35 – 1.17[a]	29.6 – 29.3	1.37 – 1.18[a]	29.7 – 29.3
16	1.25[a]	31.9	1.25[a]	31.9	1.24[a]	31.9	1.25[a]	31.9
17	1.27[a]	22.7	1.29[a]	22.7	1.27[a]	22.7	1.27[a]	22.7
18	0.880 t (7.0)	14.1	0.880 t (7.0)	14.1	0.880 t (7.0)	14.1	0.880 t (7.0)	14.1

n.d. = not detected. [a] Overlapping signals; chemical shifts were determined from ^{1}H,^{13}C HSQC correlation peaks. [b] Measured at 600 MHz. [c] [13]C chemical shifts were deduced from ^{1}H,^{13}C HSQC or ^{1}H,^{13}C HMBC spectra (recorded at 600 MHz).

6.2.3 Stereochemical assignment of compounds 6.3–6.5

Due to the high flexibility of the alkyl side chain in hygrophorones **6.3–6.5** as well as small spatial distances in five-membered ring systems, the relative configurations of **6.3–6.5** could not be assigned unambiguously on the basis of NOE correlation analyses.

For compound **6.3**, four stereoisomers are possible (Fig. S49, Supporting Information). The meso forms of **6.3** with the configuration 1*R*,4*S*,5*r* and 1*R*,4*S*,5*s*, in which the pseudoasymmetric atom C-5 carries two identical substituents with opposite configuration, are optically inactive. In contrast, the enantiomeric 1*S*,4*S* and 1*R*,4*R* isomers show an optical activity. Since hygrophorone E[12] (**6.3**) is optically active ([α]$^{24}_D$ +111.8), it was concluded that compound **6.3** is either 1*S*,4*S* or 1*R*,4*R* configured. In these isomers, the atom C-5 is achiral as it has only three different substituents due to the fact that both C-1 and C-4 have the *S* configuration. The absolute

configuration of **6.3** was finally established by comparing its experimental and calculated CD spectra. While the calculated CD spectrum of the *RR* isomer was mirror-imaged to the experimental curve of **6.3**, the CD spectrum of *SS*-**6.3** fitted very well to the spectrum of **6.3**, showing positive Cotton effects at 200 and 290 nm (Fig. 6.5). Therefore, the absolute configuration of hygrophorone E[12] (**6.3**) was assigned as 1*S*,4*S* (Fig. 6.1). Interestingly, E-type hygrophorones are found in both species *H. latitabundus* and *H. abieticola*, although *H. latitabundus* produces cyclopentenones with *trans* oriented endocyclic hydroxyl groups (D series hygrophorones), while the B-type hygrophorones isolated from *H. abieticola* show a *cis* configuration. A possible explanation for this observation is the achirality center (C-5) in hygrophorone E[12] (**6.3**), allowing that both the 4,5-*cis* and -*trans* configured cyclopentenones can principally be (bio-)converted to E series hygrophorones. A potential biosynthetic pathway is proposed in Scheme 11.1 (Chapter 11).
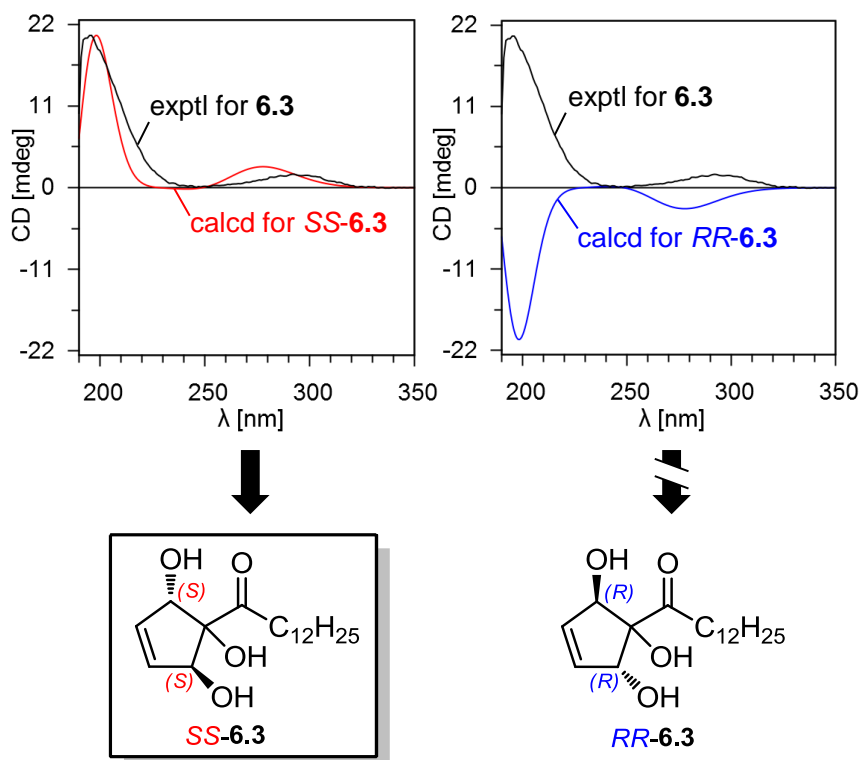
Fig. 6.5. Comparison of the Boltzmann-weighted CD spectra of *SS*-**6.3** and *RR*-**6.3** (-3 nm shift) with the experimental spectrum of hygrophorone E[12] (**6.3**).

The absolute configuration of compounds **6.4** and **6.5** was determined through semisynthesis in combination with computational studies. The semisynthetic approach involved the conversion of hygrophorone B[12] (**6.1**), whose stereostructure was assigned recently (Bette et al., 2015), to 2,3-dihydrohygrophorone H[12] (**6.5**) (Scheme 6.2). In order to do so, the hydrogenation of the double bond as well as the carbonyl group was necessary. Hygrophorones are rather sensitive towards bases arising from the reactive α,β-unsaturated carbonyl function acting as a Michael acceptor system. Therefore, the Michael acceptor system was removed under mild conditions by reduction of the endocyclic double bond with palladium-loaded activated carbon (Pd/C, 10%) under

hydrogen atmosphere (1 atm) to obtain 2,3-dihydrohygrophorone B^{12} (**6.6**). The carbonyl function was not reduced using this procedure, even at considerably higher pressure of 100 bar.
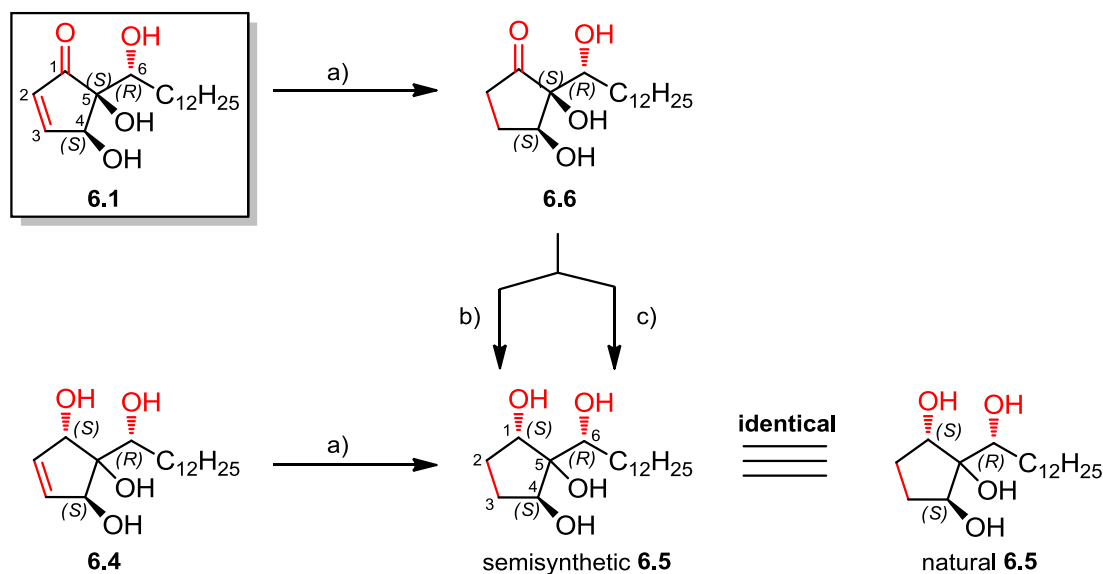
Scheme 6.2. Semisynthesis of 2,3-dihydrohygrophorone (**6.5**) from hygrophorone B^{12} (**6.1**) and hygrophorone H^{12} (**6.4**). (a) 1 atm H$_2$, 10% Pd/C, MeOH, r.t., 48 h; (b) HCOOH/NEt$_3$ 5/7, Noyori (*R,R*) catalyst, CH$_2$Cl$_2$, r.t., 7 d; (c) HCOOH/NEt$_3$ 5/7, Noyori (*S,S*) catalyst, CH$_2$Cl$_2$, r.t., 8 d.

The keto group of 2,3-dihydrohygrophorone B^{12} (**6.6**) was reduced by transfer hydrogenation using a formic acid⁄triethylamine (5/7) mixture in the presence of a chiral Ru(II)-TsDPEN complex (Noyori catalyst) (Fujii et al., 1996). The hydrogenation product using the (*R,R*) Noyori catalyst was identified as the desired 2,3-dihydrohygrophorone H^{12} (**6.5**) on the basis of 1D NMR, HRMS, and optical rotation data. Most surprisingly, the (*S,S*) Noyori catalyst afforded the same hydrogenation product as the (*R,R*) catalyst. Checking the optical rotation of the two commercial catalysts (which were enantiomeric as stated) as well as repetition of the experiment confirmed this result. For reasons to be explored, the enantiomeric ligands of the Noyori catalysts did not confer stereoselectivity onto these substrates under these conditions. Obviously, the outcome is stringently overruled by one of the existing stereocenters of the substrates, forcing the system into a highly diastereoselective reaction.

Hydrogenation on palladium-loaded activated carbon (Pd/C, 10%) in hydrogen atmosphere of compound **6.4** afforded 2,3-dihydrohygrophorone H^{12} (**6.5**) (Scheme 6.2), of which the 1D NMR data and optical rotation value were in accordance with those of natural **6.5** (Fig. S48, Supporting Information). Thus, the absolute configuration of hygrophorone H^{12} (**6.4**) and 2,3-di-hydrohygrophorone H^{12} (**6.5**) could be determined at position C^4, C^5, and C^6. However, the configuration at C-1 remained tentative due to two possible hydrogenation faces at C-1 in 2,3-dihydrohygrophorone B^{12} (**6.6**) (Scheme 6.2). Depending on the configuration of C^1 in **6.4** and **6.5**, the atom C^5 is either an achiral (1*S*,4*S*,6*R*) or a pseudoasymmetric center (1*R*,4*S*,5*s*,6*R*). A stereochemical assignment of C^1 in **6.4** and **6.5** was also not possible on the basis of circular dichroism based studies since the calculated CD spectra of both *SSR*-**6.4** and *RSsR*-**6.4** matched the experimental curve of **6.4** (Figs. 6.6A and S51A, Supporting Information).

For a final assignment of the absolute configuration of **6.4** and **6.5** as either *SSR* or *RSsR*, the Boltzmann relevant conformers of both diastereomers were analyzed to reveal spatial adjacent protons. The observed NOE correlations of **6.4** (Table S2, Supporting Information) could be reconstructed only for the energy minimized conformers of *SSR*-**6.4** (Fig. 6.6B), in particular the strong NOE correlation peak between H-1 and H-6 as well as the rather weak correlation between H-4 and H-6 (for details see Tables S5 and S7, Supporting Information). Furthermore, the experimental NOE interactions between H-1/OH-5 and H-4/OH-5 are strongly evident for a *SSR* configuration due to the spatial proximity of these protons in the energy minimized structures of *SSR*-**6.4** (Fig. 6.6B and Table S5, Supporting Information). In contrast, the *anti*-orientation of OH-5 to H-1/H-4 in the relevant conformers of *RSsR*-**6.4** makes experimental NOE interactions very unlikely (Fig. S51B and Table S7, Supporting Information). Based on these results, the absolute configuration of hygrophorone H[12] (**6.4**) and consequently 2,3-dihydrohygrophorone H[12] (**6.5**) likely can be assigned as being 1*S*,4*S*,6*R*, although final assurance is impossible at this point. However, the established stereostructure of **6.4** and **6.5** is consistent with the fact that C[1] is also *S* configured in hygrophorone E[12] (**6.3**), confirming a similar biosynthesis of these compounds (Scheme 11.1, Chapter 11).
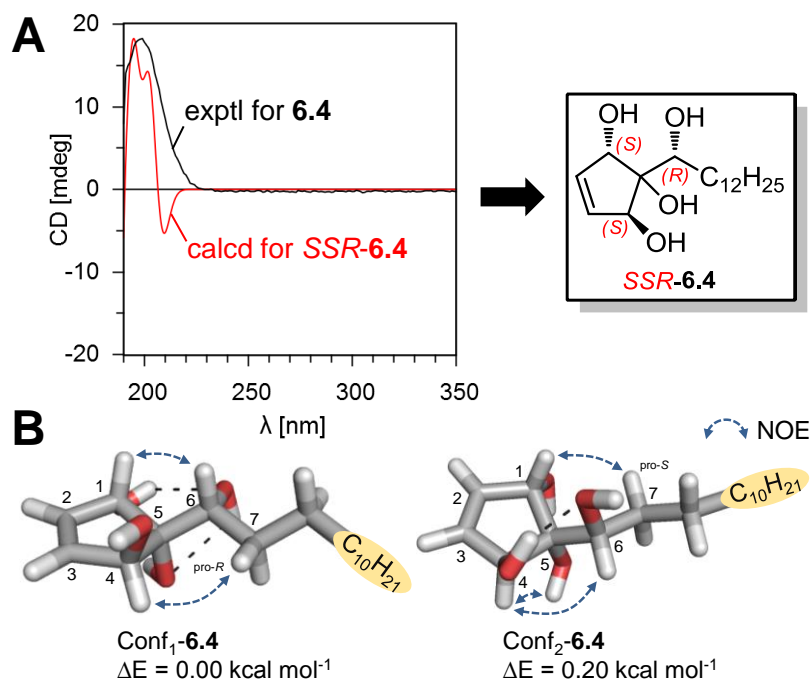
Fig. 6.6. (A) Comparison of the Boltzmann-weighted CD spectra of *SSR*-**6.4** (9 nm shift) with the experimental spectrum of hygrophorone H[12] (**6.4**). (B) Molecular structures of the main conformers of *SSR*-**6.4** for which the observed key NOE correlations can be explained.

6.2.4 Antiphytopathogenic activity

Hygrophorones are known for their strong activity against phytopathogenic organisms (Dräger, 2011; Lübken et al., 2004; Lübken, 2006). Therefore, the isolated and semisynthetic hygrophorones **6.1–6.5** and **6.1a–c** were examined towards their activity against the plant pathogenic fungi *Botrytis cinerea* (grey mold pathogen on many crops including strawberries and

wine grapes) and *Septoria tritici* (causes septoria leaf blotch of wheat) as well as the oomycete *Phytophthora infestans* (causal agent of the late blight disease on potato and tomato) using a 96 well microtiter plate assay (Table 6.3). The commercially used fungicides dodine and pyraclostrobin as well as 4-oxohexadec-2-enoic acid (**2.7**) were used as reference compounds. For the latter compound **2.7**, the *in vitro* and *in vivo* inhibitory effect on *P. infestans* was demonstrated previously (Eschen-Lippold et al., 2009).

Table 6.3. Antiphytopathogenic activity of natural hygrophorones **6.1–6.5** and semisynthetic hygrophorone B^{12} derivatives **6.1a–c** against *B. cinerea*, *S. tritici*, and *P. infestans* (IC_{50}, µM).

compound	*B. cinerea*	*S. tritici*	*P. infestans*
hygrophorone B^{12} (**6.1**)	4.9 ± 0.7	5.9 ± 0.7	1.6 ± 0.3
4-*O*-acetylhygrophorone B^{12} (**6.1a**)	13.9 ± 2.7	13.3 ± 1.2	8.0 ± 2.1
6-*O*-acetylhygrophorone B^{12} (**6.1b**)	9.1 ± 1.5	6.8 ± 0.3	5.8 ± 1.1
4,6-di-*O*-acetylhygrophorone B^{12} (**6.1c**)	12.9 ± 1.3	11.9 ± 0.8	9.6 ± 0.6
hygrophorone B^{10} (**6.2**)	14.1 ± 1.3	19.3 ± 3.9	1.6 ± 0.1
hygrophorone E^{12} (**6.3**)	58.9 ± 10.6	48.0 ± 4.3	38.4 ± 2.9
hygrophorone H^{12} (**6.4**)	23.2 ± 2.8	84.6 ± 3.2	60.7 ± 1.9
2,3-dihydrohygrophorone H^{12} (**6.5**)	> 100	> 100	> 100
4-oxohexadec-2-enoic acid (**2.7**)	6.0 ± 1.5	55.9 ± 5.2	3.4 ± 0.4
dodine[a]	9.4 ± 0.6	2.8 ± 0.2	43.8 ± 5.6
pyraclostrobin[a]	< 0.0052	< 0.0052	0.018 ± 0.002

[a] Used as reference compounds.

As shown in Table 6.3, the strongest activities were exhibited by hygrophorone B^{12} (**6.1**). The shorter chain homologue hygrophorone B^{10} (**6.2**) displayed an activity against *P. infestans* similar to that of **6.1**, but was less active against *B. cinerea* and *S. tritici*. The acetylated hygrophorone B^{12} derivatives **6.1a–c** exhibited weaker effects in comparison to **6.1**, indicating that the antiphytopathogenic activity cannot be enhanced by acetylation of the hydroxyl groups in **6.1**. The triacetylated derivative **6.1d** could not be tested due to solubility problems in the assay system. The activity of the 4-oxohexadec-2-enoic acid (**2.7**) against *B. cinerea* and *P. infestans* was comparable to hygrophorone B^{12} (**6.1**), while **2.7** was almost inactive against *S. tritici*.

Compounds **6.3** and **6.4**, lacking the endocyclic carbonyl function, showed only moderate to low antifungal activities, while compound **6.5** without the double bond was inactive against all organisms tested ($IC_{50} > 100$ µM). These results indicate, that an α,β-unsaturated carbonyl structure seems to be a prerequisite for potent bioactivity. A similar structure-activity relationship can be suggested for 4-oxoalk-2-ene fatty acids possessing the α,β-unsaturated carbonyl pharmacophor, since derivatives with the double bond at position 2 were active (Teichert et al., 2005b), while compounds without the unsaturation were less active or inactive (Gilardoni et al., 2006). A reduced activity for hygrophorones lacking the carbonyl group in conjugation to the double bond was also reported earlier for acetylated E series hygrophorones (Lübken, 2006).

6.2.5 Biological activity profile of hygrophorone B^{12}

The biological activity of hygrophorone B^{12} (**6.1**) was furthermore evaluated against the clinical bacterial isolates methicillin-resistant *Staphylococcus aureus* subsp. *aureus* (MRSA, DSM 18827), vancomycin-resistant *Enterococcus faecium* (vanA+, DSM 13590), and *Pseudomonas aeruginosa* (DSM 1117). The antimicrobial activity was evaluated by determining the minimum inhibitory concentration (MIC) using a broth microdilution assay (Table 6.4). The effect of the 4-oxohexadec-2-enoic acid (**2.7**) was examined as well.

Table 6.4. MIC values (in µg/ml) of hygrophorone B^{12} (**6.1**) and the 4-oxo fatty acid **2.7** against clinical gram-positive and gram-negative bacterial strains.

compound	*S. aureus* (MRSA) DSM 18827	*E. faecium* (vanA+) DSM 13590	*P. aeruginosa* DSM 1117
hygrophorone B^{12} (**6.1**)	0.78	0.78	> 400
4-oxohexadec-2-enoic acid (**2.7**)	91.7	5.7	> 367
ciprofloxacin[a]	0.25[b]	0.5[b]	0.5[b]
vancomycin[a]	1.0[b]	2.0[b]	---
linezolid[a]	2.0[b]	2.0[b]	---

[a] Reference compounds; [b] MICs reported in the literature (EUCAST, 2003).

Compound **6.1** exerted strong activity against MRSA and vanA+, which are comparable to those of the antibiotics ciprofloxacin, vancomycin, and linezolid reported in the literature (EUCAST, 2003). Hygrophorone B^{12} (**6.1**) was devoid of activity against the gram-negative bacterium *P. aeruginosa*. Thus, the activity spectrum of **6.1** is most likely limited to gram-positive bacteria as already reported by Lübken (2006) for similar hygrophorones. The 4-oxo fatty acid **2.7** showed modest effects against vanA+, but was inactive against MRSA and *P. aeruginosa*.
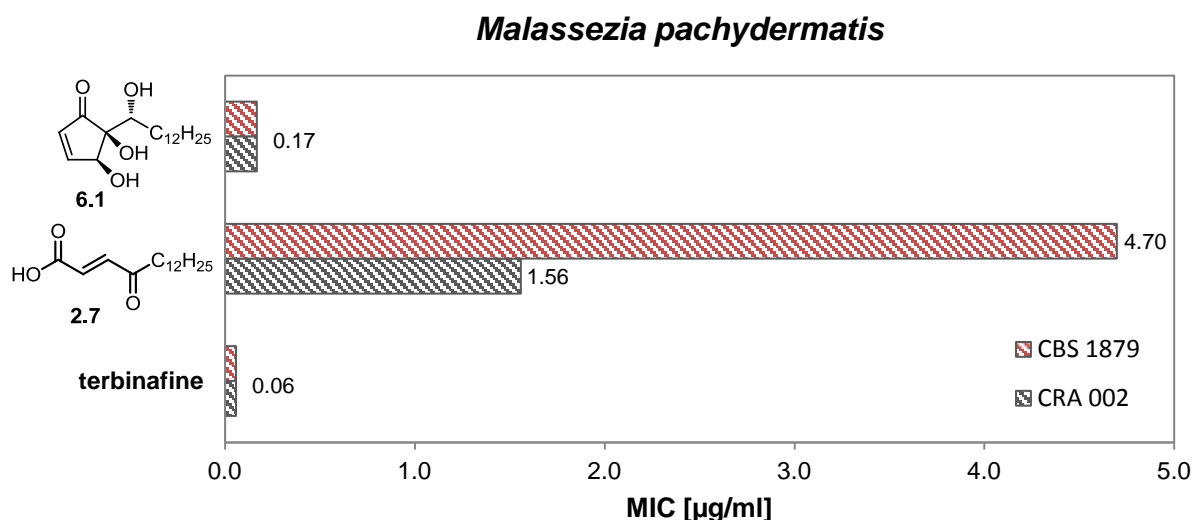
Fig. 6.7. Activity of hygrophorone B^{12} (**6.1**) and the 4-oxo fatty acid **2.7** against *M. pachydermatis* CBS 1879 and CRA 002.

Additionally, the activity of **6.1** and **2.7** was determined against two strains of *Malassezia pachydermatis*, a opportunistic pathogen causing skin and ear infections in mammals, particularly in dogs (Coutinho and Paula, 2000). Fig. 6.7 shows a strong *in vitro* activity of **6.1** against *M. pachydermatis*, which is comparable to the activity of terbinafine. Terbinafine is a synthetic antifungal drug used for many years to treat these infections (Guillot et al., 2003). In contrast to **6.1**, the 4-oxo fatty acid **2.7** exerted only modest activity against the tested strains of *M. pachydermatis*. Apart from that, it should be noted that both hygrophorone B[12] (**6.1**) and the 4-oxo fatty acid **2.7** were devoid of noticeable hemolytic activity (i.e. lysis of red blood cells) at a concentration of 10 μM. Thus, both **6.1** and **2.7** may also have potential for therapeutic use, presenting antimicrobial activity with none toxicity to human erythrocytes.

6.2.6 Mode of action of hygrophorone B[12]

It has been reported that cyclopentenones containing an α,β unsaturated carbonyl function can form covalent bonds with biological nucleophiles through Michael addition, such as cysteine residues in key regulatory enzymes (Stamatakis and Perez-Sala, 2006). In fact, *in vitro* incubation of hygrophorone B[12] (**6.1**) with L-cysteine at room temperature afforded the Michael addition product **6.7** (cysteine adduct). A rapid conversion could be monitored *via* ESI-HRMS investigations. The protonated molecular ion at *m/z* 434.2572 (calculated for $C_{21}H_{40}O_6NS^+$ 434.2571) of **6.7** indicated, that the thiol group of cysteine was alkylated accompanied by loss of the endocyclic double bond of hygrophorone B[12] (**6.1**) (Scheme 6.3). However, due to the extremely poor solubility in the tested solvents EtOAc, MeOH, DMSO, EtOH, *n*-hexane, or water, compound **6.7** could not be purified and further characterized. The fact that hygrophorone B[12] (**6.1**) reacts with L-cysteine suggests that a possible *in vivo* Michael addition may account for the observed biological activities of **6.1** and derivatives thereof.
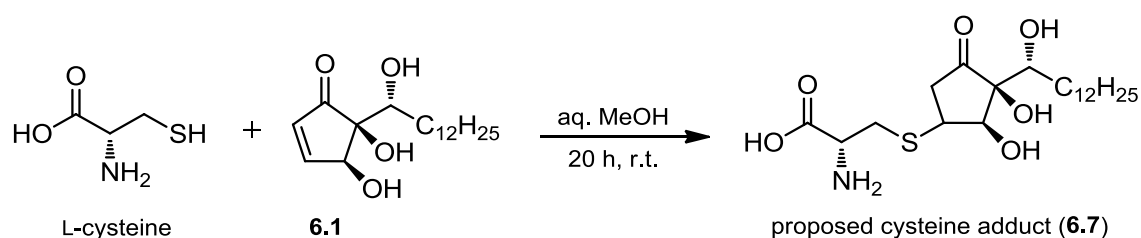
Scheme 6.3. Proposed 1,4-Michael reaction of L-cysteine with hygrophorone B[12] (**6.1**).

6.3 Conclusions

Four new hygrophorones were isolated from fruiting bodies of *H. abieticola*. Among these compounds, two previously undescribed hygrophorone types, namely hygrophorone H[12] (**6.4**) and 2,3-dihydrohygrophorone H[12] (**6.5**), were identified. The absolute configuration of hygrophorone E[12] (**6.3**) was established by quantum chemical CD calculations, while a semisynthetic approach in conjunction with computational studies and analysis of NOE interactions allowed the

elucidation of the absolute configuration of compounds **3** and **4**. The isolated compounds **6.2–6.5** and hygrophorone B[12] (**6.1**) were evaluated against phytopathogenic organisms. Hygrophorone B[12] (**6.1**) was identified as the most active compound, acting against both ascomycetous fungi and oomycetes. Therefore, **6.1** may serve as a lead structure for the development of novel antifungal plant protection agents. However, the antiphytopathogenic effects of hygrophorone B[12] (**6.1**) could not be improved by acetylation of its hydroxyl groups. The compounds **6.3** and **6.4**, lacking the endocyclic carbonyl function, showed only moderate to low antifungal activities, while compound **6.5** without the double bond was inactive against all organisms tested ($IC_{50} > 100$ μM).

These results indicate that an α,β-unsaturated carbonyl structure is likely to be a prerequisite for potent bioactivity, which might react as a Michael acceptor with biological nucleophiles. The important role for biological activity of an α,β-unsaturated carbonyl group is known not only for several phytotoxins but also for natural compounds with anticancer activity (Cimmino et al., 2014; Evidente et al., 2014). The mechanism of "lethal metabolism" (Hassal, 1990) could explain the reduced activity of the acetyl derivatives **6.1a–c** in respect to the parent compound **6.1**, since these compounds may be only partially hydrolyzed at physiological pH values (Cimmino et al., 2015). Particularly strong growth inhibitions were observed against *Phytophthora infestans* indicating that these Michael acceptor compounds are especially potent against oomycetes. Besides, hygrophorone B[12] (**6.1**) showed remarkable activity against clinical isolates of resistant gram positive bacteria (MRSA and VRE) as well as *Malassezia pachydermatis*, a opportunistic pathogen causing skin and ear infections in mammals.

6.4 Experimental Section

General Experimental Procedures. Column chromatography was performed on silica gel 60 (Merck, 40–63 μm particle size) and Sephadex LH 20 (Fluka) using cylindrical glass columns with glass frits or plugged with cotton wool, while analytical TLC was performed on precoated silica gel F_{254} plates (Merck). The compound spots were detected by their UV absorbance at λ 254 nm and/or by spraying of the TLC plates with vanillin-sulfuric acid reagent followed by heating in a hot air stream. IR spectra were obtained from a Thermo Nicolet 5700 FT-IR spectrometer using a diamond ATR accessory. UV spectra were measured with a Jasco V-560 UV/Vis spectrophotometer, whereas CD spectra were acquired on a Jasco J-815 CD spectrophotometer. The specific rotation was acquired with a Jasco P-2000 polarimeter. Chromabond® SPE cartridges (SiOH and C18) were purchased from Macherey-Nagel, Germany.
^{1}H and ^{13}C as well as ^{1}H,^{13}C gHSQCAD (optimized for a one-bond ^{1}H,^{13}C coupling constant of 146 Hz), ^{1}H,^{13}C gHMBCAD (optimized for a long-range ^{1}H,^{13}C coupling constant of 8 Hz), ^{1}H,^{1}H gDQCOSY and ^{1}H,^{1}H ROESY (mixing time 0.4 s) NMR spectra were obtained from an Agilent DD2-400 and an Agilent VNMRS 600 system. The spectra were recorded at 400/600 MHz (^{1}H) and 100/150 MHz (^{13}C), respectively. Chemical shifts were referenced to internal TMS (δ_H 0, ^{1}H) or CDCl$_3$ (δ_C 77.0, ^{13}C).

The positive and negative ion high resolution ESI mass spectra were obtained from an Orbitrap Elite mass spectrometer (Thermo Fisher Scientific, Germany) equipped with an HESI electrospray ion source (spray voltage 3.5 kV, capillary temperature 275 °C, source heater temperature 40 °C, FTMS resolution 60.000). Nitrogen was used as sheath gas. The sample solutions were introduced continuously *via* a 500 μl Hamilton syringe pump with a flow rate of 5 μl min^{-1}. The instrument was externally calibrated by the Pierce LTQ Velos ESI calibration solution (product no. 88324) from Thermo Fisher Scientific. The data were evaluated by the Xcalibur software 2.7 SP1.

Preparative HPLC was performed on a Knauer system equipped with a WellChrom K-1001 pump and a WellChrom K-2501 UV detector using an ODS-A column (5 μm, 120 Å, 150 × 10 mm ID, YMC, USA) eluting with H_2O (A) and CH_3CN (B) at a flow rate of 3.5 ml/min.

Fungal Material. Fruiting bodies of *Hygrophorus abieticola* Krieglst. ex Gröger & Bresinsky were collected under *Abies alba* Mill. in Paintner Forst near Kelheim, Bavaria, Germany (October 11, 2007, leg./det. A. Bresinsky). A voucher specimen (coll. 57/07) is deposited at the Leibniz Institute of Plant Biochemistry (IPB), Halle, Germany.

Fruiting bodies of *Hygrophorus latitabundus* Britzelm. were collected under *Pinus sylvestris* L. near Bad Bibra, Saxony Anhalt, Germany (October 30, 2002, leg./det. N. Arnold). A voucher specimen (coll. 51/02) is deposited at the Leibniz Institute of Plant Biochemistry (IPB), Halle, Germany.

Chemicals. All commercial reagents were purchased from Fluka, Merck or Aldrich and used without further purification. Dry CH_2Cl_2 was distilled from calcium hydride. All solvents (except Chloroform Rotisolv HPLC, purchased from Roth) were distilled prior to use. Spectral grade solvents were used for spectroscopic measurements. LC grade acetonitrile (LiChroSolv HPLC, Roth) was used for HPLC measurements. $CDCl_3$ was purchased from Deutero GmbH, Kastellaun, Germany. Bidistilled water was obtained from Millipore apparatus. The reference compounds dodine and pyraclostrobin were purchased from Sigma Aldrich (Germany), while the 4-oxo-hexadec-2-enoic acid (**2.7**) was obtained from the in-house compound library of the Leibniz Institute of Plant Biochemistry (IPB).

Extraction and isolation of compounds 6.1–6.5 from *Hygrophorus abieticola*. Frozen fruiting bodies of *H. abieticola* (2.5 kg) were macerated using a blender and extracted with EtOAc (3 × 3 l). The slight yellow solution was evaporated *in vacuo* to dryness. The crude extract (20.2 g) was subjected to silica gel column chromatography (CC, 450 × 45 mm) eluting with $CHCl_3$/MeOH (100:0→0:100) to obtain 10 fractions (A1–10, each 50 ml). Fraction A6 (3.05 g) was further purified by size exclusion CC on Sephadex LH 20 (400 × 40 mm, eluent CH_2Cl_2/MeOH 1:1) yielding 7 fractions (B1–7, each 50 ml). Fraction B5 (1.40 g) was applied to silica gel CC (450 × 45 mm) eluting with *n*-hexane/EtOAc 1:1 to afford 230 fractions (each 20 ml).

Fraction 79 (5.2 mg) was finally purified by preparative RP18 HPLC (0–19 min, 55–80% B) to afford **6.3** (t_R 13.6 min, 3.3 mg). Fractions 173–180 (32.3 mg) were finally purified by preparative RP18 HPLC (0–24 min, 55–75% B) to yield **6.1** (t_R 13.6–15.2 min, 20.1 mg), **6.2** (t_R 7.8 min, 0.6 mg), and **6.5** (t_R 11.0–13.5 min, 6.3 mg). Fraction 213–215 were combined (18.7 mg) and purified by preparative RP18 HPLC (0–15 min, 50–70% B) to obtain **6.4** (t_R 13.0 min, 5.9 mg).

Hygrophorone B[12] (6.1): white solid; TLC R_f 0.31 (n-hexane/EtOAc 1:1); $[\alpha]_D$ +19.9 (c 0.130, MeOH); CD (MeOH) $[\theta]_{201}$ –27159, $[\theta]_{219}$ +37657, $[\theta]_{306}$ –2027 $°×cm^2×dmol^{-1}$; IR, ^{1}H NMR, ^{13}C NMR, and ESI-HRMS in agreement with literature data (Bette et al., 2015; Otto et al., 2016a).

Hygrophorone B[10] (6.2): colorless oil; TLC R_f 0.24 (n-hexane/EtOAc 1:1); $[\alpha]^{27}_D$ +6.4 (c 0.060, CHCl$_3$); IR (ATR) υ_{max} 3510 (br, w), 3401 (w), 2915 (s), 2849 (s), 1715 (s), 1692 (s), 1594 (w), 1470 (m), 1398 (w), 1354 (w), 1251 (w), 1214 (w), 1114 (m), 1071 (m), 1000 (m), 960 (m), 930 (w), 842 (m), 796 (w), 718 (w), 705 (w), 686 (w) cm^{-1}; ^{1}H NMR and ^{13}C NMR see Table 6.1; ESI-HRMS m/z 319.1680 ([M+Cl]$^-$, calculated for $C_{16}H_{28}O_4Cl^-$ 319.1682).

Hygrophorone E[12] (6.3): colorless oil; TLC R_f 0.29 (n-hexane/EtOAc 1:1); $[\alpha]^{24}_D$ +111.8 (c 0.310, CHCl$_3$); CD (MeOH) $[\theta]_{196}$ +26703, $[\theta]_{292}$ +2375 $°×cm^2×dmol^{-1}$; UV (MeOH) λ_{max} (log ε) 200 (3.50) nm; IR (ATR) υ_{max} 3384 (br, w), 2917 (s), 2851 (s), 2360 (w), 1703 (s), 1466 (m), 1397 (w), 1336 (w), 1264 (w), 1182 (w), 1073 (m), 1019 (m), 959 (w), 832 (w), 737 (m) cm^{-1}; ^{1}H NMR and ^{13}C NMR see Table 6.1; ESI-HRMS m/z 311.2231 ([M–H]$^-$, calculated for $C_{18}H_{31}O_4^-$ 311.2228).

Hygrophorone H[12] (6.4): colorless oil; TLC R_f 0.33 (n-hexane/EtOAc 1:1); $[\alpha]^{24}_D$ +81.8 (c 0.380, CHCl$_3$); CD (MeOH) $[\theta]_{199}$ +21282 $°×cm^2×dmol^{-1}$; UV (MeOH) λ_{max} (log ε) 199 (3.37) nm; IR (ATR) υ_{max} 3355 (br, w), 2913 (s), 2848 (s), 1737 (w), 1466 (m), 1373 (w), 1341 (w), 1293 (w), 1217 (w), 1155 (w), 1107 (m), 1006 (s), 954 (w), 916 (w), 877 (w), 837 (m), 790 (w), 766 (w), 712 (w) cm^{-1}; ^{1}H NMR and ^{13}C NMR see Table 6.1; ESI-HRMS m/z 313.2390 ([M–H]$^-$, calculated for $C_{18}H_{33}O_4^-$ 313.2384).

2,3-Dihydrohygrophorone H[12] (6.5): white solid; TLC R_f 0.30 (n-hexane/EtOAc 1:1); $[\alpha]^{24}_D$ +31.7 (c 0.540, CHCl$_3$); IR (ATR) υ_{max} 3378 (br, w), 2913 (s), 2848 (s), 2362 (w), 2341 (w), 1465 (m), 1300 (w), 1100 (w), 1027 (m), 963 (w), 936 (w), 890 (w), 720 (w), 670 (w) cm^{-1}; ^{1}H NMR and ^{13}C NMR see Table 6.1; ESI-HRMS m/z 315.2551 ([M–H]$^-$, calculated for $C_{18}H_{35}O_4^-$ 315.2541).

Extraction and isolation of natural 6.3a from *Hygrophorus latitabundus*. Frozen fruiting bodies of *H. latitabundus* (212 g) were macerated using a blender and extracted with EtOAc (3 × 2 l). The slight yellow solution was evaporated *in vacuo* to dryness. The crude extract (1.60 g) was purified by sequential fractionation on a Chromabond® SiOH cartridge (3 ml,

500 mg, Macherey-Nagel) eluting with a petroleum ether/EtOAc gradient (100:0→0:100). The 80:20 and 70:30 eluates were combined (37.9 mg) and purified by preparative RP18 HPLC (0–20 min, 70–100% B) to obtain pure 1,4-di-*O*-acetylhygrophorone E[12] (**6.3a**) (t_R 12.8 min, 2.8 mg) as a colorless oil. TLC R_f 0.69 (*n*-hexane/EtOAc 1:1); $[\alpha]^{27}_D$ +119.6 (*c* 0.130, MeOH); ^{1}H NMR (400 MHz, CDCl$_3$) 6.185 (1H, ddd, *J* = 6.2/1.9/1.1 Hz, H-3), 6.154 (1H, ddd, *J* = 6.2/2.1/1.1 Hz, H-2), 5.721 (1H, m, H-4), 5.710 (1H, m, H-1), 3.985 (1H, br s, OH-5), 2.663 (1H, ddd, *J* = 17.7/8.7/6.1 Hz, H$_A$-7), 2.582 (1H, ddd, *J* = 17.7/8.7/6.2 Hz, H$_7$-B), 2.105 (3H, s, OAc-1), 2.015 (3H, s, OAc-4), 1.632 (2H, m, H$_2$-8), 1.33 – 1.21 (18H, m, H$_2$-9 – H$_2$-17), 0.880 (3H, t, *J* = 7.0 Hz, H$_3$-18); ^{13}C NMR (100 MHz, CDCl$_3$) 208.0 C-6, 170.6 OAc-1, 169.9 OAc-4, 134.7 C-3, 133.9 C-2, 86.2 C-4, 83.7 C-5, 77.6 C-1, 38.2 C-7, 31.9 C-16, 29.6 – 29.3 C-9 – C-15, 23.6 C-8, 22.7 C-17, 20.8 OAc-4, 20.6 OAc-1, 14.1 C-18; ESI-HRMS *m/z* 419.2412 ([M+Na]$^+$, calculated for C$_{22}$H$_{36}$O$_6$Na$^+$ 419.2404).

Semisynthesis of 4-*O*- and 6-*O*-acetylhygrophorone B[12] (6.1a and 6.1b). To a solution of 9.1 mg **6.1** in 3 ml pyridine, 7 drops of acetic anhydride were added. The mixture was stirred for 2 h at room temperature, and unreacted acetic anhydride was quenched with water. The solution was concentrated *in vacuo* to dryness and subsequently purified by preparative RP18 HPLC (0–15 min, 60–90% B, 15–16 min, 90–100% B) to yield **6.1a** (t_R 12.3 min, 4.1 mg) and **6.1b** (t_R 14.0 min, 0.6 mg).

4-*O*-Acetylhygrophorone B[12] (6.1a): colorless oil; TLC R_f 0.51 (*n*-hexane/EtOAc 1:1); $[\alpha]^{24}_D$ +12.2 (*c* 0.280, CHCl$_3$); ^{1}H NMR and ^{13}C NMR see Table 6.2; ESI-HRMS *m/z* 377.2298 ([M+Na]$^+$, calculated for C$_{20}$H$_{34}$O$_5$Na$^+$ 337.2298).

6-*O*-Acetylhygrophorone B[12] (6.1b): colorless oil; TLC R_f 0.50 (*n*-hexane/EtOAc 1:1); ^{1}H NMR and ^{13}C NMR see Table 6.2; ESI-HRMS *m/z* 377.2298 ([M+Na]$^+$, calculated for C$_{20}$H$_{34}$O$_5$Na$^+$ 377.2298).

Semisynthesis of 4,6-di-*O*-acetylhygrophorone B[12] (6.1c). To a solution of 4.9 mg **6.1** in pyridine (1.5 ml) an excess of acetic anhydride (2 ml) was added. The mixture was stirred for 15 h at room temperature, and unreacted acetic anhydride was quenched with water. The solution was concentrated *in vacuo* to dryness and subsequently purified by preparative RP18 HPLC (0–15 min, 60–90% B, 15–16 min, 90–100% B) to yield **6.1c** (t_R 14.8 min, 3.0 mg) as a colorless oil. TLC R_f 0.69 (*n*-hexane/EtOAc 1:1); $[\alpha]^{24}_D$ +16.0 (*c* 0.310, CHCl$_3$); ^{1}H NMR and ^{13}C NMR see Table 6.2; ESI-HRMS *m/z* 419.2398 ([M+Na]$^+$, calculated for C$_{22}$H$_{36}$O$_6$Na$^+$ 419.2404).

Semisynthesis of 4,5,6-tri-*O*-acetylhygrophorone B[12] (6.1d). To a solution of 6.0 mg **6.1** in pyridine (2 ml) catalytic amounts of DMAP and an excess of acetic anhydride (2 ml) were added. The mixture was stirred for 50 h at room temperature, and unreacted acetic anhydride was quenched with water. The solution was concentrated *in vacuo* to dryness and subsequently

purified by preparative RP18 HPLC (0–20 min, 60–100% B) to yield **6.1d** (t_R 17.8 min, 3.7 mg) as a colorless oil. TLC R_f 0.89 (*n*-hexane/EtOAc 1:1); $[\alpha]^{24}_D$ +29.3 (*c* 0.470, CHCl$_3$); ^{1}H NMR and ^{13}C NMR see Table 6.2; ESI-HRMS *m/z* 461.2512 ([M+Na]$^+$, calculated for C$_{24}$H$_{38}$O$_7$Na$^+$ 461.2510).

Semisynthesis of 1,4-di-*O*-acetylhygrophorone E[12] (6.3a). To a solution of 5.1 mg **6.3** in pyridine (3 ml) an excess of acetic anhydride (2 ml) was added. The mixture was stirred for 15 h at room temperature, and unreacted acetic anhydride was quenched with water. The solution was concentrated *in vacuo* to dryness and subsequently purified by preparative RP18 HPLC (0–20 min, 70–85% B) to obtain **6.3a** (t_R 15.4 min, 3.7 mg) as a colorless oil. TLC R_f 0.70 (*n*-hexane/EtOAc 1:1); $[\alpha]^{27}_D$ +137.9 (*c* 0.310, MeOH); ^{1}H NMR (400 MHz, CDCl$_3$) 6.186 (1H, ddd, J = 6.2/1.9/1.1 Hz, H-3), 6.154 (1H, ddd, J = 6.2/2.1/1.1 Hz, H-2), 5.721 (1H, m, H-4), 5.709 (1H, m, H-1), 3.990 (1H, br s, OH-5), 2.663 (1H, ddd, J = 17.7/8.8/6.2 Hz, H$_A$-7), 2.582 (1H, ddd, J = 17.7/8.6/6.1 Hz, H$_7$-B), 2.104 (3H, s, OAc-1), 2.014 (3H, s, OAc-4), 1.639 (2H, m, H$_2$-8), 1.33 – 1.21 (18H, m, H$_2$-9 – H$_2$-17), 0.880 (3H, t, J = 7.0 Hz, H$_3$-18); ^{13}C NMR (100 MHz, CDCl$_3$) 208.0 C-6, 170.6 OAc-1, 169.9 OAc-4, 134.7 C-3, 133.9 C-2, 86.2 C-4, 83.7 C-5, 77.6 C-1, 38.2 C-7, 31.9 C-16, 29.6 – 29.3 C-9 – C-15, 23.6 C-8, 22.7 C-17, 20.8 OAc-4, 20.6 OAc-1, 14.1 C-18; ESI-HRMS *m/z* 419.2412 ([M+Na]$^+$, calculated for C$_{22}$H$_{36}$O$_6$Na$^+$ 419.2404).

Semisynthesis of 2,3-dihydrohygrophorone B[12] (6.6). To a solution of 8.0 mg **6.1** in MeOH (2 ml) a catalytic amount of palladium-loaded activated carbon (Pd/C, 10%) was added and the reaction was stirred for 48 hours at room temperature in hydrogen atmosphere (1 atm). The reaction mixture was filtered through a membrane filter (PTFE, pore size 0.2 μm), and the MeOH was removed *in vacuo* to yield **6.6** (7.5 mg) as a colorless oil. TLC R_f 0.30 (*n*-hexane/ EtOAc 1:1); ^{1}H NMR (600 MHz, CDCl$_3$) 4.399 (1H, m, H-4), 3.629 (1H, dd, J = 8.7/4.2 Hz, H-6), 2.53 – 2.44 (1H, m, H$_A$-2), 2.35 – 2.24 (2H, m, H$_B$-2 & H$_A$-3), 2.11 – 2.03 (1H, m, H$_B$-3), 1.400 (2H, m, H$_2$-7), 1.33 – 1.21 (20H, m, H$_2$-8 – H$_2$-17), 0.881 (3H, t, J = 7.0 Hz, H$_3$-18); ^{13}C NMR (150 MHz, CDCl$_3$) 217.2 C-1, 83.2 C-5, 71.8 C-6, 71.1 C-4, 32.5 C-2, 31.9 C-16, 31.6 C-7, 29.7 – 29.3 C-9 – C-15, 25.9 C-8, 25.4 C-3, 22.7 C-17, 14.1 C-18; ESI-HRMS *m/z* 313.2391 ([M–H]$^-$, calculated for C$_{18}$H$_{33}$O$_4^-$ 313.2384).

Semisynthesis of 2,3-dihydrohygrophorone H[12] (6.5) from 2,3-dihydrohygrophorone B[12] (6.6) (*R,R* catalyst). To a solution of 7.5 mg **6.6** in dry CH$_2$Cl$_2$ (1 ml), formic acid/trimethylamine (5/7 v/v, 1.1 ml) and catalytic amounts of (*R,R*) Noyori hydrogenation catalyst [RuCl{(*R,R*)-TsDPEN}(mesitylene)] ($[\alpha]^{27}_D$ –257.4, *c* 0.205, CHCl$_3$) was added. The resulting solution was stirred at room temperature under nitrogen atmosphere for seven days. Water (2 ml) was added and the solution was extracted thrice with CH$_2$Cl$_2$ (each 3 ml). The combined organic layers were dried over Na$_2$SO$_4$, concentrated *in vacuo* to dryness and purified by sequential fractionation on a Chromabond® SiOH cartridge (3 ml, 500 mg, Macherey-Nagel) eluting with a CH$_2$Cl$_2$/EtOAc gradient (100:0→0:100). The 40:60, 50:50, 60:40, and 70:30 eluates were combined to yield pure

6.5 (4.2 mg) as a yellowish solid. TLC R_f 0.29 (*n*-hexane/EtOAc 1:1); $[\alpha]^{24}_D$ +26.3 (*c* 0.310, CHCl$_3$); ^{1}H NMR (400 MHz, CDCl$_3$) 4.458 (1H, dd, J = 8.1/7.6 Hz, H-1), 4.082 (1H, m, H-4), 3.955 (1H, dd, J = 9.4/2.5 Hz, H-6), 2.32 – 2.18 (2H, m, H$_A$-2 & H$_A$-3), 1.65 – 1.57 (3H, m, H$_B$-2 & H$_2$-7), 1.55 – 1.20 (21H, m, H$_B$-3 & H$_2$-8 – H$_2$-17), 0.880 (3H, t, J = 7.0 Hz, H$_3$-18); ^{13}C NMR (100 MHz, CDCl$_3$) 80.7 C-5, 78.4 C-4, 75.9 C-1, 75.4 C-6, 31.9 C-16, 31.4 C-7, 31.1 C-3, 29.7 – 29.3 C-9 – C-15, 29.1 C-2, 25.9 C-8, 22.7 C-17, 14.1 C-18; ESI-HRMS *m/z* 315.2544 ([M–H]$^-$, calculated for C$_{18}$H$_{35}$O$_4^-$ 315.2541).

Semisynthesis of 2,3-dihydrohygrophorone H^{12} (6.5) from 2,3-dihydrohygrophorone B^{12} (6.6) (*S,S* catalyst). To a solution of 5.2 mg **6.6** in dry CH$_2$Cl$_2$ (1 ml), formic acid/trimethylamine (5/7 v/v, 1.1 ml) and catalytic amounts of (*S,S*) Noyori hydrogenation catalyst [RuCl{(*S,S*)-TsDPEN}(mesitylene)] ($[\alpha]^{27}_D$ +281.7, *c* 0.265, CHCl$_3$) was added. The resulting solution was stirred at room temperature under nitrogen atmosphere for eight days. Water (2 ml) was added and the solution was extracted thrice with CH$_2$Cl$_2$ (each 3 ml). The combined organic layers were dried over Na$_2$SO$_4$, concentrated *in vacuo* to dryness and purified by sequential fractionation on a Chromabond® SiOH cartridge (3 ml, 500 mg, Macherey-Nagel) eluting with a CH$_2$Cl$_2$/EtOAc gradient (100:0→0:100). The 40:60, 50:50, 60:40, and 70:30 eluates were combined to yield **6.5** (2.9 mg) as a white solid. TLC R_f 0.30 (*n*-hexane/EtOAc 1:1); ^{1}H NMR (400 MHz, CDCl$_3$) 4.459 (1H, dd, 8.1/7.6 Hz, H-1), 4.084 (1H, m, H-4), 3.956 (1H, m, H-6), 2.43 – 2.18 (2H, m, H$_A$-2 & H$_A$-3), 1.68 – 1.56 (3H, m, H$_B$-2 & H$_2$-7), 1.55 – 1.20 (21H, m, H$_B$-3 & H$_2$-8 – H$_2$-17), 0.880 (3H, t, J = 7.0 Hz, H$_3$-18); ^{13}C NMR (100 MHz, CDCl$_3$) 80.7 C-5, 78.3 C-4, 75.9 C-1, 75.4 C-6, 31.9 C-16, 31.4 C-7, 31.1 C-3, 29.7 – 29.3 C-9 – C-15, 29.0 C-2, 25.9 C-8, 22.7 C-17, 14.1 C-18; ESI-HRMS *m/z* 315.2541 ([M–H]$^-$, calculated for C$_{18}$H$_{35}$O$_4^-$ 315.2541).

Semisynthesis of 2,3-dihydrohygrophorone H^{12} (6.5) from hygrophorone H^{12} (6.4). To a solution of 3.8 mg **6.4** in MeOH (2 ml) a catalytic amount of palladium-loaded activated carbon (Pd/C, 10%) was added and the reaction was stirred for 48 hours at room temperature under hydrogen atmosphere (1 atm). The reaction mixture was filtered through a PTFE membrane filter (pore size 0.2 μm), and the MeOH was removed *in vacuo* to afford **6.5** (3.5 mg) as a yellowish solid. TLC R_f 0.30 (*n*-hexane/EtOAc 1:1); $[\alpha]^{24}_D$ +18.9 (*c* 0.355, CHCl$_3$); ^{1}H NMR (600 MHz, CDCl$_3$) 4.459 (1H, dd, J = 8.1/7.7 Hz, H-1), 4.085 (1H, dd, J = 5.3/2.5 Hz, H-4), 3.955 (1H, dd, J = 9.6/2.7 Hz, H-6), 2.34 – 2.19 (2H, m, H$_A$-2 & H$_A$-3), 1.65 – 1.57 (3H, m, H$_B$-2 & H$_2$-7), 1.55 – 1.20 (21H, m, H$_B$-3 & H$_2$-8 – H$_2$-17), 0.881 (3H, t, J = 7.0 Hz, H$_3$-18); ^{13}C NMR (150 MHz, CDCl$_3$) 80.7 C-5, 78.4 C-4, 75.9 C-1, 75.4 C-6, 31.9 C-16, 31.4 C-7, 31.1 C-3, 29.7 – 29.4 C-9 – C-15, 29.1 C-2, 25.9 C-8, 22.7 C-17, 14.1 C-18; ESI-HRMS *m/z* 339.1511 ([M+Na]$^+$, calculated for C$_{18}$H$_{36}$O$_4$Na$^+$ 339.2506).

Semisynthesis of hygrophorone B^{12} cysteine adduct (6.7). To a solution of 3.2 mg **6.1** in MeOH (3 ml) L-cysteine (8.5 mg) was added and stirred for 24 hours at room temperature. ESI-HRMS

and TLC analysis indicated that the conversion to **6.7** was completed. TLC R_f 0.45 (*n*-hexane/EtOAc 1:5); ESI-HRMS *m/z* 434.2572 ([M+H]$^+$, calculated for $C_{21}H_{40}O_6NS^+$ 434.2571). Due to the poor solubility of **6.7**, a final purification and further characterization was not possible.

Antiphytopathogenic activity. Crude extracts, fractions, and pure compounds were tested in a 96-well microtiter plate assay against *Botrytis cinerea* Pers., *Septoria tritici* Desm., and *Phytophthora infestans* (Mont.) De Bary as described earlier (Otto et al., 2016a).

Antibacterial activity. The antimicrobial assays were carried out by the DSMZ (Dr. Sabine Gronow). The selected compounds were tested against the gram-positive bacteria *Staphylococcus aureus* subsp. *aureus* DSM 18827 (MRSA) and *Enterococcus faecium* DSM 13590 (vanA+) as well as the gram-negative bacterium *Pseudomonas aeruginosa* DSM 1117. The antibiotic activity was evaluated by determining the minimum inhibitory concentration (MIC). The MIC corresponds to the lowest concentration of an antibacterial compound that shows growth inhibition. The MIC was determined by the broth microdilution procedure according to the European Committee on Antimicrobial Susceptibility Testing (EUCAST, 2003).

Susceptibility testing against *Malassezia pachydermatis*. The tests against *Malassezia pachydermatis* were performed in 96 well microtiter plates. Stock solutions of the tested compounds were prepared in DMSO and diluted with RPMI 1640 medium (supplemented with 0.1% Tween 40 and 0.4% glycerol) to the following final concentrations: 42 µg/ml, 14 µg/ml, 4.70 µg/ml, 1.56 µg/ml, 0.52 µg/ml, 0.17 µg/ml, 0.06 µg/ml, and 0.02 µg/ml. Strains of *Malassezia pachydermatis* CBS 1879 and CRA 002 were cultured on SDA agar plates. Then, a part of the culture was removed from the surface with a sterile cotton swab and transferred to RPMI 1640 medium. The resulting suspension was adjusted to a final inoculum size of about 1×10^3 colony forming units (CFU) per ml. Then, 50 µl of the *Malassezia* suspension and 50 µl of the respective compound dilution were mixed in each well and incubated at 37 °C for 2–4 days. The evaluation of the inhibition was carried out by visual inspection. Terbinafine was used as a reference compound, while water was used as negative control.

Measurement of hemolytic activity. The hemolytic activity assay was carried out by Dr. Katrin Vogel (Department of Pharmacology and Toxicology, Division of Clinical Pharmacology, Medicinal Faculty of the Martin-Luther University Halle-Wittenberg) as described in the literature (Kahn et al., 1981; Malinauskas, 1997; Richterich and Colombo, 1978).

Computational methods. The initial conformational analysis of the relevant stereoisomers of compounds **6.3** (*SS*-**6.3**, *RR*-**6.3**) and **6.4** (*SSR*-**6.4**, *RSsR*-**6.4**) was performed with the aid of the Molecular Operating Environment (MOE, 2015) software. Low-mode molecular dynamics simulations were applied for the conformational search using the MMFF94 molecular mechanics

force field (Halgren, 1999). The force field minimum energy structures were subsequently optimized by applying the density functional theory (DFT) using the BP86 functional with the def2-TZVPP basis set (Becke, 1988; Karton et al., 2008; Perdew, 1986; Schäfer et al., 1992; Weigend and Ahlrichs, 2005) implemented in the *ab initio* ORCA 3.0.3 program package (Neese et al., 2012). The influence of the solvent MeOH was included in the DFT calculations using the COSMO model (Sinnecker et al., 2006) to include any influence of the solvent. The quantum chemical simulation of the UV and CD spectra was also carried out using ORCA. Therefore, the first 50 excited states of each enantiomer and conformation were calculated by applying the long-range corrected hybrid functional TD CAM-B3LYP9 with the def2-TZVP(-f) and def2-TZVP/J basis sets (Karton et al., 2008; Schäfer et al., 1992; Weigend and Ahlrichs, 2005). The CD curves were visualized with the help of the software SpecDis 1.64 (Bruhn et al., 2013, 2015) from the calculated rotatory strength values using a Gaussian distribution function at a half-bandwidth of $\sigma = 0.3$ eV. The single spectra of the individual conformers were summed up according to their contribution to Boltzmann-statistical weighting (as derived from the single-point energy calculations), wavelength shifted, and compared with the experimental spectra.

6.5 References

Becke, A.D., 1988. Density-functional exchange-energy approximation with correct asymptotic behavior. *Phys. Rev. A* 38, 3098–3100.

Bette, E., Otto, A., Dräger, T., Merzweiler, K., Arnold, N., Wessjohann, L., Westermann, B., 2015. Isolation and asymmetric total synthesis of fungal secondary metabolite hygrophorone B[12]. *Eur. J. Org. Chem.* 2015, 2357–2365.

Bresinsky, A., 2008. Beiträge zu einer Mykoflora Deutschlands (2): Die Gattungen *Hydropus* bis *Hypsizygus* mit Angaben zur Ökologie und Verbreitung der Arten. *Regensburg. Mykol. Schriften* 15, 1–304.

Bruhn, T., Schaumlöffel, A., Hemberger, Y., Bringmann, G., 2015. SpecDis version 1.64, University of Würzburg, Germany.

Bruhn, T., Schaumlöffel, A., Hemberger, Y., Bringmann, G., 2013. SpecDis: Quantifying the comparison of calculated and experimental electronic circular dichroism spectra. *Chirality* 25, 243–249.

Cimmino, A., Andolfi, A., Evidente, A., 2014. Phytotoxic terpenes produced by phytopathogenic fungi and allelopathic plants. *Nat. Prod. Commun.* 9, 401–408.

Cimmino, A., Masi, M., Evidente, M., Superchi, S., Evidente, A., 2015. Fungal phytotoxins with potential herbicidal activity: Chemical and biological characterization. *Nat. Prod. Rep.* 32, 1629–1653.

Coutinho, S.D., Paula, C.R., 2000. Proteinase, phospholipase, hyaluronidase and chondroitin-sulphatase production by *Malassezia pachydermatis*. *Med. Mycol.* 38, 73–76.

Dräger, T., 2011. Synthese und biologische Testung von Naturstoffen und Naturstoff-Analoga mit Acryl-Struktureinheit. Dissertation, Martin-Luther-Universität Halle-Wittenberg.

Eschen-Lippold, L., Dräger, T., Teichert, A., Wessjohann, L., Westermann, B., Rosahl, S., Arnold, N., 2009. Antioomycete activity of γ-oxocrotonate fatty acids against *P. infestans*. *J. Agric. Food Chem.* 57, 9607–9612.

European Committee on Antimicrobial Susceptibility Testing (EUCAST), 2003. Determination of minimum inhibitory concentrations (MICs) of antibacterial agents by broth microdilution. *Clin. Microbiol. Infect.* 9, IX–XV.

Evidente, A., Kornienko, A., Cimmino, A., Andolfi, A., Lefranc, F., Mathieu, V., Kiss, R., 2014. Fungal metabolites with anticancer activity. *Nat. Prod. Rep.* 31, 617–627.

Fujii, A., Hashiguchi, S., Uematsu, N., Ikariya, T., Noyori, R., 1996. Ruthenium(II)-catalyzed asymmetric transfer hydrogenation of ketones using a formic acid−triethylamine mixture. *J. Am. Chem. Soc.* 118, 2521–2522.

Gilardoni, G., Clericuzio, M., Marchetti, A., Vita Finzi, P., Zanoni, G., Vidari, G., 2006. New oxidized 4-oxo fatty acids from *Hygrophorus discoxanthus*. *Nat. Prod. Commun.* 1, 1079–1084.

Gilardoni, G., Clericuzio, M., Tosi, S., Zanoni, G., Vidari, G., 2007. Antifungal acylcyclopentenediones from fruiting bodies of *Hygrophorus chrysodon*. *J. Nat. Prod.* 70, 137–139.

Guillot, J., Bensignor, E., Jankowski, F., Seewald, W., Chermette, R., Steffan, J., 2003. Comparative efficacies of oral ketoconazole and terbinafine for reducing *Malassezia* population sizes on the skin of Basset Hounds. *Vet. Dermatol.* 14, 153–157.

Halgren, T.A., 1999. MMFF VI. MMFF94s option for energy minimization studies. *J. Comp. Chem.* 20, 720–729.

Hassal, K.A., 1990. The biochemistry and uses of pesticides: Structure, metabolism, mode of action and uses in crop Protection. Macmillan Press Ltd, London, 297.

Kahn, S.E., Watkins, B.F., Bermes, E.W., 1981. An evaluation of a spectrophotometric scanning technique for measurement of plasma hemoglobin. *Ann. Clin. Lab. Sci.* 11, 126–131.

Karton, A., Tarnopolsky, A., Lamère, J.F., Schatz, G.C., Martin, J.M.L., 2008. Highly accurate first-principles benchmark data sets for the parametrization and validation of density functional and other approximate methods. Derivation of a robust, generally applicable, double-hybrid functional for thermochemistry and thermochemical kinetics. *J. Phys. Chem. A* 112, 12868–12886.

Krieglsteiner, G.J., Gminder, A., 2001. Die Großpilze Baden-Württembergs, Band 3: Ständerpilze. Blätterpilze 1. Ulmer, Stuttgart, 1–634.

Lübken, T., 2006. Hygrophorone – Neue antifungische Cyclopentenonderivate aus *Hygrophorus*-Arten (Basidiomycetes). Dissertation, Martin-Luther-Universität Halle-Wittenberg.

Lübken, T., Arnold, N., Wessjohann, L., Böttcher, C., Schmidt, J., 2006. Analysis of fungal cyclopentenone derivatives from *Hygrophorus* spp. by liquid chromatography/electrospray-tandem mass spectrometry. *J. Mass Spectrom.* 41, 361–371.

Lübken, T., Schmidt, J., Porzel, A., Arnold, N., Wessjohann, L., 2004. Hygrophorones A–G: Fungicidal cyclopentenones from *Hygrophorus* species (Basidiomycetes). *Phytochemistry* 65, 1061–1071.

Malinauskas, R.A., 1997. Plasma hemoglobin measurement techniques for the *in vitro* evaluation of blood damage caused by medical devices. *Artif. Organs* 21, 1255–1267.

Molecular Operating Environment (MOE) 2015.10, 2015. Chemical Computing Group Inc.: Montreal, QC, Canada.

Neese, F., 2012. The ORCA program system. *Wiley Interdiscip. Rev.: Comput. Mol. Sci.* 2, 73–78.

Otto A., Porzel A., Schmidt J., Wessjohann L., Arnold N., 2014. Penarines A–F, (nor-) sesquiterpene carboxylic acids from *Hygrophorus penarius* (Basidiomycetes). *Phytochemistry* 108, 229–233.

Otto, A., Porzel, A., Schmidt, J., Wessjohann, L., Arnold, N., 2015b. A study on the biosynthesis of hygrophorone B[12] in the mushroom *Hygrophorus abieticola* reveals an unexpected labelling pattern in the cyclopentenone moiety. *Phytochemistry* 118, 174–180.

Otto, A., Porzel, A., Schmidt, J., Brandt, W., Wessjohann, L., Arnold, N., 2016a. Structure and absolute configuration of pseudohygrophorones A[12] and B[12], alkyl cyclohexenone derivatives from *Hygrophorus abieticola* (Basidiomycetes). *J. Nat. Prod.* 79, 74–80.

Perdew, J.P., 1986. Density-functional approximation for the correlation energy of the inhomogeneous electron gas. *Phys. Rev. B* 33, 8822–8824.

Richterich, R., Colombo, J.P., 1978. Klinische Chemie: Theorie, Praxis, Interpretation. Karger, Freiburg, 435–446.

Schäfer, A., Horn, H., Ahlrichs, R., 1992. Fully optimized contracted gaussian-basis sets for atoms Li to Kr. *J. Chem. Phys.* 97, 2571–2577.

Schmidts, V., Fredersdorf, M., Lübken, T., Porzel, A., Arnold, N., Wessjohann, L., Thiele, C.M., 2013. RDC-based determination of the relative configuration of the fungicidal cyclopentenone 4,6-diacetylhygrophorone A[12]. *J. Nat. Prod.* 76, 839–844.

Sinnecker, S., Rajendran, A., Klamt, A., Diedenhofen, M., Neese, F., 2006. Calculation of solvent shifts on electronic g-tensors with the conductor-like screening model (COSMO) and its self-consistent generalization to real solvents (direct COSMO-RS). *J. Phys. Chem. A* 110, 2235–2245.

Stamatakis, K., Perez-Sala, D., 2006. Prostanoids with cyclopentenone structure as tools for the characterization of electrophilic lipid-protein interactomes. *Ann. N. Y. Acad. Sci.* 1091, 548–570.

Teichert, A., Lübken, T., Schmidt, J., Porzel, A., Arnold, N., Wessjohann, L., 2005b. Unusual bioactive 4-oxo-2-alkenoic fatty acids from *Hygrophorus eburneus*. *Z. Naturforsch.* 60b, 25–32.

Weigend, F., Ahlrichs, R., 2005. Balanced basis sets of split valence, triple zeta valence and quadruple zeta valence quality for H to Rn: Design and assessment of accuracy. *Phys. Chem. Chem. Phys.* 7, 3297–3305.

6.6 Supporting Information

Supplementary data associated with this Chapter can be found at http://dx.doi.org/10.1016/ j.tet.2017.02.013.

7 Penarines A–F, (nor-)sesquiterpene carboxylic acids from *Hygrophorus penarius* (Basidiomycetes)
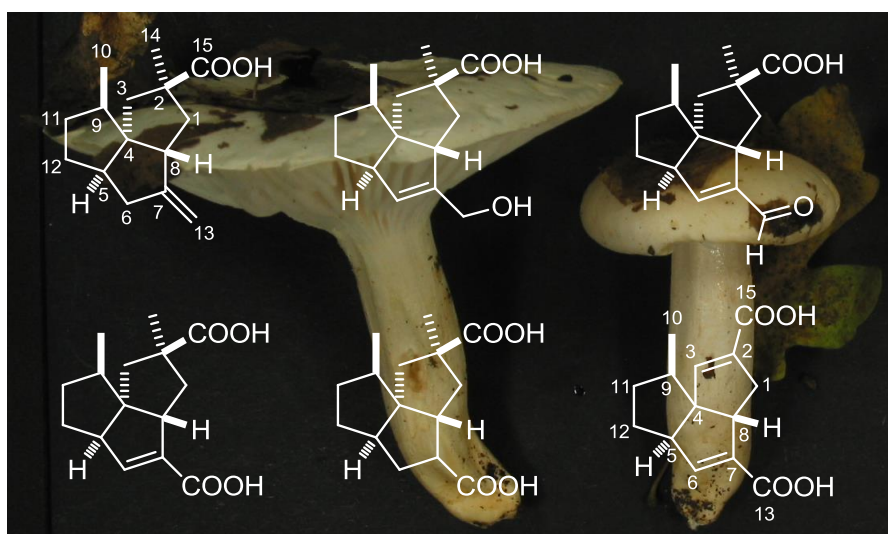
Abstract

Five novel sesquiterpene carboxylic acids (**7.1**–**7.5**) and one new nor-sesquiterpene carboxylic acid (**7.6**) of the very rare ventricosane type, named penarines A–F, were isolated from fruiting bodies of the basidiomycete *Hygrophorus penarius* (Hygrophoraceae). This is the first report of (nor-)sesquiterpenes isolated from basidiocarps of the family Hygrophoraceae. Their structures were elucidated on the basis of extensive 1D (^{1}H, ^{13}C) and 2D (HSQC, HMBC, COSY, ROESY) NMR spectroscopic analyses as well as high-resolution mass spectrometry studies. Additionally, the only known member of this rare type of sesquiterpenes, ventricos-7(13)-ene (**7.7**), could be identified *via* headspace GC-MS analysis in a fruiting body of *H. penarius*. Compounds **7.1**–**7.6** were devoid of remarkable antifungal activity against *Cladosporium cucumerinum.* Additionally, the cytotoxic activities of compounds **7.1** and **7.2** were evaluated against the human prostate cancer cell line PC-3 and the colon cancer cell line HT-29 showing no significant cytotoxic activity.

7.1 Introduction

Basidiomycetous fungal fruiting bodies are a rich source for structural highly diverse secondary metabolites. Earlier investigations showed that species of the genus *Hygrophorus* (Hygrophoraceae) produce compounds like cyclopentenone derivatives (Lübken et al., 2004; Gilardoni et al., 2007), unusual 4-oxo-2-ene fatty acids (Teichert et al., 2005b; Gilardoni et al., 2006) and ceramides (Qu et al., 2004). During our ongoing work regarding secondary metabolites from fungal basidiocarps, the EtOAc extract of *Hygrophorus penarius* Fr. (section Pudorini, subsection Clitocyboides) was investigated (Lodge et al., 2014). The medium-sized to large fruiting bodies (4–9 cm) are obligate mycorrhizal symbionts with deciduous trees, especially with *Fagus* and *Quercus*, on calcareous soils. The pale ochraceous basidiocarps are characterized by a slimy surface soon becoming dry. The present paper describes the isolation, structure elucidation and biological evaluation of novel ventricosane-type (nor-)sesquiterpenes (**7.1**–**7.6**) named penarines A–F.

7.2 Results and discussion

After repeated column chromatography on silica gel, Sephadex LH 20, and preparative HPLC, compounds **7.1**–**7.6** could be isolated from the EtOAc extract of *H. penarius* (see Chapter 7.4).
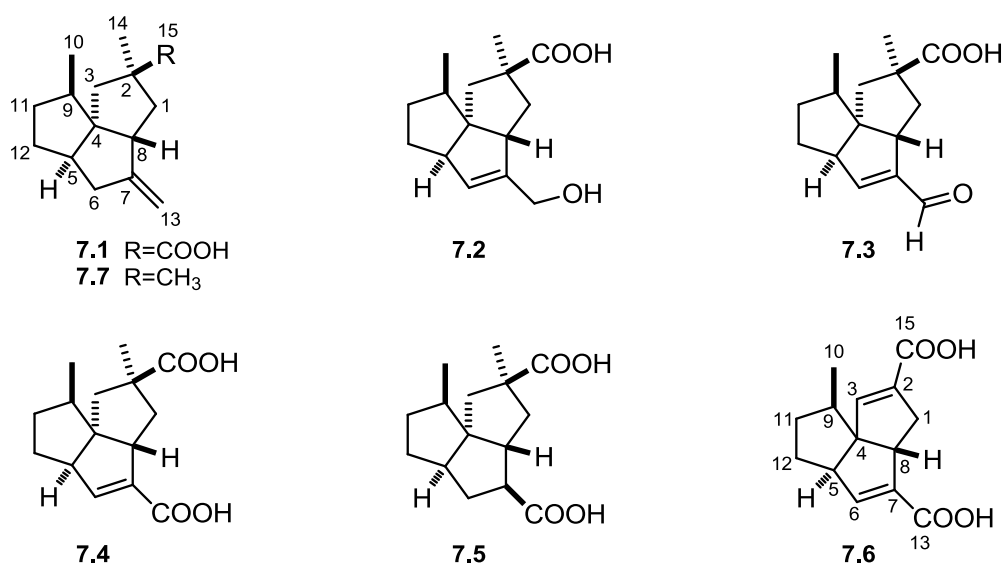
Fig. 7.1. Structures of compounds **7.1**–**7.7**.

Compound **7.1** was obtained as a colorless oil. The molecular formula $C_{15}H_{22}O_2$ was determined by HR-ESI-MS (negative mode) as *m/z* 233.1548 ([M–H]$^-$, calculated for $C_{15}H_{21}O_2^-$ 233.1547), indicating five double bond equivalents (DBEs). A strong IR absorption band at 1693 cm^{-1} indicated the presence of a carbonyl functionality. The ^{13}C NMR (Table 7.2) and DEPT-135 spectra of compound **7.1** exhibited signals for two primary carbons (δ_C 14.5 and 25.7), six secondary carbons (δ_C 32.3, 33.7, 40.5, 44.8, 52.2 and 104.2), three tertiary carbons (δ_C 45.2,

49.8 and 51.5) and four quaternary carbons (δ_C 50.4, 64.7, 158.1 and 183.5). These data suggested the presence of one carboxylic group and one double bond. Thus, the remaining three DBEs indicated the presence of a tricyclic system. The ^{1}H NMR spectroscopic data (Table 7.1) of **7.1** displayed signals at δ_H 0.921 (3H, d, J = 6.8 Hz) and δ_H 1.301 (3H, s) representing CH$_3$-groups. The signals at δ_H 4.753 (1H, br s) and δ_H 4.741 (1H, br s) indicated an exocyclic double bond which was further confirmed by olefinic carbon signals at δ_C 104.2 (C-13) and δ_C 158.1 (C-7). HMBC correlations demonstrated, that both the methyl group at δ_H 1.301 (H$_3$-14) and the carboxylic moiety (C-15; δ_C 183.5) are connected to a quaternary carbon (C-2, δ_C 50.4) being neighbored by two methylene functionalities (C-1 and C-3, Table 7.2). The HMBC correlations of H$_A$-3 (δ_H 2.321) with C-5 and C-9 on the one hand and of H$_B$-3 (δ_H 1.798) with C-8 on the other hand demonstrated the quaternary carbon C-4 to be center of three five-membered rings. Further analyses of 2D NMR experiments (HMBC and COSY) of compound **7.1** revealed the presence of a tricyclic ventricosane skeleton with a carboxylic group at C-15 (Lu et al., 2005). Key HMBC and COSY correlations of **7.1** are shown in Fig. 7.2.

The NOE spectrum of **7.1** indicated spatial proximity between H-5 (δ_H 2.257) and the methyl group H$_3$-14 (δ_H 1.301) as well as among H-8 (δ_H 2.852) and H$_3$-10 (δ_H 0.921). These observations were in accordance with a computer generated energy minimized 3D model of **7.1** (Fig. 7.2) using MM2 force field (CS Chem 3D). Thus, the relative stereochemistry of **7.1** was demonstrated to be equal to that of the known ventricos-7(13)-ene (**7**) (Lu et al., 2005). Therefore, the structure of compound **7.1** was established as ventricos-7(13)-ene-15-oic acid and named penarine A (Fig. 7.1).
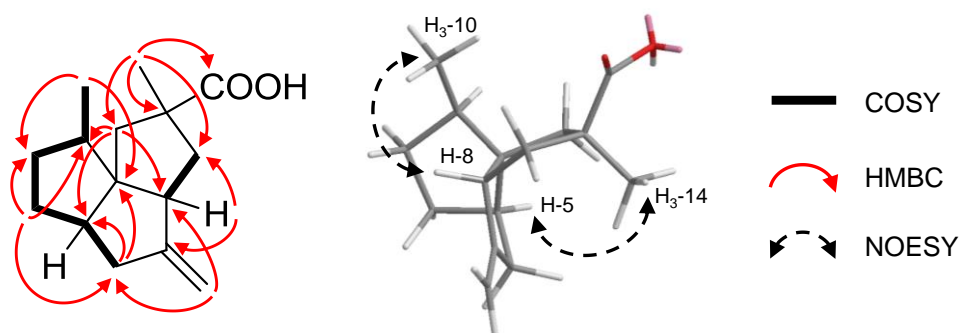
Fig. 7.2. Key HMBC, COSY and NOE correlations of penarine A (**7.1**).

Compound **7.2** was isolated as a colorless oil. HR-MS measurements revealed the elemental composition of C$_{15}$H$_{22}$O$_3$ revealing the presence of an additional oxygen function in comparison to **7.1**. Instead of proton signals of the exo methylene group in **7.1**, an ^{1}H signal at δ_H 5.375 (1H, br s) was found to be apparent indicating an endocyclic double bond. An ^{1}H,^{1}H COSY cross peak of the olefinic signal to H-5 and its HMBC correlation to C-4 and C-13 proofed the location of the double bond between C-6 and C-7. Additionally, an AB system with signals at δ_H 4.215 (1H, d, J = 14.1 Hz) and δ_H 4.160 (1H, d, J = 14.1 Hz) suggested the presence of a hydroxymethylene substituent. HMBC correlations of these methylene protons to C-6 and C-7 indicated the connectivity of this group to C-7. Detailed NOE studies of compound **7.2** demonstrated the

relative stereochemistry to be equal to penarine A (**7.1**). Based on these observations, the structure of **7.2** was determined as ventricos-6(7)-ene-13-ol-15-oic acid and named penarine B (Fig. 7.1).

Table 7.1. ^{1}H NMR data of compounds **7.1–7.6** in CDCl$_3$ (600 MHz, δ$_H$ in ppm, mult, *J* in Hz).

Pos.	7.1	7.2	7.3	7.4	7.5	7.6
1	2.408 dd (13.2/8.6);	2.087 dd (13.4/9.9);	2.263 dd (13.6/10.2);	2.266 dd (13.7/10.0);	2.478 dd (14.3/8.4);	2.814 ddd (17.6/9.1/2.4);
	1.611 dd (13.2/6.2)	1.710 br d (13.4)	1.875 br d (13.6)	1.915 br d (13.7)	1.721 dd (14.3/2.6)	2.643 br d (17.6)
3	2.321 d (13.9);	2.257 d (13.6);	2.320 d (13.6);	2.318 d (13.7);	2.366 d (14.2);	6.604 br s
	1.798 d (13.9)	1.808 dd (13.6/1.4)	1.817 dd (13.6/1.4)	1.814 d (13.7)	1.838 d (14.2)	
5	2.257 m	2.933 br d (9.5)	3.184 br d (10.3)	3.105 br d (10.0)	2.341 m	3.149 br d (10.9)
6	2.789 br dd (16.2/9.0);	5.375 br s	6.608 br s	6.665 br s	2.226 ddd (13.0/7.6/6.8);	6.727 br s
	2.017 br dd (16.2/4.8)				1.570 ddd (13.0/11.4/10.0)	
7	---	---	---	---	2.703 ddd (11.4/9.6/6.8)	---
8	2.852 br dd (8.6/6.2)	3.020 br d (9.9)	3.293 br d (10.2)	3.290 br d (10.0)	2.645 ddd (9.6/8.4/2.6)	3.472 br d (9.1)
9	1.78[a]	1.72[a]	1.77[a]	1.77[a]	1.68[a]	2.023 m
10	0.921 d (6.8)	0.963 d (6.8)	0.987 d (6.8)	0.994 d (6.6)	0.936 d (6.6)	0.933 d (6.7)
11	1.60[a];	1.565 br ddd (12.0/5.5/5.5);	1.64[a];	1.625 m;	1.64[a];	1.752 m;
	1.172 m	1.020 m	0.95[a]	1.00[a]	1.39[a]	1.219 m
12	1.725 dddd (12.6/11.2/8.4/6.7);	1.69[a];	1.86[a];	1.79[a];	1.66[a];	1.838 m;
	1.333 br dd (12.6/6.9)	1.466 br dd (12.4/6.3)	1.60[a]	1.576 m	1.31[a]	1.570 ddd (13.2/7.2/1.5)
13	4.753 br s;	4.215 br d (14.1);	9.730 s	---	---	---
	4.741 br s	4.160 br d (14.1)				
14	1.301 s	1.295 s	1.227 s	1.280 s	1.437 s	---

[a] Overlapping signals; chemical shifts were determined from ^{1}H,^{13}C HSQC correlation peaks.

The ^{1}H NMR spectrum of compound **7.3** (= penarine C) differed from **7.2** by replacement of the hydroxymethylene proton signals with a lowfield singlet at δ$_H$ 9.730. Additionally, a signal of a tertiary carbon atom at δ$_C$ 189.6 indicated an aldehyde function at C-7. This was supported by HR-ESI-MS data and HMBC correlations of H-13 to C-7 and C-8, respectively. According to NOE correlations, the relative configuration was found to be equal to compound **7.1**. Hence, the structure of penarine C (**7.3**) was established as ventricos-6(7)-ene-13-al-15-oic acid (Fig. 7.1).

HR-ESI-MS measurements of compound **7.4** revealed the elemental composition C$_{15}$H$_{20}$O$_4$. The ^{1}H and ^{13}C NMR spectra of **7.4** were almost similar to those of **7.3**, except for the absence of the aldehyde resonance peak which was found to be replaced by a carboxylate signal (C-13, δ$_C$ 168.3). The connectivity of this second acidic group to C-7 was confirmed by HMBC correlation of the endocyclic double bond signal H-6 (δ$_H$ 6.665, br s) to C-13. Deduced from NOE

investigations, the relative stereochemistry of **7.4** was identified to be similar to **7.1**. In conclusion, the structure of **7.4** was assigned as ventricos-6(7)-ene-13,15-dioic acid and named penarine D (Fig. 7.1).

In comparison to penarine D (**7.4**), the ^{13}C NMR spectrum of compound **7.5** (molecular formula $C_{15}H_{22}O_4$) lacked signals of an endocyclic double bond, but showed an additional methylene signal at δ_C 38.3 (C-6) as well as a methine signal at δ_C 51.9 (C-7) (Table 7.2). NOE studies of compound **7.5** demonstrated the relative configuration at C-2, C-4, C-5, C-8 and C-9 to be equal to compound **7.1**. In contrast to **7.1–7.4**, compound **7.5** possesses an additional stereocenter at C-7. The relative configuration at C-7 was established by NOE cross peaks between H-7 and H$_3$-14. Thus, the structure of **7.5** was confirmed as ventricos-13,15-dioic acid and named penarine E (Fig. 7.1).

Table 7.2. ^{13}C NMR data of compounds **7.1–7.6** in CDCl$_3$ (150 MHz, δ_C in ppm).

Pos.	**7.1**	**7.2**[a]	**7.3**	**7.4**	**7.5**	**7.6**
1	44.8	39.4	40.5	41.0	42.3	35.8
2	50.4	49.9	49.6	49.7	50.7	133.4
3	52.2	49.5	49.3	49.7	53.1	150.4
4	64.7	63.2	63.5	63.1	65.4	72.4
5	51.5	58.9	60.0	59.8	53.8	55.5
6	40.5	128.9	155.6	149.2	38.3	148.2
7	158.1	147.5	150.8	139.1	51.9	137.4
8	49.8	49.8	46.8	48.9	50.1	46.2
9	45.2	44.8	44.8	44.9	45.6	43.3
10	14.5	13.4	13.3	13.4	14.8	13.9
11	33.7	32.6	32.7	32.7	33.8	33.5
12	32.3	31.0	30.4	30.3	30.9	30.4
13	104.2	61.2	189.6	168.3	179.1	169.5
14	25.7	23.7	24.0	23.9	27.4	---
15	183.5	182.4	179.8	182.5	182.3	169.7

[a] Measured at 100 MHz.

Compound **7.6** was isolated as a colorless oil. HR-MS measurements of **7.6** revealed the elemental composition $C_{14}H_{16}O_4$ indicating the presence of a nor-sesquiterpene with seven degrees of unsaturation. This was further confirmed by ^{1}H and ^{13}C NMR spectra, where the resonance signals of the CH$_3$ substituent (C-14 in **7.1–7.5**) were identified to be absent. Nonetheless, the ^{1}H NMR spectrum of **7.6** resembled that of compound **7.4** except for the presence of an additional endocyclic double bond signal at δ_H 6.604 (1H, br s) exhibiting HMBC correlations to C-1, C-4, C-8 and C-15. Therefore, the position of the double bond was confirmed at C-2 and C-3. NOE correlations between H-3/H-5 as well as H-8/H$_3$-10 established the relative

stereochemistry and thus the structure of **7.6** as 14-nor-ventricos-2(3),6(7)-diene-13,15-dioic acid, named penarine F (Fig. 7.1).

Until now, only one ventricosane-type sesquiterpene (ventricos-7(13)-ene, **7.7**) has been described, which was solely isolated from the essential oil of the liverwort *Lophozia ventricosa* (Lu et al., 2005). Compound **7.7** could be identified in a fruiting body of *H. penarius via* headspace GC-EI-MS using key ions in the selected ion monitoring (SIM) mode (Fig. 7.3). Both, the EI mass spectrum and the retention index of **7.7** were found to be in perfect accordance with published data (Lu et al., 2005).
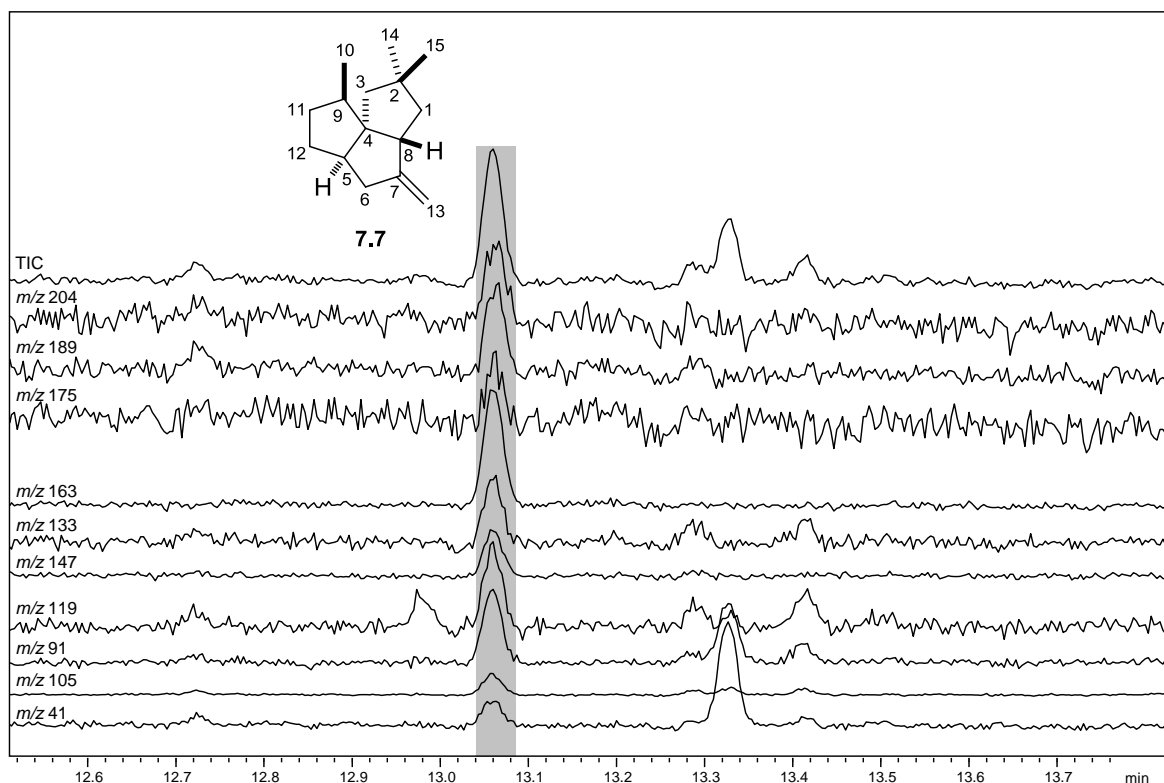
Fig. 7.3. Detection of ventricos-7(13)-ene (**7.7**) *in H. penarius via* headspace GC-SIM-MS.

7.3 Conclusions

Five novel ventricosane-type sesquiterpene carboxylic acids (**7.1–7.5**) and one new nor-sesquiterpene carboxylic acid (**7.6**) were isolated from fruiting bodies of *H. penarius*. Their structures were unambiguously established on the basis of extensive 1D and 2D NMR spectroscopic analyses as well as HR-MS experiments. The isolated compounds **7.1–7.6** were inactive against the phytopathogenic fungus *C. cucumerinum*. Moreover, the tested compounds **7.1** and **7.2** exhibited no cytotoxic activity against the human prostate cancer cell line PC-3 and the colon cancer cell line HT-29.

In general, sesquiterpenoids are common metabolites in fungal fruiting bodies like the families Russulaceae (e.g. *Russula*, *Lactarius*) and Tricholomataceae (e.g. *Lepista*) (Fraga, 2007). However, the present study is, to the best of our knowledge, the first report on the occurrence of

sesquiterpenes within the family Hygrophoraceae. Until now, only one ventricosane-type sesquiterpene (ventricos-7(13)-ene, **7.7**) has been described, which was solely isolated from the essential oil of the liverwort *Lophozia ventricosa* (Lu et al., 2005). Recently, ventricos-7(13)-ene (**7.7**) was synthesized by using Au(I)-catalyzed ring expanding cycloisomerization reactions (Sethofer et al., 2008). Hence the present paper describes a novel natural source of several new members of the very rare ventricosane-type (nor)-sesquiterpenes.

7.4   Experimental Section

General Experimental Procedures. Column chromatography was performed on silica gel (Merck, 40–63 µm) and Sephadex LH 20 (Fluka), while thin layer chromatography (TLC) was performed on precoated silica gel F_{254} plates (Merck). IR spectra were measured on a Thermo Nicolet 5700 FT-IR spectrometer. The specific rotation was measured with a JASCO DIP-2000 polarimeter. 1D (^{1}H, ^{13}C) and 2D (HSQC, HMBC, COSY, ROESY) NMR spectra were obtained from an Agilent VNMRS 600 system. The spectra were recorded at 600 MHz (^{1}H) and 150 MHz (^{13}C), respectively. Chemical shifts were referenced to internal TMS (δ_H 0 ppm, ^{1}H) and CDCl$_3$ (δ_C 77.0 ppm, ^{13}C). The high resolution negative ion ESI mass spectra were obtained from a Bruker Apex III Fourier transform ion cyclotron resonance (FT-ICR) mass spectrometer (Bruker Daltonics, Billerica, USA) equipped with an Infinity™ cell, a 7.0 Tesla superconducting magnet (Bruker, Karlsruhe, Germany), an RF-only hexapole ion guide and an external electrospray ion source (Agilent, off axis spray). The sample solutions were introduced continuously *via* a syringe pump with a flow rate of 120 µl h^{-1}. Preparative HPLC was performed on a Knauer system equipped with a WellChrom K-1001 pump and a WellChrom K-2501 UV detector using an ODS-A column (5 µm, 120 Å, 150 × 10 mm ID, YMC, USA) at a flow rate of 3.5 ml/min.

Fungal Material. *Hygrophorus penarius* Fr. was collected under *Fagus sylvatica* L. near Freyburg/Unstrut, Saxony Anhalt, Germany in September 2006 (leg./det. N. Arnold). A voucher specimen (coll. 120/13) is deposited at the Leibniz Institute of Plant Biochemistry, Halle, Germany.

Headspace GC-MS investigation. One frozen fruiting body of *H. penarius* was grinded and applied to a headspace vial. After incubation for 30 min at 40 °C the measurement started. The static headspace GC-EI-MS measurements were performed on a QP-2010 Ultra (Shimadzu Corporation, Kyoto, Japan) by using the following conditions: electron energy 70 eV, detection mode: selected ion monitoring (SIM) by using the following *m/z* values: 204, 189, 175, 163, 147, 133, 119, 105, 91, 41; source temperature 200 °C; column: ZB-5MS (Phenomenex, 30 m × 0.25 mm, 0.25 µm film thickness), injector temperature 220 °C, interface temperature 300 °C, carrier gas Helium, column flow 1.02 ml/min, constant flow mode, column temperature program: 40 °C for 1 min, then raised to 300 °C at a rate of 10 °C min^{-1} and then held on 300 °C for 5 min. Static

headspace conditions: split injection (split ratio 1:5), incubation temperature 40 °C; incubation time 30 min; syringe temperature 45 °C; injection volume 500 μl.

Extraction and isolation. Frozen fruiting bodies of *Hygrophorus penarius* Fr. (3.4 kg) were crushed in a blender and exhaustively extracted with MeOH (3 × 2.5 l) at room temperature. The light yellow solution was concentrated *in vacuo* to dryness and the extract (110.3 g) was redissolved in H_2O and partitioned with EtOAc (3 × 1 l). The slight yellow organic layers were combined, dried over anhydrous Na_2SO_4 and evaporated to dryness in *vacuo*. The resulting crude extract (29.7 g) was subjected to column chromatography (CC) on silica gel (420 × 55 mm) eluting with $CHCl_3$-MeOH (100:0→0:100) to afford 8 fractions (A1–8).

Fraction A3 (6.4 g) was applied to silica gel CC (410 × 55 mm) with $CHCl_3$-MeOH (93:7→0:100) to give 4 fractions (B1–4). Fraction B2 (1.65 g) was further separated by Sephadex LH 20 CC (400 × 40 mm, CH_2Cl_2-MeOH 1:1) yielding 6 fractions (B2.1–6). Fraction B2.5 (16.1 mg) was finally purified by preparative HPLC with H_2O (A) and CH_3CN (B) as solvents (0–14 min, 50–80% B) to afford **7.1** (t_R 12.9 min, 6.0 mg).

Fraction B3 (4.0 g) was further purified with Sephadex LH 20 CC (400 × 40 mm, CH_2Cl_2-MeOH 1:1) to give 9 fractions (C1–9). Fraction C8 (159.1 mg) was further purified with silica gel CC (420 × 55 mm) eluted with $CHCl_3$-MeOH to obtain 7 fractions (C8.1–7). Fraction C8.5 (10.9 mg) was finally purified by preparative HPLC with H_2O + 0.1% TFA (A) and CH_3CN + 0.1% TFA (B) as solvents (0–25 min, 5–100% B) to afford **7.3** 14.7 min, 5.1 mg) and **7.3** (t_R 16.3°min, 1.0 mg). Fraction C8.7 (5.5 mg) was finally purified by preparative HPLC with H_2O + 0.1% TFA (A) and CH_3CN + 0.1% TFA (B) as solvents (0–10 min, 20–50% B, 10–20 min, 50–100% B) to afford **7.5** (t_R 18.2 min, 1.3 mg).

Fraction A4 (7.6 g) was applied to Sephadex LH 20 CC (400 × 40 mm, CH_2Cl_2-MeOH 1:1) to obtain 7 fractions (A4.1–7). Fraction A4.6 (15.8 mg) was finally purified by preparative HPLC with H_2O + 0.1% TFA (A) and CH_3CN + 0.1% TFA (B) as solvents (0–25 min, 15–55% B) to yield **7.4** (t_R 20.8 min, 3.3 mg) and **7.6** (t_R 19.1 min, 4.9 mg).

Penarine A (7.1): colorless oil; $[\alpha]^{24}_D$ –8.4 (*c* 0.420, $CHCl_3$); IR (ATR) υ_{max} 2934 (br, m), 2866 (br, w), 1693 (s), 1463 (w), 1407 (w), 1234 (m), 1171 (m), 1132 (w), 1009 (m), 949 (w), 901 (w), 755 (w), 702 (w) cm^{-1}; ^{1}H NMR see Table 7.1; ^{13}C NMR see Table 7.2; ESI-FT-ICR-MS *m/z* 233.1548 ([M–H]$^-$, calculated for $C_{15}H_{21}O_2^-$ 233.1547).

Penarine B (7.2): colorless oil; $[\alpha]^{26}_D$ –34.3 (*c* 0.420, $CHCl_3$); IR (ATR) υ_{max} 2934 (br, m), 2867 (br, w), 1694 (s), 1463 (w), 1405 (w), 1208 (m), 1124 (w), 1009 (m), 949 (m), 903 (w), 751 (s), 701 (w) cm^{-1}; ^{1}H NMR see Table 7.1; ^{13}C NMR see Table 7.2; ESI-FT-ICR-MS *m/z* 249.1491 ([M–H]$^-$, calculated for $C_{15}H_{21}O_3^-$ 249.1496).

Penarine C (7.3): colorless oil; $[\alpha]^{23}_D$ –21.1 (*c* 0.030, $CHCl_3$); IR (ATR) υ_{max} 2924 (br m), 2853 (w), 2359 (w), 2159 (w), 1700 (s), 1462 (w), 1411 (w), 1379 (w), 1232 (w), 1174 (w), 1021 (w),

936 (w), 802 (w), 721 (w) cm^{-1}; ^{1}H NMR see Table 7.1; ^{13}C NMR see Table 7.2; ESI-FT-ICR-MS: *m/z* 247.1336 ([M–H]$^{-}$, calculated for $C_{15}H_{19}O_3^-$ 247.1340).

Penarine D (7.4): colorless oil; $[\alpha]^{26}_D$ –33.1 (*c* 0.250; CHCl$_3$); IR (ATR) υ_{max} 2930 (br, m), 2859 (br, w), 1692 (s), 1441 (w), 1410 (w), 1379 (w), 1224 (br, m), 1134 (w), 1078 (w), 1008 (m), 949 (m), 921 (w), 754 (m), 699 (w) cm^{-1}; ^{1}H NMR see Table 7.1; ^{13}C NMR see Table 7.2; ESI-FT-ICR-MS: *m/z* 263.1288 ([M–H]$^{-}$, calculated for $C_{15}H_{19}O_4^-$ 263.1289).

Penarine E (7.5): colorless oil; $[\alpha]^{24}_D$ +16.2 (*c* 0.050, CHCl$_3$); IR (ATR) υ_{max} 2925 (br, w), 1857 (w), 1695 (s), 1464 (w), 1412 (w), 1378 (w), 1258 (w), 1090 (w), 1011 (w), 938 (w), 795 (w), 756 (m) cm^{-1}; ^{1}H NMR see Table 7.1; ^{13}C NMR see Table 7.2; ESI-FT-ICR-MS: *m/z* 265.1440 ([M–H]$^{-}$, calculated for $C_{15}H_{21}O_4^-$ 265.1445).

Penarine F (7.6): colorless oil; $[\alpha]^{26}_D$ –66.8 (*c* 0.400, CHCl$_3$); IR (ATR) υ_{max} 2929 (br, m), 2866 (br, w), 1683 (s), 1628 (m), 1415 (w), 1378 (w), 1206 (br, m), 1141 (w), 1091 (w), 1006 (s), 948 (m), 921 (w), 751 (m), 687 (w) cm^{-1}; ^{1}H NMR see Table 7.1; ^{13}C NMR see Table 7.2; ESI-FT-ICR-MS: *m/z* 247.0973 ([M–H]$^{-}$, calculated for $C_{14}H_{15}O_4^-$ 247.0976).

Ventricos-7(13)-ene (7.7): RI (ZB-5MS) 1352; EI-MS (70 eV) *m/z* (rel. int.) 204 [M]$^{+}$ (20), 189 (27), 175 (18), 163 (85), 147 (63), 133 (51), 119 (43), 105 (62), 91 (100), 41 (50).

Antifungal bioassay. The antifungal bioassay against *Cladosporium cucumerinum* Ell. et Arth. was performed following the method described in literature (Gottstein et al., 1982).

Cytotoxicity assay. The human prostate cancer cell line PC-3 and the colon cancer cell line HT-29 were maintained in RPMI 1640 medium supplemented with 10% fetal bovine serum, 2 mM L-alanyl-L-glutamine and 16 mM HEPES buffer. 5×10^2 PC-3 cells per well and 1.5×10^3 HT-29 cells per well were seeded overnight into 96-well plates and exposed to different concentrations of each compound (10 µM down to 10 nM in 1:4 dilution steps) for three days. Cytotoxicity was determined by utilizing the modified XTT method (Scudiere et al., 1988). Digitonin was used as a positive control, while DMSO served as a negative control.

7.5 References

Fraga, B.M., 2007. Natural sesquiterpenoids. *Nat. Prod. Rep.* 24, 1350–1381.

Gilardoni, G., Clericuzio, M., Marchetti, A., Finzi, P.V., Zanoni, G., Vidari, G., 2006. New oxidized 4-oxo fatty acids from *Hygrophorus discoxanthus. Nat. Prod. Commun.* 12, 1079–1084.

Gilardoni, G., Clericuzio, M., Tosi, S., Zanoni G., Vidari, G., 2007. Antifungal acylcyclopentenediones from fruiting bodies of *Hygrophorus chrysodon.* J. Nat. Prod. 70, 137–139.

Gottstein, D., Gross, D., Lehmann, H., 1982. Mikrobiotest mit *Cladosporium cucumerinum* Ell. et Arth. zum Nachweis fungitoxischer Verbindungen auf Dünnschichtplatten. *Arch. Phytopathol. Pflanzenschutz* 20, 111–116.

Lodge, D.J., Padamsee, M., Matheny, P.B., Aime, M.C., Cantrell, S.A., Boertmann, D., Kovalenko, A., Vizzini, A., Dentinger, B.T.M., Kirk, P.M., Ainsworth, A.M., Moncalvo, J., Vilgalys, R., Larsson, E., Lucking, R., Griffith, G.W., Smith, M.E., Norvell, L.L., Desjardin, D.E., Redhead, S.A., Ovrebo, C.L., Lickey, E.B., Ercole, E., Hughes, K.W., Courtecuisse, R., Young, A., Binder, M., Minnis, A.M., Lindner, D.L., Ortiz-Santana, B., Haight, J., Laessoe, T., Baroni, T.J., Geml, J., Hattori, T., 2014. Molecular phylogeny, morphology, pigment chemistry and ecology in Hygrophoraceae (Agaricales). *Fungal Divers.* 64, 1–99.

Lu, R., Paul, C., Basarb, S., König, W.A., 2005. Sesquiterpene constituents of the liverwort *Lophozia ventricosa*. *Tetrahedron: Asymmetry* 16, 883–887.

Lübken, T., Schmidt, J., Porzel, A., Arnold, N., Wessjohann, L., 2004. Hygrophorones A–G: fungicidal cyclopentenones from *Hygrophorus* species (Basidiomycetes). *Phytochemistry* 65, 1061–1071.

Qu, Y., Zhang, H.-B., Liu, J.-K., 2004. Isolation and structure of a new ceramide from the basidiomycete *Hygrophorus eburnesus*. *Z. Naturforsch.* 59b, 241–244.

Scudiere, D.A., Schoemaker, R.H., Monks, A., Tierney, S., Nofziger, T.H., Currens, M.J., Seniff, D., Boyd, M.R., 1988. Evaluation of a soluble tetrazolium/formazan assay for cell growth and drug sensitivity in culture using human and other tumor cell lines. *Cancer Res.* 48, 4827–4833.

Sethofer, S.G., Staben, S.T., Hung, O.Y., Toste, F.D., 2008. Au(I)-Catalyzed ring expanding cycloisomerizations: total synthesis of ventricosene. *Org. Lett.* 10, 4315–4318.

Teichert, A., Lübken, T., Schmidt, J., Porzel, A., Arnold, N., Wessjohann, L., 2005b. Unusual bioactive 4-oxo-2-alkenoic fatty acids from *Hygrophorus eburneus*. *Z. Naturforsch.* 60b, 25–32.

7.6 Supporting Information

Supplementary data associated with this article can be found at http://dx.doi.org/10.1016/j.phytochem.2014.09.005.

8   Chilenopeptins A and B, peptaibols from the Chilean *Sepedonium* aff. *chalcipori* KSH 883
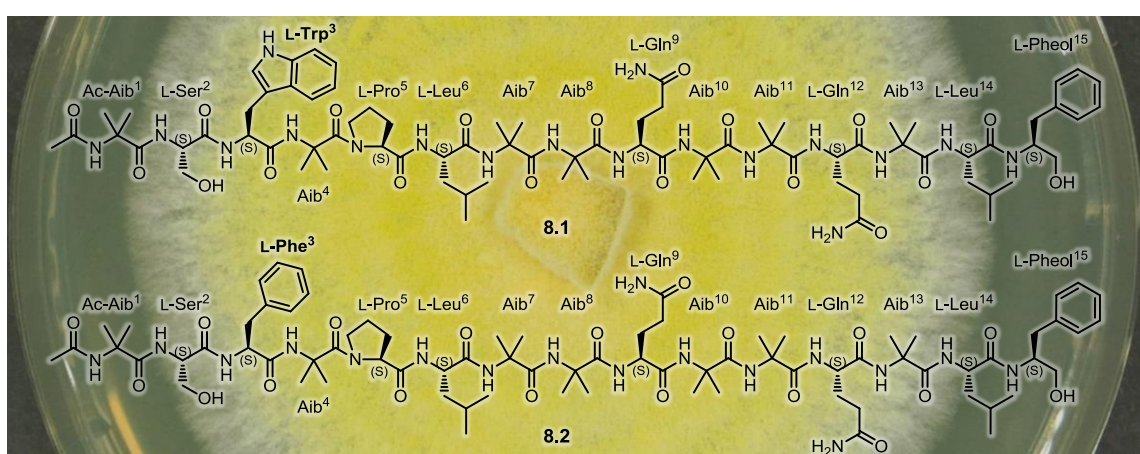
Abstract

The Chilean *Sepedonium* aff. *chalcipori* strain KSH 883, isolated from the endemic *Boletus loyo* Philippi, was studied in a polythetic approach based on chemical, molecular, and biological data. A taxonomic study of the strain using molecular data of the ITS, EF1-α, and RPB2 barcoding genes confirmed the position of the isolated strain within the *S. chalcipori* clade, but also suggested the separation of this clade into three different species. Two new linear 15-residue peptaibols, named chilenopeptins A (**8.1**) and B (**8.2**), together with the known peptaibols tylopeptins A (**8.3**) and B (**8.4**) were isolated from the semi-solid culture of strain KSH 883. The structures of **8.1** and **8.2** were elucidated on the basis of ESI-HRMS^n experiments in conjunction with comprehensive 1D and 2D NMR analyses. Thus, the sequence of chilenopeptin A (**8.1**) was identified as Ac-Aib^1-Ser^2-**Trp^3**-Aib^4-Pro^5-Leu^6-Aib^7-Aib^8-Gln^9-Aib^{10}-Aib^{11}-Gln^{12}-Aib^{13}-Leu^{14}-Pheol^{15}, while chilenopeptin B (**8.2**) differs from **8.1** by the replacement of Trp^3 by Phe^3. Additionally, the total synthesis of **8.1** and **8.2** was accomplished by a solid-phase approach confirming the absolute configuration of all chiral amino acids as ʟ. Both the chilenopeptins (**8.1** and **8.2**) and tylopeptins (**8.3** and **8.4**) were evaluated for their potential to inhibit the growth of phytopathogenic organisms.

8.1 Introduction

The genus *Sepedonium* (Hypocreaceae, Ascomycota) comprises asexual states of fungi that parasitize on basidiocarps of the order Boletales (Sahr et al., 1999). In natural habitats, we observed that Boletales fruiting bodies primarily infected by *Sepedonium* spp. are rarely colonized by secondary fungal parasites competing with *Sepedonium* for host nutrients. It is therefore supposed that *Sepedonium* species produce defense molecules to prevent further infections.

The most common secondary metabolites isolated from the genus *Sepedonium* include tropolones (Divekar and Vining, 1964; Divekar et al., 1965), mono- and bisanthraquinones (Shibata et al., 1957), an isoquinoline alkaloid (Quang et al., 2010), an azaphilone (Closse and Hauser, 1973), and peptaibols (Dornberger et al., 1995; Hülsmann et al., 1998; Kronen et al., 2001; Mitova et al., 2008; Neuhof et al., 2007; Ritzau et al., 1997; Stadler et al., 2001). The latter represent a class of linear 5 to 21-residue peptides, generally characterized by a high proportion of the non-proteinogenic, α,α-dialkylated amino acid α-aminoisobutyric acid (Aib). An additional structural feature is an acetylated *N*-terminus, while the *C*-terminal amino acid is reduced to an amino alcohol such as leucinol (Leuol) or phenylalaninol (Pheol) (Degenkolb et al., 2007). Their amphipathic nature and helical secondary structure allows these non-ribosomally biosynthesized peptides to form voltage-gated ion channels in lipid bilayer membranes, causing alterations in the osmotic balance of the cell (Chugh and Wallace, 2001; Rahaman and Lazaridis, 2014; Rodriguez et al., 2011). Consequently, peptaibols exhibit a broad spectrum of biological effects including antibiotic (Gräfe et al., 1995; Lee et al., 1999), antiviral (Stadler et al., 2001; Yun et al., 2000), neuroleptic (Kronen et al., 2001; Ritzau et al., 1997), cytotoxic (Ayers et al., 2012; Tavano et al., 2015), antiparasitic (Ayers et al., 2012; Schiell et al., 2001), and antifungal (Berg et al., 1996; Gräfe et al., 1995) activities.

During field research in Chile, the *Sepedonium* strain KSH 883 was isolated from the endemic host *Boletus loyo* Philippi. *B. loyo* is limited to the *Nothofagus* forests between the coastal zone and the Andean foothills of central Chile. Although an infection by *Sepedonium* spp. is a common sight on endemic Chilean boletes, no investigation on their identity and/or chemical properties had been performed previously. The European species *Sepedonium chalcipori* was separated from *S. chrysospermum* s.l. based on conidiophore morphology, ornamentation of aleurioconidia, and most importantly, the restriction to its host *Chalciporus piperatus* (Helfer, 1991). The separate position of the species was confirmed by molecular data using ITS sequencing (Sahr et al., 1999).

In the present paper, the phylogenetic position of the Chilean strain KSH 883 is evaluated in a polythetic approach based on chemical, molecular, and biological data. The isolation and structural elucidation of two new peptaibols (**8.1** and **8.2**) as well as tylopeptins A (**8.3**) and B (**8.4**) from the semi-solid culture of strain KSH 883 are also reported. The solid-phase total synthesis of **8.1** and **8.2** afforded the absolute configuration of all stereocenters. Moreover, the peptaibols **8.1**–**8.4** were evaluated towards their biological activity against the phytopathogenic organisms *Botrytis cinerea*, *Septoria tritici*, and *Phytophthora infestans*.

8.2 Results and discussion

8.2.1 Isolation and structural elucidation of chilenopeptins A and B

The chromatographic separation of the culture broth and mycelial crude extract using Diaion HP 20 and Sephadex LH 20 in combination with preparative HPLC yielded compounds **8.1**–**8.4** (Fig. 8.1). The presence of *N*-protected peptides such as peptaibols was suggested from TLC spots showing no reaction with neutral ninhydrin solution, but a positive color reaction when a modified acidic ninhydrin reagent was sprayed (see Chapter 8.4).
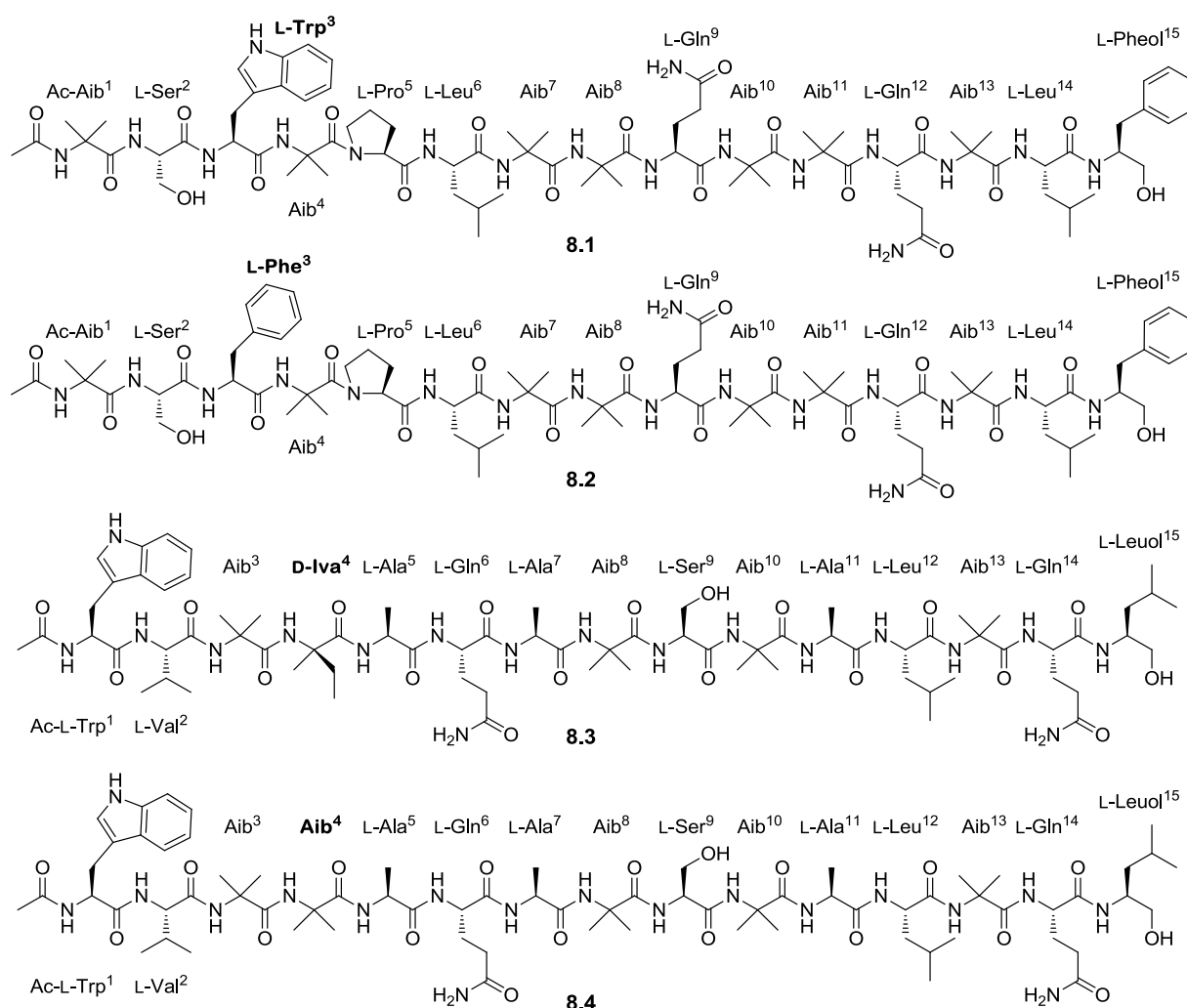
Fig. 8.1. Structures of chilenopeptins A and B (**8.1** and **8.2**) as well as tylopeptins A and B (**8.3** and **8.4**). Differences in amino acid sequences are highlighted in bold.

Compound **8.1** was isolated as a white, amorphous solid. The amino acid sequence of **8.1** was determined on the basis of ESI-HRMS^n investigations. Fragments in the positive mode were predominantly ions of the b-series, while under negative ion mode conditions y ions were mainly produced. The [M+2H]$^{2+}$ ion at *m/z* 821.4735 (calcd for $C_{80}H_{126}N_{18}O_{19}{}^{2+}$ 821.4718) was most abundant in the positive ion full scan spectrum of **8.1** (Fig. 8.2), accompanied by the protonated molecular ion at *m/z* 1641.9368 corresponding to the molecular formula $C_{80}H_{124}N_{18}O_{19}$. The MS^2 spectrum of the [M+2H]$^{2+}$ ion displayed two intense fragment ions at *m/z* 486.2355 (b$_4{}^+$,

N-terminal fragment) and *m/z* 1156.7105 (y_{11}^+, *C*-terminal ion) arising from cleavage of the labile Aib^4-Pro^5 bond (Przybylski et al., 1984).
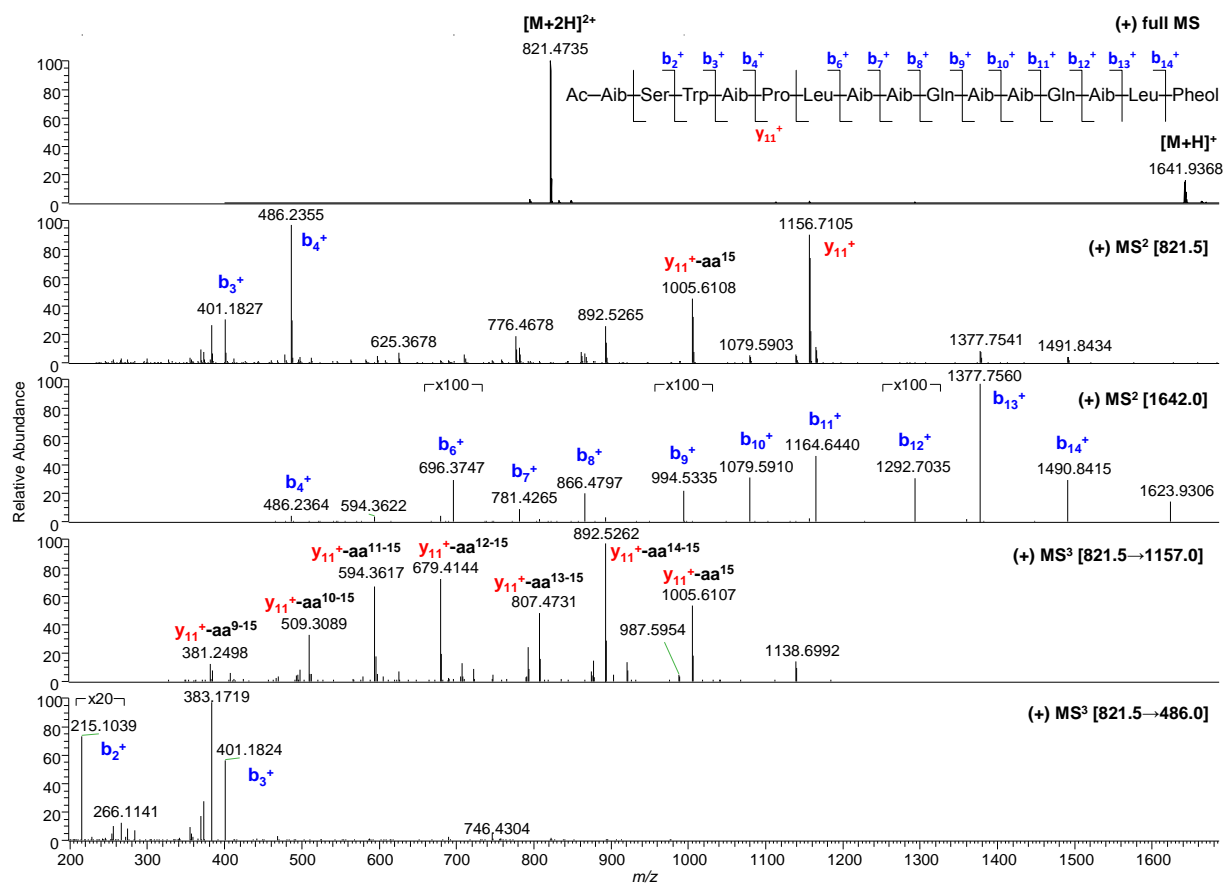
Fig. 8.2. Positive ion ESI-HRMS^n spectra of chilenopeptin A (**8.1**).

Fragmentation of the $[M+H]^+$ ion generated a series of product ions b_6^+ to b_{14}^+ providing successive losses of Aib^7, Aib^8, Gln^9, Aib^{10}, Aib^{11}, Gln^{12} (glutamine), Aib^{13}, and Lxx^{14} as well as phenylalaninol ($Pheol^{15}$) as *C*-terminal amino acid (Table 8.1). The negative ion MS^2 spectrum (Fig. 8.3) of the *C*-terminal moiety (y_{11}^-, *m/z* 1154.6945) yielded diagnostic fragment ions y_{10}^- and y_9^- corresponding to Pro^5 and Lxx^6, respectively. In addition, the observed ion series y_8^- to y_3^- fully supported the sequence deduced from the b ion series. Hence, the *C*-terminal peptide part was shown to be Pro^5-Lxx^6-Aib^7-Aib^8-Gln^9-Aib^{10}-Aib^{11}-Gln^{12}-Aib^{13}-Lxx^{14}-$Pheol^{15}$.

The positive ion MS^3 spectrum of the *N*-terminal fragment b_4^+ showed characteristic mass differences of 85 amu (b_3^+, *m/z* 401.1826) as well as 186 amu (b_2^+, *m/z* 215.1039) corresponding to Aib^4 and Trp^3 (tryptophan). The b_1^+ fragment ion representing the acetylated *N*-terminal amino acid was not detected under these conditions. Thus, the *N*-terminal dipeptide sequence of **8.1** was determined from the negative mode MS^2 spectrum (Fig. 8.3) of the $[M–H]^-$ ion, which yielded a predominant loss of 30 amu (v_{15}^-), corresponding to the side chain loss (CH_2O) of a serine (Ser) residue (Li et al., 2006). The mass differences of v_{15}^- and v_{14}^- (127 amu) as well as of v_{14}^- and y_{13}^- (57 amu) were assigned to the *N*-terminal dipeptide Ac-Aib^1-Ser^2. Based on the above mass spectrometric analyses (Table 8.1), the tentative sequence of **8.1** was proposed to be Ac-Aib^1-Ser^2-Trp^3-Aib^4-Pro^5-Lxx^6-Aib^7-Aib^8-Gln^9-Aib^{10}-Aib^{11}-Gln^{12}-Aib^{13}-Lxx^{14}-$Pheol^{15}$ (Fig. 8.1).

Table 8.1. Diagnostic fragment ions [*m/z*] of chilenopeptins A (**8.1**) and B (**8.2**) deduced from positive and negative ion ESI-HRMS^n experiments (for further details see Table S1, Supporting Information).

	8.1	8.2		8.1	8.2
t_R [min]^a	10.1	11.5	$y_{11}^+ - aa^{11-15}$	594.3617	594.3614
$[M+2H]^{2+}$	821.4735	801.9671	$y_{11}^+ - aa^{10-15}$	509.3089	509.3084
$[M+H]^+$	1641.9368	1602.9260	$y_{11}^+ - aa^{9-15}$	381.2498	381.2506
b_1^+	*n.d.*	*n.d.*	$y_{11}^+ - aa^{8-15}$	*n.d.*	*n.d.*
b_2^+	215.1039	215.1029	$y_{11}^+ - aa^{7-15}$	*n.d.*	*n.d.*
b_3^+	401.1824	362.1715	$y_{11}^+ - aa^{6-15}$	*n.d.*	*n.d.*
b_4^+	486.2355	447.2243	$[M-H]^-$	1639.9235	1600.9127
b_5^+	*n.d.*	*n.d.*	y_2^-	*n.d.*	*n.d.*
b_6^+	696.3747	657.3605	y_3^-	348.2279	348.2299
b_7^+	781.4265	742.4158	y_4^-	476.2884	476.2885
b_8^+	866.4797	827.4687	y_5^-	561.3411	561.3412
b_9^+	994.5335	955.5270	y_6^-	646.3943	646.3939
b_{10}^+	1079.5910	1040.5799	y_7^-	774.4520	774.4526
b_{11}^+	1164.6440	1125.6324	y_8^-	859.5060	859.5053
b_{12}^+	1292.7035	1253.6842	y_9^-	944.5600	944.5581
b_{13}^+	1377.7560	1338.7446	y_{10}^-	1057.6410	1057.6416
b_{14}^+	1490.8415	1451.8303	y_{11}^-	1154.6945	1154.6952
y_{11}^+	1156.7105	1156.7098	y_{12}^-	1239.7488	1239.7493
$y_{11}^+ - aa^{15}$	1005.6107	1005.6105	y_{13}^-	1425.8292	1386.8170
$y_{11}^+ - aa^{14-15}$	892.5262	892.5259	y_{14}^-	*n.d.*	*n.d.*
$y_{11}^+ - aa^{13-15}$	807.4731	807.4726	v_{14}^-	1482.8400	1443.8381
$y_{11}^+ - aa^{12-15}$	679.4144	679.4142	v_{15}^-	1609.9102	1570.9005

n.d. = not detected; b^+ = positively charged b ion; y^+ = positively charged y ion with amino acid (aa) abstraction. y^- = negatively charged y ion; v^- = negatively charged v ion without serine side chain (30 amu) ^{a} Hypersil GOLD RP18 column (particle size 1.9 μm, pore size 175 Å, 50 × 2.1 mm ID), flow rate 0.2 ml/min, gradient 0–5 min, 45–55% B; 5–13 min, 55–95% B (A=H$_2$O + 0.2% FA; B=CH$_3$CN + 0.2% FA).

The amino acid sequence of **8.1** obtained from MS^n studies comprises Lxx as either leucine (Leu) or isoleucine (Ile), since these constitutional isomers are difficult to distinguish based on tandem mass spectrometry sequencing. To clarify the proposed structure of **8.1**, detailed 1D and 2D NMR studies were carried out. The ^{1}H NMR spectrum of **8.1** (Table 8.2) in DMSO-d_6 displayed four characteristic high field doublets (δ_H 0.938, 0.880, 0.827, and 0.744; each J = 6.6 Hz), which were unambiguously assigned to CH$_3$ groups of Leu^6 and Leu^{14}.

Additionally, resonances of fourteen N-H groups, two N-H$_2$ (δ_N 113.7, Gln^9 and δ_N 113.5, Gln^{12}) as well as one tertiary nitrogen atom signal (δ_N 129.2, Pro^5) were detected and assigned on the basis of ^{1}H,^{15}N HSQC and ^{1}H,^{15}N HMBC experiments. The ^{13}C NMR spectrum showed seventeen carbonyl resonances at δ_C 170.2–176.0, belonging to amide carbonyl atoms. HMBC correlation peaks of the acetyl CH$_3$ resonance (δ_H 1.973) as well as the N-H signal of Aib^1

(δ_H 8.598) to the carbonyl carbon at δ_C 171.0 demonstrated the presence of an acetylated *N*-terminal Aib residue.
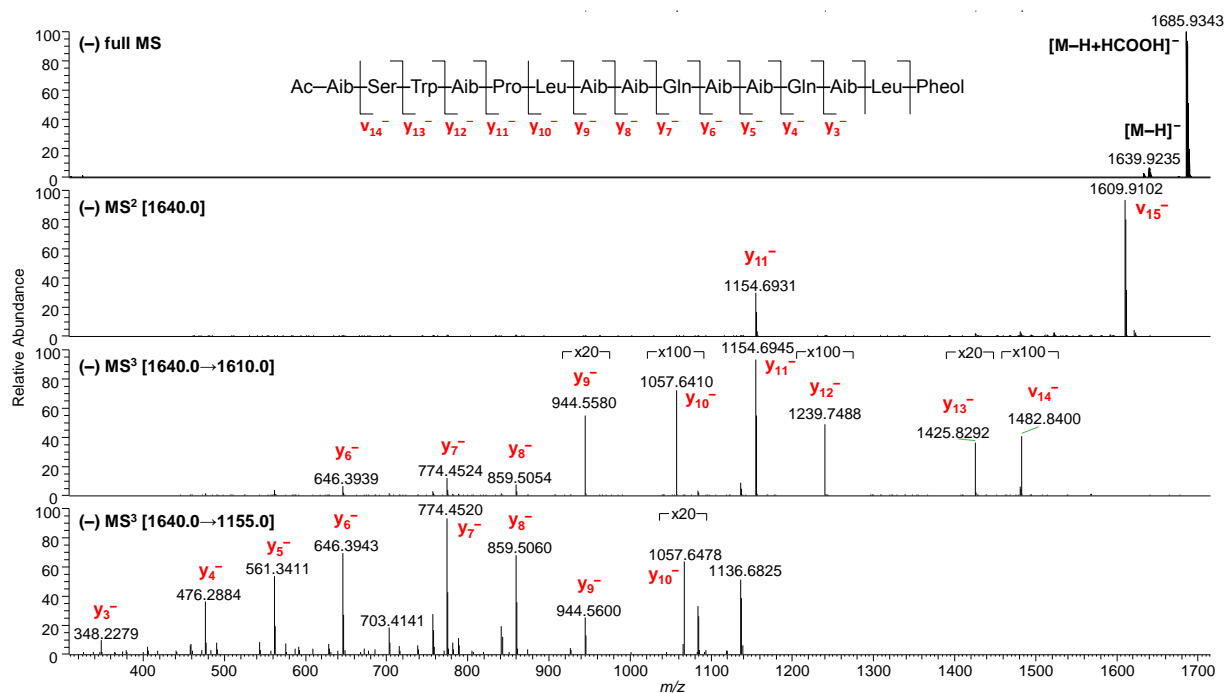
Fig. 8.3. Negative ion ESI-HRMS^n spectra of chilenopeptin A (**8.1**).

Seven N-H signals appeared as ^{1}H singlets (δ_H 8.598, 7.991, 7.848, 7.649, 7.587, 7.455, and 7.430) as a result of the linkage with quaternary C-α atoms resonating at δ_C 55.6–58.6. Multiple overlapping ^{1}H singlet methyl signals at δ_H 1.39–1.51 and their corresponding ^{13}C resonances (δ_C 22.7–26.7) confirmed the presence of seven Aib residues. A broad low field shifted singlet at δ_H 10.807 was assigned to the aromatic indole nitrogen proton of Trp^3.

Intraresidual HMBC, COSY, and TOCSY correlations allowed an unambiguous assignment of side chain signals with their respective peptide backbone resonances. The amino acid sequence of **8.1** was confirmed by analyses of NOE interactions between neighbored (*i*-1) and (*i*+1) nitrogen proton signals as well as HMBC correlations of N-H signals through $^3J_{CH}$ couplings to (*i*) carbonyl signals and $^2J_{CH}$ couplings to (*i*-1) carbonyl atoms and (*i*) C-α resonances (Fig. 8.4). For instance, the sequence position of tryptophan was deduced from HMBC correlation peaks between δ_C 172.8 (C=O, Trp^3) and N-H (δ_H 7.991, Aib^4) as well as N-H (δ_H 7.979, Trp^3) and δ_C 170.2 (C=O, Ser^2). In addition, NOE interaction between N-H resonances of Ser^2, Trp^3, and Aib^4 were observed (Fig. 8.4). As proline is characterized by a tertiary amide structure, the position was established on the basis of HMBC correlations between H-δ_A of the pyrrolidine ring (δ_H 3.663, Pro^5) and δ_C 172.6 (C=O, Aib^4) as well as C=O of Pro^5 (δ_C 173.3) and N-H of Leu^6 (δ_H 7.562). Based on comprehensive 2D NMR investigations exemplified above (Fig. 8.4), the primary structure of **8.1** was unambiguously confirmed as Ac-Aib^1-Ser^2-Trp^3-Aib^4-Pro^5-Leu^6-Aib^7-Aib^8-Gln^9-Aib^{10}-Aib^{11}-Gln^{12}-Aib^{13}-Leu^{14}-Pheol^{15} and given the trivial name chilenopeptin A (Fig. 8.1).
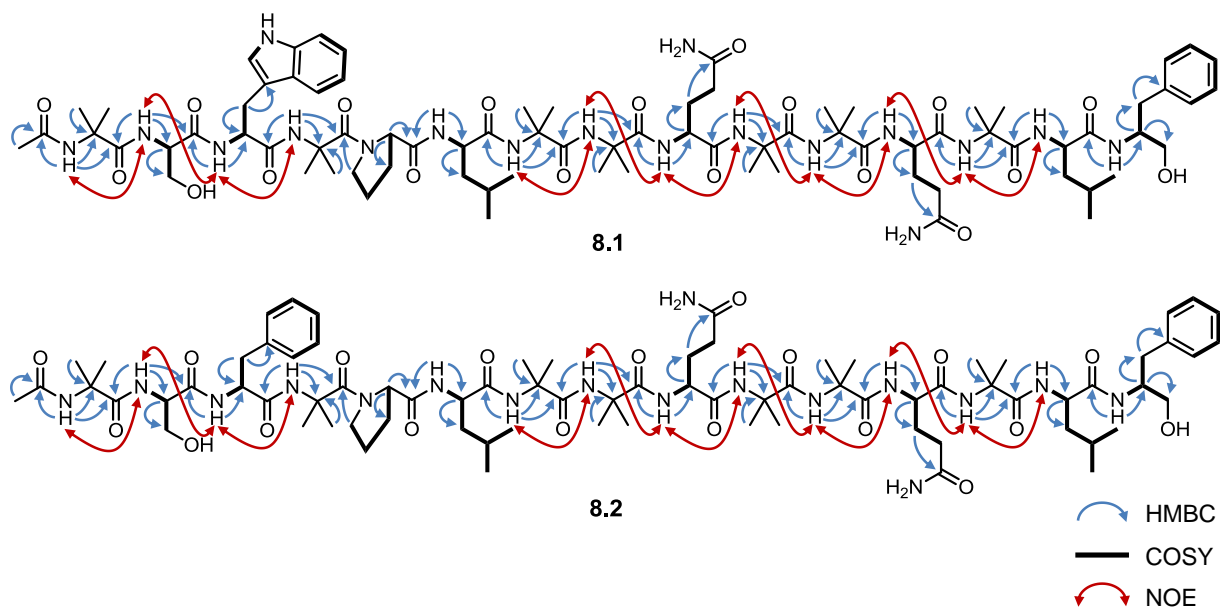
Fig. 8.4. Key HMBC (H to C), COSY, and NOE correlations of chilenopeptins A (**8.1**) and B (**8.2**).

Compound **8.2** was isolated as white, amorphous solid. The positive mode spectrum of **8.2** displayed an intense doubly charged ion at *m/z* 801.9671 (calcd for $C_{78}H_{125}N_{17}O_{19}{}^{2+}$ 801.9663). As with chilenopeptin A (**8.1**), the MS^2 spectrum of the $[M+2H]^{2+}$ ion showed two highly abundant fragment ions at *m/z* 447.2243 ($b_4{}^+$, *N*-terminal fragment) and *m/z* 1156.7098 ($y_{11}{}^+$, *C*-terminus). In comparison to **8.1**, the mass difference of 39 amu (corresponding to C_2HN) in the *N*-terminal fragment $b_4{}^+$ indicated an exchange of Trp^3 by Phe^3. This was supported by the missing characteristic UV absorption maxima of tryptophan and ESI-HRMS^n investigations (Table 8.1).

The ^1H NMR spectrum (Table 8.3) of **8.2** was almost identical to that of chilenopeptin A (**8.1**). Four doublets at δ_H 0.975, 0.886, 0.828, and 0.745 confirmed the presence of two Leu residues. In contrast to **8.1**, the low field ^1H singlet of the aromatic nitrogen proton as well as indole signals of Trp^3 were absent. Instead, additional aromatic proton resonances between δ_H 7.21–7.27 were observed and assigned to Phe^3. Based on extensive analyses of HMBC, COSY, and NOE correlations (Fig. 8.4), the structure of compound **8.2** was unambiguously confirmed as Ac-Aib^1-Ser^2-Phe^3-Aib^4-Pro^5-Leu^6-Aib^7-Aib^8-Gln^9-Aib^{10}-Aib^{11}-Gln^{12}-Aib^{13}-Leu^{14}-$Pheol^{15}$ and consequently named chilenopeptin B (Fig. 8.1).

Table 8.2. ^{1}H, ^{13}C, and ^{15}N NMR data of chilenopeptin A (**8.1**) (600/150 MHz, DMSO-d_6, 40 °C, δ in ppm).

Pos.	δ_H, mult. J (Hz)	δ_C/δ_N[d]	Pos.	δ_H, mult. J (Hz)	δ_C/δ_N[d]	Pos.	δ_H, mult. J (Hz)	δ_C/δ_N[d]
Ac			β	2.23[a]; 1.63[a]	28.3	C=O	---	176.2
CH$_3$	1.973 s	23.0	γ	1.82[a]	25.4	α	---	55.8
C=O	---	171.0	δ	3.663 dt-like 11.1/5.9;	48.2	β	1.484 s	26.7
Aib[1]				3.471 dt-like 11.1/7.0		γ	1.435 s	22.4
N-H	8.598 s	138.6	**L-Leu[6]**			**L-Gln[12]**		
C=O	---	176.0	N-H	7.562 d 7.2	114.3	N-H	7.772 d 5.1	113.5
α	---	55.7	C=O	---	173.9	C=O	---	173.2
β	1.42[a]	24.0	α	4.060 ddd 10.4/7.2/5.0	53.8	α	3.758 td-like 7.5/5.1	56.1
γ	1.40[a]	25.9	β	1.82[a]; 1.62[a]	38.5	β	2.02[a]	25.9[b]
L-Ser[2]			γ	1.713 m	24.8	γ	2.35[a]; 2.19[a]	31.4
N-H	8.089 d 5.4	108.1	δ	0.938 d 6.5	22.7	C=O	---	173.2
C=O	---	170.2	ε	0.880 d 6.5	21.4	N-H$_2$	7.12[a]; 6.691 s[c]	107.5
α	3.99[a]	58.0	**Aib[7]**			**Aib[13]**		
β	3.565 m	60.2	N-H	7.587 s	128.9	N-H	7.649 s	125.3
O-H	4.907 br t 6.3	---	C=O	---	174.8	C=O	---	173.9
L-Trp[3]			α	---	55.8	α	---	56.1
N-H	7.979 d 8.5	116.9	β	1.42[a]	25.9	β	1.430 s	23.2
C=O	---	172.8	γ	1.40[a]	22.7	γ	1.394 s	26.7
α	4.472 ddd 10.3/8.5/4.4	54.4	**Aib[8]**			**L-Leu[14]**		
β	3.293 dd 14.8/4.4;	26.5	N-H	7.430 s	123.9	N-H	7.10[a]	110.0
	3.136 dd 14.8/10.3		C=O	---	175.7	C=O	---	171.4
1-N-H	10.807 br s	131.2	α	---	55.6	α	3.98[a]	52.2
2	7.13[a]	123.4	β	1.446 s	26.5	β	1.53[a]; 1.37[a]	39.7
3	---	109.8	γ	1.41[a]	22.5	γ	1.60[a]	24.1
3a	---	126.9	**L-Gln[9]**			δ	0.827 d 6.5	22.8
4	7.505 br d 8.0	117.8	N-H	7.713 d 5.2	113.7	ε	0.744 d 6.5	20.5
5	6.956 ddd 8.0/7.1/0.9	118.1	C=O	---	173.7	**L-Pheol[15]**		
6	7.065 ddd 8.1/7.1/1.1	120.8	α	3.865 ddd 8.3/6.8/5.2	55.9	N-H	7.10[a]	116.7
7	7.333 dt-like 8.1/0.9	111.3	β	2.02[a]	26.0[b]	α	3.904 m	52.3
7a	---	136.0	γ	2.34[a]; 2.18[a]	31.4	β	2.903 dd 13.8/4.7;	36.6
Aib[4]			C=O	---	173.2		2.622 dd 13.8/9.2	
N-H	7.991 s	132.4	N-H$_2$	7.12[a]; 6.679 s[c]	107.5	1	---	139.1
C=O	---	172.6	**Aib[10]**			2 & 6	7.261 d-like 7.7	129.2
α	---	56.0	N-H	7.848 s	127.9	4	7.13[a]	125.5
β	1.513 s	23.1	C=O	---	175.1	3 & 5	7.194 t-like 7.7	127.7
γ	1.42[a]	25.9	α	---	55.8	β'	3.402 dt-like 11.0/5.6;	63.0
L-Pro[5]			β	1.454 s	26.1		3.349 dt-like 11.0/6.5	
N	---	129.2	γ	1.41[a]	22.7	O-H	4.575 t-like 6.1	---
C=O	---	173.3	**Aib[11]**					
α	4.268 dd 8.3/7.2	62.7	N-H	7.455 s	123.1			

[a] Overlapping signals; ^{1}H chemical shifts were determined from ^{1}H,^{13}C or ^{1}H,^{15}N HSQC correlation peaks. [b, c] Assignments may be interchanged. [d] ^{15}N chemical shifts were determined from ^{1}H,^{15}N HSQC or ^{1}H,^{15}N HMBC correlation peaks.

Table 8.3. ^{1}H, ^{13}C, and ^{15}N NMR data of chilenopeptin B (**8.2**) (600/150 MHz, DMSO-d_6, 40 °C, δ in ppm).

Pos.	δH, mult. *J* (Hz)	δC/δN[c]	Pos.	δH, mult. *J* (Hz)	δC/δN[c]	Pos.	δH, mult. *J* (Hz)	δC/δN[c]
Ac			δ	3.674 dt-like 11.0/5.8;	48.2	C=O	---	176.2
CH₃	1.994 s	23.0		3.480 dt-like 11.0/7.2		α	---	55.8
C=O	---	171.2	**L-Leu⁶**			β	1.484 s	26.7
Aib¹			N-H	7.542 d 7.2	114.0	γ	1.44[a]	22.4
N-H	8.643 s	139.0	C=O	---	173.9	**L-Gln¹²**		
C=O	---	176.1	α	4.030 ddd 10.9/7.2/5.2	53.8	N-H	7.776 d 5.1	113.5
α	---	55.7	β	1.802 ddd 13.5/10.9/5.2;	38.4	C=O	---	173.2
β	1.417 s	23.9		1.57[a]		α	3.758 td-like 7.4/5.1	56.1
γ	1.40[a]	25.9	γ	1.715 m	24.6	β	2.02[a]	26.0
L-Ser²			δ	0.975 d 6.5	22.8	γ	2.36[a]; 2.20[a]	31.4
N-H	8.137 d 5.1	108.3	ε	0.886 d 6.5	21.1	C=O	---	173.2
C=O	---	170.0	**Aib⁷**			N-H₂	7.11[a]; 6.692 s[b]	107.6
α	3.97[a]	58.1	N-H	7.535 s	128.7	**Aib¹³**		
β	3.55[a]; 3.52[a]	60.1	C=O	---	174.8	N-H	7.650 s	125.2
O-H	4.877 br s	---	α	---	55.8	C=O	---	173.9
L-Phe³			β	1.44[a]	25.9	α	---	56.1
N-H	8.016 d 8.4	115.2	γ	1.40[a]	22.8	β	1.429 s	23.2
C=O	---	172.2	**Aib⁸**			γ	1.40[a]	26.7
α	4.416 ddd 10.5/8.4/4.8	54.7	N-H	7.408 s	124.0	**L-Leu¹⁴**		
β	3.160 dd 13.9/4.8;	36.2	C=O	---	175.7	N-H	7.11[a]	110.0
	3.018 dd 13.9/10.5		α	---	55.6	C=O	---	171.4
1	---	137.5	β	1.447 s	26.5	α	3.98[a]	52.2
2 & 6	7.21[a]	128.7	γ	1.41[a]	22.5	β	1.53[a]; 1.37[a]	39.7
4	7.21[a]	126.3	**L-Gln⁹**			γ	1.60[a]	24.1
3 & 5	7.266 t-like 7.3	128.0	N-H	7.714 d 5.1	113.6	δ	0.828 d 6.5	22.8
Aib⁴			C=O	---	173.7	ε	0.745 d 6.5	20.5
N-H	7.947 s	132.6	α	3.863 m	55.9	**L-Pheol¹⁵**		
C=O	---	172.5	β	2.03[a]	26.0	N-H	7.11[a]	116.6
α	---	56.1	γ	2.31[a]; 2.16[a]	31.4	α	3.904 m	52.3
β	1.518 s	23.1	C=O	---	173.2	β	2.904 dd 13.8/4.7;	36.6
γ	1.43[a]	25.8	N-H₂	7.12[a]; 6.680 s[b]	107.5		2.622 dd 13.8/9.0	
L-Pro⁵			**Aib¹⁰**			1	---	139.1
N	---	129.2	N-H	7.832 s	127.9	2 & 6	7.260 d-like 7.6	129.2
C=O	---	173.3	C=O	---	175.1	4	7.13[a]	125.5
α	4.270 dd 8.2/7.2	62.7	α	---	55.8	3 & 5	7.194 t-like 7.6	127.7
β	2.24[a];	28.3	β	1.453 s	26.0	β'	3.403 dt-like 11.0/5.5;	63.0
	1.647 dq-like 12.9/7.2		γ	1.41[a]	22.8		3.348 dt-like 11.0/6.5	
γ	1.86[a]	25.4	**Aib¹¹**			O-H	4.570 t-like 6.1	---
			N-H	7.447 s	123.1			

[a] Overlapping signals; chemical shifts were determined from ^{1}H,^{13}C or ^{1}H,^{15}N HSQC correlation peaks. [b] Assignments may be interchanged. [c] [15]N shifts were determined from ^{1}H,^{15}N HSQC or ^{1}H,^{15}N HMBC correlation peaks.

8.2.2 Solid-phase synthesis and absolute configuration of chilenopeptins

The stereochemical assignment of compounds **8.1** and **8.2** was established on the basis of solid-phase peptide synthesis (SPPS) using Fmoc protected, L-configured amino acids (except the achiral Aib) and tetramethylfluoroformamidinium hexafluorophosphate (TFFH) as coupling reagent (Scheme 8.1).

Scheme 8.1. Solid-phase synthesis of chilenopeptins A (**8.1**) and B (**8.2**)[a].

a) activation and coupling with Fmoc-L-Leu^{14}

Fmoc-L-Leu^{14}-L-Pheol^{15}—

b) deprotection of Fmoc group
c) activation and coupling with aa$^{1-13}$

Fmoc-Aib^1-L-Ser^2(tBu)-X$_{aa}$^{3}-Aib^4-L-Pro^5-L-Leu^6-Aib^7-Aib^8-L-Gln^9(Trt)-Aib^{10}-Aib^{11}-L-Gln^{12}(Trt)-Aib^{13}-L-Leu^{14}-L-Pheol^{15}—

d) deprotection of Fmoc group
e) acetylation of N-terminus

Ac-Aib^1-L-Ser^2(tBu)-X$_{aa}$^{3}-Aib^4-L-Pro^5-L-Leu^6-Aib^7-Aib^8-L-Gln^9(Trt)-Aib^{10}-Aib^{11}-L-Gln^{12}(Trt)-Aib^{13}-L-Leu^{14}-L-Pheol^{15}—

f) final deprotection and cleavage from resin

Ac-Aib^1-L-Ser^2-X$_{aa}$^{3}-Aib^4-L-Pro^5-L-Leu^6-Aib^7-Aib^8-L-Gln^9-Aib^{10}-Aib^{11}-L-Gln^{12}-Aib^{13}-L-Leu^{14}-L-Pheol^{15}

	X$_{aa}$^{3}
8.1	L-Trp
8.2	L-Phe

[a] Reagents and conditions: (a) 5 eq. Fmoc-L-Leu^{14}, 10 eq. DIPEA, 5 eq. TFFH, 18/60 min; (b) 20% piperidine/DMF, 5 min; (c) 5 eq. Fmoc-aa$^{1-13}$, 10 eq. DIPEA, 5 eq. TFFH, 12/60 min; (d) 20% piperidine/DMF, 8 min; (e) Ac$_2$O/DIPEA/DMF (15/15/70, v/v/v), 4 ml, 30 min; (f) TFA/CH$_2$Cl$_2$/H$_2$O/TIPS (47/47/4/2, v/v/v/v), 5 ml, 60 min.

Our initial attempts using PyBOP-mediated Fmoc SPPS with either single or double coupling cycles failed. Significant improvement could be achieved while using TFFH, which is as an *in situ* reagent to obtain reactive amino acid fluorides (El-Faham and Khattab, 2009). Recently, TFFH was already successfully applied as a coupling reagent for the sterically hindered, weakly reactive α,α-dialkyl amino acids including Aib or isovaline (Iva) (Otto et al., 2015a). A commercially available L-phenylalaninol loaded 2-chlorotrityl polystyrene resin was used as solid support. After complete peptide assembly, the *N*-terminus was acetylated with Ac$_2$O and DIPEA, and subsequently detached from the resin by treatment with TFA. The synthesized polypeptides **8.1**

and **8.2** were purified by size exclusion column chromatography on Sephadex LH 20 followed by preparative HPLC. The ESI-HRMS^n, 1D NMR as well as CD spectra of the synthetic peptaibols **8.1** and **8.2** were consistent with those of the natural chilenopeptins A (**8.1**) and B (**8.2**) (see Supporting Information). Consequently, all chiral amino acids naturally present in **8.1** and **8.2** possess the L-configuration.

8.2.3 Tylopeptins A and B

Compound **8.3** was isolated as white, amorphous solid. ESI-HRMS studies of the [M+H]$^+$ ion at *m/z* 1553.9010 afforded the molecular formula $C_{73}H_{120}N_{18}O_{19}$ (calcd for $C_{73}H_{121}N_{18}O_{19}^+$ 1553.9050). Deduced from positive and negative ion high-resolution tandem MS studies as well as 1D NMR experiments (see Supporting Information), compound **8.3** (Fig. 8.1) was identified as the peptaibol tylopeptin A (Ac-Trp^1-Val^2-Aib^3-Iva^4-Ala^5-Gln^6-Ala^7-Aib^8-Ser^9-Aib^{10}-Ala^{11}-Leu^{12}-Aib^{13}-Gln^{14}-Leuol^{15}).

Compound **8.4,** isolated as white amorphous solid, exhibited the molecular formula $C_{72}H_{118}N_{18}O_{19}$ as deduced from HRMS measurements of the protonated molecular ion at *m/z* 1539.8864 (calcd for $C_{72}H_{119}N_{18}O_{19}^+$ 1539.8893). The diagnostic fragment ions deduced from the positive and negative ion mode as well as 1D NMR spectroscopic data (see Supporting Information) were in accordance with those of tylopeptin B (**8.4**) showing an exchange of Iva^4 in **8.3** by Aib^4 in **8.4** (Fig. 8.1). Both tylopeptins A (**8.3**) and B (**8.4**) were originally isolated from fruiting bodies of the basidiomycete *Tylopilus neofelleus* (Lee et al., 1999) and later synthesized (Gobbo et al., 2010; Hjørringgaard et al., 2009).

Interestingly, compounds **8.3** and **8.4** were additionally detected in a solid-state culture of *Sepedonium chalcipori* S33 using MALDI-TOF mass spectrometry (Neuhof et al., 2007). Our finding of tylopeptins A (**8.3**) and B (**8.4**) in the culture of *Sepedonium* aff. *chalcipori* KSH 883 strongly support the proposed hypothesis of Neuhof and co-workers that fruiting bodies of *Tylopilus neofelleus* were putatively infected by a tylopeptin-producing *Sepedonium* strain (Neuhof et al., 2007). Most notably, the production of **8.3** and **8.4** strongly indicates that the present Chilean *Sepedonium* strain KSH 883 is closely related to *S. chalcipori*.

8.2.4 Phylogenetic analyses

The taxonomic status of the herein studied Chilean *Sepedonium* strain KSH 883 was investigated by initial morphological studies (Fig. S1, Supporting Information) and molecular analysis using ITS, EF1-α, and RPB2 sequences of 29 strains (Table 8.4), including two *Sepedonium* strains (S44 and S46) from New Zealand that were determined earlier as *S. chalcipori* (Sahr et al., 1999). *Trichoderma aerugineum*, a representative of a closely related genus, was used as outgroup to root the phylogenetic trees. The phylogeny derived from the ITS data (Fig. 8.5A) is largely in agreement with the data published previously by Sahr and co-workers (Sahr et al., 1999).

Table 8.4. List of specimens and reference sequences used for molecular phylogeny. Type strains are indicated by (**T**).

Species	Strain no.	Origin	GenBank accession			References
			ITS	**EF1-α**	**RPB2**	
Hypomyces lactifluorum	TAA 171006	N/A	---	---	EU710773	(Jaklitsch et al., 2008)
H. lactifluorum	TAAM 170476	USA	FN859432	FN868751	---	(Põldmaa, 2011)
H. rosellus	N/A	N/A	EU340833	---	---	Sharma and Singh (direct submission)
H. rosellus	TFC 95-105	N/A	---	HF911695	EU710774	(Jaklitsch et al., 2008); (Tamm and Põldmaa, 2013)
H. subiculosus	DAOM 226568	N/A	EU280093	---	---	(Hoyos-Carvajal et al., 2009)
H. subiculosus	TFC 97-166	Puerto Rico	---	FN868770	EU710776	(Jaklitsch et al., 2008); (Põldmaa, 2011)
Sepedonium ampullosporum	CBS 392.52	Netherlands (**T**)	AF054854	---	---	(Sahr et al., 1999)
S. ampullosporum	S15	Germany	AF054853	---	---	(Sahr et al., 1999)
S. brunneum	S171	USA	KT946841	KU041491	KU041503	This study*
S. brunneum	S172	USA	KT946842	KU041492	KU041504	This study*
S. chalcipori	S33	Germany	KT946845	KU041495	KU041507	This study*
S. chalcipori	S35	Germany	KT946840	KU041490	KU041502	This study*
S. chalcipori	S44	New Zealand	KT946846	KU041496	KU041508	This study*
S. chalcipori	S46	New Zealand	KT946847	KU041497	KU041509	This study*
S. aff. *chalcipori*	**KSH 883**	**Chile**	**KT946848**	**KU041498**	**KU041510**	**This study**
S. chlorinum	S247	USA	KT946843	KU041493	KU041505	This study
S. chlorinum	S248	USA	KT946844	KU041494	KU041506	This study
S. chlorinum	S38	Germany	AF054866	---	---	(Sahr et al., 1999)
S. chrysospermum	S160	Germany	AF054845	---	---	(Sahr et al., 1999)
S. chrysospermum	S47	Germany	AF054844	---	---	(Sahr et al., 1999)
S. laevigatum	CBS 101645	USA (**T**)	AF054858	---	---	(Sahr et al., 1999)
S. laevigatum	S88	Germany	AF054857	---	---	(Sahr et al., 1999)
S. microspermum	S177	USA	AF054852	---	---	(Sahr et al., 1999)
S. microspermum	S23	Germany	AF054851	---	---	(Sahr et al., 1999)
S. microspermum	S24	Germany	AF054847	---	---	(Sahr et al., 1999)
S. tulasneanum	S165	Germany	AF054860	---	---	(Sahr et al., 1999)
S. tulasneanum	S29	Germany	AF054859	---	---	(Sahr et al., 1999)
Trichoderma aerugineum	CBS 120541	Germany (**T**)	FJ860720	FJ860608	FJ860516	(Jaklitsch and Voglmayr, 2015)

N/A = no information available. * Strains were sequenced before by Sahr et al. (1999), but not considered in this study.

Here, the separation of the *S. chalcipori* clade to other *Sepedonium* species was confirmed with 97% bootstrap support. *Sepedonium* aff. *chalcipori* strain KSH 883 clustered as a sister taxon to isolates from Germany due, in part, to a deletion within the ITS1 region that was not present in specimens from New Zealand. The inclusion of the additional DNA loci EF1-α and RPB2 as molecular markers resulted in a multigene alignment with ~2–3% sequence differences. The corresponding phylogenetic tree confirmed the separation of the *S. chalcipori* taxon into three different clades that are in accordance with their origin (Fig. 8.5B). However, a comprehensive molecular analysis using multiple gene loci and a detailed morphological (re-)characterization of the specimens involved remains to be done in order to confirm the hypothesis whether these three clades represent different species.

(A) ITS-RAxML Tree
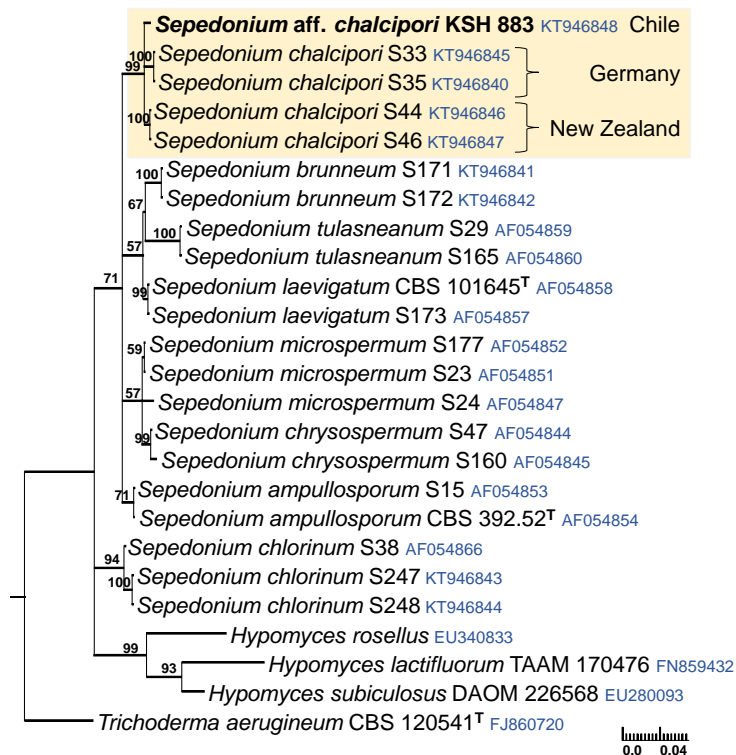
(B) MGA-RAxML Tree (ITS, EF1-α, RPB2)
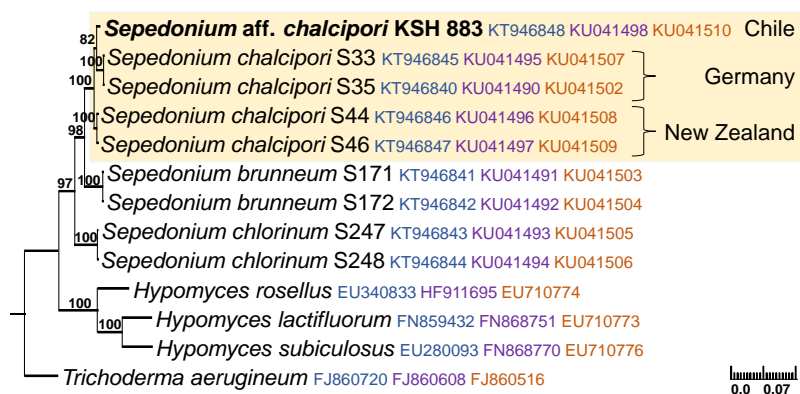
Fig. 8.5. Phylogenetic relationships of selected *Sepedonium* and *Hypomyces* spp. (with *Trichoderma aerugineum* as outgroup) inferred from (A) the nuclear ITS region and (B) a multigene alignment (MGA) of ITS, EF1-α, and RPB2 sequences by using MAFFT, RAxML, GTR+G, and 1000 bootstraps (Likelihood: ITS ln(L)= –2219.1484 & MGA ln(L)= –8709.4025). The calculated ITS tree is depicted as 50% majority-rule consensus tree. Calculated bootstrap support values of ≥50% are indicated above branches of the respective nodes.

8.2.5 Evaluation of antiphytopathogenic activity

The biological activity of peptaibols **8.1–8.4** was examined against the phytopathogenic ascomycetous fungi *Botrytis cinerea* (grey mold pathogen found on many crops including strawberries and wine grapes) and *Septoria tritici* (responsible for septoria leaf blotch of wheat) as well as the hemibiotrophic oomycete *Phytophthora infestans* (causal agent of the late blight disease on potato and tomato) using a 96 well microtiter plate assay (Table 8.5). The commercial

fungicides dodine and pyraclostrobin were used as reference compounds for a membrane-active fungicide and a respiration inhibitor fungicide, respectively.

Chilenopeptins A (**8.1**) and B (**8.2**) exhibited strong growth inhibitory activity against *B. cinerea*, modest activity towards *P. infestans*, and only slight effects against *S. tritici*. Tylopeptins A (**8.3**) and B (**8.4**) were reported to be inactive against several phytopathogens including *Magnaporthe grisea* IFO 5994, *Colletotrichum lagenarium* IFO 7513, and *Alternaria mali* IFO 8594 (Lee et al., 1999). In our biological assay, however, potent antagonistic effects were observed against *B. cinerea* as well as moderate activity towards *P. infestans*. In contrast to **8.1** and **8.2**, compounds **8.3** and **8.4** were devoid of any substantial activity towards *S. tritici*.

Table 8.5. Antiphytopathogenic activity of compounds **8.1–8.4** against *B. cinerea*, *S. tritici*, and *P. infestans* (IC_{50}, µM).

compound	*B. cinerea*	*S. tritici*	*P. infestans*
8.1	5.3 ± 0.2	53.0 ± 4.1	10.1 ± 0.3
8.2	7.0 ± 0.2	55.7 ± 6.2	17.8 ± 1.0
8.3	5.3 ± 0.2	> 80	13.3 ± 2.2
8.4	11.0 ± 0.7	> 80	17.5 ± 1.5
dodine[a]	9.4 ± 0.6	2.8 ± 0.2	43.8 ± 5.6
pyraclostrobin[a]	< 0.0052	< 0.0052	0.018 ± 0.002

[a] Used as reference compounds.

8.3   Conclusions

In summary, the present study represents the very first investigation of a Chilean *Sepedonium* isolate, which was parasitizing on an endemic bolete. The phylogenetic position of the *Sepedonium* aff. *chalcipori* strain KSH 883 was studied in a polythetic approach based on chemical, molecular, and biological data. Semi-solid cultivation, isolation, and structural elucidation yielded two new linear 15-residue peptaibols, designated chilenopeptins A (**8.1**) and B (**8.2**), as well as the known 15-mer peptaibols tylopeptins A (**8.3**) and B (**8.4**). Additionally, the total synthesis of **8.1** and **8.2** was accomplished by a solid-phase peptide approach, confirming the absolute configuration of all chiral amino acids as L. The antiphytopathogenic activity of peptaibols **8.1–8.4** was evaluated against the ascomycetous fungi *B. cinerea* and *S. tritici* as well as the oomycete *P. infestans*.

8.4   Experimental Section

General Experimental Procedures. Size exclusion column chromatography was performed using Sephadex LH 20 (Fluka, Germany), while analytical TLC was carried out on precoated silica gel F_{254} plates from Merck (Germany). Diaion HP 20 was purchased from Supelco (USA). Peptaibols were visualized on TLC plates using a modified acidic ninhydrin reagent as described

previously (Otto et al., 2015a). UV spectra were obtained from a Jasco V-560 UV/Vis spectrophotometer, while CD spectra were acquired on a Jasco J-815 CD spectrophotometer. The specific rotation was measured with a Jasco P-2000 polarimeter.

The NMR spectra were obtained from an Agilent VNMRS 600 system at +40 °C. The compounds were dissolved in DMSO-d_6 (99.96% D) and spectra were recorded at 599.83 MHz (^{1}H) and 150.84 MHz (^{13}C), respectively. 1D (^{1}H, ^{13}C) and 2D spectra (^{1}H,^{13}C and ^{1}H,^{15}N gHSQCAD, ^{1}H,^{13}C and ^{1}H,^{15}N gHMBCAD, ^{1}H,^{1}H gDQCOSY, ^{1}H,^{1}H zTOCSY, ^{1}H,^{1}H ROESY) were measured using standard CHEMPACK 5 pulse sequences implemented in the VnmrJ 4.0 spectrometer software. The mixing times for the TOCSY and ROESY spectra were set to 80 and 250 ms, respectively, and the ^{1}H,^{15}N HMBC experiment was optimized for a long range coupling constant of 8 Hz. ^{1}H and ^{13}C chemical shifts were referenced to internal DMSO-d_6 (δ_H 2.510 ppm and δ_C 39.5 ppm), while ^{15}N chemical shifts are given relative to liquid NH_3 (δ_N 0 ppm).

The solid-phase peptide synthesis was performed on a ResPep SL peptide synthesizer (Intavis Bioanalytical Instruments, Germany). The L-configured Fmoc-amino acids Fmoc-Ser(*t*Bu)-OH, Fmoc-Trp(Boc)-OH, Fmoc-Pro-OH, Fmoc-Leu-OH, Fmoc-Gln(Trt)-OH were supplied by Novabiochem (Germany), while Fmoc-Aib-OH and the L-phenylalaninol 2-chlorotrityl polystyrene resin were purchased from Iris Biotech GmbH (Germany). TFFH was obtained from Carbolution Chemicals (Germany). Piperidine, Ac_2O, DIPEA, and DMF were purchased from Sigma Aldrich (Germany).

The positive and negative ion high-resolution ESI and collision induced dissociation (CID) MS^n spectra were obtained from an Orbitrap Elite mass spectrometer (Thermo Fisher Scientific, Germany) equipped with a HESI electrospray ion source (positive spray voltage 4.0 kV, negative spray voltage 3.5 kV, capillary temperature 275 °C, source heater temperature 200 °C, FTMS resolution 30.000). Nitrogen was used as sheath and auxiliary gas. The MS system was coupled to an ultra-high performance liquid chromatography (UHPLC) system (Dionex UltiMate 3000, Thermo Fisher Scientific), equipped with a RP18 column (particle size 1.9 μm, pore size 175 Å, 50 × 2.1 mm ID, Hypersil GOLD, Thermo Fisher Scientific; column temperature 40 °C) and a photodiode array detector (200–600 nm, Thermo Fisher Scientific). The mobile phases were H_2O (A; Fluka Analytical, LC-MS Chromasolv) and CH_3CN (B; Fluka Analytical, LC-MS Chromasolv) with 0.2% formic acid using a gradient system (0–5 min, 45–55% B; 5–13 min, 55–95% B; 13–16 min, 95% B; 16–17 min 95–45% B; flow rate 0.2 ml/min).

The CID mass spectra (buffer gas: helium) were recorded using normalized collision energies (NCE) of 45–65% (see Supporting Information). The instrument was externally calibrated by the Pierce LTQ Velos ESI positive ion calibration solution (product no. 88323) and Pierce ESI negative ion calibration solution (product no. 88324) from Thermo Fisher Scientific. The data were evaluated using the software Xcalibur 2.7 SP1.

Preparative HPLC was performed on a Knauer system equipped with a WellChrom K-1001 pump and a WellChrom K-2501 UV detector using either column 1 (ODS-A, 5 μm, 120 Å,

150 × 10 mm ID, YMC, USA) or column 2 (polymeric C18, 8 μm, 300 Å, 250 × 9 mm ID, VYDAC, USA).

Fungal strain and cultivation. The fungal strain *Sepedonium* aff. *chalcipori* KSH 883 was isolated in May 2011 from *Boletus loyo* Phillippi (leg./det. N. Arnold/G. Palfner) under *Nothofagus obliqua* (Mirb.) Oerst. in Chile (region Bío Bío, province Ňuble, district Quillón, Cerro Cayumanqui). A voucher specimen (CONC-F 0738) is deposited at the fungarium of the University of Concepción, Chile. The living strain is preserved at the Leibniz Institute of Plant Biochemistry, Halle. For isolation, the conidia were aseptically removed from the infected host, transferred to malt peptone agar (MPA) plates (10 g malt, 2.5 g peptone, and 15 g agar in 1000 ml deionized water), and transferred periodically. Large scale semi-solid cultures, used for isolation of peptaibols, were grown in 20 Erlenmeyer flasks (size 1 l) each containing 1.5 g of cotton wool and 250 ml of malt peptone medium (2.5 g malt and 0.625 g peptone in 250 ml deionized water) resulting in a total volume of 5 l. Each culture flask was inoculated with a 10 × 10 mm agar plug of colonized fungus and incubated for 28 days at room temperature without agitation.

Molecular phylogenetic analyses. Genomic DNA was extracted from 3–5 week old mycelial cultures on MPA plates using a gene extraction kit (Bio Basic Inc., Canada). The internal transcribed spacer region (ITS) was amplified and sequenced using the primer pair ITS1F/ITS4 (Gardes and Bruns, 1993; White et al., 1990). The sequences of the EF1-α gene were generated using EF1-983F/EF1-1577F/EF1-1567R/EF1-2218R, while the primers fRPB2-5F/ fRPB2-7cR were used to maintain RPB2 gene sequences (Liu et al., 2006; Rehner and Buckley, 2005). PCR products were purified using EZ-10 Spin Column PCR Purification Kit (Bio Basic Inc., Canada) and FastGene Gel/PCR Extraction Kit (NIPPON Genetics EUROPE GmbH, Germany). DNA sequences of the three molecular markers were aligned by MAFFT v7.017 (Katoh and Toh, 2008) using Geneious version 7.1.5 (http://www.geneious.com) (Kearse et al., 2012), the ends were replenished with "N", and the alignments were cured with low stringency using Gblocks v0.91b (http://molevol.cmima.csic.es/castresana/Gblocks_server.html) (Castresana, 2000). The multigene alignment was constructed by concatemerization of the aligned ITS, EF1-α, and RPB2 sequences. Model tests for the ITS and multigene alignment were performed in MEGA6 (Tamura et al., 2013). The phylogenetic trees were calculated with RAxML (Stamatakis, 2006) in Geneious version 7.1.5, using GTR+G as substitution model and 1000 bootstraps. *Trichoderma aerugineum* was used as outgroup. Phylogenetic trees were edited in TreeGraph 2.4.0-456 beta (http://treegraph.bioinfweb.info) (Stöver and Müller, 2010).

Scanning electron microscopy of aleurioconidia. A thin layer of aleurioconidia originating from a 2–3 week old culture was fixed on metal stubs. After drying overnight at room temperature, samples were coated with a 1.4 nm gold-palladium layer in a Polaron SEM SC 515 Sputter

Coater. Microscopy and photography were performed on a Digital Scanning Electron Microscop DSM 950 (Zeiss, Germany).

Extraction and isolation. The mycelia were separated from the culture broth by vacuum filtration, frozen with liquid nitrogen, and extracted with MeOH (3×3 l). The MeOH extract was evaporated to dryness, redissolved in H_2O, and combined with the culture broth. Activated Diaion HP 20 (30 g) was added and agitated for 12 hours at room temperature. The Diaion HP 20 resin was removed by vacuum filtration, washed with H_2O, eluted with MeOH, and evaporated *in vacuo* to dryness. The resulting yellow crude extract (2.0 g) was subjected to size exclusion column chromatography (450×35 mm) using Sephadex LH 20 (eluent: MeOH) to afford 90 fractions (each 10 ml). Fractions 18–19 showing a positive ninhydrin reaction were combined (95.1 mg) and finally purified by preparative HPLC using column 1 with H_2O (A) and CH_3CN (B) as eluents (0–20 min, 50–80% B; flow rate 3.5 ml/min) to afford **8.1** (t_R 14.7 min, 8.2 mg), **8.2** (t_R 17.3 min, 10.4 mg), **8.3** (t_R 9.7 min, 5.5 mg), and **8.4** (t_R 8.4 min, 3.9 mg).

Automated solid-phase peptide synthesis. Compounds **8.1** and **8.2** were synthesized in a 0.1 mmol scale starting from a L-phenylalaninol 2-chlorotrityl resin (200–400 mesh, loading 0.67 mmol/g resin). The used coupling cycle protocol (Scheme 8.1) was modified from the standard Intavis protocol by increasing the activation (12 min) and coupling time (60 min). The Fmoc amino acids, piperidine, and TFFH were dissolved in DMF. DIPEA was used as a base during the activation steps (for detailed protocol see Supporting Information). *N*-Terminal acetylation was performed after complete peptide assembly by treating the resin with Ac_2O and DIPEA in DMF (15/15/70, v/v/v) for 30 min.

Solid-phase cleavage and deprotection of peptide **8.1** was achieved by treatment with 5 ml TFA/CH_2Cl_2/H_2O/TIPS (47/47/4/2, v/v/v/v) for 60 min. The cleavage mixture was concentrated under reduced pressure to approximately 1 ml. After precipitation in water, the sample was lyophilized to obtain the crude peptide mixture (143.8 mg), which was dissolved in MeOH and subsequently separated by Sephadex LH 20 column chromatography (360×30 mm) eluting with MeOH to afford 33 fractions (each 10 ml). Fractions 12–14 were combined (37.5 mg) and purified by preparative HPLC using column 2 with H_2O + 0.1% TFA (A) and CH_3CN + 0.1% TFA (B) as eluents (0–30 min, 40–50% B; flow rate 4.5 ml/min) to afford **8.1** in 1.2% total yield (t_R 17.1 min, 1.9 mg).

Cleavage and deprotection of compound **8.2** was performed by treating the resin with 5 ml TFA/CH_2Cl_2/H_2O/TIPS (47/47/4/2, v/v/v/v) for 60 min. The cleavage mixture was concentrated under reduced pressure to approximately 1 ml. After precipitation in water, the sample was lyophilized to afford the crude peptide product (145.9 mg). The mixture was dissolved in MeOH and purified by Sephadex LH 20 column chromatography (360×30 mm) eluting with MeOH to afford 34 fractions (each 10 ml). Fractions 13–15 were combined (37.6 mg) and purified by preparative HPLC using column 2 with H_2O + 0.1% TFA (A) and CH_3CN + 0.1% TFA (B) as

eluents (0–20 min, 35–50% B; flow rate 4.5 ml/min) to afford **8.2** in 1.5% total yield (t_R 19.6 min, 2.4 mg).

Natural chilenopeptin A (8.1): white, amorphous solid; TLC R_f 0.61 (*n*-BuOH/AcOH/H$_2$O 4:1:1); $[\alpha]^{23}_D$ –18.9 (*c* 0.200, MeOH); CD (MeOH) $[\theta]_{194}$ +380655, $[\theta]_{207}$ –219414, $[\theta]_{222}$ –147364 $°\times cm^2\times dmol^{-1}$; UV (MeOH) λ_{max} (log ε) 200 (4.84), 218 (4.62), 282 (3.74), 290 (3.69) nm; ^{1}H NMR and ^{13}C NMR see Table 8.2; ESI-HRMS *m/z* 821.4735 ([M+2H]$^{2+}$, calcd for $C_{80}H_{126}N_{18}O_{19}{}^{2+}$ 821.4718); ESI-HRMS^n see Tables 8.1 and S1.

Synthetic chilenopeptin A (8.1): white, amorphous solid; CD (MeOH) $[\theta]_{193}$ +281793, $[\theta]_{207}$ –160020, $[\theta]_{222}$ –106074 $°\times cm^2\times dmol^{-1}$; UV (MeOH) λ_{max} (log ε) 200 (4.94), 218 (4.67), 281 (3.82), 290 (3.75) nm; ^{1}H NMR and ^{13}C NMR in agreement with natural **8.1** (^{13}C difference below 0.1 ppm); ESI-HRMS *m/z* 821.4759 ([M+2H]$^{2+}$, calcd for $C_{80}H_{126}N_{18}O_{19}{}^{2+}$ 821.4718); ESI-HRMS^n in accordance with data of natural **8.1**.

Natural chilenopeptin B (8.2): white, amorphous solid; TLC R_f 0.62 (*n*-BuOH/AcOH/H$_2$O 4:1:1); $[\alpha]^{25}_D$ –34.0 (*c* 0.185, MeOH); CD (MeOH) $[\theta]_{194}$ +471416, $[\theta]_{208}$ –186003, $[\theta]_{222}$ –130126 $°\times cm^2\times dmol^{-1}$; UV (MeOH) λ_{max} (log ε) 200 (4.77) nm; ^{1}H NMR and ^{13}C NMR see Table 8.3; ESI-HRMS *m/z* 801.9671 ([M+2H]$^{2+}$, calcd for $C_{78}H_{125}N_{17}O_{19}{}^{2+}$ 801.9663); ESI-HRMS^n see Tables 8.1 and S1.

Synthetic chilenopeptin B (8.2): white, amorphous solid; CD (MeOH) $[\theta]_{193}$ +408041, $[\theta]_{208}$ –152517, $[\theta]_{222}$ –109078 $°\times cm^2\times dmol^{-1}$; UV (MeOH) λ_{max} (log ε) 200 (4.83) nm; ^{1}H and ^{13}C NMR in agreement with natural **8.2** (^{13}C difference below 0.1 ppm); ESI-HRMS *m/z* 801.9693 ([M+2H]$^{2+}$, calcd for $C_{78}H_{125}N_{17}O_{19}{}^{2+}$ 801.9663); ESI-HRMS^n in accordance with data of natural **8.2**.

Natural tylopeptin A (8.3): white, amorphous solid; TLC R_f 0.70 (*n*-BuOH/AcOH/H$_2$O 4:1:1); ^{1}H NMR and ^{13}C NMR in accordance with data of Lee et al. (1999) (^{13}C difference below 0.1 ppm); ESI-HRMS *m/z* 777.4565 ([M+2H]$^{2+}$, calcd for $C_{73}H_{122}N_{18}O_{19}{}^{2+}$ 777.4562); ESI-HRMS^n see Table S2, Supporting Information.

Natural tylopeptin B (8.4): white, amorphous solid; TLC R_f 0.66 (*n*-BuOH/AcOH/H$_2$O 4:1:1); ^{1}H NMR and ^{13}C NMR in accordance with data of Lee et al. (1999) (^{13}C difference below 0.1 ppm); ESI-HRMS *m/z* 770.4480 ([M+2H]$^{2+}$, calcd for $C_{72}H_{120}N_{18}O_{19}{}^{2+}$ 770.4483); ESI-HRMS^n see Table S2, Supporting Information.

Antiphytopathogenic bioassay. Crude extracts, fractions, and pure compounds were tested in a 96-well microtiter plate assay against *Botrytis cinerea*, *Septoria tritici*, and *Phytophthora infestans* according to the fungicide resistance action committee (FRAC) with minor modifications (Otto et al., 2015a; Stammler and Semar, 2011; Stammler and Speakman, 2006;

Stammler, 2006): Crude extracts and fractions were examined at a final concentration of 125 µg/ml, while pure compounds were tested in a serial dilution ranging from 80 µM to 0.1 µM. The solvent DMSO was used as a negative control (max. concentration 2.5%), and the commercially used fungicides dodine and pyraclostrobin (from Sigma Aldrich) served as reference compounds. Seven days after inoculation, the pathogen growth was evaluated by measurement of the optical density (OD) at λ 405 nm with a Tecan GENios Pro microplate reader (5 measurements per well using multiple reads in a 3×3 square). Each experiment was carried out in triplicates. IC_{50} values were calculated from dose-response curves on the basis of sigmoidal curve fitting (four parameter logistic) using the software SigmaPlot 12.0.

8.5 References

Ayers, S., Ehrmann, B.M., Adcock, A.F., Kroll, D.J., Carcache de Blanco, E.J., Shen, Q., Swanson, S.M., Falkinham, J.O., Wani, M.C., Mitchell, S.M., Pearce, C.J., Oberlies, N.H., 2012. Peptaibols from two unidentified fungi of the order Hypocreales with cytotoxic, antibiotic, and anthelmintic activities. *J. Pept. Sci.* 18, 500–510.

Berg, A., Ritzau, M., Ihn, W., Schlegel, B., Fleck, W.F., Heinze, S., Gräfe, U., 1996. Isolation and structure of bergofungin, a new antifungal peptaibol from *Emericellopsis donezkii* HKI 0059. *J. Antibiot.* 49, 817–820.

Castresana, J., 2000. Selection of conserved blocks from multiple alignments for their use in phylogenetic analysis. *Mol. Biol. Evol.* 17, 540–552.

Chugh, J.K., Wallace, B.A., 2001. Peptaibols: Models for ion channels. *Biochem. Soc. Trans.* 29, 565–570.

Closse, A., Hauser, D., 1973. Isolierung und Konstitutionsermittlung von Chrysodin. *Helv. Chim. Acta* 56, 2694–2698.

Degenkolb, T., Kirschbaum, J., Brückner, H., 2007. New sequences, constituents, and producers of peptaibiotics: An updated review. *Chem. Biodivers.* 4, 1052–1067.

Divekar, P.V., Raistrick, H., Dobson, T.A., Vining, L.C., 1965. Studies in the biochemistry of microorganisms: Part 117. Sepedonin, a tropolone metabolite of *Sepedonium chrysospermum* Fries. *Can. J. Chem.* 43, 1835–1848.

Divekar, P.V., Vining, L.C., 1964. Reaction of anhydrosepedonin with alkali synthesis of a degradation product and some related dimethylhydroxybenzoic acids. *Can. J. Chem.* 42, 63–68.

Dornberger, K., Ihn, W., Ritzau, M., Gräfe, U., Schlegel, B., Fleck, W.F., Metzger, J.W., 1995. Chrysospermins, new peptaibol antibiotics from *Apiocrea chrysosperma* Ap101. *J. Antibiot.* 48, 977–989.

El-Faham, A., Khattab, S.N., 2009. Utilization of N,N,N,'N'-tetramethylfluoroformamidinium hexafluorophosphate (TFFH) in peptide and organic synthesis. *Synlett* 6, 886–904.

Gardes, M., Bruns, T.D., 1993. ITS primers with enhanced specificity for basidiomycetes - application to the identification of mycorrhizae and rusts. *Mol. Ecol.* 2, 113–118.

Gobbo, M., Poloni, C., De Zotti, M., Peggion, C., Biondi, B., Ballano, G., Formaggio, F., Toniolo, C., 2010. Synthesis, preferred conformation, and membrane activity of medium-length peptaibiotics: Tylopeptin B. *Chem. Biol. Drug Des.* 75, 169–181.

Gräfe, U., Ihn, W., Ritzau, M., Schade, W., Stengel, C., Schlegel, B., Fleck, W.F., Künkel, W., Härtl, A., Gutsche, W., 1995. Helioferins; novel antifungal lipopeptides from *Mycogone rosea*: screening, isolation, structures and biological properties. *J. Antibiot.* 48, 126–133.

Helfer, W., 1991. Pilze auf Pilzfruchtkörpern: Untersuchungen zur Ökologie, Systematik und Chemie. IHW-Verlag, Eching, pp. 1–157.

Hjørringgaard, C.U., Pedersen, J.M., Vosegaard, T., Nielsen, N.C., Skrydstrup, T., 2009. An automatic solid-phase synthesis of peptaibols. *J. Org. Chem.* 74, 1329–1332.

Hoyos-Carvajal, L., Orduz, S., Bissett, J., 2009. Genetic and metabolic biodiversity of *Trichoderma* from Colombia and adjacent neotropic regions. *Fungal Genet. Biol.* 46, 615–631.

Hülsmann, H., Heinze, S., Ritzau, M., Schlegel, B., Gräfe, U., 1998. Isolation and structure of peptaibolin, a new peptaibol from *Sepedonium* strains. *J. Antibiot.* 51, 1055–1058.

Jaklitsch, W.M., Põldmaa, K., Samuels, G.J., 2008. Reconsideration of Protocrea (Hypocreales, Hypocreaceae). *Mycologia* 100, 962–984.

Jaklitsch, W.M., Voglmayr, H., 2015. Biodiversity of *Trichoderma* (Hypocreaceae) in Southern Europe and Macaronesia. *Stud. Mycol.* 80, 1–87.

Katoh, K., Toh, H., 2008. Recent developments in the MAFFT multiple sequence alignment program. *Brief. Bioinform.* 9, 286–298.

Kearse, M., Moir, R., Wilson, A., Stones-Havas, S., Cheung, M., Sturrock, S., Buxton, S., Cooper, A., Markowitz, S., Duran, C., Thierer, T., Ashton, B., Meintjes, P., Drummond, A., 2012. Geneious Basic: An integrated and extendable desktop software platform for the organization and analysis of sequence data. *Bioinformatics* 28, 1647–1649.

Kronen, M., Kleinwächter, P., Schlegel, B., Härtl, A., Gräfe, U., 2001. Ampullosporines B, C, D, E1, E2, E3 and E4 from *Sepedonium ampullosporum* HKI-0053: structures and biological activities. *J. Antibiot.* 54, 175–178.

Lee, S.J., Yun, B.S., Cho, D.H., Yoo, I.D., 1999. Tylopeptins A and B, new antibiotic peptides from *Tylopilus neofelleus*. *J. Antibiot.* 52, 998–1006.

Li, Z., Yalcin, T., Cassady, C.J., 2006. *C*-terminal amino acid residue loss for deprotonated peptide ions containing glutamic acid, aspartic acid, or serine residues at the *C*-terminus. *J. Mass Spectrom.* 41, 939–949.

Liu, Y.J., Hodson, M.C., Hall, B.D., 2006. Loss of the flagellum happened only once in the fungal lineage: phylogenetic structure of Kingdom Fungi inferred from RNA polymerase II subunit genes. *BMC Evol. Biol.* 6, 74.

Mitova, M.I., Murphy, A.C., Lang, G., Blunt, J.W., Cole, A.L.J., Ellis, G., Munro, M.H.G., 2008. Evolving trends in the dereplication of natural product extracts. 2. The isolation of chrysaibol, an antibiotic peptaibol from a New Zealand sample of the mycoparasitic fungus *Sepedonium chrysospermum*. *J. Nat. Prod.* 71, 1600–1603.

Neuhof, T., Berg, A., Besl, H., Schwecke, T., Dieckmann, R., von Döhren, H., 2007. Peptaibol production by *Sepedonium* strains parasitizing Boletales. *Chem. Biodivers.* 4, 1103–1115.

Otto, A., Laub, A., Porzel, A., Schmidt, J., Wessjohann, L., Westermann, B., Arnold, N., 2015a. Isolation and total synthesis of albupeptins A–D: 11-residue peptaibols from the fungus *Gliocladium album*. *Eur. J. Org. Chem.* 2015, 7449–7459.

Põldmaa, K., 2011. Tropical species of *Cladobotryum* and *Hypomyces* producing red pigments. *Stud. Mycol.* 68, 1–34.

Przybylski, M., Dietrich, I., Manz, I., Brückner, H., 1984. Elucidation of structure and microheterogeneity of the polypeptide antibiotics paracelsin and trichotoxin A-50 by fast atom bombardment mass spectrometry in combination with selective *in situ* hydrolysis. *Biol. Mass Spectrom.* 11, 569–582.

Quang, D.N., Schmidt, J., Porzel, A., Wessjohann, L., Haid, M., Arnold, N., 2010. Ampullosine, a new isoquinoline alkaloid from *Sepedonium ampullosporum* (Ascomycetes). *Nat. Prod. Commun.* 5, 869–872.

Rahaman, A., Lazaridis, T., 2014. A thermodynamic approach to alamethicin pore formation. *BBA - Biomembr.* 1838, 98–105.

Rehner, S.A., Buckley, E., 2005. A Beauveria phylogeny inferred from nuclear ITS and EF1-sequences: evidence for cryptic diversification and links to *Cordyceps* teleomorphs. *Mycologia* 97, 84–98.

Ritzau, M., Heinze, S., Dornberger, K., Berg, A., Fleck, W., Schlegel, B., Hartl, A., Gräfe, U., 1997. Ampullosporin, a new peptaibol-type antibiotic from *Sepedonium ampullosporum* HKI-0053 with neuroleptic activity in mice. *J. Antibiot.* 50, 722–728.

Rodriguez, M.A., Cabrera, G., Gozzo, F.C., Eberlin, M.N., Godeas, A., 2011. *Clonostachys rosea* BAFC3874 as a *Sclerotinia sclerotiorum* antagonist: Mechanisms involved and potential as a biocontrol agent. *J. Appl. Microbiol.* 110, 1177–1186.

Sahr, T., Ammer, H., Besl, H., Fischer, M., 1999. Infrageneric classification of the boleticolous genus *Sepedonium*: Species delimitation and phylogenetic relationships. *Mycologia* 91, 935–943.

Schiell, M., Hofmann, J., Kurz, M., Schmidt, F.R., Vértesy, L., Vogel, M., Wink, J., Seibert, G., 2001. Cephaibols, new peptaibol antibiotics with anthelmintic properties from *Acremonium tubakii* DSM 12774. *J. Antibiot.* 54, 220–233.

Shibata, S., Shoji, J., Ohta, A., Watanabe, M., 1957. Metabolic products of fungi. XI. Some observation on the occurrence of skyrin and rugulosin in mold metabolites, with a reference to structural relationship between penicilliopsin and skyrin. *Pharm. Bull.* 5, 380–382.

Stadler, M., Seip, S., Müller, H., Henkel, T., Lagojda, A., Kleymann, G., 2001. New antiviral peptaibols from the mycoparasitic fungus *Sepedonium microspermum*, in: Book of Abstracts, 13. Irseer Naturstofftage der DECHEMA, Irsee.

Stamatakis, A., 2006. RAxML-VI-HPC: maximum likelihood-based phylogenetic analyses with thousands of taxa and mixed models. *Bioinformatics* 22, 2688–2690.

Stammler, G., 2006. *Phytophthora infestans* microtiter method with sporangia. URL http://www.frac.info/docs/default-source/monitoring-methods/approved-methods/phytin-microtiter-method-sporangia-basf-2006-v1.pdf?sfvrsn=4 (accessed 24th October 2015).

Stammler, G., Semar, M., 2011. Sensitivity of *Mycosphaerella graminicola* (anamorph: *Septoria tritici*) to DMI fungicides across Europe and impact on field performance. *EPPO Bull.* 41, 149–155.

Stammler, G., Speakman, J., 2006. Microtiter method to test the sensitivity of *Botrytis cinerea* to boscalid. *J. Phytopathol.* 154, 508–510.

Stöver, B.C., Müller, K.F., 2010. TreeGraph 2: Combining and visualizing evidence from different phylogenetic analyses. *BMC Bioinformatics* 11, 7.

Tamm, H., Põldmaa, K., 2013. Diversity, host associations, and phylogeography of temperate aurofusarin-producing *Hypomyces/Cladobotryum* including causal agents of cobweb disease of cultivated mushrooms. *Fungal Biol.* 117, 348–367.

Tamura, K., Stecher, G., Peterson, D., Filipski, A., Kumar, S., 2013. MEGA6: Molecular Evolutionary Genetics Analysis version 6.0. *Mol. Biol. Evol.* 30, 2725–2729.

Tavano, R., Malachin, G., De Zotti, M., Peggion, C., Biondi, B., Formaggio, F., Papini, E., 2015. The peculiar *N-* and *C*-termini of trichogin GA IV are needed for membrane interaction and human cell death induction at doses lacking antibiotic activity. *BBA - Biomembr.* 1848, 134–144.

White, T.J., Bruns, S., Lee, S., Taylor, J., 1990. Amplification and direct sequencing of fungal ribosomal RNA genes for phylogenetics, in: Innis, M.A., Gelfand, D.H., Sninsky, J.J., White, T.J. (Eds.), PCR Protocols: A guide to methods and applications. Academic Press, London, pp. 315–322.

Yun, B.S., Yoo, I.D., Kim, Y.S.H., Kim, Y.S.H., Lee, S.J., Kim, K.S., Yeo, W.H., 2000. Peptaivirins A and B, two new antiviral peptaibols against TMV infection. *Tetrahedron Lett.* 41, 1429–1431.

8.6 Supporting Information

Supplementary data associated with this article (^{1}H and ^{13}C NMR spectra of natural and synthetic **8.1** and **8.2** as well as natural **8.3** and **8.4**; ^{1}H,^{13}C and ^{1}H,^{15}N HSQC, ^{1}H,^{13}C and ^{1}H,^{15}N HMBC, COSY, and ROESY spectra of **8.1** and **8.2**; ESI-HRMS^n data of **8.1**–**8.4**; CD spectra of natural and synthetic **8.1** and **8.2**; initial morphological analysis of *Sepedonium* aff. *chalcipori* KSH 883) can be found at http://dx.doi.org/10.1021/acs.jnatprod.5b01018.

9 Isolation and total synthesis of albupeptins A–D: 11-residue peptaibols from the fungus *Gliocladium album*

Ac-**Aib/D-Iva^1**-Aib^2-Val^3-Leu^4-**Aib/L-Iva^5**-Pro^6-D-Iva^7-Leu^8-Gln^9-Aib^{10}-Leuol^{11}
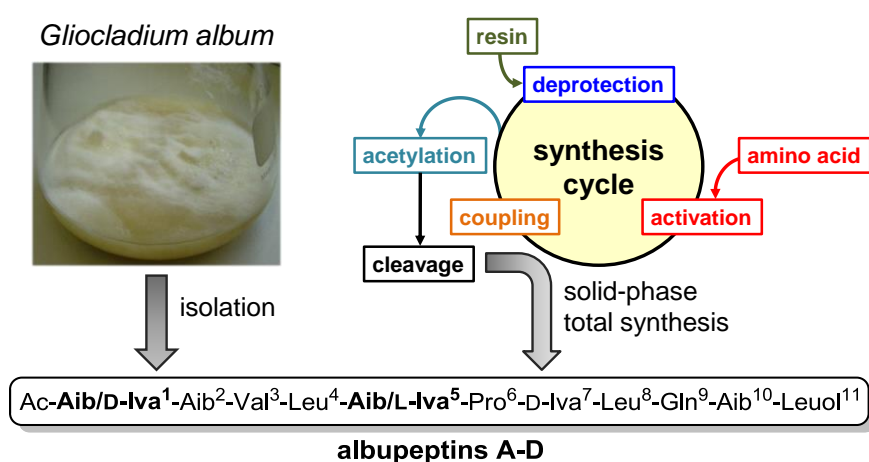
albupeptins A-D

Abstract

Four new 11-mer peptaibols, named albupeptins A–D (**9.1**–**9.4**), were isolated from cultures of the fungus *Gliocladium album*. Their structures were elucidated on the basis of 1D and 2D NMR experiments as well as ESI-HRMS^n analyses. The sequence of albupeptin A (**9.1**) was thus identified as Ac-Aib^1-Aib^2-Val^3-Leu^4-Aib^5-Pro^6-Iva^7-Leu^8-Gln^9-Aib^{10}-Leuol^{11}. Albupeptin B (**9.2**) and C (**9.3**) feature an exchange of Aib^5 by Iva^5 and Aib^1 by Iva^1, respectively, and albupeptin D (**9.4**) contains both Iva^1 and Iva^5 residues. The stereochemistry of the isolated peptaibols **9.1**–**9.4** was unambiguously assigned by proton NMR chemical shift analyses in conjunction with solid-phase peptide synthesis. By using this approach, the absolute configuration of Iva residues in albupeptins A (**9.1**) and C (**9.3**) was determined as D, whereas albupeptins B (**9.2**) and D (**9.4**) feature an additional Iva^5 in L-configuration. Thus, albupeptins B (**9.2**) and D (**9.4**) belong to the rare class of peptaibols that exhibit both stereoisomers of Iva in the same sequence.

9.1 Introduction

Fungi of the anamorphic genus *Gliocladium* (Hypocreaceae, Ascomycota) are well known for their production of bioactive secondary metabolites with high structural diversity, such as polyterpenoids (Joshi et al., 1999; Nishida et al., 1992; Thines et al., 1998), polyketide glycosides (Kasai et al., 2005; Tomoda et al., 1999), di- and triketopiperazines (Chu et al., 1995; Dong et al., 2006, 2005; Joshi et al., 1999; Usami et al., 2004), a bisindole (Bertinetti et al., 2010), and peptaibols (Brückner and Przybylski, 1984; Jaworski and Brückner, 2000).

Peptaibols are a family of fungal peptides that consist of 5 to 21 amino acids and are biosynthesized by non-ribosomal peptide synthetases (NRPS). They are characterized by the presence of non-proteinogenic, helix inducing α,α-dialkyl amino acids such as α-aminoisobutyric acid (Aib) and its chiral homologue isovaline (Iva), which can occur as the D- and/or the L-enantiomer (Degenkolb and Brückner, 2008). A further structural feature is an acetylated *N*-terminus, and the *C*-terminal amino acid is reduced to an amino alcohol such as leucinol (Leuol) or phenylalaninol (Pheol) (Degenkolb et al., 2007). Their amphipathic nature and helical secondary structure allows these compounds to form voltage-dependent ion channels into biological membranes, leading to alterations in the osmotic balance of the cell (Chugh and Wallace, 2001; Rahaman and Lazaridis, 2014; Rodriguez et al., 2011). Consequently, peptaibols exhibit a broad range of biological and pharmacological properties, including antibiotic (Gräfe et al., 1995; Lee et al., 1999), antiviral (Stadler et al., 2001; Yun et al., 2000), neuroleptic (Kronen et al., 2001; Ritzau et al., 1997), cytotoxic (Ayers et al., 2012; Tavano et al., 2015), antiparasitic (Ayers et al., 2012; Schiell et al., 2001), and antifungal activities (Berg et al., 1996; Shi et al., 2012).

As part of ongoing screening studies for new bioactive metabolites based on our highly diverse fungal strain collection, the culture extract of *Gliocladium album* (Preuss) Petch significantly inhibited the growth of various phytopathogenic organisms. *G. album* has so far only been observed on slime molds (myxomycetes) (Ellis and Ellis, 1988; Gams, 1971b; Petch, 1939) such as *Stemonitis fusca* or *Fuligo septica* (Helfer, 1991).

The present study reports the bioactivity guided isolation, structural elucidation, and total synthesis of four new linear 11-residue peptaibols (**9.1–9.4**) from the semi-solid culture of *G. album*. The absolute configuration of compounds **9.1–9.4** was clarified by proton chemical shift analyses in combination with solid-phase synthesis. The isolated peptaibols **9.1–9.4** were evaluated for their biological activity against the plant pathogenic organisms *Botrytis cinerea*, *Septoria tritici*, and *Phytophthora infestans*.

9.2 Results and discussion

9.2.1 Isolation and structural elucidation of albupeptins A–D

The chromatographic separation of the culture broth and mycelial crude extract using Diaion HP 20 and Sephadex LH 20 in combination with preparative RP18 HPLC resulted in the isolation of compounds **9.1–9.4** (Fig. 9.1). The presence of *N*-protected peptides such as peptaibols was suggested from TLC spots showing no reaction using neutral ninhydrin spray solution, but a positive color reaction when a modified acidic ninhydrin reagent was applied (see Chapter 9.4).
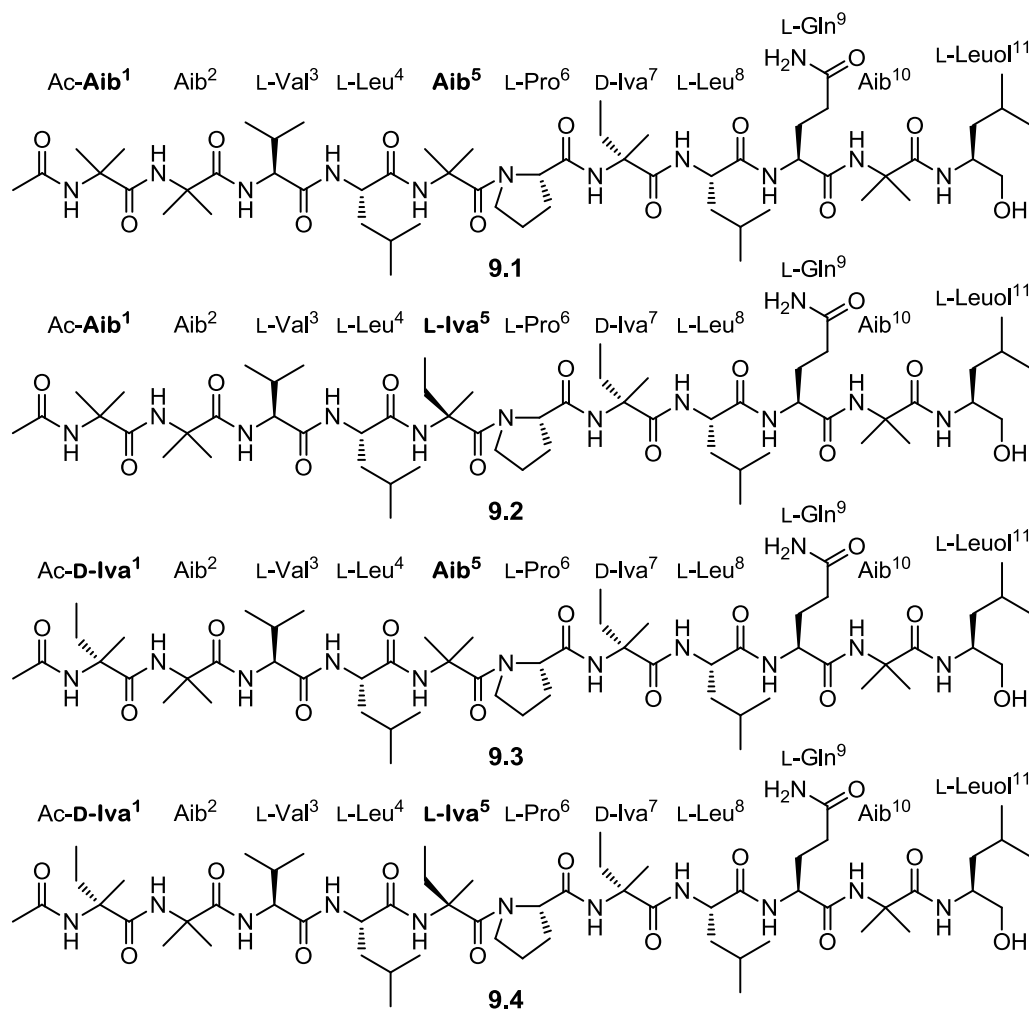
Fig. 9.1. Structures of albupeptins A–D (**9.1–9.4**). Differences in amino acid sequences are highlighted in bold.

Compound **9.1** was isolated as a white, amorphous solid. The molecular formula $C_{56}H_{100}N_{12}O_{13}$ was deduced from ESI-HRMS of the pseudomolecular $[M+H]^+$ ion at m/z 1149.7639 (calculated for $C_{56}H_{101}N_{12}O_{13}^+$ 1149.7606). The ^1H NMR spectrum of **9.1** in DMSO-d_6 (Table 9.1) displayed 10 N-H resonances corresponding to amide protons. Among them, five N-H signals appeared as ^1H singlets (δ_H 8.455, 8.284, 7.797, 7.404, and 7.107) and five resonances as ^1H doublets (δ_H 7.630, 7.600, 7.535, 7.436, and 6.622). Moreover, the presence of a secondary amino group corresponding to a glutamine (Gln) residue was evident from the $^1H, ^{15}N$

HSQC spectrum. Among the five N-H singlets, the four resonances at δ_H 8.455, 8.284, 7.797, and 7.107 were attributed to Aib residues as deduced from HMBC correlation peaks of these N-H resonances to quaternary Cα atoms resonating around δ_C 56 and β/γ-methyl groups between δ_C 22.8–27.1. Furthermore, the presence of one Iva residue was concluded from long-range correlations of the N-H singlet (δ_H 7.404) and the characteristic γ-methyl triplet (δ_H 0.755, J = 7.6 Hz) to the Cα signal at δ_C 58.6.
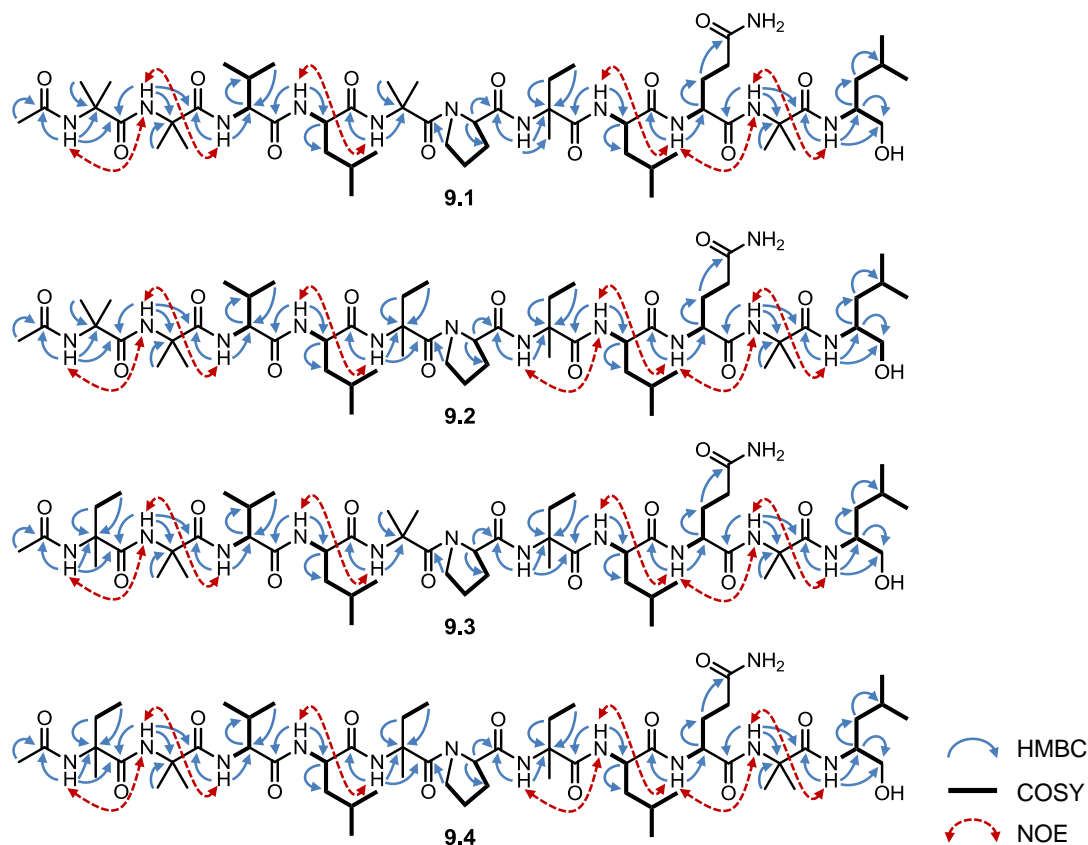
Fig. 9.2. Key HMBC (H to C), COSY, and NOE correlations of albupeptins A–D (**9.1–9.4**).

The ^{13}C NMR spectrum (Table 9.1) showed 12 carbonyl signals between δ_C 170.4–176.2 confirming **9.1** to be a polypeptide. HMBC interactions of the acetyl CH$_3$ group (δ_H 1.927) as well as the N-H signal of Aib[1] (δ_H 8.455) to the carbonyl carbon resonating at δ_C 170.4 demonstrated the presence of an acetylated *N*-terminal Aib residue (Fig. 9.2). The TOCSY spectrum of **9.1** displayed characteristic spin systems corresponding to one valine, one proline, one glutamine, and two leucine residues (Fig. 9.3). Another leucine-related coupling system, showing additional hydroxymethylene signals at δ_H 3.274 (H$_A$-β') and 3.120 (H$_B$-β') as well as a hydroxyl resonance at δ_H 4.274 was assigned to a *C*-terminal Leuol[11] residue.

The amino acid sequence was established on the basis of HMBC interactions through $^2J_{CH}$ and $^3J_{CH}$ couplings of N-H resonances with carbonyl and Cα signals as well as NOE correlation peaks between neighboring nitrogen proton signals (Fig. 9.2). Subsequently, the HMBC interactions of N-H (δ_H 8.455, Aib[1]) with δ_C 170.4 (C=O, Ac) and δ_C 175.0 (C=O, Aib[1]), N-H (δ_H 8.284, Aib[2]) with δ_C 175.0 (C=O, Aib[1]) and δ_C 176.2 (C=O, Aib[2]), N-H (δ_H 7.630, Val[3]) with δ_C 176.2 (C=O, Aib[2]), N-H (δ_H 7.600, Leu[4]) with δ_C 171.4 (C=O, Val[3]), N-H (δ_H 7.797, Aib[5]) with δ_C 172.8 (C=O,

Leu[4]), N-H (δ_H 7.404, Iva[7]) with δ_C 173.5 (C=O, Pro[6]), N-H (δ_H 7.436, Leu[8]) with δ_C 175.9 (C=O, Iva[7]), N-H (δ_H 7.535, Gln[9]) with δ_C 173.0 (C=O, Leu[8]), N-H (δ_H 7.107, Aib[10]) with δ_C 170.7 (C=O, Gln[9]) and δ_C 173.2 (C=O, Aib[10]) as well as N-H (δ_H 6.622, Leuol[11]) with δ_C 173.2 (C=O, Aib[10]) established the sequence of **9.1** as Ac-Aib[1]-Aib[2]-Val[3]-Leu[4]-Iva[5]-Pro[6]-Iva[7]-Leu[8]-Gln[9]-Aib[10]-Leuol[11]. The sequence deduced from NMR analyses was consistent with positive and negative ion ESI-HRMS[n] investigations, showing diagnostic fragment ions of the b and y series (Fig. 9.4, Table S2). Thus, the structure of compound **9.1** was confirmed as proposed above and trivially named albupeptin A (Fig. 9.1).
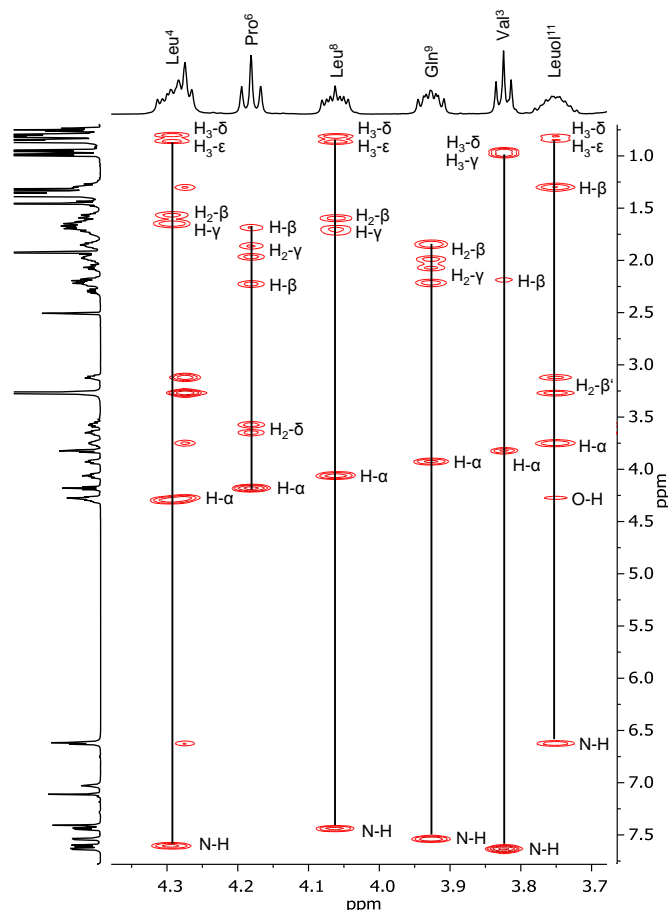
Fig. 9.3. H-α region in the TOCSY spectrum of **9.1** (600 MHz, DMSO-d_6, 40 °C, 80 ms mixing time), displaying characteristic spin systems of Val[3], Leu[4], Pro[6], Leu[8], Gln[9], and Leuol[11].

Compound **9.2** was isolated as a white, amorphous solid. Its prominent peak at *m/z* 1163.7781 ([M+H]$^+$, calculated for $C_{57}H_{103}N_{12}O_{13}^+$ 1163.7762) displayed a difference of 14 atomic mass units (amu) from **9.1** to **9.2**, indicative of an additional methylene group. Comprehensive 1D and 2D NMR studies (Table 9.1) demonstrated that peptide **9.2** contained only three Aib residues, one less than in **9.1**. Instead, two Iva residues were identified. The HMBC correlation peak between C=O of Leu[4] (δ_C 172.7) and the N-H signal of the additional Iva residue (δ_H 7.698) confirmed its insertion at position 5 (Fig. 9.2). Diagnostic fragment ions obtained from positive and negative ion high-resolution tandem mass spectrometry sequencing were consistent with these observations (Table S2). Therefore, the sequence of albupeptin B (**9.2**) was determined as Ac-Aib[1]-Aib[2]-Val[3]-Leu[4]-Iva[5]-Pro[6]-Iva[7]-Leu[8]-Gln[9]-Aib[10]-Leuol[11] (Fig. 9.1).
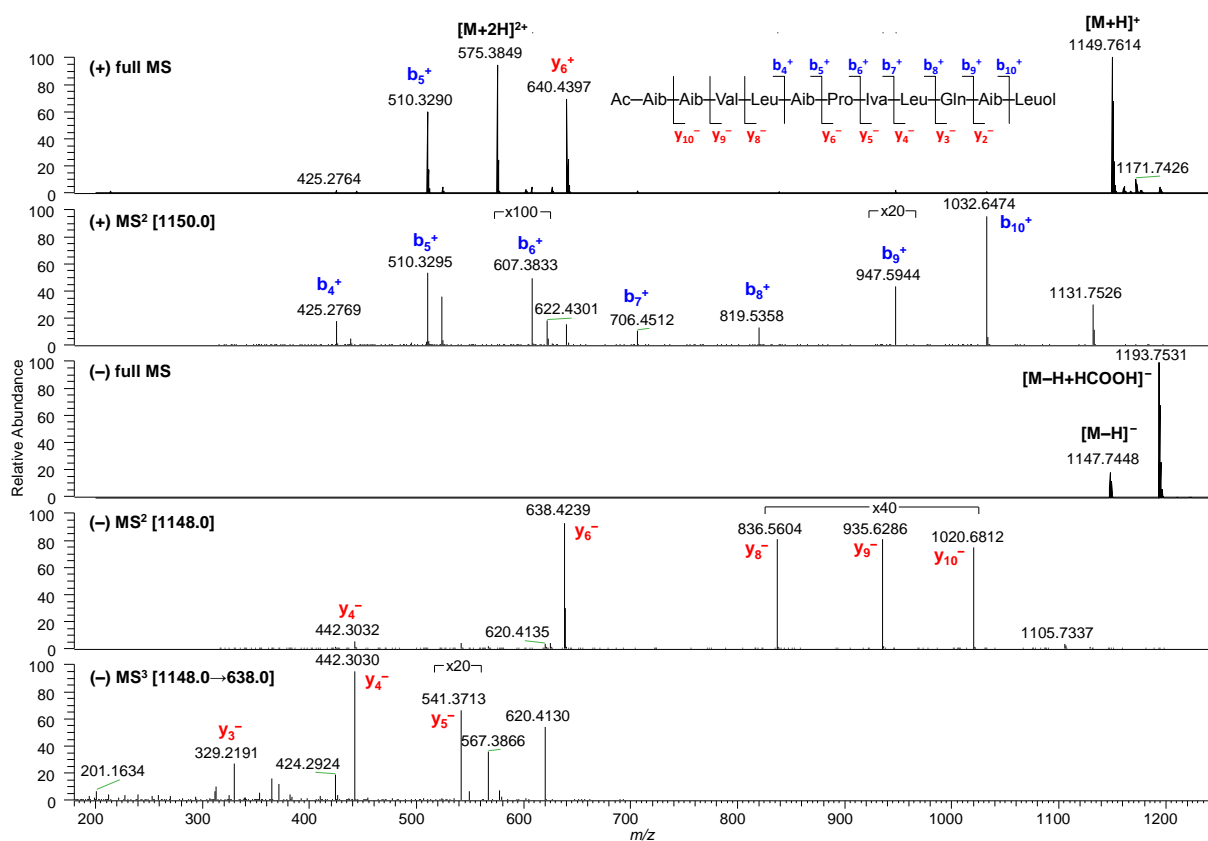
Fig. 9.4. Positive and negative ion ESI-HRMS^n spectra of albupeptin A (**9.1**).

Compound **9.3** was isolated as a white, amorphous solid. ESI-HRMS studies demonstrated that **9.3** had the same molecular formula ($C_{57}H_{102}N_{12}O_{13}$) as compound **9.2**. Detailed analyses of 1D and 2D NMR data (Table 9.1) revealed that **9.3** is a constitutional isomer of albupeptin B (**9.2**). The only disparity between the compounds is the positional exchange of Aib^1/Iva^5 (in **9.2**) by Iva^1/Aib^5 (in **9.3**) as deduced from the HMBC correlation between the N-H-Iva^1 resonance (δ_H 8.313) and the carbonyl signal (δ_C 170.4) of the *N*-terminal acetyl residue (Fig. 9.2). The proposed sequence was corroborated by ESI-HRMS^n analyses (Table S2). Based on the above spectroscopic data, compound **9.3** was identified as Ac-Iva^1-Aib^2-Val^3-Leu^4-Aib^5-Pro^6-Iva^7-Leu^8-Gln^9-Aib^{10}-Leuol^{11} and consequently named albupeptin C (Fig. 9.1).

The molecular formula of albupeptin D (**9.4**), isolated as a white, amorphous solid, was established on the basis of ESI-HRMS investigations as $C_{58}H_{104}N_{12}O_{13}$, demonstrating that the sequence of **9.4** holds one more CH_2 group than compounds **9.2** and **9.3**. In fact, the HSQC spectrum of **9.4** revealed the presence of three Iva residues, instead of two in **9.2** and **9.3**. Extensive analyses of HMBC correlations (Fig. 9.2) as well as ESI-HRMS^n studies (Table S2) confirmed Iva residues at position 1, 5, and 7. The structure of albupeptin D (**9.4**) was thus established as Ac-Iva^1-Aib^2-Val^3-Leu^4-Iva^5-Pro^6-Iva^7-Leu^8-Gln^9-Aib^{10}-Leuol^{11} (Fig. 9.1).

Table 9.1. ^{1}H and ^{13}C NMR data of albupeptins A–D (**9.1–9.4**) (600/150 MHz, DMSO-d_6, 40 °C, δ in ppm).

Pos.	9.1 δ$_H$, mult. *J* (Hz)	δ$_C$	9.2 δ$_H$, mult. *J* (Hz)	δ$_C$	9.3 δ$_H$, mult. *J* (Hz)	δ$_C$	9.4 δ$_H$, mult. *J* (Hz)	δ$_C$
	Ac		**Ac**		**Ac**		**Ac**	
CH$_3$	1.927 s	22.9	1.924 s	22.9	1.943 s	22.8	1.941 s	22.8
C=O	---	170.4	---	170.5	---	170.4	---	170.4
	Aib[1]		**Aib[1]**		**D-Iva[1]**		**D-Iva[1]**	
N-H	8.455 s	---	8.473 s	---	8.313 s	---	8.346 s	---
C=O	---	175.0	---	174.9	---	175.3	---	175.3
α	---	55.6	---	55.6	---	58.4	---	58.4
β	1.346 s	25.7	1.343 s	25.7	1.97[a]; 1.67[a]	26.5	1.97[a]; 1.67[a]	26.5
γ	1.324 s	23.4	1.323 s	23.5	0.782 t 7.6	7.3	0.780 t 7.6	7.3
δ	---	---	---	---	1.272 s	21.9	1.271 s	21.9
	Aib[2]		**Aib[2]**		**Aib[2]**		**Aib[2]**	
N-H	8.284 s	---	8.276 s	---	8.280 s	---	8.281 s	---
C=O	---	176.2	---	176.0	---	176.2	---	176.0
α	---	55.9	---	55.9	---	55.9	---	55.9
β	1.387 s	22.8	1.370 s	22.8	1.390 s	22.9	1.372 s	22.9
γ	1.351 s	27.1	1.348 s	27.1	1.354 s	27.1	1.353 s	27.0
	L-Val[3]		**L-Val[3]**		**L-Val[3]**		**L-Val[3]**	
N-H	7.630 d 6.6	---	7.609 d 6.6	---	7.629 d 6.6	---	7.604 d 6.6	---
C=O	---	171.4	---	171.4	---	171.4	---	171.4
α	3.824 t-like 6.6	60.7	3.827 t-like 6.6	60.6	3.817 t-like 6.6	60.7	3.822 t-like 6.7	60.6
β	2.197 m	28.7	2.18[a]	28.7	2.191 m	28.7	2.177 m	28.7
γ	0.995 d 6.8	18.4	0.989 d 6.8	18.4	0.987 d 6.8	18.4	0.982 d 6.8	18.4
δ	0.957 d 6.8	18.8	0.953 d 6.8	18.8	0.950 d 6.8	18.8	0.946 d 6.8	18.8
	L-Leu[4]		**L-Leu[4]**		**L-Leu[4]**		**L-Leu[4]**	
N-H	7.600 d 8.1	---	7.622 d 8.1	---	7.582 d 8.2	---	7.604 d 8.1	---
C=O	---	172.8	---	172.7	---	172.7	---	172.6
α	4.294 ddd 11.0/8.1/4.2	51.1	4.273 m	51.3	4.300 ddd 11.0/8.2/4.1	51.0	4.280 m	51.2
β	1.65[a]; 1.56[a]	39.4	1.65[a]; 1.57[a]	39.4	1.64[a]; 1.56[a]	39.3	1.65[a]; 1.57[a]	39.3
γ	1.65[a]	24.0	1.65[a]	24.0	1.63[a]	24.0	1.65[a]	24.0
δ	0.863 d 6.4	22.7	0.865 d 6.5	22.6	0.868 d 6.5	22.6	0.869 d 6.5	22.6
ε	0.805 d 6.4	20.4	0.806 d 6.5	20.5	0.805 d 6.5	20.4	0.806 d 6.7	20.5
	Aib[5]		**L-Iva[5]**		**Aib[5]**		**L-Iva[5]**	
N-H	7.797 s	---	7.698 s	---	7.769 s	---	7.673 s	---
C=O	---	172.7	---	171.6	---	172.7	---	171.6
α	---	55.7	---	59.5	---	55.7	---	59.5
β	1.461 s	22.9	1.98[a]; 1.80[a]	28.2	1.458 s	22.9	1.98[a]; 1.814 dq 14.1/7.6	28.2
γ	1.381 s	25.4	0.779 t 7.6	7.7	1.378 s	25.5	0.776 t 7.6	7.7
δ	---	---	1.357 s	22.2	---	---	1.353 s	22.2
	L-Pro[6]		**L-Pro[6]**		**L-Pro[6]**		**L-Pro[6]**	
N	---	---	---	---	---	---	---	---
C=O	---	173.5	---	173.7	---	173.5	---	173.7
α	4.181 t-like 8.2	63.6	4.237 dd 8.5/7.0	63.5	4.179 t-like 8.2	63.6	4.235 dd 8.5/7.2	63.4
β	2.23[a]; 1.69[a]	28.3	2.20[a]; 1.70[a]	28.2	2.23[a]; 1.69[a]	28.3	2.20[a]; 1.70[a]	28.2
γ	1.97[a]; 1.86[a]	25.6	1.97[a]; 1.86[a]	25.6	1.97[a]; 1.86[a]	25.6	1.97[a]; 1.86[a]	25.6
δ	3.652 ddd 11.1/7.0/4.2; 3.572 ddd 11.1/8.6/6.2	48.2	3.662 dt-like 11.2/6.9; 3.607 dt-like 11.2/6.1	47.9	3.655 ddd 11.2/6.9/4.1; 3.566 ddd 11.2/8.6/6.2	48.2	3.651 dt-like 11.1/6.9; 3.613 dt-like 11.1/6.1	47.9
	D-Iva[7]		**D-Iva[7]**		**D-Iva[7]**		**D-Iva[7]**	
N-H	7.404 s	---	7.328 s	---	7.404 s	---	7.331 s	---
C=O	---	175.9	---	175.9	---	175.9	---	175.9
α	---	58.6	---	58.6	---	58.6	---	58.6
β	2.297 dq 14.3/7.6; 1.69[a]	25.6	2.310 dq 14.2/7.6; 1.68[a]	25.5	2.30[a]; 1.69[a]	25.6	2.307 dq 14.4/7.6; 1.69[a]	25.5
γ	0.755 t 7.6	7.1	0.753 t 7.6	7.1	0.754 t 7.6	7.1	0.752 t 7.6	7.1
δ	1.369 s	22.4	1.379 s	22.3	1.367 s	22.4	1.378 s	22.3

	L-Leu[8]		**L-Leu[8]**		**L-Leu[8]**		**L-Leu[8]**	
N-H	7.436 d 7.1	---	7.434 d 7.1	---	7.435 d 7.2	---	7.432 d 7.2	---
C=O	---	173.0	---	173.0	---	173.0	---	173.0
α	4.062 ddd 11.4/7.1/4.0	52.5	4.058 ddd 11.2/7.1/4.0	52.6	4.061 ddd 11.3/7.2/3.9	52.5	4.058 ddd 11.4/7.2/3.9	52.6
β	1.70[a]; 1.59[a]	39.0	1.72[a]; 1.59[a]	39.0	1.70[a]; 1.59[a]	39.0	1.72[a]; 1.59[a]	39.0
γ	1.74[a]	24.2	1.75[a]	24.2	1.74[a]	24.2	1.76[a]	24.2
δ	0.869 d 6.6	22.7	0.873 d 6.6	22.7	0.868 d 6.5	22.7	0.873 d 6.7	22.7
ε	0.816 d 6.6	20.3	0.819 d 6.6	20.3	0.816 d 6.5	20.3	0.819 d 6.7	20.3
	L-Gln[9]		**L-Gln[9]**		**L-Gln[9]**		**L-Gln[9]**	
N-H	7.535 d 7.0		7.536 d 7.0	---	7.536 d 7.1	---	7.519 d 7.1	---
C=O	---	170.7	---	170.7	---	170.7	---	170.7
α	3.927 ddd 10.3/7.0/4.7	53.7	3.935 ddd 10.5/7.0/4.6	53.7	3.926 ddd 10.3/7.1/4.7	53.7	3.937 ddd 10.4/7.1/4.6	53.7
β	1.99[a]; 1.84[a]	26.4	1.98[a]; 1.87[a]	26.4	1.98[a]; 1.84[a]	26.4	1.98[a]; 1.87[a]	26.4
γ	2.22[a]; 2.072 ddd 15.1/10.1/6.1	31.5	2.23[a]; 2.059 ddd 14.9/10.1/5.9	31.5	2.22[a]; 2.072 ddd 15.0/10.1/6.1	31.5	2.23[a]; 2.059 ddd 14.9/10.2/6.0	31.5
C=O	---	173.3	---	173.3	---	173.3	---	173.3
N-H₂	7.025 br s; 6.614 br s	---	7.005 br s; 6.581 br s	---	7.024 br s; 6.614 br s	---	7.005 br s; 6.581 br s	---
	Aib[10]		**Aib[10]**		**Aib[10]**		**Aib[10]**	
N-H	7.107 s	---	7.083 s	---	7.108 s	---	7.085 s	---
C=O	---	173.2	---	173.2	---	173.2	---	173.2
α	---	56.1	---	56.1	---	56.1	---	56.1
β	1.379 s	24.9	1.379 s	24.8	1.378 s	24.9	1.378 s	24.8
γ	1.364 s	25.5	1.365 s	25.5	1.364 s	25.4	1.364 s	25.4
	L-Leuol[11]		**L-Leuol[11]**		**L-Leuol[11]**		**L-Leuol[11]**	
N-H	6.622 d 9.0	---	6.624 d 9.0	---	6.622 d 9.1	---	6.625 d 9.0	---
α	3.750 m	48.7	3.750 m	48.7	3.750 m	48.7	3.750 m	48.7
β	1.30[a]	39.8	1.30[a]	39.8	1.30[a]	39.8	1.31[a]	39.8
γ	1.64[a]	23.7	1.64[a]	23.7	1.64[a]	23.7	1.64[a]	23.7
δ	0.854 d 6.6	23.4	0.851 d 6.7	23.4	0.854 d 6.6	23.4	0.851 d 6.7	23.4
ε	0.816 d 6.6	21.6	0.814 d 6.7	21.6	0.816 d 6.6	21.6	0.813 d 6.7	21.6
β'	3.274 m; 3.120 m	64.0	3.27[a]; 3.114 dt-like 10.6/6.8	64.0	3.27[a]; 3.120 m	64.0	3.27[a]; 3.114 dt-like 10.4/6.5	64.0
O-H	4.274 t-like 5.9	---	4.275 m	---	4.273 t-like 5.9	---	4.275 m	---

[a] Overlapping signals, ^{1}H chemical shifts were assigned from ^{1}H,^{13}C HSQC correlation peaks.

9.2.2 Solid-phase synthesis and absolute configuration of albupeptins A–D

The stereochemistry of Iva residues in albupeptins A–D (**9.1**–**9.4**) was investigated using a 2D NMR based approach (Table 9.2, Fig. 9.5) (De Zotti et al., 2010), which is non-destructive unlike Marfey's analysis. This methodology is based on ^{1}H chemical shift difference analyses between the diastereotopic β-methylene protons of Iva residues. Right-handed helical peptaibols exhibit large chemical shift differences of these protons for D-Iva ($\Delta\delta_H > 0.28$) and low values for L-Iva ($\Delta\delta_H < 0.20$) residues, whereas an opposite behavior is observed for left-handed helicity (De Zotti et al., 2010).

The large $\Delta\delta_H$ values of the geminal protons in the β-methylene group of Iva[7] in albupeptin A (**9.1**) as well as of Iva[1] and Iva[7] in **9.3** indicated the presence of D-configured Iva residues in case of right-handed helicity (Table 9.2). To elucidate the absolute configuration of albupeptins A (**9.1**) and C (**9.3**), a solid-phase synthesis of **9.1** and **9.3** was performed on a L-leucinol loaded

2-chlorotrityl polystyrene resin using Fmoc protected amino acids and tetramethylfluoro-formamidinium hexafluorophosphate (TFFH) as coupling reagent (Scheme 9.1).

Table 9.2. Chemical shift differences ($\Delta\delta_H$) of β-methylene protons of Iva residues in synthetic and natural albupeptins.

compound	$\Delta\delta_H$ in ppm			
	D-Iva[1]	L-Iva[5]	D-Iva[5]	D-Iva[7]
natural **9.1**	---	---	---	0.61
syn. **9.1**	---	---	---	0.60
natural **9.2**	---	0.18	---	0.63
syn. LD-**9.2**	---	0.18	---	0.63
syn. DD-**9.2**	---	---	0.40	0.60
natural **9.3**	0.30	---	---	0.61
syn. **9.3**	0.29	---	---	0.60
natural **9.4**	0.30	0.17	---	0.62
syn. DLD-**9.4**	0.30	0.17	---	0.63
syn. DDD-**9.4**	0.32	---	0.40	0.61

syn. = synthetic
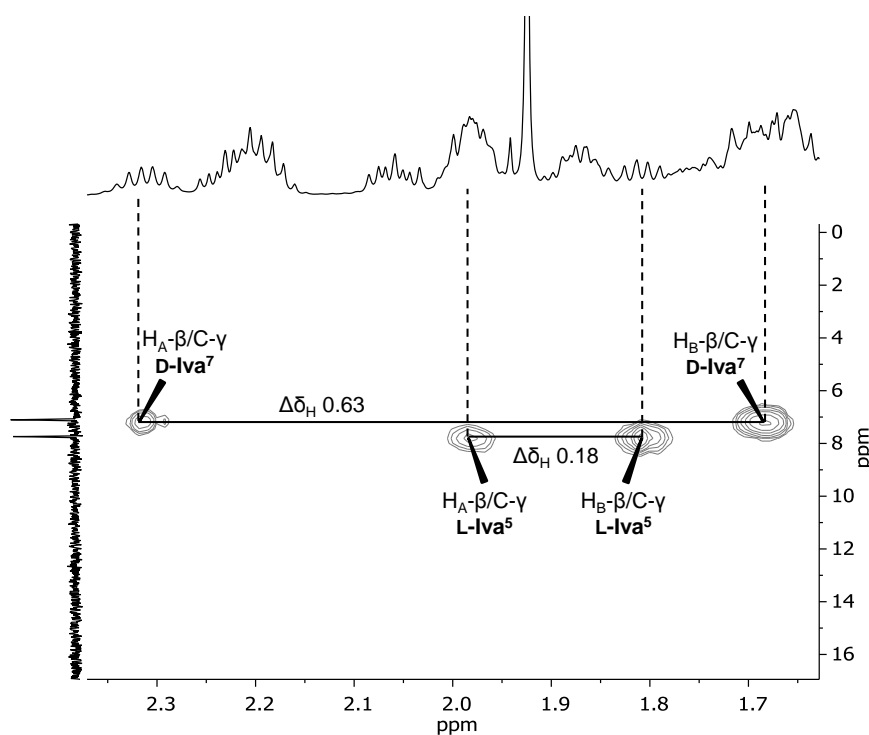
Fig. 9.5. Expanded ^{1}H,^{13}C HMBC spectrum of **9.2** (600 MHz, DMSO-d_6, 40 °C) displaying correlations between H-β signals and γ-methyl carbon resonances of L-Iva[5] and D-Iva[7], respectively (for further details see Table 9.2).

TFFH was used as an *in situ* reagent to obtain reactive amino acid fluorides (El-Faham and Khattab, 2009). It has been described as a useful coupling reagent for sterically hindered, poorly reactive α,α-dialkyl amino acids such as Aib and Iva (Hjørringgaard et al., 2009; Wenschuh et al., 1995). It proved to be superior to other coupling reagents, since well-known strategies such as PyBOP coupling did not lead to noticeable product formation in our preliminary studies. The total yields of the 11-mer peptaibols ranged from 1.0% to 3.5% (Table 9.4) which was sufficient to

support the structure elucidation. *N*-Terminal acetylation was accomplished after complete peptide assembly by treating the resin with Ac$_2$O followed by cleavage from the solid support using TFA or HCl in hexafluoroisopropanol (HFIP) (for details, see Chapter 9.4).

Scheme 9.1. Solid-phase peptide synthesis of albupeptins A–D (**9.1**, LD-**9.2**, **9.3**, DLD-**9.4**) and their isomers (DD-**9.2**, DDD-**9.4**)[a].

	X_{aa}^1	X_{aa}^5
9.1	Aib	Aib
LD-**9.2**	Aib	L-Iva
DD-**9.2**	Aib	D-Iva
9.3	D-Iva	Aib
DLD-**9.4**	D-Iva	L-Iva
DDD-**9.4**	D-Iva	D-Iva
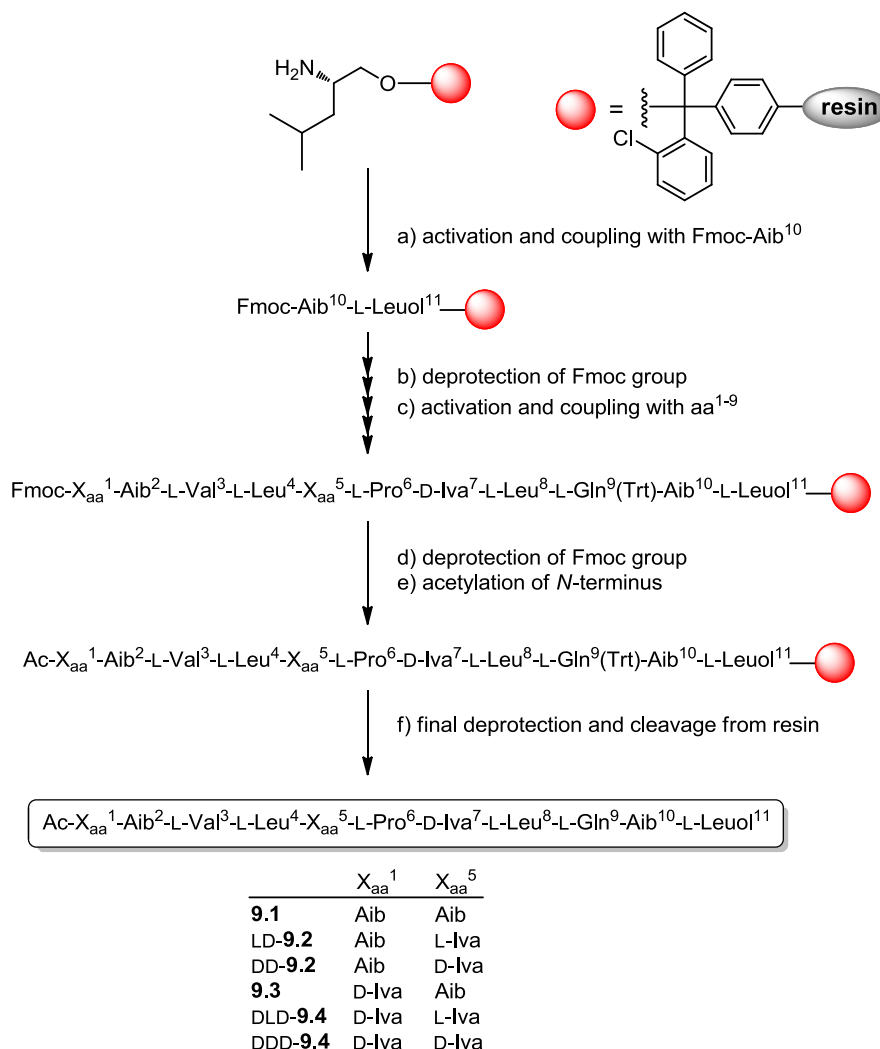
[a] Reagents and conditions: (a) 5 eq. Fmoc-Aib^{10}, 10 eq. DIPEA, 5 eq. TFFH, 18/60 min; (b) 20% piperidine/DMF, 5 min; (c) 5 eq. Fmoc-aa$^{1-9}$, 10 eq. DIPEA, 5 eq. TFFH, 12/60 min; (d) 20% piperidine/DMF, 8 min; (e) Ac$_2$O/DIPEA/DMF (15/15/70, v/v/v), 4 ml, 30 min; (f) TFA/CH$_2$Cl$_2$/H$_2$O/TIPS (47/47/4/2, v/v/v/v), 5 ml, 60 min.

The spectroscopic data from 1D NMR and CD experiments of the synthetic albupeptins **9.1** and **9.3** having Iva^7 and Iva^1/Iva^7 residues in D-configuration (and the other chiral amino acids in L-configuration) were in accordance with that of the corresponding natural albupeptins A (**9.1**) and C (**9.3**) (see Supporting Information). These investigations additionally indicate that albupeptins A (**9.1**) and C (**9.3**) form right-handed helical structures.

For albupeptins B (**9.2**) and D (**9.4**), however, the β-methylene proton chemical shift differences of Iva^5 were lower than 0.20 ppm, indicating an L-configuration, whereas large $\Delta\delta_H$

values for Iva[7] in **9.2** as well as Iva[1] and Iva[7] in **9.4** suggested the presence of D-configured residues (Table 9.2, Fig. 9.5).
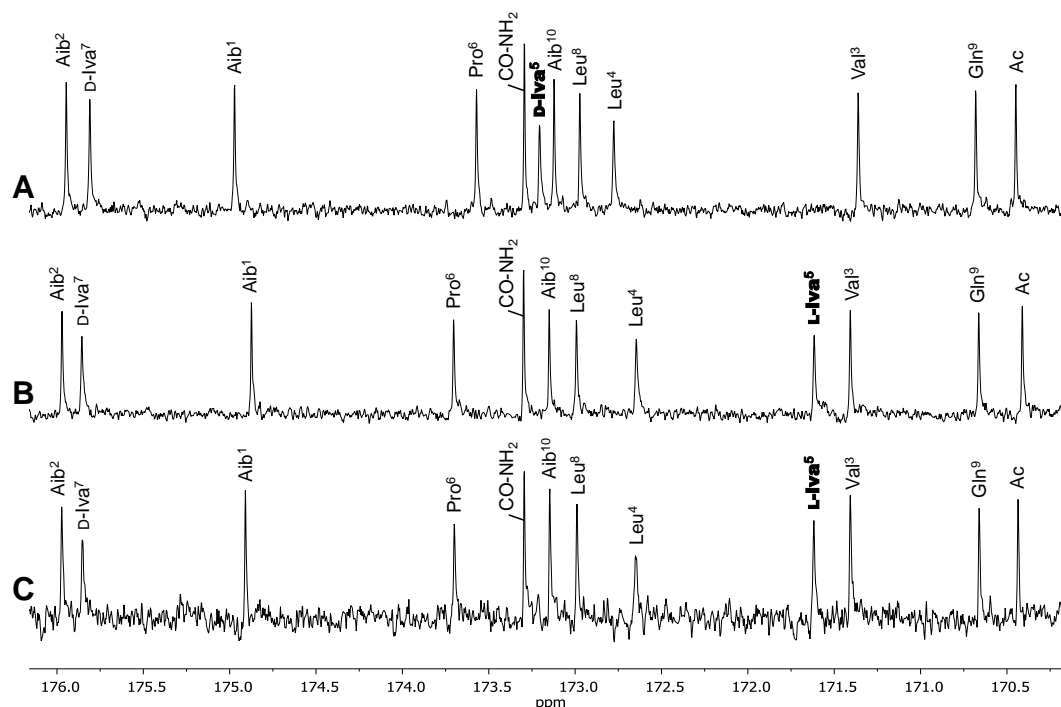
Fig. 9.6. Carbonyl region in the ^{13}C NMR spectra of the synthetic diastereomers (A) D-Iva[5]-D-Iva[7] (DD-**9.2**) and (B) L-Iva[5]-D-Iva[7] (LD-**9.2**) as well as (C) natural albupeptin B (**9.2**) (150 MHz, DMSO-d_6, 40 °C). The chemical shift of the Iva[5] carbonyl signal (annotated in bold) is strongly influenced by the configuration of the adjacent stereogenic center.

As albupeptins B (**9.2**) and D (**9.4**) were proposed to contain both L- and D-Iva residues in the same structure, the classical derivatization approach by using Marfey's reagent could not be applied. Therefore, the solid-phase synthesis of the L-Iva[5]-D-Iva[7] and additionally the D-Iva[5]-D-Iva[7] isomer of **9.2** was performed (Scheme 9.1). While the D-D-isomer (DD-**9.2**) showed in fact significantly different NMR spectra from those of natural product **9.2**, the spectroscopic data of the corresponding L-D-isomer (LD-**9.2**) were consistent with the natural albupeptin B (**9.2**) (Figs. 9.6 and S34). This was supported by RP18 HPLC analyses, since DD-**9.2** showed a clearly different chromatographic behavior than natural **9.2**, while the peak corresponding to LD-**9.2** co-eluted with albupeptin B (**9.2**) (Fig. S31). Subsequent solid-phase synthesis of DDD-**9.4** and DLD-**9.4** combined with comparison of spectroscopic data with the natural albupeptin D (**9.4**) confirmed the absolute configuration of Iva[5] to be L as well, accompanied by D-configured Iva[1] and Iva[7] residues (Figs. S37 and S38). The above results highlight that albupeptins B (**9.2**) and D (**9.4**) are members of the rare class of peptaibols that contain both stereoisomers of Iva in the same sequence (Degenkolb et al., 2007).

9.2.3 Antiphytopathogenic activity

The biological activity of peptaibols **9.1–9.4** were examined against the phytopathogenic ascomycetous fungi *Botrytis cinerea* (grey mold pathogen on many crops including strawberries

and wine grapes) and *Septoria tritici* (causing septoria leaf blotch of wheat) as well as the oomycete *Phytophthora infestans* (causal agent of the late blight disease on potato and tomato) using a 96 well microtiter plate assay (Table 9.3). The commercial fungicides dodine and pyraclostrobin were used as references for a membrane active fungicide and a protein inhibitor fungicide, respectively. It is noteworthy that among all peptaibols reported in the literature, only a few were tested against plant pathogenic organisms such as trichokonin VI, which exhibited activity against *Phytophthora parasitica*, *Fusarium oxysporum*, and *Botrytis cinerea* (Shi et al., 2012). Albupeptins **9.1–9.4** exhibited modest activity against *B. cinerea* and were inactive against *S. tritici* ($IC_{50} > 100$ μM). Notably, the growth inhibitory effects of **9.1–9.4** against *B. cinerea* increased with the number of present Iva residues (IC_{50} **9.1**: 49.6 μM, **9.2**: 38.9 μM, **9.3**: 35.2 μM, **9.4**: 24.5 μM). While albupeptin A (**9.1**) was devoid of significant activity against *P. infestans* ($IC_{50} > 100$ μM), compounds **9.2–9.4** showed minor effects (IC_{50} **9.2**: 97.6 μM, **9.3**: 84.7 μM, **9.4**: 84.3 μM).

Table 9.3. Antiphytopathogenic activity of compounds **9.1–9.4** against *B. cinerea*, *S. tritici*, and *P. infestans* (IC_{50}, μM).

compound	*B. cinerea*	*S. tritici*	*P. infestans*
9.1	49.6 ± 2.1	> 100	> 100
9.2	38.9 ± 2.8	> 100	97.6 ± 0.9
9.3	35.2 ± 1.0	> 100	84.7 ± 1.2
9.4	24.5 ± 2.9	> 100	84.3 ± 6.3
dodine[a]	9.4 ± 0.6	2.8 ± 0.2	43.8 ± 5.6
pyraclostrobin[a]	< 0.0052	< 0.0052	0.018 ± 0.002

[a] Used as reference compounds.

9.3 Conclusions

In summary, four new 11-residue peptaibols (**9.1–9.4**) were isolated from the mycelial culture of *G. album* KSH 719. Their structures were elucidated on the basis of 1D and 2D NMR analyses as well as ESI-HRMS[n] experiments. The absolute configuration of compounds **9.1–9.4** was elucidated with the aid of ^{1}H NMR chemical shift analyses in conjunction with solid-phase peptide synthesis. The present study demonstrates that albupeptins B (**9.2**) and D (**9.4**) belong to the rare class of peptaibols that contain both stereoisomers of Iva (D- and L-configured) in the same sequence. Finally, peptaibols **9.1–9.4** showed moderate activity towards *B. cinerea*, modest effects against *P. infestans* and were devoid of substantial activity towards *S. tritici*.

9.4 Experimental Section

General Experimental Procedures. Size exclusion column chromatography was performed on Sephadex LH 20 (Fluka), while analytical TLC was performed on precoated silica gel F_{254} plates

(Merck, Germany). Diaion HP 20 was purchased from Supelco (USA). Peptaibols were visualized on TLC plates according to the method of Chinard (1952) that was modified by exchange of acetic acid and phosphoric acid by *p*-toluenesulfonic acid (*p*-TsOH). Therefore, the plates were sprayed with an ethanolic solution of 1.0% ninhydrin and 2.5% *p*-TsOH, and heated to 110 °C with a hot air gun, resulting in pink to purple-brownish spots. In comparison to the widely used two-step hydrochloric acid based ninhydrin analysis (Pandey et al., 1979), we found this simple and fast *p*-TsOH based procedure also convenient for silica gel coated aluminium TLC plates. UV spectra were obtained from a Jasco V-560 UV/Vis spectrophotometer, whereas CD spectra were acquired on a Jasco J-815 CD spectrophotometer. The specific rotation was measured with a Jasco P-2000 polarimeter.

The NMR spectra were obtained from an Agilent VNMRS 600 system at +40 °C. The compounds were dissolved in DMSO-d_6 (99.96% D) and spectra were recorded at 599.83 MHz (^{1}H) and 150.84 MHz (^{13}C), respectively. 1D (^{1}H, ^{13}C) and 2D spectra (^{1}H,^{13}C and ^{1}H,^{15}N gHSQCAD, ^{1}H,^{13}C gHMBCAD, ^{1}H,^{1}H gDQCOSY, ^{1}H,^{1}H zTOCSY, ^{1}H,^{1}H ROESY) were measured using standard CHEMPACK 5 pulse sequences implemented in the VnmrJ 4.0 spectrometer software. The mixing time for the TOCSY and ROESY spectra was set to 80 and 200 ms, respectively. ^{1}H and ^{13}C chemical shifts are given relative to internal DMSO-d_6 (δ_H 2.510 ppm and δ_C 39.5 ppm), while ^{15}N chemical shifts were referenced to liquid NH$_3$ (δ_N 0 ppm).

The solid-phase peptide synthesis was performed on a ResPep SL peptide synthesizer (Intavis Bioanalytical Instruments, Germany). The L-configured Fmoc-amino acids Fmoc-Pro-OH, Fmoc-Leu-OH, Fmoc-Gln(Trt)-OH were supplied by Novabiochem (Germany), while Fmoc-Aib-OH and the L-leucinol 2-chlorotrityl polystyrene resin were purchased from Iris Biotech GmbH (Germany). D- and L-Fmoc-Iva-OH were purchased from Peptech Corp. (USA), while TFFH and HFIP were obtained from Carbolution Chemicals (Germany). Piperidine, Ac$_2$O, DIPEA, TFA, HCl, and DMF were purchased from Sigma Aldrich (Germany).

The positive and negative ion high-resolution ESI and collision induced dissociation (CID) MS^n spectra were obtained from an Orbitrap Elite mass spectrometer (Thermo Fisher Scientific, Germany) equipped with a HESI electrospray ion source (positive spray voltage 4.0 kV, negative spray voltage 3.5 kV, capillary temperature 275 °C, source heater temperature 200 °C, FTMS resolution 30.000). Nitrogen was used as a sheath and auxiliary gas. The MS system was coupled to an ultra-high performance liquid chromatography (UHPLC) system (Dionex UltiMate 3000, Thermo Fisher Scientific), equipped with a RP18 column (particle size 1.9 μm, pore size 175 Å, 50 × 2.1 mm ID, Hypersil GOLD; Thermo Fisher Scientific; column temperature 40 °C) and a photodiode array detector (200–600 nm, Thermo Fisher Scientific). The mobile phases were H$_2$O (A; Fluka Analytical, LC-MS Chromasolv) and CH$_3$CN (B; Fluka Analytical, LC-MS Chromasolv) with 0.2% formic acid by using a gradient system (0–5 min, 45–55% B; 5–13 min, 55–95% B, 13–16 min, 95% B, 16–17 min 95–45% B, flow rate 0.2 ml/min). The CID mass spectra (buffer gas: helium) were recorded using normalized collision energies (NCE) of 35–55%

(see Supporting Information). The instrument was externally calibrated by the Pierce LTQ Velos ESI positive ion calibration solution (product no. 88323) and Pierce ESI negative ion calibration solution (product no. 88324) from Thermo Fisher Scientific. The data were evaluated using the software Xcalibur 2.7 SP1.

Preparative RP18 HPLC was performed on a Knauer system equipped with a WellChrom K-1001 pump and a WellChrom K-2501 UV detector using either column 1 (ODS-A, 5 μm, 120 Å, 150 × 10 mm ID, YMC, USA) or column 2 (polymeric C18, 8 μm, 300 Å, 250 × 9 mm ID, VYDAC, USA).

Fungal strain and cultivation. *Gliocladium album* (Preuss) Petch (strain KSH 719) was isolated in September 1987 from the myxomycete *Fuligo septica* in Himmelreich near Aichach, Bavaria, Germany (leg./det. W. Helfer) (Helfer, 1991). A voucher specimen (M20/87) is deposited at the herbarium of the University Regensburg. The fungal culture of *G. album* KSH 719 was stored on malt peptone agar (MPA) plates and transferred periodically. The upscaled semi-solid cultures, used for isolation of peptaibols, were grown in 20 Erlenmeyer flasks (size 1 l) each containing 1.5 g of cotton wool and 250 ml of malt peptone medium (2.5 g malt and 0.625 g peptone in 250 ml deionized water) resulting in a total volume of 5 l. Each culture flask was inoculated with a 10 × 10 mm agar plug of colonized fungus and incubated for 28 days at room temperature without agitation.

Extraction and isolation. The mycelia were separated from the culture broth by vacuum filtration, frozen with liquid nitrogen, and extracted with MeOH (3 × 3 l). The yellow solution was evaporated to dryness, redissolved in H_2O, and combined with the culture broth. Activated Diaion HP 20 (30 g) was added and agitated for 12 hours at room temperature. Diaion HP 20 was removed by vacuum filtration, washed with H_2O, eluted with MeOH, and the extract was evaporated *in vacuo* to dryness. The resulting yellow crude MeOH extract (3.2 g) was subjected to size exclusion column chromatography on Sephadex LH 20 (470 × 50 mm) eluting with MeOH to afford 63 fractions (10 ml each). Fractions 28–31 were combined (112.5 mg) and finally purified by preparative RP18 HPLC using column 1 with H_2O (A) and CH_3CN (B) as eluents (0–20 min, 55–62% B, flow rate 3.5 ml/min) to afford **9.1** (t_R 15.4 min, 12.3 mg), **9.2** (t_R 16.3 min, 2.1 mg), **9.3** (t_R 18.0 min, 14.2 mg), and **9.4** (t_R 19.1 min, 2.3 mg).

Natural albupeptin A (9.1): white, amorphous solid; TLC R_f 0.65 (*n*-BuOH/AcOH/H_2O 4:1:1); $[\alpha]^{23}_D$ +3.5 (*c* 0.250, MeOH); CD (MeOH) $[\theta]_{193}$ +99496, $[\theta]_{206}$ −90392, $[\theta]_{222}$ −38712 °×cm²×dmol⁻¹; UV (MeOH) λ_{max} (log ε) 200 (4.49) nm; ¹H NMR and ¹³C NMR see Table 9.1; ESI-HRMS *m/z* 1149.7639 ([M+H]⁺, calculated for $C_{56}H_{101}N_{12}O_{13}^+$ 1149.7606); ESI-HRMSⁿ see Tables S2 and S3.

Synthetic albupeptin A (9.1): white, amorphous solid; CD (MeOH) $[\theta]_{193}$ +95365, $[\theta]_{206}$ −82745, $[\theta]_{222}$ −34085 °×cm²×dmol⁻¹; UV (MeOH) λ_{max} (log ε) 200 (4.46) nm; ¹H NMR and ¹³C NMR in

agreement with natural **9.1** (^{13}C difference below 0.1 ppm); ESI-HRMS *m/z* 1149.7636 ([M+H]$^+$, calculated for $C_{56}H_{101}N_{12}O_{13}^+$ 1149.7606); ESI-HRMS^n in accordance with natural **9.1**.

Natural albupeptin B (9.2): white, amorphous solid; TLC R_f 0.66 (*n*-BuOH/AcOH/H$_2$O 4:1:1); $[\alpha]^{25}_D$ +1.3 (*c* 0.372, MeOH); CD (MeOH) $[\theta]_{193}$ +110932, $[\theta]_{206}$ −86627, $[\theta]_{222}$ −41277 $°\times cm^2\times dmol^{-1}$; UV (MeOH) λ_{max} (log ε) 200 (4.47) nm; ^{1}H NMR and ^{13}C NMR see Table 9.1; ESI-HRMS *m/z* 1163.7781 ([M+H]$^+$, calculated for $C_{57}H_{103}N_{12}O_{13}^+$ 1163.7762); ESI-HRMS^n see Tables S2 and S3.

Synthetic albupeptin B (LD-9.2): white, amorphous solid; CD (MeOH) $[\theta]_{193}$ +80069, $[\theta]_{206}$ −71352, $[\theta]_{222}$ −33569 $°\times cm^2\times dmol^{-1}$; UV (MeOH) λ_{max} (log ε) 200 (4.49) nm; ^{1}H NMR and ^{13}C NMR in agreement with natural **9.2** (^{13}C difference below 0.1 ppm); ESI-HRMS *m/z* 1163.7763 ([M+H]$^+$, calculated for $C_{57}H_{103}N_{12}O_{13}^+$ 1163.7762); ESI-HRMS^n in accordance with natural **9.2**.

Synthetic diastereomer of albupeptin B (DD-9.2): white, amorphous solid; CD (MeOH) $[\theta]_{193}$ +106018, $[\theta]_{206}$ −93294, $[\theta]_{222}$ −43029 $°\times cm^2\times dmol^{-1}$; UV (MeOH) λ_{max} (log ε) 200 (4.51) nm; ESI-HRMS *m/z* 1163.7768 ([M+H]$^+$, calculated for $C_{57}H_{103}N_{12}O_{13}^+$ 1163.7762).

Natural albupeptin C (9.3): white, amorphous solid; TLC R_f 0.66 (*n*-BuOH/AcOH/H$_2$O 4:1:1); $[\alpha]^{24}_D$ +11.7 (*c* 0.290, MeOH); CD (MeOH) $[\theta]_{193}$ +103910, $[\theta]_{206}$ −86661, $[\theta]_{222}$ −37700 $°\times cm^2\times dmol^{-1}$; UV (MeOH) λ_{max} (log ε) 200 (4.49) nm; ^{1}H NMR and ^{13}C NMR see Table 9.1; ESI-HRMS *m/z* 1163.7768 ([M+H]$^+$, calculated for $C_{57}H_{103}N_{12}O_{13}^+$ 1163.7762); ESI-HRMS^n see Tables S2 and S3.

Synthetic albupeptin C (9.3): white, amorphous solid; CD (MeOH) $[\theta]_{193}$ +75581, $[\theta]_{206}$ −68795, $[\theta]_{222}$ −28763 $°\times cm^2\times dmol^{-1}$; UV (MeOH) λ_{max} (log ε) 200 (4.15) nm; ^{1}H NMR and ^{13}C NMR in agreement with natural **9.3** (^{13}C difference below 0.1 ppm); ESI-HRMS *m/z* 1163.7771 ([M+H]$^+$, calculated for $C_{57}H_{103}N_{12}O_{13}^+$ 1163.7762); ESI-HRMS^n in accordance with natural **9.3**.

Natural albupeptin D (9.4): white, amorphous solid; TLC R_f 0.68 (*n*-BuOH/AcOH/H$_2$O 4:1:1); $[\alpha]^{26}_D$ +7.2 (*c* 0.326, MeOH); CD (MeOH) $[\theta]_{193}$ +109018, $[\theta]_{206}$ −76991, $[\theta]_{222}$ −38243 $°\times cm^2\times dmol^{-1}$; UV (MeOH) λ_{max} (log ε) 200 (4.47) nm; ^{1}H NMR and ^{13}C NMR see Table 9.1; ESI-HRMS *m/z* 1177.7929 ([M+H]$^+$, calculated for $C_{58}H_{105}N_{12}O_{13}^+$ 1177.7919); ESI-HRMS^n see Tables S2 and S3.

Synthetic albupeptin D (DLD-9.4): white, amorphous solid; CD (MeOH) $[\theta]_{193}$ +90226, $[\theta]_{206}$ −78074, $[\theta]_{222}$ −39060 $°\times cm^2\times dmol^{-1}$; UV (MeOH) λ_{max} (log ε) 200 (4.46) nm; ^{1}H NMR and ^{13}C NMR in agreement with natural **9.4** (^{13}C difference below 0.1 ppm); ESI-HRMS *m/z* 1177.7927 ([M+H]$^+$, calculated for $C_{58}H_{105}N_{12}O_{13}^+$ 1177.7919); ESI-HRMS^n in accordance with natural **9.4**.

Synthetic diastereomer of albupeptin D (DDD-9.4): white, amorphous solid; CD (MeOH) $[\theta]_{193}$ +65235, $[\theta]_{206}$ −56358, $[\theta]_{222}$ −24281 $°\times cm^2 \times dmol^{-1}$; UV (MeOH) λ_{max} (log ε) 200 (4.44) nm; ESI-HRMS m/z 1177.7913 ($[M+H]^+$, calculated for $C_{58}H_{105}N_{12}O_{13}^+$ 1177.7919).

Automated solid-phase peptide synthesis. Compounds **9.1**–**9.4** were synthesized in a 0.1 or 0.2 mmol scale (Table 9.4), starting from a L-leucinol 2-chlorotrityl polystyrene resin (200–400 mesh, loading 0.62 mmol/g resin). The used coupling cycle (Scheme 9.1) was modified from the standard Intavis protocol regarding the activation (12 min) and coupling time (60 min). The Fmoc amino acids, piperidine and TFFH were dissolved in DMF. DIPEA was used as a base during the activation steps (for detailed protocol see Table S1). *N*-Terminal acetylation was performed after complete peptide assembly by treating the resin with Ac_2O and DIPEA in DMF (15/15/70, v/v/v) for 30 min. Solid-phase cleavage and deprotection of peptides **9.1** and **9.3** was achieved by treatment with 5 ml TFA/CH_2Cl_2/H_2O/TIPS (47/47/4/2, v/v/v/v) for 60 min. For peptides LD-**9.2**, DD-**9.2**, DLD-**9.4**, and DDD-**9.4**, the cleavage and deprotection was accomplished by treatment with 10.1 ml HCl/HFIP/DCM (0.1/2/8, v/v/v) for 3 hours and shaking at 550 rpm. The cleavage mixture was concentrated under reduced pressure and subsequently lyophilized to obtain the crude peptide mixture. The crude products were dissolved in MeOH and subjected to size exclusion column chromatography on Sephadex LH 20 (360 × 30 mm) eluting with MeOH. Fractions containing the respective peptaibol were combined and finally purified by preparative RP18 HPLC using column 2 with H_2O + 0.1% TFA or FA (A) and CH_3CN + 0.1% TFA or FA (B) as eluents at a flow rate of 4.5 ml/min, affording total yields between 1.0% and 3.5%. Further experimental details are given in Table 9.4.

Table 9.4. Experimental purification details of synthesized albupeptins.

compound	crude product	synthesis scale	HPLC method	t_R	amount	total yield
9.1	59.5 mg	0.1 mmol	0–21 min, 35–44% B + TFA	21.8 min	3.4 mg	3.0%
LD-**9.2**	238.0 mg	0.2 mmol	0–20 min; 45–50% B + FA	8.2 min	8.2 mg	3.5%
DD-**9.2**	203.1 mg	0.2 mmol	0–20 min; 45–50% B + FA	8.4 min	5.8 mg	2.5%
9.3	69.6 mg	0.1 mmol	0–20 min, 35–47% B + TFA	23.4 min	3.6 mg	3.1%
DLD-**9.4**	260.7 mg	0.2 mmol	0–20 min; 45–55% B + FA	9.3 min	6.3 mg	2.7%
DDD-**9.4**	277.2 mg	0.2 mmol	0–20 min; 45–55% B + FA	9.4 min	2.4 mg	1.0%

Antiphytopathogenic bioassay. Crude extracts, fractions, and pure compounds were tested in a 96-well microtiter plate assay against *Botrytis cinerea* Pers., *Septoria tritici* Desm., and *Phytophthora infestans* (Mont.) De Bary according to the fungicide resistance action committee (FRAC) with minor modifications (Stammler and Semar, 2011; Stammler and Speakman, 2006; Stammler, 2006): Crude extracts and fractions were examined at a final concentration of 125 µg/ml, whereas pure compounds were tested in a serial dilution ranging from 100 µM to 0.1 µM. The solvent DMSO was used as a negative control (max. concentration 2.5%), and the

commercially used fungicides dodine and pyraclostrobin (from Sigma Aldrich) served as reference compounds. Seven days after inoculation, the pathogen growth was evaluated by measurement of the optical density (OD) at λ 405 nm with a Tecan GENios Pro microplate reader (5 measurements per well using multiple reads in a 3×3 square). Each experiment was carried out in triplicates. IC_{50} values were calculated from dose-response curves on the basis of sigmoidal curve fitting (four parameter logistic) using the software SigmaPlot 12.0.

9.5 References

Ayers, S., Ehrmann, B.M., Adcock, A.F., Kroll, D.J., Carcache de Blanco, E.J., Shen, Q., Swanson, S.M., Falkinham, J.O., Wani, M.C., Mitchell, S.M., Pearce, C.J., Oberlies, N.H., 2012. Peptaibols from two unidentified fungi of the order Hypocreales with cytotoxic, antibiotic, and anthelmintic activities. *J. Pept. Sci.* 18, 500–510.

Berg, A., Ritzau, M., Ihn, W., Schlegel, B., Fleck, W.F., Heinze, S., Gräfe, U., 1996. Isolation and structure of bergofungin, a new antifungal peptaibol from *Emericellopsis donezkii* HKI 0059. *J. Antibiot.* 49, 817–820.

Bertinetti, B. V, Rodriguez, M.A., Godeas, A.M., Cabrera, G.M., 2010. 1H,1'H-[3,3']biindolyl from the terrestrial fungus *Gliocladium catenulatum*. *J. Antibiot.* 63, 681–683.

Brückner, H., Przybylski, M., 1984. Methods for the rapid detection, isolation and sequence determination of "peptaibols" and other aib-containing peptides of fungal origin. I. Gliodeliquescin a from *Gliocladium deliquescens*. *Chromatographia* 19, 188–199.

Chinard, F.P., 1952. Photometric estimation of proline and ornithine. *J. Biol. Chem.* 199, 91–95.

Chu, M., Truumees, I., Rothofsky, M.L., Patel, M.G., Gentile, F., Das, P.R., Puar, M.S., Lin, S.L., 1995. Inhibition of c-fos proto-oncogene induction by Sch 52900 and Sch 52901, novel diketopiperazine produced by *Gliocladium* sp. *J. Antibiot.* 48, 1440–1445.

Chugh, J.K., Wallace, B.A., 2001. Peptaibols: Models for ion channels. *Biochem. Soc. Trans.* 29, 565–570.

De Zotti, M., Schievano, E., Mammi, S., Kaptein, B., Broxterman, Q.B., Singh, S.B., Brückner, H., Toniolo, C., 2010. Configurational assignment of D- and L-isovalines in intact, natural, and synthetic peptides by 2D-NMR spectroscopy. *Chem. Biodivers.* 7, 1612–1624.

Degenkolb, T., Brückner, H., 2008. Peptaibiomics: Towards a myriad of bioactive peptides containing C^{α}-dialkylamino acids? *Chem. Biodivers.* 5, 1817–1843.

Degenkolb, T., Kirschbaum, J., Brückner, H., 2007. New sequences, constituents, and producers of peptaibiotics: An updated review. *Chem. Biodivers.* 4, 1052–1067.

Dong, J.Y., He, H.P., Shen, Y.M., Zhang, K.Q., 2005. Nematicidal epipolysulfanyldioxopiperazines from *Gliocladium roseum*. *J. Nat. Prod.* 68, 1510–1513.

Dong, J.Y., Zhou, W., Li, L., Li, G.H., Liu, Y.J., Zhang, K.Q., 2006. A new epidithiodioxopiperazine metabolite isolated from *Gliocladium roseum* YMF1.00133. *Chinese Chem. Lett.* 17, 922–924.

El-Faham, A., Khattab, S.N., 2009. Utilization of N,N,N,'N'-tetramethylfluoroformamidinium hexafluorophosphate (TFFH) in peptide and organic synthesis. *Synlett* 6, 886–904.

Ellis, M.B., Ellis, J.P., 1988. Microfungi on miscellaneous substrates: An identification handbook, Brittonia. Croom Helm, London.

Gams, W., 1971b. Cephalosporium-artige Schimmelpilze (Hyphomycetes). VEB Gustav Fischer Verlag, Jena, pp. 1–252.

Gräfe, U., Ihn, W., Ritzau, M., Schade, W., Stengel, C., Schlegel, B., Fleck, W.F., Künkel, W., Härtl, A., Gutsche, W., 1995. Helioferins; novel antifungal lipopeptides from *Mycogone rosea*: screening, isolation, structures and biological properties. *J. Antibiot.* 48, 126–133.

Helfer, W., 1991. Pilze auf Pilzfruchtkörpern: Untersuchungen zur Ökologie, Systematik und Chemie. IHW-Verlag, Eching, pp. 1–157.

Hjørringgaard, C.U., Pedersen, J.M., Vosegaard, T., Nielsen, N.C., Skrydstrup, T., 2009. An automatic solid-phase synthesis of peptaibols. *J. Org. Chem.* 74, 1329–1332.

Jaworski, A., Brückner, H., 2000. New sequences and new fungal producers of peptaibol antibiotics antiamoebins. *J. Pept. Sci.* 6, 149–167.

Joshi, B.K., Gloer, J.B., Wicklow, D.T., 1999. New verticillin and glisoprenin analogues from *Gliocladium catenulatum*, a mycoparasite of *Aspergillus flavus* sclerotia. *J. Nat. Prod.* 62, 730–733.

Kasai, Y., Komatsu, K., Shigemori, H., Tsuda, M., Mikami, Y., Kobayashi, J., 2005. Cladionol A, a polyketide glycoside from marine-derived fungus *Gliocladium species*. *J. Nat. Prod.* 68, 777–779.

Kronen, M., Kleinwächter, P., Schlegel, B., Härtl, A., Gräfe, U., 2001. Ampullosporines B, C, D, E1, E2, E3 and E4 from *Sepedonium ampullosporum* HKI-0053: structures and biological activities. *J. Antibiot.* 54, 175–178.

Lee, S.J., Yun, B.S., Cho, D.H., Yoo, I.D., 1999. Tylopeptins A and B, new antibiotic peptides from *Tylopilus neofelleus*. *J. Antibiot.* 52, 998–1006.

Nishida, H., Huang, X.H., Tomoda, H., Omura, S., 1992. Glisoprenins, new inhibitors of acyl-CoA: cholesterol acyltransferase produced by *Gliocladium* sp. FO-1513. II. Structure elucidation of glisoprenins A and B. *J. Antibiot.* 45, 1669–1676.

Pandey, R.C., Misra, R., Rinehart, K.L., 1979. Visualization of N-protected peptides, amino acids and aminocyclitol antibiotics on a thin-layer chromatogram by ninhydrin. *J. Chromatogr. A* 170, 498–501.

Petch, T., 1939. *Gliocladium. Trans. Br. Mycol. Soc.* 22, 257–263.

Rahaman, A., Lazaridis, T., 2014. A thermodynamic approach to alamethicin pore formation. *BBA - Biomembr.* 1838, 98–105.

Ritzau, M., Heinze, S., Dornberger, K., Berg, A., Fleck, W., Schlegel, B., Hartl, A., Gräfe, U., 1997. Ampullosporin, a new peptaibol-type antibiotic from *Sepedonium ampull*osporum HKI-0053 with neuroleptic activity in mice. *J. Antibiot.* 50, 722–728.

Rodriguez, M.A., Cabrera, G., Gozzo, F.C., Eberlin, M.N., Godeas, A., 2011. *Clonostachys rosea* BAFC3874 as a *Sclerotinia sclerotiorum* antagonist: Mechanisms involved and potential as a biocontrol agent. *J. Appl. Microbiol.* 110, 1177–1186.

Schiell, M., Hofmann, J., Kurz, M., Schmidt, F.R., Vértesy, L., Vogel, M., Wink, J., Seibert, G., 2001. Cephaibols, new peptaibol antibiotics with anthelmintic properties from *Acremonium tubakii* DSM 12774. *J. Antibiot.* 54, 220–233.

Shi, M., Chen, L., Wang, X.W., Zhang, T., Zhao, P.B., Song, X.Y., Sun, C.Y., Chen, X.L., Zhou, B.C., Zhang, Y.Z., 2012. Antimicrobial peptaibols from *Trichoderma pseudokoningii* induce programmed cell death in plant fungal pathogens. *Microbiology* 158, 166–175.

Stadler, M., Seip, S., Müller, H., Henkel, T., Lagojda, A., Kleymann, G., 2001. New antiviral peptaibols from the mycoparasitic fungus *Sepedonium microspermum*, in: Book of Abstracts, 13. Irseer Naturstofftage der DECHEMA, Irsee.

Stammler, G., 2006. *Phytophthora infestans* microtiter method with sporangia. URL http://www.frac.info/docs/default-source/monitoring-methods/approved-methods/phytin-microtiter-method-sporangia-basf-2006-v1.pdf?sfvrsn=4 (accessed 24th October 2015).

Stammler, G., Semar, M., 2011. Sensitivity of *Mycosphaerella graminicola* (anamorph: *Septoria tritici*) to DMI fungicides across Europe and impact on field performance. *EPPO Bull.* 41, 149–155.

Stammler, G., Speakman, J., 2006. Microtiter method to test the sensitivity of *Botrytis cinerea* to boscalid. *J. Phytopathol.* 154, 508–510.

Tavano, R., Malachin, G., De Zotti, M., Peggion, C., Biondi, B., Formaggio, F., Papini, E., 2015. The peculiar *N*- and *C*-termini of trichogin GA IV are needed for membrane interaction and human cell death induction at doses lacking antibiotic activity. *BBA - Biomembr.* 1848, 134–144.

Thines, E., Eilbert, F., Anke, H., Sterner, O., 1998. Glisoprenins C, D and E, new inhibitors of appressorium formation in *Magnaporthe grisea*, from cultures of *Gliocladium roseum*. 1. Production and biological activities. *J. Antibiot.* 51, 117–122.

Tomoda, H., Ohyama, Y., Abe, T., Tabata, N., Namikoshi, M., Yamaguchi, Y., Masuma, R., Omura, S., 1999. Roselipins, inhibitors of diacylglycerol acyltransferase, produced by *Gliocladium roseum* KF-1040. *J. Antibiot.* 52, 689–694.

Usami, Y., Yamaguchi, J., Numata, A., 2004. Gliocladins A–C and glioperazine; cytotoxic dioxo- or trioxopiperazine metabolites from a *Gliocladium* sp. separated from a sea hare. *Heterocycles* 63, 1123–1129.

Wenschuh, H., Beyermann, M., Haber, H., Seydel, J.K., Krause, E., Bienert, M., Carpino, L.A., El-Faham, A., Albericio, F., 1995. Stepwise automated solid phase synthesis of naturally occurring peptaibols using FMOC amino acid fluorides. *J. Org. Chem.* 60, 405–410.

Yun, B.S., Yoo, I.D., Kim, Y.S.H., Kim, Y.S.H., Lee, S.J., Kim, K.S., Yeo, W.H., 2000. Peptaivirins A and B, two new antiviral peptaibols against TMV infection. *Tetrahedron Lett.* 41, 1429–1431.

9.6 Supporting Information

Supplementary data associated with this article (spectroscopic data and comparison of synthetic and natural albupeptins A–D (**9.1**–**9.4**); ESI-HRMS[n] data of natural albupeptins A–D; protocol for solid-phase peptide synthesis) can be found at http://dx.doi.org/10.1002/ejoc.201501124.

10 Tulasporins A–D, 19-residue peptaibols from the mycoparasitic fungus *Sepedonium tulasneanum*

	R^1	X$_{aa}$^{5}	R^2	X$_{aa}$^{8}
tulasporin A	CH$_3$	Aib	H	Gly
tulasporin B	CH$_2$CH$_3$	Iva	H	Gly
tulasporin C	CH$_3$	Aib	CH$_3$	Ala
tulasporin D	CH$_2$CH$_3$	Iva	CH$_3$	Ala
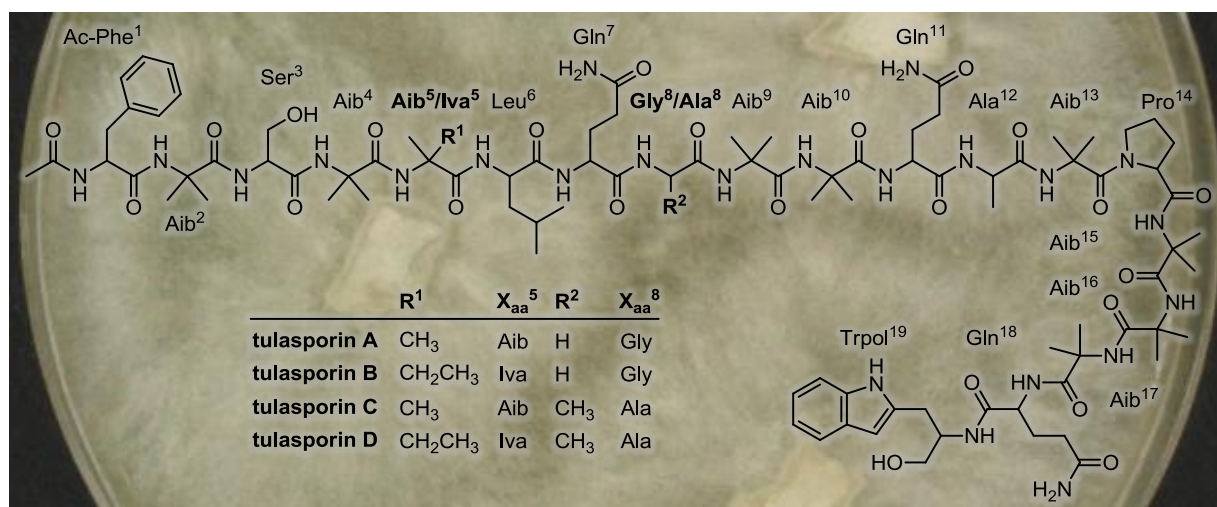
Abstract

Four new 19-residue peptaibols, named tulasporins A–D (**10.1**–**10.4**), were isolated from the semi-solid cultures of *Sepedonium tulasneanum*. Their structures were elucidated on the basis of extensive ESI-HRMS^n fragmentation studies as well as ^{1}H NMR spectroscopic analyses. Interestingly, the structures of tulasporins A–D (**10.1**–**10.4**) resemble those of chrysospermins isolated earlier from cultures of *S. chrysospermum*. Previously, it was hypothesized that the peptaibol production by *Sepedonium* species correlates with the morphology of the aleurioconidia, as exclusively round-shaped aleurioconidia forming species produced peptaibols. Since the investigated *Sepedonium tulasneanum* produces oval aleurioconidia, this study can be considered as the first report of peptaibols from a *Sepedonium* strain with oval-shaped aleurioconidia. Thus, it could be demonstrated that both round as well as oval aleurioconidia forming *Sepedonium* species are able to produce peptaibols. Tulasporins A–D (**10.1**–**10.4**), when tested against phytopathogenic organisms, exhibited good growth inhibitory activity against *Botrytis cinerea* and *Phytophthora infestans*, while they were devoid of significant activity against *Septoria tritici*.

10.1 Introduction

The genus *Sepedonium* (Hypocreaceae, Ascomycota) comprises asexual states of fungi that parasitize basidiocarps of Boletales s.l. (Sahr et al., 1999). In natural habitats, we observed that Boletales fruiting bodies primarily infected by *Sepedonium* spp. are rarely colonized by secondary fungal parasites competing with *Sepedonium* for host nutrients. A variety of interesting secondary metabolites (Closse and Hauser, 1973; Divekar and Vining, 1964; Divekar et al., 1965; Dornberger et al., 1995; Hülsmann et al., 1998; Kronen et al., 2001; Mitova et al., 2008, 2006; Neuhof et al., 2007; Quang et al., 2010; Ritzau et al., 1997; Shibata et al., 1957; Stadler et al., 2001) were isolated from *Sepedonium* species which may be responsible for the observed biological phenomenon. One of the most prominent structural class within this genus is represented by the peptaibols due to their biological activity against molds (Berg et al., 1996; Gräfe et al., 1995; Otto et al., 2016b, 2015a) and striking mode of action (Bobone et al., 2013).

Very recently, we reported the first investigation of a Chilean *Sepedonium* species, parasitizing an endemic bolete, in a polythetic approach based on chemical, biological, and phylogenetic data. It could be demonstrated that the investigated strain is strongly related to the European species *S. chalcipori*. Semi-solid cultivation and isolation yielded chilenopeptins A and B, two new linear 15-residue peptaibols. Additionally, the total synthesis of the chilenopeptins was accomplished by a solid-phase peptide approach. (Otto et al., 2016b)

The production of peptaibols in different *Sepedonium* species was investigated earlier by Neuhof et al. (2007) using MALDI-TOF mass spectrometry. It was concluded, that the production of peptaibols in *Sepedonium* may correlate with the shape of the aleurioconidia. Peptaibols were only identified in strains forming round-shaped aleurioconidia, and in contrast, not detected in *Sepedonium* strains with oval-shaped aleurioconidia, such as *S. tulasneanum* (Plowr.) Sacc. (Neuhof et al., 2007; Sahr et al., 1999). The herein investigated *S. tulasneanum* strain KSH 535 was isolated from the lurid bolete *Boletus luridus* Schaeff., a common European host of this species (Sahr et al., 1999). Due to the characteristic oval-shaped chlamydospores, *S. tulasneanum* was never confused with round aleurioconidia producing species like *S. chrysospermum* (Bull.) Fr. (Sahr et al., 1999).

The present study describes the isolation of four new 19-residue peptaibols **10.1–10.4** from semi-solid cultures of *S. tulasneanum* KSH 535. Consequently, this is the first report of peptaibols from a *Sepedonium* strain with oval- to lemon-shaped aleurioconidia.

10.2 Results and discussion

The chromatographic separation of the culture broth and mycelial crude extract of the strain KSH 535 using adsorption chromatography on Diaion HP 20 and size exclusion chromatography on Sephadex LH 20 in combination with preparative RP18 HPLC afforded compounds **10.1–10.4** (see Chapter 10.4).
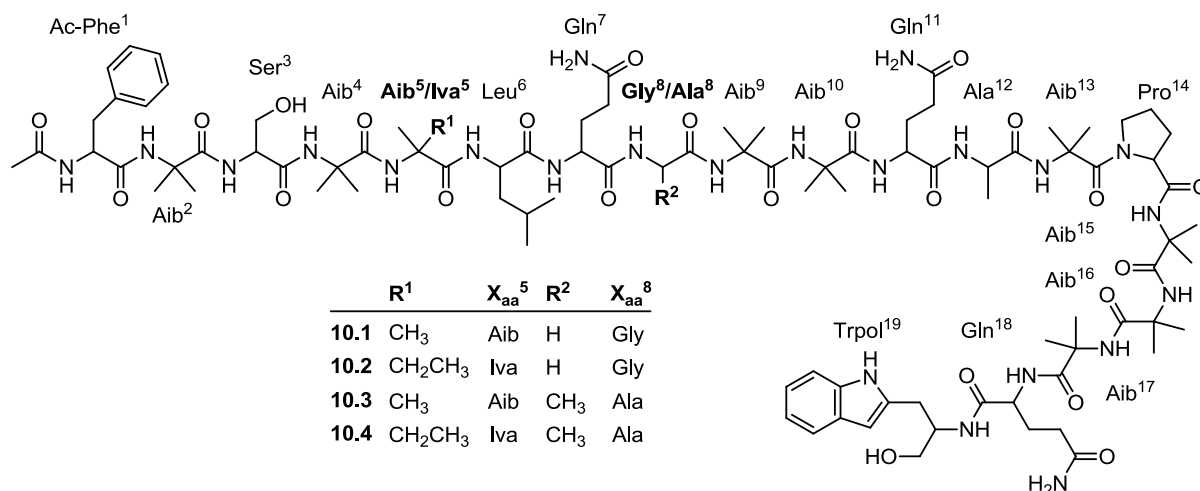
Fig. 10.1. Constitutions of tulasporins A–D (**10.1–10.4**). Differences in amino acid sequences are highlighted in bold.

Compound **10.1** was isolated as a white, amorphous solid. A positive ninhydrin reaction on TLC solely in the presence of the hydrolyzing agent *p*-TsOH indicated the presence of *N*-protected peptides. The positive ion full scan MS (Fig. 10.2) displayed the protonated molecular ion at *m/z* 1955.0740 ([M+H]$^+$, calculated for $C_{92}H_{144}N_{23}O_{24}^+$ 1955.0749) as well as the [M+2H]$^{2+}$ ion at *m/z* 978.0443 (calculated for $C_{92}H_{145}N_{23}O_{24}^{2+}$ 978.0411). Similarly to chilenopeptins A (**8.1**) and B (**8.2**) (Otto et al., 2016b), the MS^2 spectrum of the [M+2H]$^{2+}$ ion generated highly abundant fragment ions at *m/z* 1284.6946 (b_{13}^+, *N*-terminal fragment) and *m/z* 671.3869 (y_6^+, *C*-terminal fragment) being indicative for an Aib-Pro bond. The MS^2 analysis of the y_6^+ ion produced y-series fragments corresponding to the residues 17 to 19 and demonstrated a *C*-terminal tryptophanol (Trpol^{19}) residue (Fig. 10.3). MS^2 analysis of the [M+H]$^+$ ion as well as MS^3 studies of the b_{10}^+ ion displayed diagnostic fragment ions b_{13}^+ to b_3^+ affording the sequence between amino acids 13 and 3.

On the other hand, the negative ion MS^2 spectrum (Fig. 10.3) of *m/z* 1953.0606 ([M–H]$^-$, calculated for $C_{92}H_{142}N_{23}O_{24}^-$ 1953.0604) displayed a predominant *C*-terminal fragment ion at *m/z* 1923.0462, corresponding to v_{19}^-, generated by a neutral side chain loss of CH_2O (30 amu) indicating a Ser residue. MS/MS analyses of v_{19}^- showed the diagnostic fragment ions of the y_n/v_n series including v_{18}^- (*m/z* 1733.9669) suggesting the insertion of Ac-Phe at the *N*-terminus. Furthermore, a mass difference of 57 mass units between v_{17}^- and the y_{16}^- ion afforded the location of Ser at position 3. The tandem mass spectrometric analyses of **10.1**, as compiled in Tables 10.1 and 10.2, indicated the presence of either Ile or Leu at position 6 (Lxx^6). The ^{1}H NMR spectrum displayed two high field doublets resonating at δ_H 0.920 and δ_H 0.840 (each *J* = 6.5 Hz) corresponding to CH_3 groups of the leucine residue. Based on the above observations, the sequence of **1** was assigned as Ac-Phe^1-Aib^2-Ser^3-Aib^4-Aib^5-Leu^6-Gln^7-Gly^8-Aib^9-Aib^{10}-Gln^{11}-Ala^{12}-Aib^{13}-Pro^{14}-Aib^{15}-Aib^{16}-Aib^{17}-Gln^{18}-Trpol^{19} and trivially named tulasporin A (Fig. 10.1).
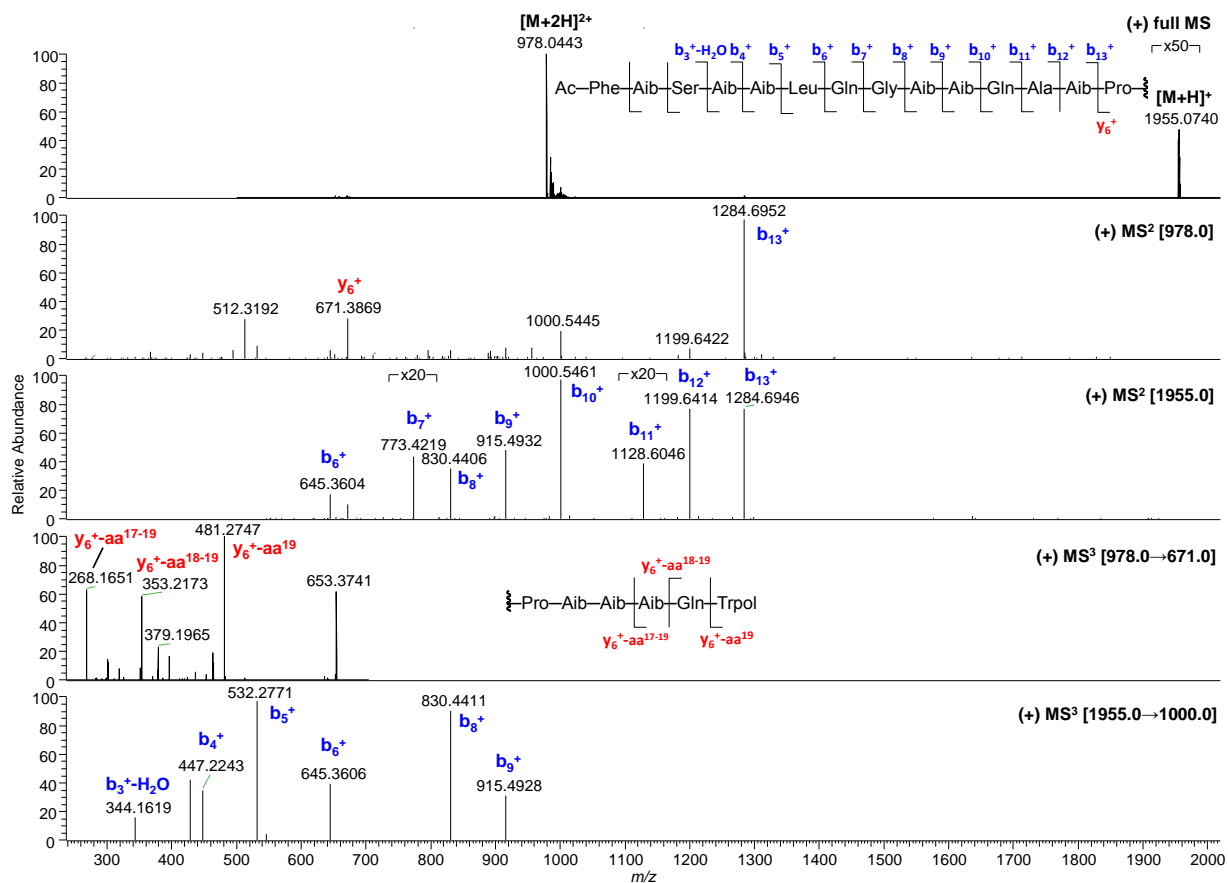
Fig. 10.2. Positive ion ESI-HRMS^n spectra of tulasporin A (**10.1**).
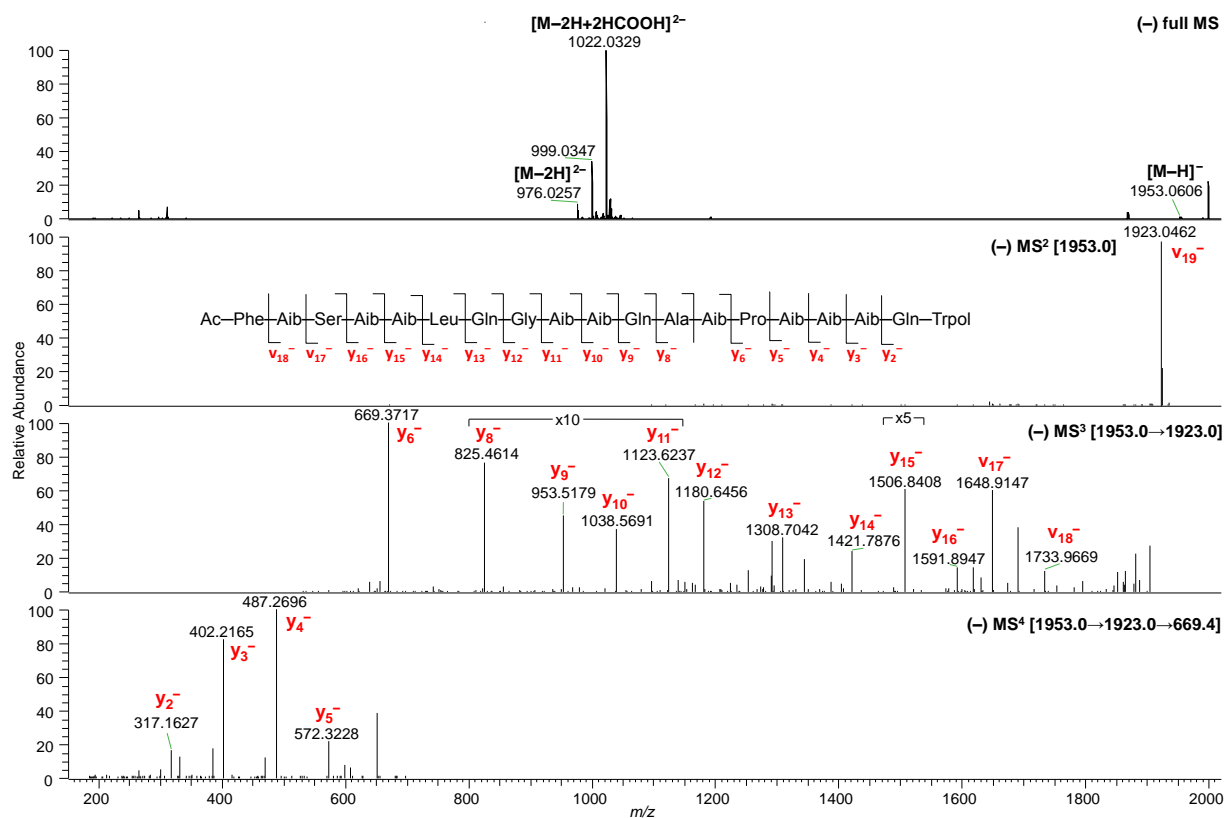
Fig. 10.3. Negative ion ESI-HRMS^n spectra of tulasporin A (**10.1**).

Table 10.1. Diagnostic fragment ions [m/z] of tulasporins A–D (**10.1**–**10.4**) obtained from positive ion ESI-HRMS^n experiments.

	10.1	10.2	10.3	10.4
t_R [min]^a	2.8	4.7	7.4	8.8
$[M+H]^+$	1955.0740	1969.0900	1969.0911	1983.1087
$[M+2H]^{2+}$	978.0443	985.0500	985.0509	992.0598
b_1^+	n.d.	n.d.	n.d.	n.d.
b_2^+	n.d.	n.d.	n.d.	n.d.
$b_3^+ - H_2O$	344.1619	344.1596	344.1609	344.1614
b_3^+	n.d.	n.d.	n.d.	n.d.
b_4^+	447.2243	447.2240	447.2244	447.2255
b_5^+	532.2771	546.2925	532.2771	546.2933
b_6^+	645.3604	659.3768	645.3611	659.3778
b_7^+	773.4219	787.4391	773.4186	787.4371
b_8^+	830.4406	844.4571	844.4569	858.4738
b_9^+	915.4932	929.5096	929.5097	943.5266
b_{10}^+	1000.5461	1014.5624	1014.5626	1028.5797
b_{11}^+	1128.6046	1142.6161	1142.6178	1156.6370
b_{12}^+	1199.6414	1213.6580	1213.6581	1227.6761
b_{13}^+	1284.6946	1298.7111	1298.7113	1312.7290
$b_{14}^+ - b_{19}^+$	n.d.	n.d.	n.d.	n.d.
y_6^+	671.3869	671.3879	671.3857	671.3872
$y_6^+ - aa^{19}$	481.2747	481.2752	481.2752	481.2750
$y_6^+ - aa^{18-19}$	353.2173	353.2176	353.2172	353.2160
$y_6^+ - aa^{17-19}$	268.1651	268.1655	268.1649	268.1646
$y_6^+ - aa^{15-19}$	n.d.	n.d.	n.d.	n.d.

n.d. = not detected; b^+ = positively charged b ion; y^+ = positively charged y ion with amino acid (aa) abstraction.
^{a} Hypersil GOLD RP18 column (1.9 μm, 50 × 2.1 mm), flow rate 0.2 ml/min, gradient 0–5 min, 45–55% B; 5–13 min, 55–95% B (A=H_2O + 0.2% FA; B=CH_3CN + 0.2% FA).

Compound **10.2** was isolated as a white, amorphous solid. The molecular formula $C_{93}H_{145}N_{23}O_{24}$ was deduced from HR-MS measurements of the pseudomolecular $[M+H]^+$ ion at m/z 1969.0900 (calculated for $C_{93}H_{146}N_{23}O_{24}^+$ 1969.0906). The difference of 14 atomic mass units (amu) between **10.1** and **10.2** was indicative for the presence of an additional methylene group. Again, the MS^2 spectrum of the $[M+2H]^{2+}$ ion displayed two main fragments at m/z 1298.7132 (b_{13}^+, *N*-terminal fragment) and m/z 671.3879 (y_6^+, *C*-terminus). In comparison with **10.1**, the 14 amu shift in **10.2** was observed in the *N*-terminal fragment b_{13}^+. Detailed analyses of the b_n^+ ion series (Table 10.1) revealed that Aib^5 was exchanged by either valine or isovaline (Val or Iva). The presence of Iva at position 5 was evident from the characteristic triplet signal at δ_H 0.680 (J = 7.5 Hz) corresponding to its γ methyl group. Therefore, the structure of **10.2** was assigned as Ac-Phe^1-Aib^2-Ser^3-Aib^4-Iva^5-Leu^6-Gln^7-Gly^8-Aib^9-Aib^{10}-Gln^{11}-Ala^{12}-Aib^{13}-Pro^{14}-Aib^{15}-Aib^{16}-Aib^{17}-Gln^{18}-Trpol^{19}, named tulasporin B (Fig. 10.1).

Table 10.2. Diagnostic fragment ions [*m/z*] of tulasporins A–D (**10.1–10.4**) obtained from negative ion ESI-HRMS^n experiments.

	10.1	10.2	10.3	10.4
[M–H]$^-$	1953.0606	1967.0798	1967.0793	1981.0937
[M–2H]$^{2-}$	976.0257	983.0376	983.0346	990.0429
y_1^-	*n.d.*	*n.d.*	*n.d.*	*n.d.*
y_2^-	317.1627	317.1618	317.1620	317.1621
y_3^-	402.2165	402.2150	402.2152	402.2150
y_4^-	487.2696	487.2679	487.2679	487.2677
y_5^-	572.3228	572.3212	572.3211	572.3219
y_6^-	669.3717	669.3717	669.3717	669.3715
y_7^-	*n.d.*	*n.d.*	*n.d.*	*n.d.*
y_8^-	825.4614	825.4611	825.4604	825.4611
y_9^-	953.5179	953.5187	953.5187	953.5181
y_{10}^-	1038.5691	1038.5719	1038.5686	1038.5693
y_{11}^-	1123.6237	1123.6239	1123.6244	1123.6244
y_{12}^-	1180.6456	1180.6456	1194.6614	1194.6609
y_{13}^-	1308.7042	1308.7039	1322.7200	1322.7190
y_{14}^-	1421.7876	1421.7880	1435.8034	1435.8036
y_{15}^-	1506.8408	1520.8576	1520.8569	1534.8708
y_{16}^-	1591.8947	1605.9110	1605.9089	1619.9230
v_{17}^-	1648.9147	1662.9299	1662.9301	1676.9452
y_{17}^-	*n.d.*	*n.d.*	*n.d.*	*n.d.*
v_{18}^-	1733.9669	1747.9803	1747.9806	1761.9979
y_{18}^-	*n.d.*	*n.d.*	*n.d.*	*n.d.*
v_{19}^-	1923.0462	1937.0612	1937.0614	1951.0765

n.d. = not detected; y^- = negatively charged y ion; v^- = negatively charged v ion without serine side chain (30 amu).

Compound **10.3** was isolated as a white, amorphous solid. ESI-HRMS studies demonstrated that **10.3** exhibited the same molecular formula ($C_{93}H_{145}N_{23}O_{24}$) as compound **10.2**. As in **10.1**, the characteristic triplet signal of Iva was not observed in the ^{1}H NMR spectrum of **10.3**. Positive and negative ion ESI-HRMS^n investigations (Tables 10.1 and 10.2) confirmed that Gly^8 was exchanged by Ala^8 in comparison with **10.1**. Thus, the structure of **10.3** was determined as Ac-Phe^1-Aib^2-Ser^3-Aib^4-Aib^5-Leu^6-Gln^7-Ala^8-Aib^9-Aib^{10}-Gln^{11}-Ala^{12}-Aib^{13}-Pro^{14}-Aib^{15}-Aib^{16}-Aib^{17}-Gln^{18}-Trpol^{19} and consequently named tulasporin C (Fig. 10.1).

ESI-HRMS measurements of compound **10.4**, isolated as a white amorphous solid, afforded the molecular formula $C_{94}H_{147}N_{23}O_{24}$, demonstrating that the sequence of **10.4** holds a CH_2 group more than **10.2** and **10.3**. In contrast to **10.1**, exchanges of Aib^5 by Iva^5 and Gly^8 by Ala^8 in **10.4** were deduced from extensive tandem mass spectrometric studies (Tables 10.1 and 10.2) as well as ^{1}H NMR analyses. The sequence of compound **10.4** (tulasporin D) was therefore established as

Ac-Phe^1-Aib^2-Ser^3-Aib^4-Iva^5-Leu^6-Gln^7-Ala^8-Aib^9-Aib^{10}-Gln^{11}-Ala^{12}-Aib^{13}-Pro^{14}-Aib^{15}-Aib^{16}-Aib^{17}-Gln^{18}-Trpol^{19} (Fig. 10.1).

The structures of **10.1**–**10.4** are very similar to each other, differences being found only in position 5 (Iva/Aib) and in position 8 (Ala/Gly). It should be noted that tulasporin sequences are related to those of chrysospermins, isolated earlier from cultures of *S. chrysospermum* (Dornberger et al., 1995) (see also Chapter 2.3.1). For instance, the sequence of tulasporin A (**10.1**) differs from chrysospermin A (**2.52**) only by the exchange of Ala^{11} by Gln^{11} (Table B1, Appendix). As a result of the herein identified tulasporins A–D (**10.1**–**10.4**) in *S. tulasneanum* KSH 535, this study reports for the very first time peptaibols from a *Sepedonium* strain with oval-shaped aleurioconidia. Thus, the hypothesis of Neuhof et al. (2007) that the peptaibol production in *Sepedonium* strains may correlate with the morphology of the aleurioconidia has to be revised, since both round- as well as oval-shaped aleurioconidia forming *Sepedonium* species are able to produce peptaibols.

The biological activity of tulasporins A–D (**10.1**–**10.4**) was evaluated against the phytopathogenic ascomycetous fungi *Botrytis cinerea* (grey mold pathogen on many crops including strawberries and wine grapes) and *Septoria tritici* (causing septoria leaf blotch of wheat) as well as the oomycete *Phytophthora infestans* (causal agent of late blight disease on potato and tomato) using a 96 well microtiter plate assay (Table 10.3). The commercial fungicides dodine and pyraclostrobin were used as references for a membrane active fungicide and a respiration inhibitor fungicide, respectively.

The tulasporins **10.1**–**10.4** exhibited good growth inhibitory activity against both *B. cinerea* and *P. infestans*, while they were devoid of significant activity against *S. tritici* (IC$_{50}$ > 60 µM). As already observed for albupeptins A–D (**9.1**–**9.4**) (Otto et al., 2015a), the antiphytopathogenic activity of compounds **10.1**–**10.4** increased with rising lipophilicity, with tulasporin D (**10.4**) being the most active and at the same time the most lipophilic compound.

Table 10.3. Antiphytopathogenic activity of tulasporins A–D (**10.1**–**10.4**) against *B. cinerea*, *S. tritici*, and *P. infestans* (IC$_{50}$, µM).

compound	*B. cinerea*	*S. tritici*	*P. infestans*
10.1	10.7 ± 1.7	> 60	22.6 ± 3.7
10.2	5.2 ± 0.6	> 60	6.3 ± 1.0
10.3	5.2 ± 0.4	> 60	5.9 ± 1.4
10.4	3.7 ± 0.3	> 60	4.0 ± 0.2
dodine[a]	9.4 ± 0.6	2.8 ± 0.2	43.8 ± 5.6
pyraclostrobin[a]	< 0.0052	< 0.0052	0.018 ± 0.002

[a] Used as reference compounds.

10.3   Conclusions

Four new 19-residue peptaibols, named tulasporins A–D (**10.1**–**10.4**), were isolated from the semi-solid cultures of *Sepedonium tulasneanum*. Their structures resemble those of the chrysospermins and were elucidated on the basis of extensive ESI-HRMS^n fragmentation studies as well as ^{1}H NMR spectroscopic analyses. For the very first time, peptaibols were isolated from a *Sepedonium strain* with oval-shaped aleurioconidia. An earlier proposal that the peptaibol production may correlate with the morphology of aleurioconidia was thus disproved.

10.4   Experimental Section

General Experimental Procedures. Size exclusion column chromatography was performed using Sephadex LH 20 (Fluka, Germany), while analytical TLC was carried out on precoated silica gel F_{254} plates from Merck (Germany). Diaion HP 20 was purchased from Supelco (USA). Peptaibols were visualized on TLC plates using a modified acidic ninhydrin reagent as described previously (Otto et al., 2015a). UV spectra were obtained from a Jasco V-560 UV/Vis spectrophotometer, while CD spectra were acquired on a Jasco J-815 CD spectrophotometer. The specific rotation was measured with a Jasco P-2000 polarimeter.

The ^{1}H NMR spectra were recorded in DMSO-d_6 (99.96% D) at +40 °C on an Agilent VNMRS 600 system (599.83 MHz). ^{1}H chemical shifts were referenced to internal DMSO-d_6 (δ_H 2.510 ppm).

The positive and negative ion high-resolution ESI and collision induced dissociation (CID) MS^n spectra were obtained from an Orbitrap Elite mass spectrometer (Thermo Fisher Scientific, Germany) equipped with a HESI electrospray ion source (positive spray voltage 4.0 kV, negative spray voltage 3.5 kV, capillary temperature 275 °C, source heater temperature 200 °C, FTMS resolution 30.000). Nitrogen was used as sheath and auxiliary gas. The MS system was coupled to an ultra-high performance liquid chromatography (UHPLC) system (Dionex UltiMate 3000, Thermo Fisher Scientific), equipped with a RP18 column (particle size 1.9 μm, pore size 175 Å, 50 × 2.1 mm ID, Hypersil GOLD, Thermo Fisher Scientific; column temperature 40 °C) and a photodiode array detector (200–600 nm, Thermo Fisher Scientific). The mobile phases were H_2O (A; Fluka Analytical, LC-MS Chromasolv) and CH_3CN (B; Fluka Analytical, LC-MS Chromasolv) with 0.2% formic acid using a gradient system (0–5 min, 45–55% B; 5–13 min, 55–95% B; 13–16 min, 95% B; 16–17 min 95–45% B; flow rate 0.2 ml/min).

The CID mass spectra (buffer gas: helium) were recorded using normalized collision energies (NCE) of 45–65% (see Supporting Information). The instrument was externally calibrated by the Pierce LTQ Velos ESI positive ion calibration solution (product no. 88323) and Pierce ESI negative ion calibration solution (product no. 88324) from Thermo Fisher Scientific. The data were evaluated using the software Xcalibur 2.7 SP1.

Preparative HPLC was performed on a Knauer system equipped with a WellChrom K-1001 pump and a WellChrom K-2501 UV detector using an ODS-A column (5 μm, 120 Å, 150 × 10 mm ID, YMC, USA) eluting with H_2O (A) and CH_3CN (B).

Fungal strain and cultivation. *Sepedonium tulasneanum* (Plowr.) Sacc. (strain KSH 535) was isolated in August 1999 from *Boletus luridus* Schaeff. in Crista Acri near Cosenza, Italy (leg./det. C. Lavorato). A voucher specimen (990811-27) is deposited at the herbarium of the University Regensburg. The fungal culture of *S. tulasneanum* KSH 535 was stored on malt peptone agar (MPA) plates and transferred periodically. The upscaled semi-solid cultures, used for isolation of peptaibols, were grown in 32 Erlenmeyer flasks (size 1 l) each containing 1.5 g of cotton wool and 250 ml of malt peptone medium (2.5 g malt and 0.625 g peptone in 250 ml deionized water), resulting in a total volume of 8 l. Each culture flask was inoculated with a 10 × 10 mm agar plug of colonized fungus, and incubated for 35 days at room temperature without agitation.

Extraction and isolation. The mycelia were separated from the culture broth by vacuum filtration, frozen with liquid nitrogen and extracted with MeOH (3 × 3 l). The yellow solution was evaporated to dryness, redissolved in H_2O and combined with the culture broth. Activated Diaion HP 20 (40 g) was added and agitated for 12 hours at room temperature. Diaion HP 20 was removed by vacuum filtration, washed with H_2O, and eluted with MeOH. The resulting yellow crude MeOH extract (10.7 g) was evaporated *in vacuo* to dryness and subjected to Sephadex LH 20 column chromatography (470 × 50 mm) eluting with MeOH to afford 59 fractions (10 ml each). Fractions 11–13 were combined (112.5 mg) and finally purified by preparative HPLC (0–20 min, 45–70% B, flow rate 3.5 ml/min) to afford **10.1** (t_R 11.3 min, 3.2 mg), **10.2** (t_R 13.5 min, 11.3 mg), **10.3** (t_R 15.8 min, 8.7 mg), and **10.4** (t_R 18.4 min, 15.9 mg).

Tulasporin A (10.1): white, amorphous solid; TLC R_f 0.36 (*n*-BuOH/AcOH/H_2O 8:1:1); $[\alpha]_D^{27}$ +7.3 (*c* 0.126, MeOH); CD (MeOH) $[\theta]_{193}$ +399166, $[\theta]_{207}$ −177612, $[\theta]_{225}$ −131533 $°×cm^2×dmol^{-1}$; UV (MeOH) λ_{max} (log ε) 200 (4.85), 217 (4.53), 282 (3.50), 290 (3.45) nm; ^1H NMR (600 MHz, DMSO-d_6) 0.920 (3H, d, J = 6.5 Hz, H_3-δ Leu[6]), 0.840 (3H, d, J = 6.5 Hz, H_3-ε Leu[6]); ESI-HRMS *m/z* 978.0443 ([M+2H]$^{2+}$, calculated for $C_{92}H_{145}N_{23}O_{24}^{2+}$ 978.0411); ESI-HRMS^n see Tables 10.1 and 10.2.

Tulasporin B (10.2): white, amorphous solid; TLC R_f 0.38 (*n*-BuOH/AcOH/H_2O 8:1:1); $[\alpha]_D^{27}$ +7.6 (*c* 0.161, MeOH); CD (MeOH) $[\theta]_{193}$ +320965, $[\theta]_{207}$ −166557, $[\theta]_{224}$ −130700 $°×cm^2×dmol^{-1}$; UV (MeOH) λ_{max} (log ε) 200 (4.76), 217 (4.51), 281 (3.64), 290 (3.58) nm; ^1H NMR (600 MHz, DMSO-d_6) 0.922 (3H, d, J = 6.5 Hz, H_3-δ Leu[6]), 0.843 (3H, d, J = 6.5 Hz, H_3-ε Leu[6]), 0.680 (3H, t, J = 6.5 Hz, H_3-γ Iva[5]); ESI-HRMS *m/z* 985.0500 ([M+2H]$^{2+}$, calculated for $C_{93}H_{147}N_{23}O_{24}^{2+}$ 985.0489); ESI-HRMS^n see Tables 10.1 and 10.2.

Tulasporin C (10.3): white, amorphous solid; TLC R_f 0.39 (*n*-BuOH/AcOH/H$_2$O 8:1:1); $[\alpha]^{27}_D$ –2.7 (*c* 0.167, MeOH); CD (MeOH) $[\theta]_{193}$ +599866, $[\theta]_{207}$ –212919, $[\theta]_{225}$ –187601 °×cm^2× dmol^{-1}; UV (MeOH) λ_{max} (log ε) 200 (4.89), 217 (4.63), 281 (3.74), 290 (3.69) nm; ^{1}H NMR (600 MHz, DMSO-d_6) 0.931 (3H, d, J = 6.5 Hz, H$_3$-δ Leu^6), 0.845 (3H, d, J = 6.5 Hz, H$_3$-ε Leu^6); ESI-HRMS *m/z* 985.0509 ([M+2H]$^{2+}$, calculated for C$_{93}$H$_{147}$N$_{23}$O$_{24}$$^{2+}$ 985.0489); ESI-HRMS^n see Tables 10.1 and 10.2.

Tulasporin D (10.4): white, amorphous solid; TLC R_f 0.40 (*n*-BuOH/AcOH/H$_2$O 8:1:1); $[\alpha]^{25}_D$ +1.5 (*c* 0.214, MeOH); CD (MeOH) $[\theta]_{193}$ +401477, $[\theta]_{208}$ –184917, $[\theta]_{224}$ –150305 °×cm^2× dmol^{-1}; UV (MeOH) λ_{max} (log ε) 200 (4.81), 217 (4.53), 281 (3.65), 290 (3.59) nm; ^{1}H NMR (600 MHz, DMSO-d_6) 0.934 (3H, d, J = 6.5 Hz, H$_3$-δ Leu^6), 0.849 (3H, d, J = 6.5 Hz, H$_3$-ε Leu^6), 0.689 (3H, t, J = 6.5 Hz, H$_3$-γ Iva^5); ESI-HRMS *m/z* 992.0598 ([M+2H]$^{2+}$, calculated for C$_{94}$H$_{149}$N$_{23}$O$_{24}$$^{2+}$ 992.0568); ESI-HRMS^n see Tables 10.1 and 10.2.

Antiphytopathogenic bioassay. Pure compounds were tested in a 96-well microtiter plate assay against *Botrytis cinerea* Pers., *Septoria tritici* Desm., and *Phytophthora infestans* (Mont.) De Bary as described earlier (Otto et al., 2015a).

10.5   References

Berg, A., Ritzau, M., Ihn, W., Schlegel, B., Fleck, W.F., Heinze, S., Gräfe, U., 1996. Isolation and structure of bergofungin, a new antifungal peptaibol from *Emericellopsis donezkii* HKI 0059. *J. Antibiot.* 49, 817–820.

Bobone, S., Gerelli, Y., De Zotti, M., Bocchinfuso, G., Farrotti, A., Orioni, B., Sebastiani, F., Latter, E., Penfold, J., Senesi, R., Formaggio, F., Palleschi, A., Toniolo, C., Fragneto, G., Stella, L., 2013. Membrane thickness and the mechanism of action of the short peptaibol trichogin GA IV. *BBA - Biomembr.* 1828, 1013–1024.

Closse, A., Hauser, D., 1973. Isolierung und Konstitutionsermittlung von Chrysodin. *Helv. Chim. Acta* 56, 2694–2698.

Divekar, P.V., Raistrick, H., Dobson, T.A., Vining, L.C., 1965. Studies in the biochemistry of microorganisms: Part 117. Sepedonin, a tropolone metabolite of *Sepedonium chrysospermum* Fries. *Can. J. Chem.* 43, 1835–1848.

Divekar, P.V., Vining, L.C., 1964. Reaction of anhydrosepedonin with alkali synthesis of a degradation product and some related dimethylhydroxybenzoic acids. *Can. J. Chem.* 42, 63–68.

Dornberger, K., Ihn, W., Ritzau, M., Gräfe, U., Schlegel, B., Fleck, W.F., Metzger, J.W., 1995. Chrysospermins, new peptaibol antibiotics from *Apiocrea chrysosperma* Ap101. *J. Antibiot.* 48, 977–989.

Gräfe, U., Ihn, W., Ritzau, M., Schade, W., Stengel, C., Schlegel, B., Fleck, W.F., Künkel, W., Härtl, A., Gutsche, W., 1995. Helioferins; novel antifungal lipopeptides from *Mycogone rosea*: screening, isolation, structures and biological properties. *J. Antibiot.* 48, 126–133.

Hülsmann, H., Heinze, S., Ritzau, M., Schlegel, B., Gräfe, U., 1998. Isolation and structure of peptaibolin, a new peptaibol from *Sepedonium* strains. *J. Antibiot.* 51, 1055–1058.

Kronen, M., Kleinwächter, P., Schlegel, B., Härtl, A., Gräfe, U., 2001. Ampullosporins B, C, D, E1, E2, E3 and E4 from *Sepedonium ampullosporum* HKI-0053: Structures and biological activities. *J. Antibiot.* 54, 175–178.

Mitova, M.I., Murphy, A.C., Lang, G., Blunt, J.W., Cole, A.L.J., Ellis, G., Munro, M.H.G., 2008. Evolving trends in the dereplication of natural product extracts. 2. The isolation of chrysaibol, an antibiotic peptaibol from a New Zealand sample of the mycoparasitic fungus *Sepedonium chrysospermum. J. Nat. Prod.* 71, 1600–1603.

Mitova, M.I., Stuart, B.G., Cao, G.H., Blunt, J.W., Cole, A.L.J., Munro, M.H.G., 2006. Chrysosporide, a cyclic pentapeptide from a New Zealand sample of the fungus *Sepedonium chrysospermum. J. Nat. Prod.* 69, 1481–1484.

Neuhof, T., Berg, A., Besl, H., Schwecke, T., Dieckmann, R., von Döhren, H., 2007. Peptaibol production by *Sepedonium* strains parasitizing Boletales. *Chem. Biodivers.* 4, 1103–1115.

Otto, A., Laub, A., Porzel, A., Schmidt, J., Wessjohann, L., Westermann, B., Arnold, N., 2015a. Isolation and total synthesis of albupeptins A–D: 11-residue peptaibols from the fungus *Gliocladium album. Eur. J. Org. Chem.* 2015, 7449–7459.

Otto, A., Laub, A., Wendt, L., Porzel, A., Schmidt, J., Palfner, G., Becerra, J., Krüger, D., Stadler, M., Wessjohann, L., Westermann, B., Arnold, N., 2016b. Chilenopeptins A and B, peptaibols from the Chilean *Sepedonium* aff. *chalcipori* KSH 883. *J. Nat. Prod.* 79, 928–938.

Quang, D.N., Schmidt, J., Porzel, A., Wessjohann, L., Haid, M., Arnold, N., 2010. Ampullosine, a new isoquinoline alkaloid from *Sepedonium ampullosporum* (Ascomycetes). *Nat. Prod. Commun.* 5, 869–872.

Ritzau, M., Heinze, S., Dornberger, K., Berg, A., Fleck, W., Schlegel, B., Hartl, A., Gräfe, U., 1997. Ampullosporin, a new peptaibol-type antibiotic from *Sepedonium ampullosporum* HKI-0053 with neuroleptic activity in mice. *J. Antibiot.* 50, 722–728.

Sahr, T., Ammer, H., Besl, H., Fischer, M., 1999. Infrageneric classification of the boleticolous genus *Sepedonium*: species delimitation and phylogenetic relationships. *Mycologia* 91, 935–943.

Shibata, S., Shoji, J., Ohta, A., Watanabe, M., 1957. Metabolic products of fungi. XI. Some observation on the occurrence of skyrin and rugulosin in mold metabolites, with a reference to structural relationship between penicilliopsin and skyrin. *Pharm. Bull.* 5, 380–382.

Stadler, M., Seip, S., Müller, H., Henkel, T., Lagojda, A., Kleymann, G., 2001. New antiviral peptaibols from the mycoparasitic fungus *Sepedonium microspermum*, in: Book of Abstracts, 13. Irseer Naturstofftage der DECHEMA. Irsee.

10.6 Supporting Information

Supplementary data associated with this article (ESI-HRMS^n data as well as ^{1}H NMR, CD, and UV spectra of **10.1**–**10.4**) are available in electronic form on the publisher's website.

11   General discussion and conclusions

Fungi are of great interest to the pharmaceutical and agrochemical industry due to the diverse bioactive natural products produced by these organisms. It is well recognized that the heterogeneity of fungi is also reflected in the chemical diversity of their secondary metabolites. However, several fungi and fungi-like organisms are also economically important pathogens in plants. A major problem is the increasing resistance development of phytopathogenic organisms against commercial fungicides, causing an urgent need of novel lead structures which are ideally associated with new mode of actions. This thesis was therefore focused on the isolation and identification of new natural products from chemically unexplored fungal sources that potentially can serve as lead structures for the development of novel plant protective agents or pharmaceutical drugs.

The present thesis describes mycochemical studies on basidiomycetous fruiting bodies (e.g. genus *Hygrophorus*) as well as cultivars of ascomycetous fungi (e.g. genera *Sepedonium* and *Gliocladium*). While the majority of Ascomycetes are saprophytes, basidiomycetous fungi are mainly characterized by a symbiotic lifestyle by forming mycorrhiza with roots of plants. Due to the high specialization of mycorrhizal fungi, they are less cultivable than saprophytic fungi. However, since both fungal ecotypes produce interesting compounds worth to study, fungal fruiting bodies as well as mycelial cultures were collected in Germany and Chile, and subsequently analyzed. Based on a bioactivity screening of approximately 150 different fungal extracts against various phytopathogenic organisms (for details, see Tables A1–A4, Appendix), several extracts with remarkable activity were identified. The subsequent chemical investigation on fruiting bodies of *H. abieticola* and *H. penarius* as well as mycelial cultures of *G. album*, *S. chalcipori*, and *S. tulasneanum* afforded in total 23 natural products that were never described before.

The (nor-)sesquiterpenes, penarines A–F (**7.1**–**7.6**), isolated from *H. penarius*, represent the first finding of this structural class not only in the genus *Hygrophorus*, but also within the family Hygrophoraceae (Chapter 7). In general, sesquiterpenoids are common metabolites in fungal fruiting bodies of species from the families Russulaceae (e.g. *Russula*, *Lactarius*) and Tricholomataceae (e.g. *Lepista*) (Fraga, 2007). Depending on further studies of selected *Hygrophorus* species, these sesquiterpenes may be used as chemotaxonomic marker compounds for particular sections or species within the genus *Hygrophorus*.

Investigations on fruiting bodies of *H. abieticola* afforded five new hygrophorones (Chapters 3 and 6) and two previously undescribed cyclohexenone derivatives, named pseudohygrophorones (Chapter 5). Among these constituents, two new tetrahydroxylated hygrophorone types were identified. Whereas the cyclopentenone-type hygrophorones are in general well known constituents from the genus *Hygrophorus* (Lübken et al., 2004), the cyclohexenone-type pseudohygrophorones are rare in nature, as their distribution is limited to plant species of the

family Anacardiaceae (Chapter 5). A good perspective would be to study the distribution of tetrahydroxylated hygrophorones as well as pseudohygrophorones in further species of the genus *Hygrophorus* in order to propose these compounds as chemotaxonomic markers.

So far, semisynthetic modifications of hygrophorones had been described only for structure elucidation and biological evaluation purposes (Lübken, 2006), but not to allow for a stereochemical assignment. Instead, the relative configuration of hygrophorones was studied earlier by NOE interactions (Lübken et al., 2004) and residual dipolar coupling (RDC) experiments (Schmidts et al., 2013). However, the absolute configuration remained tentative using these approaches. With the first asymmetric total synthesis of enantiomerically pure hygrophorone B^{12} (Chapter 3), the absolute configuration of a hygrophorone could be elucidated for the first time. This synthetic route demonstrates at the same time an attractive alternative to afford the natural product, since the fungal fruiting body as the natural source is not permanently available, restricted to specified soil conditions (e.g. limestone areas), and most importantly this highly specified mycorrhizal organism is not cultivable under artificial conditions. Furthermore, this synthetic approach can be used as a basis for derivatization to enhance the bioactivity or to study the mode of action more intensively.

An essential part in natural product research is the study of biosynthetic pathways of the target compounds. Feeding experiments on *Hygrophorus* spp. were carried out before in the Steglich group (Gill and Steglich, 1987). The γ-butyrolactone hygrophoric acid (**2.1**), which has a similar structure to those of hygrophorones F^{12} (**2.38**) and G^{12} (**2.39**), is biosynthesized *via* caffeic acid as demonstrated by feeding of [α-^{2}H]-caffeic acid to fruiting bodies of *H. lucorum* (Gill and Steglich, 1987). A highlight of this thesis was the study on the hitherto unknown biosynthesis of hygrophorone B^{12} in fruiting bodies of *H. abieticola* by labelling experiments in the field using ^{13}C labelled precursors (Chapter 4). The advantage of using ^{13}C precursors in contrast to ^{14}C is the environmental safety, whereas ^{2}H can underlie an unwanted rapid exchange with ^{1}H combined with a poor detectability in NMR spectroscopy. Based on the results, it is suggested that structurally related 4-oxo fatty acids and cyclopentenediones (chrysotriones), metabolites which are also produced by *Hygrophorus* spp., might be involved in the natural formation of hygrophorones. The biosynthesis of other (pseudo-)hygrophorones might be strongly related to that of hygrophorone B^{12} (**6.1**), possibly proceeding *via* a similar symmetrical intermediate such as the chrysotrione B homologue **4.5** (Scheme 11.1). To validate this hypothesis with respect to pseudohygrophorones, further feeding experiments using [1-^{13}C]- or [2-^{13}C]-acetate are necessary followed by analysis of ^{13}C incorporation in the cyclohexenone system. So far, 4-oxo fatty acids and (pseudo-) hygrophorones have not been detected in the same species within the genus *Hygrophorus*, but only independently from each other. For instance, 4-oxo fatty acids are so far only known from *H. eburneus* and *H. discoxanthus* (Teichert et al., 2005b; Gilardoni et al., 2006). Moreover, cyclopentenediones (chrysotriones) were detected in fruiting bodies of *H. chrysodon*, but neither cyclopentenones (hygrophorones) nor 4-oxo fatty acids (Gilardoni et al., 2007).

Further research is recommended, whether the absence of (pseudo-)hygrophorones in the species *H. discoxanthus*, *H. eburneus*, and *H. chrysodon* correlates with the lacking expression of certain enzymes that might be able to convert these fatty acids to (pseudo-) hygrophorones. In Chapter 6, the absolute configuration of hygrophorone E^{12} (**6.3**) was established. Interestingly, compound **6.3** shows an achirality center at C^5, indicating that both 4,5-*cis* and -*trans* configured cyclopentenones can principally be (bio-)converted to E series hygrophorones. This is in agreement with the finding of E-type hygrophorones in both species *H. latitabundus* and *H. abieticola*, although *H. latitabundus* produces cyclopentenones with *trans* oriented endocyclic hydroxyl groups (D series hygrophorones), while the B-type hygrophorones isolated from *H. abieticola* show a 4,5-*cis* configuration. A potential biosynthetic pathway is proposed in Scheme 11.1.
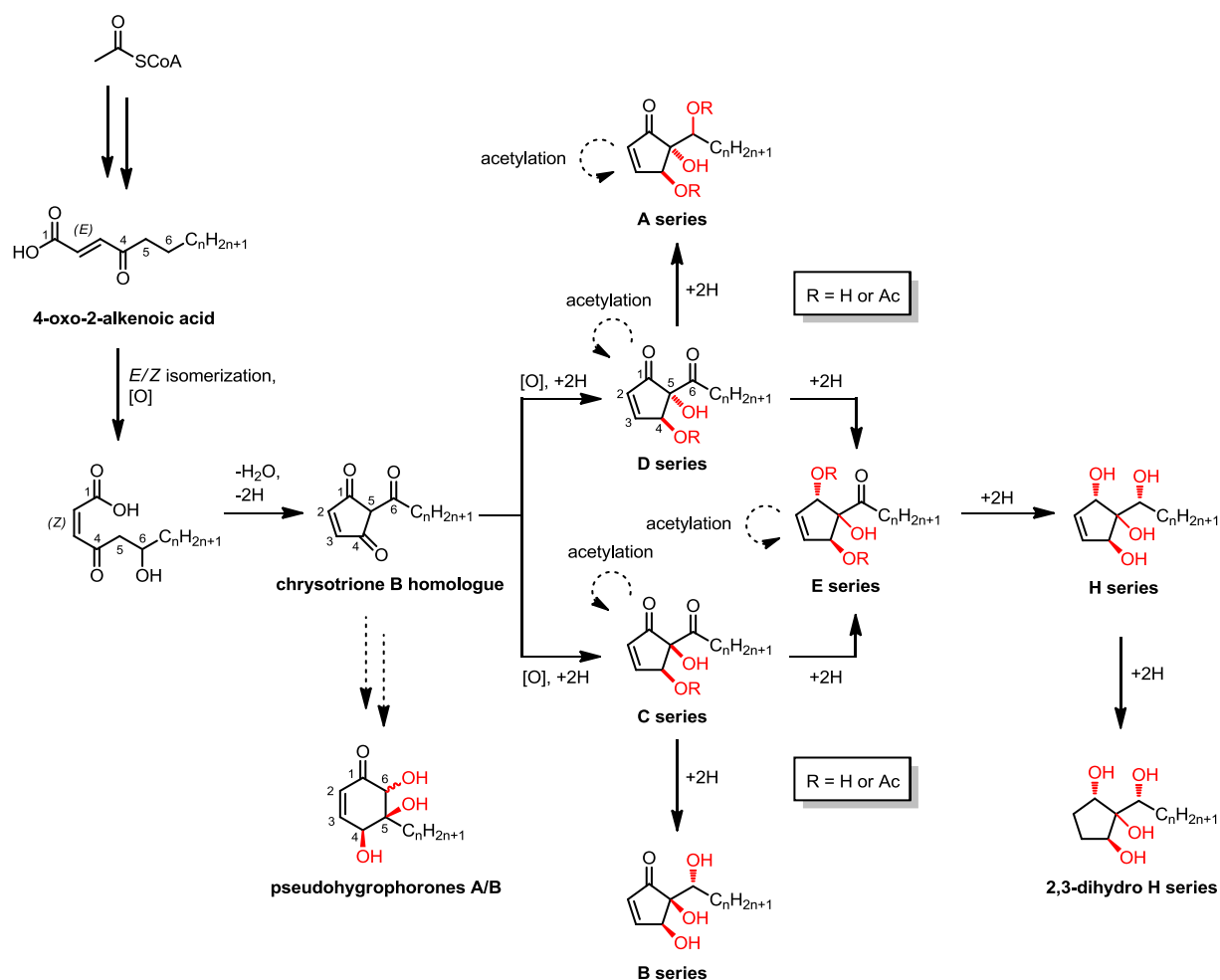
Scheme 11.1. Proposed biosynthesis of (pseudo-) hygrophorones *via* a chrysotrione B homologue as a key intermediate.

Hygrophorones were described as potent plant protective compounds, acting against the phytopathogenic organisms *Cladosporium cucumerinum* and *Phytophthora infestans* (Dräger, 2011; Lübken, 2006). In this thesis, the biological activity of the isolated and semisynthetic (pseudo-)hygrophorones was evaluated against *B. cinerea*, *S. tritici*, and *P. infestans* (Chapters 5 and 6). In general, strong growth inhibitions were observed against the oomycete *P. infestans*, indicating that the tested (pseudo-)hygrophorones especially act towards these fungus-like

organisms. The greatest antiphytopathogenic activities were observed for hygrophorone B^{12} (**6.1**), followed by hygrophorone B^{10} (**6.2**) and the pseudohygrophorones **5.1** and **5.2**. These results suggest that the length of the side chain and size of the ring system have an effect on the bioactivity. Moreover, it seems likely that an α,β-unsaturated carbonyl structure is a prerequisite for potent bioactivity, which might react as a Michael acceptor with biological nucleophiles. This was supported by the rapid reaction of hygrophorone B^{12} (**6.1**) with L-cysteine (Chapter 6). Such a mechanism of action is established for the anticancer drug ibrutinib, which covalently binds *via* Michael addition to the cysteine-481 residue of Bruton's tyrosine kinase (BTK) (Byrd et al., 2013).

Due to its potent antiphytopathogenic activity, hygrophorone B^{12} (**6.1**) may serve as a lead structure for the development of novel fungicidal plant protection agents. Initial studies towards structure-activity relationships were performed by Eileen Bette (for details, see Bette, 2017). Surprisingly, the cyclopentenone **11.1**, which lacks the exocyclic hydroxyl group at C-6 and three methylene groups in the alkyl side chain, showed a higher activity against *Botrytis cinerea* and *P. infestans* in comparison with **6.1**. At the same time, the synthesis of such dihydroxy-cyclopentenones can be accomplished in fewer steps than hygrophorone B^{12} (**6.1**). Apart from that, compounds that additionally lack the endoyclic hydroxyl group at C-5, such as **11.2**, exerted decreased activity against *Septoria tritici* (Bette, 2017). Prospective studies should be carried out to understand the mode of action of hygrophorone B^{12} (**6.1**) in order to generate biologically more active derivatives in combination with reduced synthetic effort.
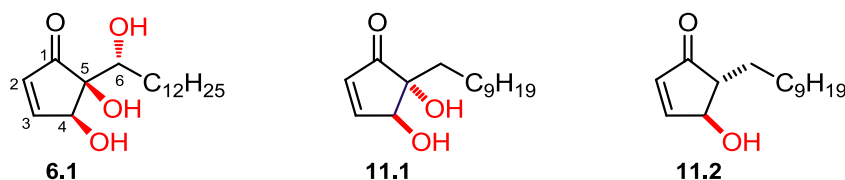
Hygrophorone B^{12} (**6.1**) and some of the hygrophorones tested by Lübken (2006) are also active against MRSA and VRE (gram-positive), and in contrast, inactive against the gram-negative bacterium *P. aeruginosa* (Chapter 6). It is well known that gram-positive bacteria are generally more sensitive to antibiotics than the gram-negative ones due to the outer membrane of gram-negative bacteria preventing the permeation of antibiotic molecules (Delcour, 2009). Because of the strong antimicrobial activity against MRSA and VRE and no toxicity to human erythrocytes, hygrophorone B^{12} (**6.1**) may have potential for therapeutic use.

While *H. abieticola* is associated with *Abies alba* as mycorrhiza partner, the macroscopically similar species *H. poetarum* exclusively occurs in beech forests (*Fagus sylvatica*). Previous studies demonstrated that *H. poetarum* produced hygrophorone B and C types, but only in small amounts (Lübken, 2006). 4-*O*-Acetylhygrophorone C^{12} (**2.28**) was also identified in basidiocarps of *H. abieticola* (results not shown). A future perspective would be thus to study the significance of (pseudo-)hygrophorones as a chemotaxonomic marker to distinguish between *H. poetarum* and *H. abieticola*. Based on recent molecular genetic results reported by Lodge et al. (2014) and

Larsson (2014), the situation becomes more complicate through the interpretation of *H. persicolor* as a synonym of *H. pudorinus*. The latter species has been confused before with *H. abieticola* (Lodge et al., 2014). To clarify these observations and support the phylogenetic trees, further mycochemical investigations within this genus are necessary.

Hygrophorones of the B series are also produced by *H. olivaceoalbus* (B^{14} and B^{16}), while hygrophorone B^{12} (**6.1**) was identified in fruiting bodies of *H. agathosmus* (Lübken, 2006). The similar species *H. exiguus* was described recently, which differs from *H. agathosmus* by having smaller fruiting bodies, a pink tint of the lamellae, and a less pronounced odour of marzipan (Larsson et al., 2014). It would be therefore interesting to study the occurrence of (pseudo-) hygrophorones, in particular of hygrophorone B^{12} (**6.1**), in fruiting bodies of *H. exiguus* as well as others so far undetermined fungal collections in our in-house collection.

The investigated ascomycetous *Sepedonium* and *Gliocladium* species are characterized by a parasitic lifestyle. It is supposed that some of these organisms produce secondary metabolites, besides lytic enzymes, in order to attack and settle on the host (Lorito et al., 1996; Schirmböck et al., 1994). Thus, certain ascomycetous fungi have gained increasing significance in the field of biological pest control, which is a considerable alternative towards chemical control strategies due to increasing public fear of such chemicals as well as resistance development of the target organisms. The biological pest control can be defined as the control of plant pathogens by another organism and is declared to be risk free and environmentally safe (Heydari and Pessarakli, 2010). However, this might be a current legal position in some countries, ecologically, the introduction of foreign organisms, especially invasory species, for controlling others should be considered more problematic than applying chemicals for a short period of time. An additional claimed advantage of the so-called biological control agents (BCAs) is the reduced risk of resistance development due to multiple modes of action (Avikainen et al., 2004). However, the biological control is not expected to fully replace chemical agents in the future, as the efficacy is generally inconsistent under field conditions and incomplete due to a shorter duration of action (Labuschagne et al., 2010).

Several peptaibols producing fungi, in particular species of the genus *Trichoderma*, are commercially available as BCAs such as *T. harzianum* (Trichosan®) (Degenkolb et al., 2015). The biofungicidal effect of *Trichoderma* spp. is believed to be based on synergistic effects through cell wall-destroying, lytic enzymes and membrane active, antibiotic peptaibols (Lorito et al., 1996; Schirmböck et al., 1994). The observed antiphytopathogenic effects of the isolated peptaibols (Chapters 8, 9, and 10) are in concordance with the proposed hypothesis of Schirmböck et al. (1994). This synergy is interpreted as a result of a weakened cell wall of the phytopathogen which improves the rate of diffusion of the antibiotic towards the cell surface (Di Pietro et al., 1993).

Peptaibols are an interesting group of peptides that have attracted considerable attention due to their mode of action and various biological activities (Chapter 2). The majority of peptaibols are

produced by ascomycetous fungi of the family Hypocreaceae, including the analyzed strains of *Sepedonium* aff. *chalcipori*, *Gliocladium album*, and *Sepedonium tulasneanum*. There are, however, only a few reports of peptaibols that were isolated from basidiomycetes. These findings are according to Degenkolb (2008) highly doubtful. For instance, Lee et al. (1999) isolated tylopeptin A (**8.3**) and B (**8.4**) from fruiting bodies of the basidiomycete *Tylopilus neofelleus*. Later, tylopeptins were detected in a solid-state culture of *Sepedonium chalcipori* S33 (Neuhof et al., 2007). Our finding of tylopeptins A (**8.3**) and B (**8.4**) in the culture of *Sepedonium* aff. *chalcipori* KSH 883 strongly support the proposed hypothesis of Neuhof and co-workers that the material of *Tylopilus neofelleus* was putatively infected by a tylopeptin-producing *Sepedonium* strain.

During the chemical studies on the investigated mycoparasitic fungi, an TLC based analysis method was developed to screen for peptaibol-type peptides. Due to the blocked *N*-terminus that is present in peptaibols, the ninhydrin reaction using a neutral spray solution is negative and thus not applicable. For that reason, these peptides were visualized by using a modified acidic ninhydrin reagent. In comparison to the two-step hydrochloric acid based ninhydrin analysis (Pandey et al., 1979), the herein used *p*-TsOH based procedure is simple, fast, and also applicable for silica gel coated aluminium TLC plates. Subsequently, ten new and two known peptaibols were detected and isolated from the investigated strains of *Sepedonium* aff. *chalcipori* KSH 883 (Chapter 8), *Gliocladium album* KSH 719 (Chapter 9), and *Sepedonium tulasneanum* KSH 535 (Chapter 10).

The *Sepedonium* aff. *chalcipori* KSH 883 was isolated in Chile from fruiting bodies of *Boletus loyo*. Chilean *Sepedonium* strains have hitherto neither been described nor investigated. The finding of tylopeptins combined with phylogenetic analyses revealed that the Chilean strain KSH 883 is strongly related to the European species *S. chalcipori*, thus forming a sister clade of the European and New Zealand *S. chalcipori* clades (Chapter 8). Further studies are necessary to demonstrate if these three clades represent different species. Interestingly, the highly specialized European *S. chalcipori* is restricted to *Chalciporus piperatus* as a host (Helfer, 1991), while the Chilean strain KSH 883 was isolated from *Boletus loyo*, which is endemic in the Southern Hemisphere due to the association with *Nothofagus* trees. The 15-residue chilenopeptins A (**8.1**) and B (**8.2**) were newly isolated from *S.* aff. *chalcipori* KSH 883 along with the known tylopeptins A (**8.3**) and B (**8.4**) (Chapter 8). Furthermore, the Chilean *Sepedonium* strain KSH 928, that was isolated from the host *B. loyita*, produced also both the chilenopeptins and tylopeptins and clustered to the clade of strain KSH 883 (results not shown). It can be concluded that both *B. loyita* and *B. loyo* are hosts of the Chilean *S.* aff. *chalcipori*, suggesting that the Chilean species is less specialized regarding its host than the European *S. chalcipori*, which parasitizes only on *C. piperatus*. The phylogenetic relationship and possible co-evolution of Southern and Northern Hemisphere *Sepedonium* species should be investigated in the future by detailed mycochemical and molecular studies.

Further studies demonstrated that the newly characterized chilenopeptins **8.1** and **8.2** could be also identified in the European *S. chalcipori* strains S33 and S35, but not in the tested strains of the New Zealand *S. chalcipori* isolates S44 and S46 (results not shown). Thus, chilenoeptins A (**8.1**) and B (**8.2**) are not specifically produced by the Chilean *Sepedonium* strains KSH 883 and KSH 928. An outlook would be thus to find chemotaxonomic markers to distinguish European and Chilean *S. chalcipori* isolates.

In addition, Neuhof and co-workers isolated the 15-mer peptaibols chalciporins A (**2.58**) and B (**2.59**), which are structurally related to the tylopeptins, from a solid-state culture (growth medium wheat) of *S. chalcipori* S33 (Neuhof et al., 2007). In this thesis, however, the chalciporins **2.58** and **2.59** could be neither detected in the malt-peptone agar culture of *S. chalcipori* S33 nor in the semi-solid malt-peptone cultures of *Sepedonium* aff. *chalcipori* KSH 883 (results not shown). It might therefore well be that chalciporins are only produced by solid-state cultures of *S. chalcipori*.

So far, peptaibols were only isolated from *Sepedonium* strains forming round aleurioconidia. Species like *S. brunneum* and *S. tulasneanum* were investigated earlier by Neuhof et al. (2007), and peptaibols could not be detected. Neuhof et al. therefore hypothesized that the peptaibol production in *Sepedonium* species correlates with the morphology of their aleurioconidia, since only round aleurioconidia forming strains produced peptaibols. This hypothesis can be considered as invalid, since the *Sepedonium tulasneanum* KSH 535 produces the 19-mer tulasporins A–D (**10.1**–**10.4**), forming at the same time oval-shaped aleurioconidia (Chapter 10).

Peptaibols contain non-proteinogenic amino acids such as α-aminoisobutyric acid (Aib) or isovaline (Iva), while the latter can principally occur in two enantiomeric forms (L- and D-). Among the over 1350 peptaibiotics published in the "Peptaibiotics Database", the stereochemistry of Iva residues is elucidated in just a few cases. Out of these structures with known stereochemistry, only a handful are known to contain both Iva enantiomers in the same sequence (Brückner et al., 2009) such as the MS-681 compounds (Ikuina et al., 1997). The herein characterized 11-residue albupeptins B (**9.2**) and D (**9.4**) from *Gliocladium album* are new members of this rare class of peptaibiotics that possess both stereoisomers of Iva (Chapter 9).

The majority of the published peptaibols were solely sequenced based on LC-MS/MS methods and not isolated in order to be characterized by NMR studies. Among the pure compounds that were tested for biological effects, only a few peptaibols had been evaluated before for their potential to inhibit the growth of phytopathogenic organisms. In this thesis, the isolated peptaibols were evaluated against the phytopathogens *B. cinerea*, *S. tritici*, and *P. infestans* (Chapters 8, 9, and 10). An antiphytopathogenic activity of peptaibols against the oomycete *P. infestans* was reported for the first time (Chapter 8). The strongest antiphytopathogenic effects were observed for the 19-residue tulasporins A–D (**10.1**–**10.4**), followed by the 15-mer chilenopeptins and tylopeptins. Thus, the biological activity of the tested peptaibols correlated with the length of the amino acid sequence. The modest to low antiphytopathogenic activities of the 11-residue albupeptins **9.1**–**9.4** may be explained by the limited ability of these short-sequence peptaibols to

span the entire membrane, as only long-chain peptaibols (> 17 residues) have the length comparable to the lipid bilayer (Bobone et al., 2013). In earlier studies, Grigoriev et al. (2003) already demonstrated that the peptaibol sequence length corresponded not only to their biological activity, but also to their membrane activity. Shorter sequence peptaibols, which exerted only weak membrane activities, were biologically little active. On the other hand, highly membrane-active structures such as chrysospermin C (**2.54**) displayed antifungal activities (Grigoriev et al., 2003). Two hypotheses have been proposed to explain how short- to medium-chain (lipo-) peptaibols generate their bioactivity; either by induction of membrane thinning through interaction with polar phospholipid headgroups (Bobone et al., 2013) or by formation of head-to-head dimers (Syryamina et al., 2010; Toniolo et al., 1994).

Recently, studies towards the bioactivity increase of the short-chain peptaibol albupeptin A (**9.1**) *via* chain extension were performed in our group by introducing acyl chains of differing length at the *N*-terminus (Roth, 2015). Consequently, three *N*-acyl derivatives (**11.3**–**11.5**) were yielded and evaluated for their antibiotic potency. The *N*-butyryl analogue **11.3** exhibited a slightly increased activity against both *P. infestans* and *B. cinerea* in comparison to albupeptin A (**9.1**), while the bioactivity of the *N*-octanoyl derivative **11.4** was comparable to that of **9.1**. Surprisingly, the long chain *N*-palmitoyl analogue **11.5** was biologically inactive, although **11.5** should be able to span the entire membrane. The biological inactivity of **11.5** may be explained by the incapability of the acyl chain to adopt a helical conformation.

	R		R
9.1	CH_3	**11.4**	C_8H_{17}
11.3	C_4H_9	**11.5**	$C_{16}H_{33}$
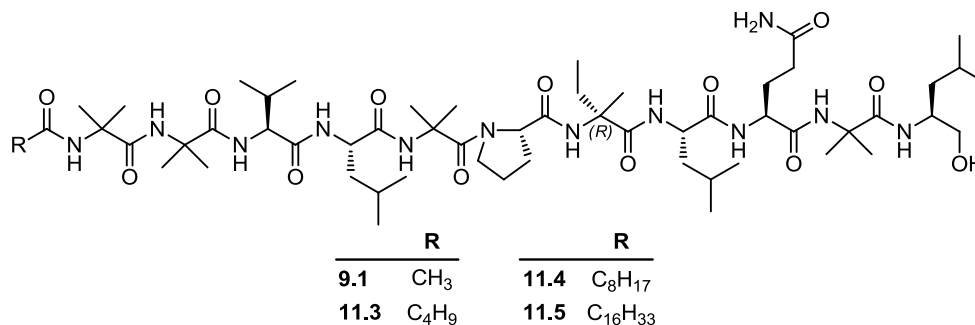
In conclusion, valuable contributions to the analysis of novel fungal secondary metabolites, to the determination of the absolute configuration by chiroptical studies, to the organic-chemical total synthesis, semisynthesis, and biosynthesis of biologically active agents have been achieved. Thus, several areas and aspects of modern natural product chemistry are covered in this thesis. The results additionally suggest that both ascomycetous and basidiomycetous fungi remain to be potential sources of new bioactive natural products that are worth to be studied. The achievements obtained in this thesis are expected to pave the way for future studies in natural product chemistry.

References

Avikainen, H.H., Keskinen, M.T., Lahdenperä, M.-L., Seiskari, P.T., Tahvonen, R.T., Teperi, E.P., Tuominen, U.A., 2004. Fungus *Gliocladium catenulatum* for biological control of plant diseases. European Patent, EP0792348 B1.

Bette, E., 2017. Synthese, Modifizierung, Strukturaufklärung und biologische Evaluierung von Naturstoffen aus Pilzen der Gattung *Hygrophorus*. Dissertation, Martin-Luther-Universität Halle-Wittenberg.

Bobone, S., Gerelli, Y., De Zotti, M., Bocchinfuso, G., Farrotti, A., Orioni, B., Sebastiani, F., Latter, E., Penfold, J., Senesi, R., Formaggio, F., Palleschi, A., Toniolo, C., Fragneto, G., Stella, L., 2013. Membrane thickness and the mechanism of action of the short peptaibol trichogin GA IV. *BBA - Biomembr.* 1828, 1013–1024.

Brückner, H., Becker, D., Gams, W., Degenkolb, T., 2009. Aib and Iva in the Biosphere: Neither rare nor necessarily extraterrestrial. *Chem. Biodivers.* 6, 38–56.

Byrd, J.C., Furman, R.R., Coutre, S.E., Flinn, I.W., Burger, J.A., Blum, K.A., Grant, B., Sharman, J.P., Coleman, M., Wierda, W.G., Jones, J.A., Zhao, W., Heerema, N.A., Johnson, A.J., Sukbuntherng, J., Chang, B.Y., Clow, F., Hedrick, E., Buggy, J.J., James, D.F., O'Brien, S., 2013. Targeting BTK with ibrutinib in relapsed chronic lymphocytic leukemia. N. *Engl. J. Med.* 369, 32–42.

Degenkolb, T., Brückner, H., 2008. Peptaibiomics: Towards a myriad of bioactive peptides containing C^α-dialkylamino acids? *Chem. Biodivers.* 5, 1817–1843.

Degenkolb, T., Fog Nielsen, K., Dieckmann, R., Branco-Rocha, F., Chaverri, P., Samuels, G.J., Thrane, U., von Döhren, H., Vilcinskas, A., Brückner, H., 2015. Peptaibol, secondary-metabolite, and hydrophobin pattern of commercial biocontrol agents formulated with species of the *Trichoderma harzianum* complex. *Chem. Biodivers.* 12, 662–684.

Delcour, A.H., 2009. Outer membrane permeability and antibiotic resistance. *BBA - Proteins Proteom.* 1794, 808–816.

Di Pietro, A., Lorito, M., Hayes, C.K., Broadway, R.M., Harman, G.E., 1993. Endochitinase from *Gliocladium virens*: Isolation, characterization, and synergistic antifungal activity in combination with gliotoxin. *Phytopathology* 83, 308–313.

Dräger, T., 2011. Synthese und biologische Testung von Naturstoffen und Naturstoff-Analoga mit Acryl-Struktureinheit. Dissertation, Martin-Luther-Universität Halle-Wittenberg.

Fraga, B.M., 2007. Natural sesquiterpenoids. *Nat. Prod. Rep.* 24, 1350–1381.

Gilardoni, G., Clericuzio, M., Marchetti, A., Finzi, P.V., Zanoni, G., Vidari, G., 2006. New oxidized 4-oxo fatty acids from *Hygrophorus discoxanthus*. *Nat. Prod. Commun.* 1, 1079–1084.

Gilardoni, G., Clericuzio, M., Tosi, S., Zanoni, G., Vidari, G., 2007. Antifungal acylcyclopentenediones from fruiting bodies of *Hygrophorus chrysodon*. *J. Nat. Prod.* 70, 137–139.

Gill, M., Steglich, W., 1987. Pigments of fungi (Macromycetes), in: Herz, W., Grisebach, H., Kirby, G.W., Tamm, C. (Eds.), Progress in the chemistry of organic natural products. Springer Verlag, Wien, New York, Vol. 51, pp. 1–317.

Grigoriev, P.A., Schlegel, B., Kronen, M., Berg, A., Härtl, A., Gräfe, U., 2003. Differences in membrane pore formation by peptaibols. *J. Pept. Sci.* 9, 763–768.

Helfer, W., 1991. Pilze auf Pilzfruchtkörpern: Untersuchungen zur Ökologie, Systematik und Chemie. IHW-Verlag, Eching, pp. 1–157.

Heydari, A., Pessarakli, M., 2010. A review on biological control of fungal plant pathogens using microbial antagonists. *J. Biol. Sci.* 10, 273–290.

Ikuina, Y., Bando, C., Yoshida, M., Yano, H., Saitoh, Y., 1997. MS-681a, b, c and d, new inhibitors of myosin light chain kinase from *Myrothecium* sp. II. Physico-chemical properties and structure elucidation. *J. Antibiot.* 50, 998–1006.

Labuschagne, N., Pretorius, T., Idris, A.H., 2010. Plant growth promoting Rhizobacteria as biocontrol agents against soil-borne plant diseases, in: Maheshwari, D. (Ed.), Plant Growth and Health Promoting Bacteria. Springer Verlag, Heidelberg, Dordrecht, London, New York, Vol. 18, pp. 211–230.

Larsson, E., Campo, E., Carbone, M., 2014. *Hygrophorus exiguus*, a new species in subgenus Colorati section Olivaceoumbrini, subsection Tephroleuci. *Karstenia* 54, 41–48.

Larsson, E., Jacobsson, S., 2014. Vilken vaxskivling var det som Fries beskrev som *Agaricus pudorinus*? *Sven. Mykolgisk Tidskr.* 35, 5–9.

Lee, S.J., Yun, B.S., Cho, D.H., Yoo, I.D., 1999. Tylopeptins A and B, new antibiotic peptides from *Tylopilus neofelleus*. *J. Antibiot.* 52, 998–1006.

Lodge, D.J., Padamsee, M., Matheny, P.B., Aime, M.C., Cantrell, S.A., Boertmann, D., Kovalenko, A., Vizzini, A., Dentinger, B.T.M., Kirk, P.M., Ainsworth, A.M., Moncalvo, J.-M., Vilgalys, R., Larsson, E., Lücking, R., Griffith, G.W., Smith, M.E., Norvell, L.L., Desjardin, D.E., Redhead, S.A., Ovrebo, C.L., Lickey, E.B., Ercole, E., Hughes, K.W., Courtecuisse, R., Young, A., Binder, M., Minnis, A.M., Lindner, D.L., Ortiz-Santana, B., Haight, J., Læssøe, T., Baroni, T.J., Geml, J., Hattori, T., 2014. Molecular phylogeny, morphology, pigment chemistry and ecology in Hygrophoraceae (Agaricales). *Fungal Divers.* 64, 1–99.

Lorito, M., Farkas, V., Rebuffat, S., Bodo, B., Kubicek, C.P., 1996. Cell wall synthesis is a major target of mycoparasitic antagonism by *Trichoderma harzianum*. *J. Bacteriol.* 178, 6382–6385.

Lübken, T., 2006. Hygrophorone – Neue antifungische Cyclopentenonderivate aus *Hygrophorus*-Arten (Basidiomycetes). Dissertation, Martin-Luther-Universität Halle-Wittenberg.

Lübken, T., Schmidt, J., Porzel, A., Arnold, N., Wessjohann, L., 2004. Hygrophorones A–G: Fungicidal cyclopentenones from *Hygrophorus* species (Basidiomycetes). *Phytochemistry* 65, 1061–1071.

Neuhof, T., Berg, A., Besl, H., Schwecke, T., Dieckmann, R., von Döhren, H., 2007. Peptaibol production by *Sepedonium* strains parasitizing Boletales. *Chem. Biodivers.* 4, 1103–1115.

Pandey, R.C., Misra, R., Rinehart, K.L., 1979. Visualization of *N*-protected peptides, amino acids and aminocyclitol antibiotics on a thin-layer chromatogram by ninhydrin. *J. Chromatogr. A* 170, 498–501.

Roth, P., 2015. *N*-Acylpeptaibole – Synthese und biologische Evaluierung. Diplomarbeit, Martin-Luther-Universität Halle-Wittenberg.

Schirmböck, M., Lorito, M., Wang, Y.L., Hayes, C.K., Arisan-Atac, I., Scala, F., Harman, G.E., Kubicek, C.P., 1994. Parallel formation and synergism of hydrolytic enzymes and peptaibol antibiotics, molecular mechanisms involved in the antagonistic action of *Trichoderma harzianum* against phytopathogenic fungi. *Appl. Environ. Microbiol.* 60, 4364–4370.

Schmidts, V., Fredersdorf, M., Lübken, T., Porzel, A., Arnold, N., Wessjohann, L., Thiele, C.M., 2013. RDC-based determination of the relative configuration of the fungicidal cyclopentenone 4,6-diacetylhygrophorone A^{12}. *J. Nat. Prod.* 76, 839–844.

Syryamina, V.N., Isaev, N.P., Peggion, C., Formaggio, F., Toniolo, C., Raap, J., Dzuba, S.A., 2010. Small-amplitude backbone motions of the spin-labeled lipopeptide trichogin GA IV in a lipid membrane as revealed by electron spin echo. *J. Phys. Chem. B* 114, 12277–12283.

Teichert, A., Lübken, T., Schmidt, J., Porzel, A., Arnold, N., Wessjohann, L., 2005b. Unusual bioactive 4-oxo-2-alkenoic fatty acids from *Hygrophorus eburneus*. *Z. Naturforsch.* 60b, 25–32.

Toniolo, C., Peggion, C., Crisma, M., Formaggio, F., Shui, X., Eggleston, D.S., 1994. Structure determination of racemic trichogin A IV using centrosymmetric crystals. *Nat. Struct. Biol.* 1, 908–914.

Appendix

A   Screening of fungal extracts against phytopathogenic organisms

EPPO (European and Mediterranean Plant Protection Organization) codes:

SEPTTR = *Septoria tritici*; **BOTRCI** = *Botrytis cinerea*; **PHYTIN** = *Phytophthora infestans*; **CLADCU** = *Cladosporium cucumerinum*

Table A1. Screening of basidiomycetous fungi of the genera *Lepista*, *Cortinarius*, and *Dermocybe*.

Species name		Collection	Extract	EPPO code			
				SEPTTR	BOTRCI	PHYTIN	CLADCU
Lepista flaccida	fr	87/11	MeOH	–	–	*n.t.*	+
Lepista flaccida	fr	87/11	EtOAc	–	–	*n.t.*	++
Lepista flaccida	fr	32/12	MeOH	*n.t.*	*n.t.*	*n.t.*	–
Lepista flaccida	fr	32/12	EtOAc	–	*n.t.*	++	+
Lepista gilva (syn. *Lepista flaccida*)	ly	150/97	MeOH	–	–	++	*n.t.*
Lepista gilva (syn. *Lepista flaccida*)	ly	150/97	EtOAc	–	+	++	*n.t.*
Lepista inversa (syn. *Lepista flaccida*)	ly	138/96	MeOH	–	–	++	*n.t.*
Lepista inversa (syn. *Lepista flaccida*)	ly	138/96	EtOAc	–	+	++	*n.t.*
Lepista inversa (syn. *Lepista flaccida*)	ly	217/96	MeOH	–	–	–	*n.t.*
Lepista inversa (syn. *Lepista flaccida*)	ly	217/96	EtOAc	–	+	–	*n.t.*
Lepista nebularis	fr	34/11	MeOH	*n.t.*	*n.t.*	*n.t.*	+
Lepista nebularis	fr	34/11	EtOAc	–	–	*n.t.*	++
Lepista nebularis	fr	89/11	MeOH	*n.t.*	*n.t.*	*n.t.*	+
Lepista nebularis	fr	89/11	EtOAc	*n.t.*	*n.t.*	*n.t.*	++
Lepista nuda	ly	331/98	EtOAc	–	–	–	*n.t.*
Lepista nuda	fr	19/02	MeOH	*n.t.*	*n.t.*	*n.t.*	–
Lepista nuda	fr	19/02	EtOAc	*n.t.*	*n.t.*	*n.t.*	–
Cortinarius anomalus	fr	31/11	MeOH	*n.t.*	*n.t.*	*n.t.*	–
Cortinarius anomalus	fr	31/11	EtOAc	*n.t.*	*n.t.*	*n.t.*	–
Cortinarius aff. *armillatus*	ad	CH 37/11	EtOAc	*n.t.*	*n.t.*	*n.t.*	–
Cortinarius dionysae	fr	28/11	MeOH	*n.t.*	*n.t.*	*n.t.*	–
Cortinarius dionysae	fr	28/11	EtOAc	*n.t.*	*n.t.*	*n.t.*	–
Cortinarius flexipes	fr	94/11	MeOH	*n.t.*	*n.t.*	*n.t.*	–
Cortinarius flexipes	fr	94/11	EtOAc	*n.t.*	*n.t.*	*n.t.*	–
Cortinarius purpurascens	fr	49/11	MeOH	*n.t.*	*n.t.*	*n.t.*	–
Cortinarius purpurascens	fr	49/11	EtOAc	*n.t.*	*n.t.*	*n.t.*	–
Cortinarius safranopes	fr	33/11	MeOH	*n.t.*	*n.t.*	*n.t.*	–
Cortinarius safranopes	fr	33/11	EtOAc	*n.t.*	*n.t.*	*n.t.*	–
Cortinarius trivialis	fr	58/12	MeOH	–	–	–	*n.t.*
Cortinarius trivialis	fr	58/12	EtOAc	–	–	–	*n.t.*
Dermocybe cinnamomeobodia	fr	50/01	MeOH	*n.t.*	*n.t.*	*n.t.*	+
Dermocybe cinnamomeobodia	fr	50/01	EtOAc	*n.t.*	*n.t.*	*n.t.*	+
Dermocybe nahuelbutensis	ad	CH 13/11	EtOAc	*n.t.*	*n.t.*	*n.t.*	–

+++ strong inhibition; ++ moderate inhibition; + weak inhibition; – no inhibition; *n.t.* = not tested; fr = fresh or frozen at –20 °C; ly = lyophilized; ad = air dried.

Table A2. Screening of basidiomycetous fungi of the genus *Hygrophorus*.

Species name		Collection	Extract	EPPO code			
				SEPTTR	BOTRCI	PHYTIN	CLADCU
Hygrophorus abieticola	fr	57/07	MeOH	+	+	*n.t.*	*n.t.*
Hygrophorus abieticola	fr	57/07	EtOAc	++	++	*n.t.*	*n.t.*
Hygrophorus abieticola	fr	58/07	MeOH	+	–	*n.t.*	*n.t.*
Hygrophorus abieticola	fr	58/07	EtOAc	++	++	*n.t.*	*n.t.*
Hygrophorus abieticola	st	19/10	MeOH	–	–	*n.t.*	*n.t.*
Hygrophorus abieticola	st	19/10	EtOAc	+	–	*n.t.*	*n.t.*
Hygrophorus abieticola	fr	90/12	MeOH	*n.t.*	*n.t.*	*n.t.*	+
Hygrophorus abieticola	fr	90/12	EtOAc	*n.t.*	*n.t.*	*n.t.*	+++
Hygrophorus chrysodon	fr	86/04	MeOH	*n.t.*	*n.t.*	*n.t.*	–
Hygrophorus chrysodon	fr	86/04	EtOAc	*n.t.*	*n.t.*	*n.t.*	+
Hygrophorus discoideus	ly	351/98	MeOH	–	–	*n.t.*	*n.t.*
Hygrophorus discoideus	ly	351/98	EtOAc	+	–	*n.t.*	*n.t.*
Hygrophorus discoideus	fr	42/05	EtOAc	–	–	*n.t.*	*n.t.*
Hygrophorus discoxanthus	fr	68/12	Acetone	+	+	–	*n.t.*
Hygrophorus discoxanthus	fr	68/12	EtOAc	++	++	+	*n.t.*
Hygrophorus discoxanthus	fr	68/05	MeOH	*n.t.*	*n.t.*	*n.t.*	+
Hygrophorus discoxanthus	fr	68/05	EtOAc	*n.t.*	*n.t.*	*n.t.*	+
Hygrophorus discoxanthus	fr	08/10	MeOH	–	–	*n.t.*	*n.t.*
Hygrophorus discoxanthus	fr	08/10	EtOAc	–	+	*n.t.*	*n.t.*
Hygrophorus discoxanthus	fr	61/11	MeOH	–	–	*n.t.*	*n.t.*
Hygrophorus discoxanthus	fr	61/11	EtOAc	–	–	*n.t.*	*n.t.*
Hygrophorus erubescens	fr	65/00	MeOH	–	–	*n.t.*	*n.t.*
Hygrophorus erubescens	fr	65/00	EtOAc	–	–	*n.t.*	*n.t.*
Hygrophorus marzuolus	fr	01/07	MeOH	–	–	*n.t.*	*n.t.*
Hygrophorus marzuolus	fr	01/07	EtOAc	–	–	*n.t.*	*n.t.*
Hygrophorus nemoreus	fr	33/02	MeOH	–	–	*n.t.*	*n.t.*
Hygrophorus nemoreus	fr	33/02	EtOAc	–	–	*n.t.*	*n.t.*
Hygrophorus penarius	fr	54/04	MeOH	–	–	*n.t.*	*n.t.*
Hygrophorus penarius	fr	54/04	EtOAc	–	–	*n.t.*	*n.t.*
Hygrophorus penarius	fr	02/06	EtOAc	*n.t.*	*n.t.*	*n.t.*	++
Hygrophorus poetarum	fr	84/11	MeOH	–	–	*n.t.*	*n.t.*
Hygrophorus poetarum	fr	84/11	EtOAc	–	–	*n.t.*	*n.t.*
Hygrophorus pudorinus	fr	53/00	MeOH	+	–	*n.t.*	+
Hygrophorus pudorinus	fr	53/00	EtOAc	++	+	*n.t.*	++
Hygrophorus pudorinus	ly	262/95	MeOH	–	–	*n.t.*	*n.t.*
Hygrophorus pudorinus	ly	262/95	EtOAc	–	–	*n.t.*	*n.t.*
Hygrophorus pudorinus	ly	332/98	MeOH	–	–	*n.t.*	*n.t.*
Hygrophorus pudorinus	ly	332/98	EtOAc	–	–	*n.t.*	*n.t.*
Hygrophorus pudorinus	ly	180/94	MeOH	–	–	*n.t.*	*n.t.*
Hygrophorus pudorinus	ly	180/94	EtOAc	–	–	*n.t.*	*n.t.*
Hygrophorus pudorinus	ad	04/09	MeOH	–	–	*n.t.*	*n.t.*
Hygrophorus pudorinus	ad	04/09	EtOAc	–	–	*n.t.*	*n.t.*

+++ strong inhibition; ++ moderate inhibition; + weak inhibition; – no inhibition; *n.t.* = not tested; fr = fresh or frozen at −20 °C; ly = lyophilized; ad = air dried; st = stored in MeOH solution until workup.

Table A3. Screening results of various basidiomycetous fungi.

Species name		Collection	Extract	EPPO code			
				SEPTTR	BOTRCI	PHYTIN	CLADCU
Tricholoma cingulatum	fr	46/07	MeOH	−	*n.t.*	−	−
Tricholoma cingulatum	fr	46/07	EtOAc	−	*n.t.*	−	−
Tricholoma inamoenum = cf. *Hygrophorus* sp.	fr	05/02	MeOH	+	*n.t.*	++	++
Tricholoma inamoenum = cf. *Hygrophorus* sp.	fr	05/02	EtOAc	+++	*n.t.*	+++	+++
Tricholoma orirubens	fr	34/07	MeOH	*n.t.*	*n.t.*	*n.t.*	−
Tricholoma orirubens	fr	34/07	EtOAc	*n.t.*	*n.t.*	*n.t.*	−
Tricholoma populinum	fr	92/00	MeOH	−	*n.t.*	−	−
Tricholoma populinum	fr	92/00	EtOAc	−	*n.t.*	−	−
Tricholoma sejunctum	fr	02/10	MeOH	−	*n.t.*	−	−
Tricholoma sejunctum	fr	02/10	EtOAc	−	*n.t.*	+	−
Tricholoma terreum	fr	60/11	MeOH	*n.t.*	*n.t.*	*n.t.*	−
Tricholoma terreum	fr	60/11	EtOAc	*n.t.*	*n.t.*	*n.t.*	−
Tricholoma ustale	fr	03/94	MeOH	−	*n.t.*	+	−
Tricholoma ustale	fr	03/94	EtOAc	−	*n.t.*	+	+
Tricholoma vaccinum	fr	78/00	MeOH	*n.t.*	*n.t.*	*n.t.*	−
Tricholoma vaccinum	fr	78/00	EtOAc	*n.t.*	*n.t.*	*n.t.*	−
Boletus luridus	fr	104/02	EtOAc	−	−	−	*n.t.*
Camarophyllus niveus	fr	43/11	EtOAc	−	−	−	*n.t.*
Camarophyllus niveus	fr	43/11	MeOH	*n.t.*	*n.t.*	*n.t.*	−
Camarophyllus niveus	fr	43/11	EtOAc	*n.t.*	*n.t.*	*n.t.*	+
Camarophyllus pratensis	fr	100/04	MeOH	*n.t.*	*n.t.*	*n.t.*	−
Camarophyllus pratensis	fr	100/04	EtOAc	*n.t.*	*n.t.*	*n.t.*	−
Chalciporus piperatus	fr	02/01	MeOH	*n.t.*	*n.t.*	*n.t.*	−
Chalciporus piperatus	fr	02/01	EtOAc	*n.t.*	*n.t.*	*n.t.*	−
Discolea pallida	ad	CH 19/12	EtOAc	−	−	−	*n.t.*
Fistulina hepatica	fr	85/11	MeOH	*n.t.*	*n.t.*	*n.t.*	−
Fistulina hepatica	fr	85/11	EtOAc	*n.t.*	*n.t.*	*n.t.*	+
Hebeloma edurum	fr	59/11	MeOH	*n.t.*	*n.t.*	*n.t.*	−
Hebeloma edurum	fr	59/11	EtOAc	*n.t.*	*n.t.*	*n.t.*	−
Hygrophoropsis aurantiaca	fr	44/03	MeOH	*n.t.*	*n.t.*	*n.t.*	−
Hygrophoropsis aurantiaca	fr	44/03	EtOAc	*n.t.*	*n.t.*	*n.t.*	−
Lycoperdon perlatum	fr	32/11	MeOH	*n.t.*	*n.t.*	*n.t.*	−
Lycoperdon perlatum	fr	32/11	EtOAc	*n.t.*	*n.t.*	*n.t.*	−
Paxillus boletinoides	ad	CH 05/11	EtOAc	*n.t.*	*n.t.*	*n.t.*	−
Paxillus statuum	ad	CH 02/11	EtOAc	*n.t.*	*n.t.*	*n.t.*	−
Paxillus statuum	ad	CH 26/12	EtOAc	−	−	−	*n.t.*
Pluteus cervinus	fr	86/11	MeOH	*n.t.*	*n.t.*	*n.t.*	−
Pluteus cervinus	fr	86/11	EtOAc	*n.t.*	*n.t.*	*n.t.*	−
Pseudoclitocybe cyathiformis	fr	86/12	MeOH	−	−	−	*n.t.*
Pseudoclitocybe cyathiformis	fr	86/12	EtOAc	−	−	−	*n.t.*
Russula sardonia	fr	88/11	MeOH	*n.t.*	*n.t.*	*n.t.*	−
Russula sardonia	fr	88/11	EtOAc	−	+	*n.t.*	++
Sarcodon imbricatum	fr	19/11	MeOH	*n.t.*	*n.t.*	*n.t.*	−
Sarcodon imbricatum	fr	19/11	EtOAc	*n.t.*	*n.t.*	*n.t.*	−
Strobilomyces floccopus	fr	87/12	EtOAc	+	−	−	*n.t.*
Stropharia aeruginosa	fr	88/12	MeOH	−	+	−	*n.t.*

+++ strong inhibition; ++ moderate inhibition; + weak inhibition; − no inhibition; *n.t.* = not tested; fr = fresh or frozen at −20 °C; ad = air dried.

Table A4. Screening of various ascomycetous fungi.

Species name		Strain	Extract	EPPO code			
				SEPTTR	BOTRCI	PHYTIN	CLADCU
Gliocladium album	cb	KSH 719	EtOAc	−	++	−	*n.t.*
Mycogone calospora	cb	KSH 742	EtOAc	−	+	++	*n.t.*
Acremonium strictum	cb	KSH 667	EtOAc	−	+	−	*n.t.*
Acremonium domschii	cb	KSH 666	EtOAc	−	+	−	*n.t.*
Sepedonium aff. *chalcipori*	cb	KSH 883	EtOAc	−	+	*n.t.*	−
Sepedonium sp.	cb	KSH 889	EtOAc	−	−	*n.t.*	−
Sepedonium tulasneanum	cb	KSH 535	EtOAc	+	++	+	*n.t.*
Sepedonium sp.	cb	KSH 885	EtOAc	+	+++	++	*n.t.*
Sepedonium sp.	cb	KSH 912	EtOAc	−	+	−	*n.t.*
Sepedonium aff. *chalcipori*	cb	KSH 883	MeOH[a]	−	+	++	*n.t.*
Sepedonium aff. *chalcipori*	cb	KSH 883	EtOAc	−	+	−	*n.t.*
Sepedonium sp.	cb	KSH 885	MeOH[a]	−	++	++	*n.t.*
Sepedonium sp.	cb	KSH 885	EtOAc	−	+	++	*n.t.*
Gliocladium album	cb	KSH 719	MeOH[a]	−	+	+	*n.t.*
Gliocladium album	cb	KSH 719	EtOAc	−	+	+	*n.t.*
Mycogone calospora	cb	KSH 742	MeOH[a]	−	+	+++	*n.t.*
Mycogone calospora	cb	KSH 742	EtOAc	+	+	++	*n.t.*
Sepedonium tulasneanum	cb	KSH 535	MeOH[a]	−	+	+	*n.t.*
Sepedonium tulasneanum	cb	KSH 535	EtOAc	−	+	−	*n.t.*

+++ strong inhibition; ++ moderate inhibition; + weak inhibition; − no inhibition; *n.t.* = not tested; cb = culture broth; [a] obtained by Diaion HP 20 purification.

B Peptaibol sequences and fragments

Table B1. Peptaibol sequences reported from *Sepedonium* species.

source / peptaibol		1	2	3	4	5	6	7	8	9	10	11	12	13	14	15	16	17	18	19
S. ampullosporum																				
peptaibolin (**2.42**)	Ac	Leu	Aib	Leu	Aib	Pheol														
ampullosporin A (**2.43**)	Ac	Trp	Ala	Aib	Aib	Leu	Aib	Gln	**Aib**	**Aib**	**Aib**	Gln	Leu	**Aib**	Gln	Leuol				
ampullosporin B (**2.44**)	Ac	Trp	Ala	Aib	Aib	Leu	Aib	Gln	**Ala**	**Aib**	**Aib**	Gln	Leu	**Aib**	Gln	Leuol				
ampullosporin C (**2.45**)	Ac	Trp	Ala	Aib	Aib	Leu	Aib	Gln	**Aib**	**Ala**	**Aib**	Gln	Leu	**Aib**	Gln	Leuol				
ampullosporin D (**2.46**)	Ac	Trp	Ala	Aib	Aib	Leu	Aib	Gln	**Aib**	**Aib**	**Ala**	Gln	Leu	**Aib**	Gln	Leuol				
ampullosporin E1 (**2.47**)	Ac	Trp	Ala	Aib	Aib	Leu	Aib	Gln	**Ala**	**Aib**	**Aib**	Gln	Leu	**Ala**	Gln	Leuol				
ampullosporin E2 (**2.48**)	Ac	Trp	Ala	Aib	Aib	Leu	Aib	Gln	**Aib**	**Aib**	**Ala**	Gln	Leu	**Aib**	Gln	Leuol				
ampullosporin E3 (**2.49**)	Ac	Trp	Ala	Aib	Aib	Leu	Aib	Gln	**Aib**	**Aib**	**Ala**	Gln	Leu	**Ala**	Gln	Leuol				
ampullosporin E4 (**2.50**)	Ac	Trp	Ala	Aib	Aib	Leu	Aib	Gln	**Ala**	**Ala**	**Aib**	Gln	Leu	**Aib**	Gln	Leuol				
S. chrysospermum																				
chrysaibol (**2.51**)	Ac	Trp	Aib	Aib	Leu	Val	Gln	Aib	Aib	Aib	Gln	Leu	Aib	Pro	Gln	Alaol				
chrysospermin A (**2.52**)	Ac	Phe	Aib	Ser	Aib	**Aib**	Leu	Gln	Gly	Aib	Aib	Ala	Ala	Aib	Pro	**Aib**	Aib	Aib	Gln	Trpol
chrysospermin B (**2.53**)	Ac	Phe	Aib	Ser	Aib	**Aib**	Leu	Gln	Gly	Aib	Aib	Ala	Ala	Aib	Pro	**Iva**	Aib	Aib	Gln	Trpol
chrysospermin C (**2.54**)	Ac	Phe	Aib	Ser	Aib	**Iva**	Leu	Gln	Gly	Aib	Aib	Ala	Ala	Aib	Pro	**Aib**	Aib	Aib	Gln	Trpol
chrysospermin D (**2.55**)	Ac	Phe	Aib	Ser	Aib	**Iva**	Leu	Gln	Gly	Aib	Aib	Ala	Ala	Aib	Pro	**Iva**	Aib	Aib	Gln	Trpol
S. chalcipori																				
tylopeptin A (**2.56**)	Ac	Trp	Val	Aib	**Iva**	Ala	Gln	Ala	Aib	Ser	Aib	Ala	Leu	Aib	Gln	Leuol				
tylopeptin B (**2.57**)	Ac	Trp	Val	Aib	**Aib**	Ala	Gln	Ala	Aib	Ser	Aib	Ala	Leu	Aib	Gln	Leuol				
chalciporin A (**2.58**)	Ac	Trp	Val	Aib	Val	Ala	Gln	Ala	Aib	**Ser**	**Leu**	Ala	Leu	Aib	Gln	Leuol				
chalciporin B (**2.59**)	Ac	Trp	Val	Aib	Val	Ala	Gln	Ala	Aib	**Gln**	**Aib**	Ala	Leu	Aib	Gln	Leuol				
S. microspermum																				
microspermin A (**2.60**)	Ac	Trp	**Aib**	Ser	Aib	**Iva**	**Trp**	Gln	Gly	Aib	Aib	Ala	Ala	Aib	Pro	Aib	Aib	**Aib**	Gln	Leuol
microspermin B (**2.61**)	Ac	Trp	**Aib**	Ser	Aib	**Aib**	**Trp**	Gln	Gly	Aib	Aib	Ala	Ala	Aib	Pro	Aib	Aib	**Iva**	Gln	Leuol
microspermin C (**2.62**)	Ac	Trp	**Iva**	Ser	Aib	**Iva**	**Trp**	Gln	Gly	Aib	Aib	Ala	Ala	Aib	Pro	Aib	Aib	**Aib**	Gln	Leuol
microspermin D (**2.63**)	Ac	Trp	**Aib**	Ser	Aib	**Iva**	**Trp**	Gln	Gly	Aib	Aib	Ala	Ala	Aib	Pro	Aib	Aib	**Iva**	Gln	Leuol
microspermin E (**2.64**)	Ac	Trp	**Iva**	Ser	Aib	**Iva**	**Trp**	Gln	Gly	Aib	Aib	Ala	Ala	Aib	Pro	Aib	Aib	**Iva**	Gln	Leuol
microspermin F (**2.65**)	Ac	Trp	**Iva**	Ser	Aib	**Iva**	**Trp**	Gln	Gly	Aib	Aib	Ala	Ala	Aib	Pro	Aib	Aib	**Aib**	Gln	Leuol
microspermin G (**2.66**)	Ac	Trp	**Aib**	Ser	Aib	**Iva**	**Leu**	Gln	Gly	Aib	Aib	Ala	Ala	Aib	Pro	Aib	Aib	**Iva**	Gln	Leuol
microspermin H (**2.67**)	Ac	Trp	**Iva**	Ser	Aib	**Iva**	**Leu**	Gln	Gly	Aib	Aib	Ala	Ala	Aib	Pro	Aib	Aib	**Iva**	Gln	Leuol

Table B2. Peptaibol sequences reported from *Gliocladium* species.

source / peptaibol		1	2	3	4	5	6	7	8	9	10	11	12	13	14	15	16	17	18	19	20
G. catenulatum																					
antiamoebin I (**2.79**)	Ac	Phe	Aib	**Aib**	Aib	**D-Iva**	**Gly**	Leu	Aib	Aib	Hyp	Gln	**D-Iva**	Hyp	Aib	Pro	Pheol				
antiamoebin III (**2.80**)	Ac	Phe	Aib	**Aib**	Aib	**Aib**	**Gly**	Leu	Aib	Aib	Hyp	Gln	**D-Iva**	Hyp	Aib	Pro	Pheol				
antiamoebin VI (**2.81**)	Ac	Phe	Aib	**Aib**	Aib	**Aib**	**Gly**	Leu	Aib	Aib	Hyp	Gln	**Aib**	Hyp	Aib	Pro	Pheol				
antiamoebin VIII (**2.82**)	Ac	Phe	Aib	**Aib**	Aib	**D-Iva**	**Gly**	Leu	Aib	Aib	Hyp	Gln	**Aib**	Hyp	Aib	Pro	Pheol				
antiamoebin IX (**2.83**)	Ac	Phe	Aib	**Ala**	Aib	**D-Iva**	**Gly**	Leu	Aib	Aib	Hyp	Gln	**D-Iva**	Hyp	Aib	Pro	Pheol				
antiamoebin XI (**2.84**)	Ac	Phe	Aib	**Aib**	Aib	**D-Iva**	**Ala**	Leu	Aib	Aib	Hyp	Gln	**D-Iva**	Hyp	Aib	Pro	Pheol				
G. deliquescens																					
gliodeliquescin A (**2.85**)	Ac	Aib	Ala	Aib	Ala	Aib	Ala	Gln	Aib	Val	Aib	Gly	Leu	Aib	Pro	Val	Aib	Aib	Gln	Gln	Pheol

Table B3. Reference monoisotopic masses of common amino acid residues and terminal modifications occurring in peptaibols with their corresponding fragments, adapted from Degenkolb (2003)[a].

Amino acid	Abbreviation		Molecular formula of the residue	Monoisotopic mass
	1LC	3LC		
α-aminoisobutyric acid	U	Aib	C_4H_7NO	85.0528
valine	V	Val	C_5H_9NO	99.0684
isovaline	J	Iva	C_5H_9NO	99.0684
leucine	L	Leu	$C_6H_{11}NO$	113.0841
isoleucine	I	Ile	$C_6H_{11}NO$	113.0841
tryptophan	W	Trp	$C_{11}H_{10}N_2O$	186.0793
phenylalanine	F	Phe	C_9H_9NO	147.0684
glycine	G	Gly	C_2H_3NO	57.0215
alanine	A	Ala	C_3H_5NO	71.0371
glutamine	Q	Gln	$C_5H_8N_2O_2$	128.0586
glutamic acid	E	Glu	$C_5H_7NO_3$	129.0426
proline	P	Pro	C_5H_7NO	97.0528
hydroxyproline	O	Hyp	$C_5H_7NO_2$	113.0477
asparagine	N	Asn	$C_4H_6N_2O_2$	114.0429
aspartic acid	D	Asp	$C_4H_5NO_3$	115.0269
serine	S	Ser	$C_3H_5NO_2$	87.0320
pyroglutamic acid	Z	Glp	$C_5H_5NO_2$	111.0320
pipecolic acid	-	Pip	C_6H_9NO	111.0684
***N*-terminal**				
acetyl α-aminoisobutyric acid	Ac-U	Ac-Aib	$C_6H_9NO_2$	127.0633
acetyl valine	Ac-V	Ac-Val	$C_7H_{11}NO_2$	141.0790
acetyl isovaline	Ac-J	Ac-Iva	$C_7H_{11}NO_2$	141.0790
acetyl alanine	Ac-A	Ac-Ala	$C_5H_7NO_2$	113.0477
acetyl leucine	Ac-L	Ac-Leu	$C_8H_{13}NO_2$	155.0946
acetyl phenylalanine	Ac-F	Ac-Phe	$C_{11}H_{11}NO_2$	189.0790
acetyl tryptophan	Ac-W	Ac-Trp	$C_{13}H_{12}N_2O_2$	228.0899
***C*-terminal**				
phenylalaninol	Fol	Pheol	$C_9H_{13}NO$	151.0997
leucinol	Lol	Leuol	$C_6H_{15}NO$	117.1154
isoleucinol	Iol	Ileol	$C_6H_{15}NO$	117.1154
tryptophanol	Wol	Trpol	$C_{11}H_{14}N_2O$	190.1106
valinol	Vol	Valol	$C_5H_{13}NO$	103.0997
2-aminoisobutanol	Uol	Aibol	$C_4H_{11}NO$	89.0841

[a] Degenkolb, T., Berg, A., Gams, W., Schlegel, B., Gräfe, U., 2003. The occurrence of peptaibols and structurally related peptaibiotics in fungi and their mass spectrometric identification *via* diagnostic fragment ions. *J. Pept. Sci.* 9, 666–678.

C Compound code assignment

Thesis compound number	Compound name	Experiment code (3LC)
4.1	Hygrophorone B^{12}	OTA 095_1B
4.1	Hygrophorone B^{12}, labelled with [2-^{13}C]-acetate	OTA 219_34_B12
4.1	Hygrophorone B^{12}, labelled with [1-^{13}C]-glucose	OTA 192_B60
4.1	Hygrophorone B^{12}, labelled with [U-^{13}C$_6$]-glucose	OTA 193_C60
4.1	Hygrophorone B^{12}, unlabelled control	OTA 196_D60, OTA 221
5.1	Pseudohygrophorone A^{12}	OTA 100_1
5.2	Pseudohygrophorone B^{12}	OTA 108_1
5.3	Hygrophorone B^{12}	OTA 095_1B
6.1	Hygrophorone B^{12}	OTA 095_1B
6.1a	4-O-Acetylhygrophorone B^{12}	OTA 122_1
6.1b	6-O-Acetylhygrophorone B^{12}	OTA 122_2
6.1c	4,6-Di-O-acetylhygrophorone B^{12}	OTA 118_1
6.1d	4,5,6-Tri-O-acetylhygrophorone B^{12}	OTA 123_1
6.2	Hygrophorone B^{10}	OTA 102_1
6.3	Hygrophorone E^{12}	OTA 100_2
6.3a	1,4-Di-O-acetylhygrophorone E^{12}	OTA 145_5, OTA 180_2
6.4	Hygrophorone H^{12}	OTA 101_1
6.5	2,3-Dihydrohygrophorone H^{12}	OTA 102_A6
7.1	Penarine A	OTA 058_2
7.2	Penarine B	OTA 041_2
7.3	Penarine C	OTA 041_3
7.4	Penarine D	OTA 056_7
7.5	Penarine E	OTA 054_4B
7.6	Penarine F	OTA 056_6
8.1	Chilenopeptin A	HEI 080_4
8.2	Chilenopeptin B	HEI 080_5
8.3	Tylopeptin A	HEI 080_3
8.4	Tylopeptin B	HEI 080_2
9.1 (nat.)	Albupeptin A, natural	OTA 168_1
9.1 (syn.)	Albupeptin A, synthetic	LAA 028
9.2	Albupeptin B, natural	OTA 168_2
LD-**9.2**	Albupeptin B, synthetic	LAA 033
DD-**9.2**	Albupeptin B, synthetic diastereomer	LAA 030
9.3 (nat.)	Albupeptin C, natural	OTA 168_3
9.3 (syn.)	Albupeptin C, synthetic	LAA 029
9.4	Albupeptin D, natural	OTA 168_4
DLD-**9.4**	Albupeptin D, synthetic	LAA 034
DDD-**9.4**	Albupeptin D, synthetic diastereomer	LAA 031
10.1	Tulasporin A	OTA 143_2
10.2	Tulasporin B	OTA 143_3
10.3	Tulasporin C	OTA 143_4
10.4	Tulasporin D	OTA 143_5

Declaration on the author contributions

Chapter 3   Bette, E., <u>Otto, A.</u>, Dräger, T., Merzweiler, K., Arnold, N., Wessjohann, L., Westermann, B. Isolation and Asymmetric Total Synthesis of Fungal Secondary Metabolite Hygrophorone B^{12}. *European Journal of Organic Chemistry* **2015**, 2015, 2357–2365.

In this work, Alexander Otto carried out the isolation and structural elucidation of hygrophorone B^{12} as a prerequisite for the total synthesis. Eileen Bette performed the asymmetric total synthesis of hygrophorone B^{12} and its stereoisomers. Initial synthetic studies have been carried out by Tobias Dräger. Kurt Merzweiler performed the X-ray analysis. Alexander Otto wrote the part of the isolation and structural elucidation of hygrophorone B^{12}, while Eileen Bette and Bernhard Westermann wrote the synthesis part of the manuscript. Norbert Arnold, Ludger Wessjohann, and Bernhard Westermann acted as supervisors of the project; they designed the project, coordinated the work, suggested the synthetic route, helped with data interpretation, and contributed to the writing and editing of the manuscript.

Chapter 4   <u>Otto, A.</u>, Porzel, A., Schmidt, J., Wessjohann, L., Arnold, N. A study on the biosynthesis of hygrophorone B^{12} in the mushroom *Hygrophorus abieticola* reveals an unexpected labelling pattern in the cyclopentenone moiety. *Phytochemistry* **2015**, 118, 174–180.

In this project, Alexander Otto carried out the feeding experiments in the field, followed by isolation of hygrophorone B^{12} and analysis of the ^{13}C incorporation patterns. Andrea Porzel performed the NMR studies and provided help with the data analysis and interpretation. The MS measurements were carried out by Jürgen Schmidt. Alexander Otto wrote the manuscript draft. The work was planned, supervised, and edited by Ludger Wessjohann and Norbert Arnold.

Chapter 5   <u>Otto, A.</u>, Porzel, A., Schmidt, J., Brandt, W., Wessjohann, L., Arnold, N. Structure and absolute configuration of pseudohygrophorones A^{12} and B^{12}, alkyl cyclohexenone derivatives from *Hygrophorus abieticola* (Basidiomycetes). *Journal of Natural Products* **2016**, 79, 74–80.

In this study, Alexander Otto carried out the isolation and structural and stereochemical assignment of the constituents as well as bioactivity testing. Andrea Porzel performed the NMR analyses and helped with the structural elucidation, while the MS measurements were carried out by Jürgen Schmidt. Wolfgang Brandt performed the computational studies and participated in writing the manuscript. Alexander Otto wrote the major part of the manuscript. The project was designed, supervised, and edited by Ludger Wessjohann and Norbert Arnold.

Chapter 6   Otto, A., Porzel, A., Westermann, B., Brandt, W., Wessjohann, L., Arnold, N. Structural and stereochemical elucidation of new hygrophorones from *Hygrophorus abieticola* (Basidiomycetes). *Tetrahedron* **2017**, 73, 1682–1690.

In this project, Alexander Otto isolated the compounds, elucidated their (stereo-)structures, and performed the semisynthetic studies as well as the antiphytopathogenic and anti-*Malassezia* activity testing. Wolfgang Brandt carried out the computational studies. Andrea Porzel performed the NMR measurements and participated in the structural and stereochemical assignment. Alexander Otto wrote the manuscript draft. The work was designed, supervised, and edited by Bernhard Westermann, Ludger Wessjohann, and Norbert Arnold.

Chapter 7   Otto, A., Porzel, A., Schmidt, J., Wessjohann, L., Arnold, N. Penarines A–F, (nor-)sesquiterpene carboxylic acids from *Hygrophorus penarius* (Basidiomycetes). *Phytochemistry* **2014**, 108, 229–233.

In this work, the isolation and structural assignment of the constituents was performed by Alexander Otto. Andrea Porzel carried out the NMR measurements and helped in the structural elucidation, while Jürgen Schmidt performed the MS studies. Alexander Otto wrote the major part of the manuscript. The work was designed, supervised, and edited by Ludger Wessjohann and Norbert Arnold.

Chapter 8   Otto, A., Laub, A., Wendt, L., Porzel, A., Schmidt, J., Palfner, G., Becerra, J., Krüger, D., Stadler, M., Wessjohann, L., Westermann, B., Arnold, N. Chilenopeptins A and B, peptaibols from the Chilean *Sepedonium* aff. *chalcipori* KSH 883. *Journal of Natural Products* **2016**, 79, 929–938.

In this project, Alexander Otto performed the mycochemical study including isolation, structural elucidation, and bioactivity testing. Andrea Porzel carried out the NMR measurements and provided help with the data analysis and interpretation. Jürgen Schmidt and Annegret Laub performed the MS studies. The solid-phase synthesis was accomplished by Annegret Laub. The phylogenetic analyses were carried out by Lucile Wendt and Dirk Krüger. Götz Palfner collected and determined the analyzed fungal material. Alexander Otto wrote the major part of the manuscript, while Lucile Wendt contributed to the phylogenetic part. Marc Stadler, José Becerra, Ludger Wessjohann, Bernhard Westermann, and Norbert Arnold acted as supervisors of the project; they designed the study, coordinated the work, and contributed to the writing and editing of the manuscript.

Chapter 9   <u>Otto, A.</u>, Laub, A., Porzel, A., Schmidt, J., Wessjohann, L., Westermann, B., Arnold, N. Isolation and total synthesis of albupeptins A–D: 11-residue peptaibols from the fungus *Gliocladium album*, *European Journal of Organic Chemistry* **2015**, 2015, 7449–7459.

In this study, Alexander Otto carried out the isolation and structural assignment of the constituents as well as antiphytopathogenic activity studies. Andrea Porzel carried out the NMR measurements and provided help with the data analysis and interpretation. Jürgen Schmidt and Annegret Laub performed the MS analyses. The solid-phase synthesis was carried out by Annegret Laub. Alexander Otto wrote the major part of the manuscript. Ludger Wessjohann, Bernhard Westermann, and Norbert Arnold supervised the project; they coordinated the work, provided helpful discussions, and contributed to the redaction of the manuscript.

Chapter 10   <u>Otto, A.</u>, Laub, A., Haid, M., Porzel, A., Schmidt, J., Wessjohann, L., Arnold, N. Tulasporins A–D, 19-residue peptaibols from the mycoparasitic fungus *Sepedonium tulasneanum*, *Natural Product Communications* **2016**, 11, 1821–1824.

In this work, Alexander Otto isolated the constituents, elucidated their structures, performed the bioactivity testing, and wrote the major part of the manuscript. NMR measurements were carried out by Andrea Porzel. Mark Haid performed initial fragmentation studies and thus contributed to the structural elucidation. The MS analyses were carried out by Jürgen Schmidt and Annegret Laub. Ludger Wessjohann and Norbert Arnold acted as supervisors of the project; they designed the study, coordinated the work, and contributed to the writing and editing of the manuscript.

Publications

Publications in peer-reviewed journals

Otto, A., Porzel, A., Schmidt, J., Wessjohann, L., Arnold, N., 2014. Penarines A–F, (nor-) sesquiterpene carboxylic acids from *Hygrophorus penarius* (Basidiomycetes). *Phytochemistry* 108, 229–233, doi: 10.1016/j.phytochem.2014.09.005

Bette, E., **Otto, A.**, Dräger, T., Merzweiler, K., Arnold, N., Wessjohann, L., Westermann, B., 2015. Isolation and Asymmetric Total Synthesis of Fungal Secondary Metabolite Hygrophorone B^{12}. *European Journal of Organic Chemistry* 2015, 2357–2365, doi: 10.1002/ejoc.201403455

Otto, A., Porzel, A., Schmidt, J., Wessjohann, L., Arnold, N., 2015. A study on the biosynthesis of hygrophorone B^{12} in the mushroom *Hygrophorus abieticola* reveals an unexpected labelling pattern in the cyclopentenone moiety. *Phytochemistry* 118, 174–180, doi: 10.1016/j.phytochem. 2015.08.018

Otto, A., Laub, A., Porzel, A., Schmidt, J., Wessjohann, L., Westermann, B., Arnold, N., 2015. Isolation and Total Synthesis of Albupeptins A–D: 11-Residue Peptaibols from the Fungus *Gliocladium album. European Journal of Organic Chemistry* 2015, 7449–7459, doi: 10.1002/ejoc.201501124

Otto, A., Porzel, A., Schmidt, J., Brandt, W., Wessjohann, L., Arnold, N., 2016. Structure and absolute configuration of pseudohygrophorones A^{12} and B^{12}, alkyl cyclohexenone derivatives from *Hygrophorus abieticola* (Basidiomycetes). *Journal of Natural Products* 79, 74–80, doi: 10.1021/acs.jnatprod.5b00675

Otto, A., Laub, A., Wendt, L., Porzel, A., Schmidt, J., Palfner, G., Becerra, J., Krüger, D., Stadler, M., Wessjohann, L., Westermann, B., Arnold, N., 2016. Chilenopeptins A and B, Peptaibols from the Chilean *Sepedonium* aff. *chalcipori* KSH 883. *Journal of Natural Products* 79, 928–938, doi: 10.1021/acs.jnatprod.5b01018

Otto, A., Laub, A., Haid, M., Porzel, A., Schmidt, J., Wessjohann, L., Arnold, N., 2016. Tulasporins A–D, 19-Residue Peptaibols from the Mycoparasitic Fungus *Sepedonium tulasneanum. Natural Product Communications* 11, 1821–1824

Otto, A., Porzel, A., Westermann, B., Brandt, W., Wessjohann, L., Arnold, N., 2017. Structural and stereochemical elucidation of new hygrophorones from *Hygrophorus abieticola* (Basidiomycetes). *Tetrahedron*, 73, 1682–1690, doi: 10.1016/j.tet.2017.02.013

Patent

Arnold, N., **Otto, A.**, Bette, E., Westermann, B., Lübken, T., Wessjohann, L., 2016. Hygrophoron B^{12} zur Verwendung bei der Behandlung einer Mykose. Europäisches Patent, EP3087981 A1.

Oral presentations

Otto, A. New hygrophorones from *Hygrophorus abieticola*: Isolation, structure elucidation, bioactivity, and biosynthesis. 48. Doktorandenworkshop "Naturstoffe: Chemie, Biologie und Ökologie", Leipzig, 10th October 2014

Otto, A. Bioactive secondary metabolites from fungi: Isolation, structure elucidation, bioactivity, and biosynthesis. Basidionet-Treffen, Halle (Saale), 13th February 2015

Poster presentations

Otto, A., Teichert, A., Lübken, T., Porzel, A., Schmidt, J., Wessjohann, L., Arnold, N. Fungicidal secondary metabolites from the genus *Hygrophorus.* 1st European Conference on Natural Products: Research and Applications, Frankfurt (Main), 22nd – 25th September 2013

Otto, A., Laub, A., Porzel, A., Schmidt, J., Palfner, G., Wessjohann, L., Arnold, N. Peptaibol pattern of Chilean *Sepedonium* strains reveal a close relationship to European *Sepedonium* species. Drei-Länder-Tagung der Deutschen Gesellschaft für Mykologie (DGfM), Mettlach-Orscholz, 29th September – 1st October 2014

Laub, A., **Otto, A.**, Arnold, N., Schmidt, J., Westermann, B. Synthese und massenspektro-metrische Charakterisierung von Aib-haltigen antibiotischen Peptiden. 48. Jahrestagung der Deutschen Gesellschaft für Massenspektrometrie (DGMS), Wuppertal, 1st – 4th March 2015

Wendt, L., **Otto, A.**, Laub, A., Porzel, A., Schmidt, J., Palfner, G., Becerra, J., Krüger, D., Stadler, M., Wessjohann, L., Westermann, B., Arnold, N. Chilenopeptins A and B, Peptaibols from the Chilean *Sepedonium* aff. *chalcipori* KSH 883. CBS Spring Symposium "Fungi and Global Challenges", Amsterdam, 14th – 16th April 2016

Video clip

Otto, A., Harmon, C., Hünecke, N., Schmidt, J., Fobofou, S., Arnold, N., Wessjohann, L., 2014. Natural antibiotics from mushrooms based on metabolic profiling. Beilstein TV series, URL http://www.beilstein.tv/tvpost/natural-antibiotics-from-mushrooms-based-on-metabolic-profiling/

Curriculum vitae

Personal details

Name: Alexander Otto

Date/place of birth: 30th December 1986 in Halle (Saale)

Nationality: German

Address: Eichendorffstraße 25, 06114 Halle (Saale)

School education

09/1997 – 06/2005 Kyffhäuser-Gymnasium, Bad Frankenhausen

Degree: General qualification for University entrance

Academic studies

10/2005 – 11/2009 Studies of Pharmacy, Martin Luther University of Halle-Wittenberg

11/2009 – 04/2010 Diploma, Martin Luther University of Halle-Wittenberg

Title: "Synthesis and characterization of 1,2-dihydropyridones as potential MDR-modulators"
(Supervisor: PD Dr. Andreas Hilgeroth)

11/2010 License to practice pharmacy

04/2011 – 08/2015 PhD candidate (Dr. rer. nat.), Leibniz Institute of Plant Biochemistry, Department of Bioorganic Chemistry, Halle (Saale)

Title: "Chemical and biological studies on bioactive secondary metabolites from fungal source"
(Supervisor: Prof. Dr. Ludger Wessjohann)

05/2014 Research stay, University of Concepción, Concepción, Chile

Work experiences

05/2010 – 10/2010 Pharmacist at practical training, St. Georg Apotheke, Halle (Saale)

11/2010 – 03/2011 Pharmacist, Anger-Apotheke, Bad Frankenhausen

04/2011 – 08/2015 Research Assistant, Leibniz Institute of Plant Biochemistry, Department of Bioorganic Chemistry, Halle (Saale)

since 09/2015 Project Leader Analytical Development, mibe GmbH Arzneimittel, Brehna-Sandersdorf

Eidesstattliche Erklärung

Ich erkläre an Eides statt, dass ich die vorliegende Arbeit selbstständig und nur unter Verwendung der angegebenen Hilfsmittel und Quellen angefertigt habe.

Alle Stellen, die wörtlich oder sinngemäß aus Veröffentlichungen entnommen sind, habe ich als solche kenntlich gemacht. Des Weiteren versichere ich, dass ich diese Arbeit an keiner anderen Institution eingereicht habe.

Mir ist bekannt, dass bei Angabe falscher Aussagen die Prüfung als nicht bestanden gilt. Mit meiner Unterschrift versichere ich die Richtigkeit dieser Angaben und erkenne die rechtlichen Grundlagen an.

Datum	(Alexander Otto)